SALTSTONE DISPOSAL FACILITY CLOSURE CAP CONCEPT AND INFILTRATION ESTIMATES

W. E. Jones
M. A. Phifer

MAY 2008

Savannah River National Laboratory
Washington Savannah River Company
Savannah River Site
Aiken, SC 29808
Prepared for the U.S. Department of Energy Under
Contract Number DE-AC09-96SR18500
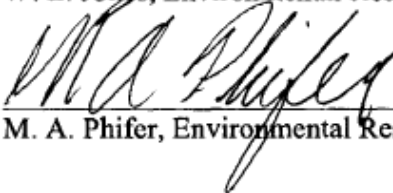
SRNL
™

DISCLAIMER

Printed in the United States of America

Prepared For
U.S. Department of Energy

SALTSTONE DISPOSAL FACILITY CLOSURE CAP CONCEPT AND INFILTRATION ESTIMATES

W. E. Jones
M. A. Phifer

MAY 2008

SRNL
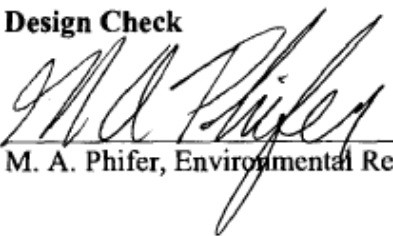
REVIEWS AND APPROVALS

Authors

_____   6/12/08
W. E. Jones, Environmental Restoration Technology Section   Date

_____   6/12/08
M. A. Phifer, Environmental Restoration Technology Section   Date

Design Check

_____   6/12/08
M. A. Phifer, Environmental Restoration Technology Section   Date

Approvals

_____   6/12/08
R. S. Aylward, Environmental Restoration Technology Section   Date

B. J. Butcher for H. Burns   6/12/08
H. H. Burns, Process Technology Programs   Date

_____   6/12/08
K. H. Rosenberger, Regulatory Interface and Planning   Date
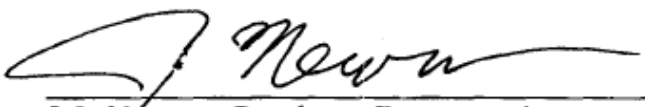
_____   6/12/08
J. L. Newman, Regulatory Documentation   Date

TABLE OF CONTENTS

LIST OF FIGURES

LIST OF TABLES

LIST OF ACRONYMS

#	number
%	percent
°C	degrees Celsius
°F	degrees Fahrenheit
η	porosity
θ_v	volumetric moisture content
ψ	suction head
ρ_b	dry bulk density
ρ_p	particle density
A	drainage area in acres
A	constant (in OIT depletion rate equation)
C	runoff coefficient (unitless)
CF	velocity correction factor
cfs	cubic feet per second
cm-H_2O	centimeters of water
cm/s	centimeters per second
D_{50}	median stone diameter
D_{100}	maximum stone diameter
E_a	activation energy of the antioxidant depletion reaction (kJ/mol);
F	flow concentration factor (unitless)
ft	feet
g/m^2-day	grams per square meter per day
g/cm^3	grams per cubic centimeter
H	elevation difference in feet
hr	hour
I	precipitation in inches/hour
in	inches
kPa	kiloPascals
K_{sat}	Saturated Hydraulic Conductivity
L	drainage length in miles
lbs/ft^2	pounds per square foot
mg/L	milligrams/liter
mil	thousandth of an inch
min	minute
mm	millimeter
MPV	maximum permissible velocity
Mrad	megarad (1,000,000 rads)
msl	mean sea level
na	not applicable
No.	number

precip	precipitation
psf	pounds per square foot
psi	pounds per square inch
Q_{cal}	calculated flow
R	hydraulic radius
P	initial geomembrane OIT value
R	universal gas constant (8.31 j/mol)
RH	polymer chain
$R^\bullet$	free radical
$ROO^\bullet$	peroxide free radical
ROOH	hydroperoxides (i.e., oxidized polymer chains)
s	saturation
S	OIT depletion rate
t	time
t_c	time of concentration
T	test temperature in absolute Kelvin (K)
UV	ultraviolet
V	velocity
vol	volume
wt%	weight percent
y	depth in feet
yr	year

AASHTO   American Association of State Highway and Transportation Officials
ASTM   ASTM International (formerly American Society of Testing and Materials)
ATG   Atmospheric Technologies Group
CCL   compacted clay liners
CD   compact disc
CL   sandy clays with low plasticity
CLM   Central Climatology Site
CLSM   Controlled Low Strength Material
CN   runoff curve number
CPT   Cone Penetrometer
CREAMS   Chemicals, Runoff, and Erosion from Agricultural Management Systems
DISPOSAL CELL   Disposal cell
D&D   Decontamination and Demolition
DRI   Desert Research Institute
GDOT   Georgia Department of Transportation
GCL   Geosynthetic Clay Liner
GRI   Geosynthetic Research Institute
GSA   General Separations Area
HDPE   High Density Polyethylene
HELP   Hydrologic Evaluation of Landfill Performance
HMR   Hydrometeorological Report
HP-OIT   high pressure-oxidative induction time
Instal.   Installation
K_{sat} Saturated Hydraulic Conductivity
LLRW   Low-Level Radioactive Waste
LVZ   Lower Vadose Zone
LS   loamy sand
NCSU   North Carolina State University
NIST   National Institutes of Standards and Technology
NRC   Nuclear Regulatory Commission
NRC-NA   National Research Council of the National Academies
NWS   National Weather Service
OIT   oxidative induction time
ORWBG   Old Radioactive Waste Burial Ground
PA   Performance Assessments
PGA   peak ground acceleration
PMP   probable maximum precipitation
PVC   polyvinyl chloride
QA/QC   quality assurance/quality control
Recirc.   recirculation
Sat. Hyd.   saturated hydraulic
SC   clayey sands
SCL   sandy clay loam
SCS   Soil Conservation Service
SDF   Saltstone Disposal Facility
SL   sandy loams
SM   silty sand

SRL	Savannah River Laboratory
SRNL	Savannah River National Laboratory
SRP	Savannah River Plant
SRS	Savannah River Site
TFBUT	Test Facility – Bentonite Umbrella Test
TIN	Triangulated Irregular Network
USACE	United States Army Corps of Engineers
USCS	Unified Soil Classification System
USDA	United States Department of Agriculture
USEPA	United States Environmental Protection Agency
USGS	United States Geological Survey
WES	Waterways Experiment Station
WSSC	Weathering System Science Consortium
XRD	x-ray diffraction

1.0 EXECUTIVE SUMMARY

The Saltstone Disposal Facility (SDF) closure cap is primarily intended to provide physical stabilization of the site, minimize infiltration, and provide an intruder deterrent. Two separate closure caps are anticipated to be constructed over the SDF Disposal cells at the end of the operational period. The anticipated SDF Closure Cap configuration and infiltration estimates over 10,000 years are provided herein. The approach is patterned after the approach used for the F-Area Tank Farm closure cap infiltration estimates presented in (Phifer et al. 2007).

The infiltration evaluation is based on an SDF closure cap system comprising two separate caps. Such a layout results in a maximum closure cap slope length of approximately 825 ft. This slope length is used as the basis for scoping level calculations conducted to determine closure cap physical stability requirements relative to erosion. The closure cap physical stability requirements (Section 4.2) were determined consistent with Nuclear Regulatory Commission (NRC) requirements relative to erosion potential resulting from a Savannah River Site (SRS) specific probable maximum precipitation (PMP) event (Abt and Johnson 1991 and Johnson 2002). These calculations result in a vegetative soil cover with a maximum 1.5 percent slope over a 825-ft slope length and specified stone sizes and thicknesses for an erosion barrier, side slopes, and toe of the side slopes. Based upon the closure cap layout and the requirements for closure cap physical stability, scoping level closure cap conceptual design and constructability are provided in Sections 4.3 and 4.4.

Based upon this scoping level conceptual design, the Hydrologic Evaluation of Landfill Performance (HELP) Model has been used to produce simulations for infiltration using annual precipitations ranging from approximately 30 to 68 inches/year (Section 5.2). The average infiltration results are shown in Table 1.

A closure cap configuration consisting of a composite hydraulic barrier with an overlaying lateral drainage layer and an erosion barrier is recommended as the SDF Closure Cap (Section 4.0) for the following reasons:
- It results in limited infiltration to the disposal cells.
- Using a composite hydraulic barrier (i.e., high density polyethylene (HDPE) geomembrane underlain by a geosynthetic clay liner (GCL)) provides defense-in-depth by the providing a HDPE geomembrane with a significantly lower saturated hydraulic conductivity underlain by the GCL to plug any holes that may develop in the HDPE geomembrane.
- Using a lateral drainage layer prevents buildup of significant hydraulic head over the composite hydraulic barrier. Head build-up could lead to significantly more infiltration as the composite hydraulic barrier degrades over time.

- Using an erosion barrier provides long-term physical stability for the closure cap. Note: The material to be used to fill the voids between barrier stones has yet to be selected.

Table 1. Summary Infiltration Results

Infiltration Through GCL With Time	
Year After Cap Construction	**Infiltration Through GCL (in/year)**
0	0.00042
100	0.00333
180	0.04520
220	0.05676
300	0.17110
380	0.47236
460	0.72342
560	1.0211
1,000	2.2638
1,800	4.340
3,200	6.795
5,412	10.6
5,600	10.6
10000	10.6

An evaluation of potential SDF Closure Cap degradation mechanisms (Section 6.0) has resulted in the identification of the following mechanisms that cannot be appropriately addressed by design and are considered applicable and significant:
- Vegetative cover succession
- Erosion of upper soil layers
- Silting-in of the lateral drainage layer
- Antioxidant depletion, thermal oxidation, and tensile stress cracking of the HDPE geomembrane
- Divalent cation exchange with the sodium bentonite GCL

The impact of these degradation mechanisms on the SDF Closure Cap (composite barrier, lateral drainage layer, and erosion barrier with sandy soil infill) layers have been estimated in terms of material property changes over time. These estimated degraded material properties over time have been input to HELP model runs (Section 7.0) to produce estimates of infiltration through the closure cap over time. These HELP-model generated infiltration estimates will serve as input to SDF PORFLOW vadose zone modeling. The results of this infiltration modeling are provided in Table 1 and graphically in Figure 1.

SDF Closure Cap Infiltration Through GCL with Time
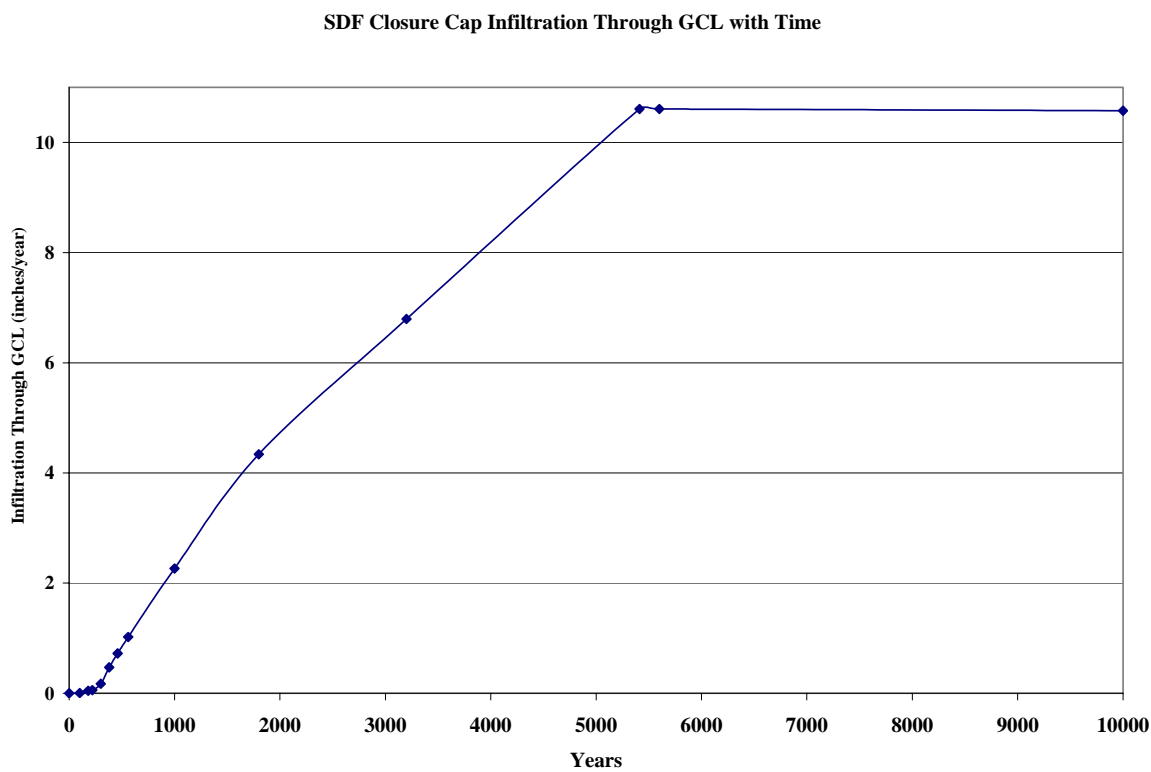
Figure 1.   Results of SDF Infiltration Modeling

The closure cap design and infiltration information provided herein is preliminary and conceptual in nature, being consistent with a scoping level concept. Final design and a re-evaluation of infiltration will be performed near the end of the operational period. During the interim, technological advances, increased knowledge, and improved modeling capabilities are likely, and will result in improvements in both closure cap design and infiltration estimates.

This page intentionally left blank.

2.0 INTRODUCTION

The SDF closure cap is primarily intended to provide physical stabilization of the site, minimize infiltration, and provide an intruder deterrent. Two closure caps are anticipated to be constructed over the SDF disposal cells at the end of the operational period. The operational period is that period of time during which waste will be placed in the disposal cells and the disposal cells will be grouted-up. During the operational period, active SDF facility maintenance sufficient to prevent both infiltration of rainwater into the disposal cells and subsurface discharge out of the disposal cells is assumed. After installation of the closure cap, a 100-year institutional control period is assumed to begin, during which active SDF facility maintenance will be conducted sufficient to prevent pine forest succession and to repair any significant erosion. After the institutional control period, a 10,000-year post-closure compliance period is assumed to begin, during which no active SDF facility maintenance will be conducted. A potential exception to the cessation of all active maintenance during the post-closure compliance period involves using bamboo as a final vegetative cover. If bamboo is determined to be a climax species that prevents or greatly slows the intrusion of pine trees, it is assumed that bamboo will be planted as the final vegetative cover at the end of the 100-year institutional control period. If bamboo is planted, maintenance, which may extend into the post-closure compliance period, will be required to establish a dense bamboo ground cover over the entire area. After such a ground cover has been established, all active SDF facility maintenance will cease. Degradation of the closure cap will accelerate once active SDF facility maintenance has ceased.

Conceptualization of the SDF closure cap, an initial infiltration estimate, and infiltration estimates over 10,000 years are provided herein. The methods and approach follow those used for the F-Area Tank Farm closure cap concept and infiltration estimates (Phifer et al. 2007), which the reader is invited to review for detailed methodology discussion. The closure cap design and infiltration information is preliminary and conceptual in nature, being consistent with a scoping level concept. In other words, it provides sufficient information for planning purposes, to evaluate the closure cap configuration relative to its constructability and functionality, and to estimate infiltration over time through modeling. It is not intended to constitute final design. Final design and a re-evaluation of infiltration will be performed near the end of the operational period. Technological advances, increased knowledge, and improved modeling capabilities are all likely and will result in improvements in both the closure cap design and infiltration estimates.

This page intentionally left blank.

3.0 BACKGROUND

3.1 SDF BACKGROUND

The General Separations Area (GSA) is located atop a ridge running southwest-northeast that forms the drainage divide between Upper Three Runs to the north and Fourmile Branch to the south. The GSA contains the F and H-Area Separations Facilities, the S-Area Defense Waste Processing Facility, the Z-Area Saltstone Facility, and the E-Area Low-Level Waste Disposal Facilities. Drainage in Z Area, which includes the Saltstone Facility, is toward Upper Three Runs, to the northwest to north, and toward McQueen Branch, to the north, east, and southeast.   Figure 2 shows the GSA topography.
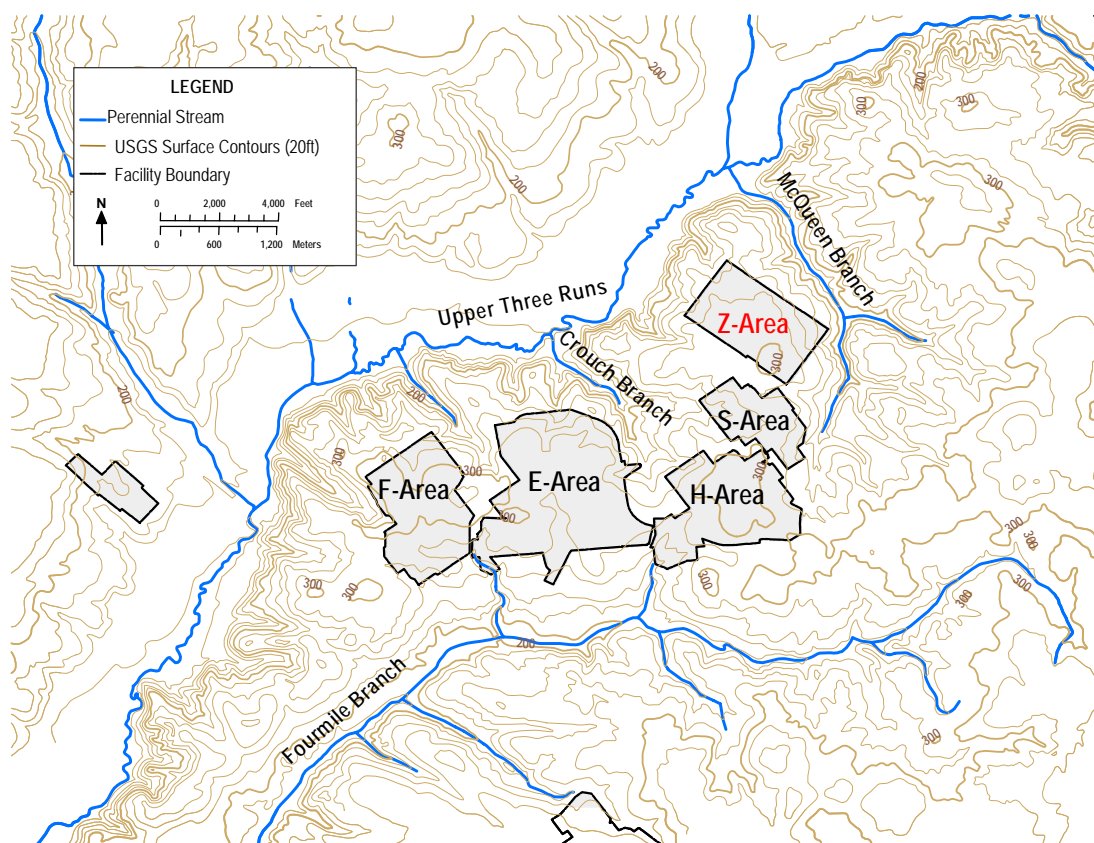
Figure 2.   General Separations Area Topography (from WSRC 2008)

Z Area at SRS, where the SDF is located, consists of approximately 650,000 meters^2 (m^2). The SDF currently includes two disposal cells, and is anticipated to eventually include sixty-six. Figure 3 provides an aerial view of the SDF, with Vaults 1 and 4, Road F, and the Z-Area perimeter road visible. Figure 4 provides an infrared aerial view of the SDF.
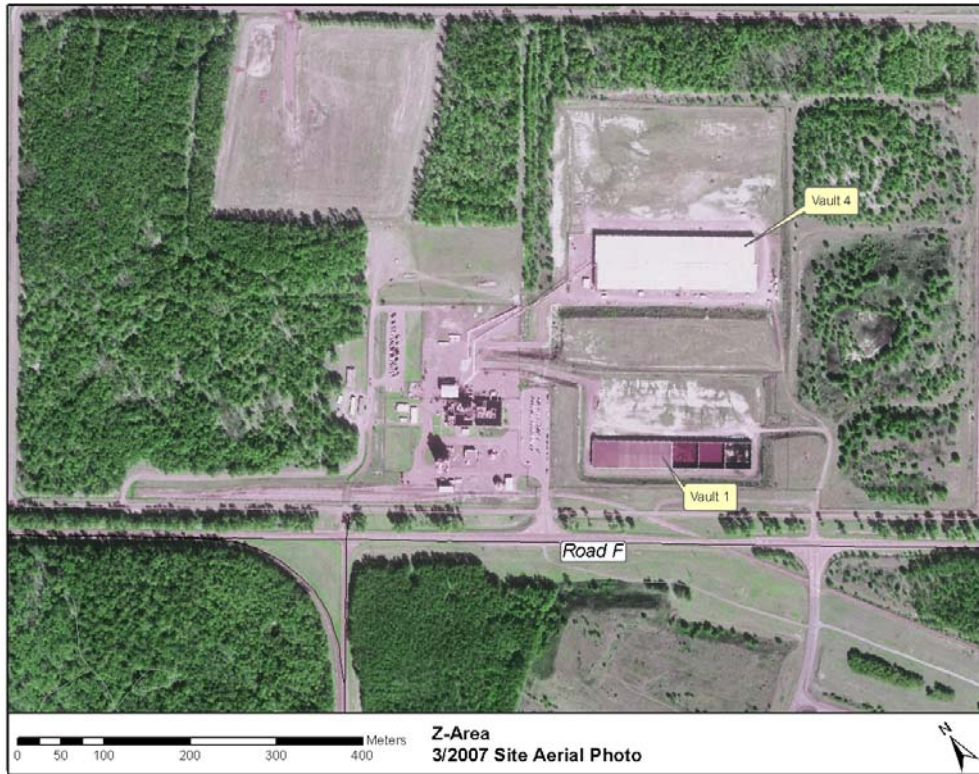
Figure 3. SDF Aerial View

Figure 4. SDF Infrared Aerial View

In general, the future disposal cells will be constructed by digging an excavation and stockpiling the excavated soil, emplacing GCL, overlain by a 100-ml thick High Density Polyethylene (HDPE) geomembrane, overlain by 6-in. thick concrete mudmat on which the disposal cell will be constructed. The stockpiled, excavated native soil will be backfilled around the disposal cells.

Within the SDF a maximum elevation difference of approximately 25 ft is anticipated in the finished grade between disposal cell groupings (between Vault #1 and Group 3). An elevation difference of approximately 45 ft is anticipated between the top of the Vault 1 and Group 3. The Saltstone Processing Facility, located between the northwestern and southeastern general disposal cell areas, will not be covered by either cap, but will undergo deactivation and decommissioning.

Figure 5 provides a layout of the anticipated SDF disposal cell groups and closure cap configurations. Figures 6 and 7 provide closure cap cross-sections. Figure 8 presents a detailed view of the closure cap layered configuration.

This page intentionally left blank.
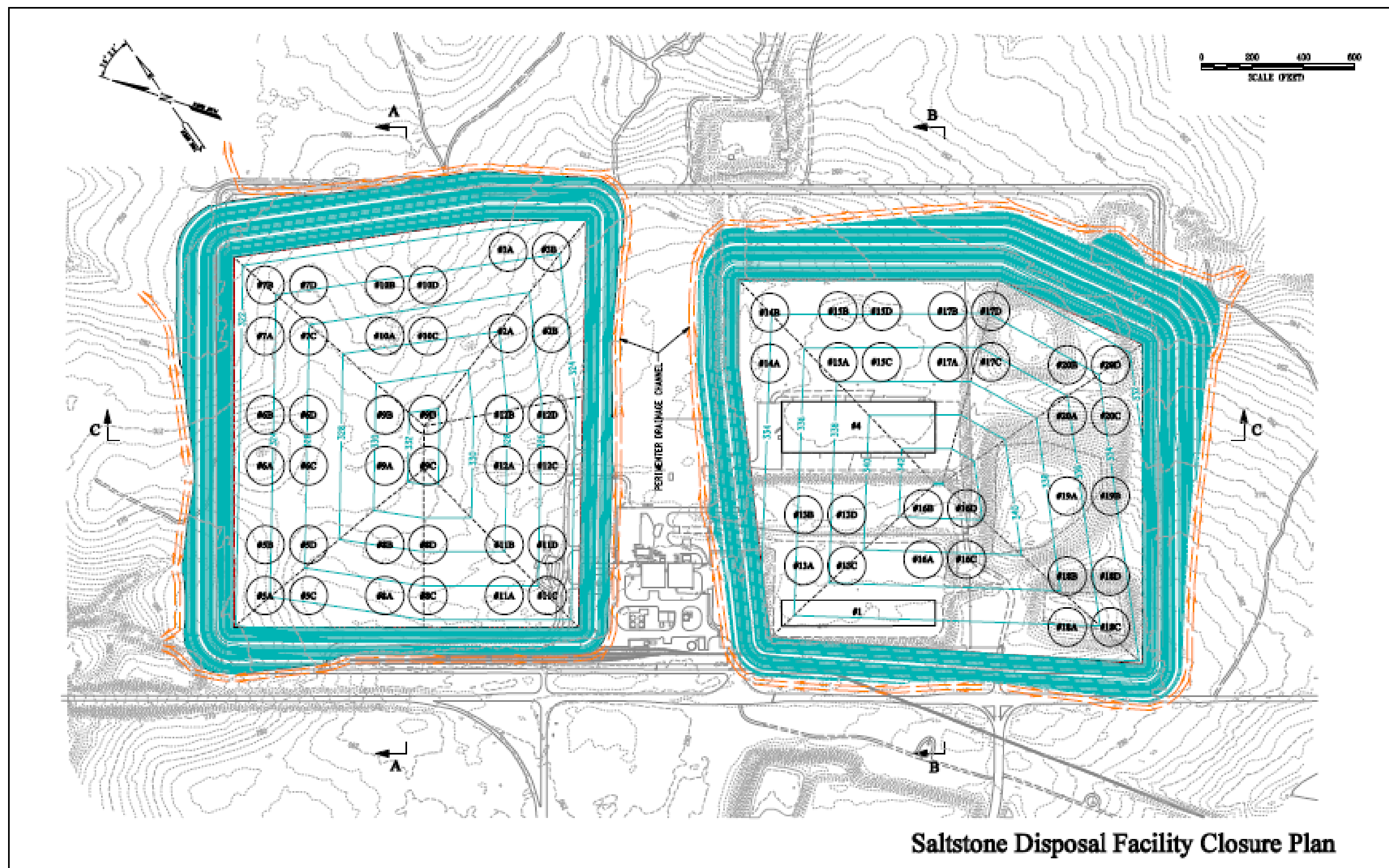
Figure 5. SDF Anticipated Disposal Cell Layout and Cap Configurations

This page intentionally left blank.
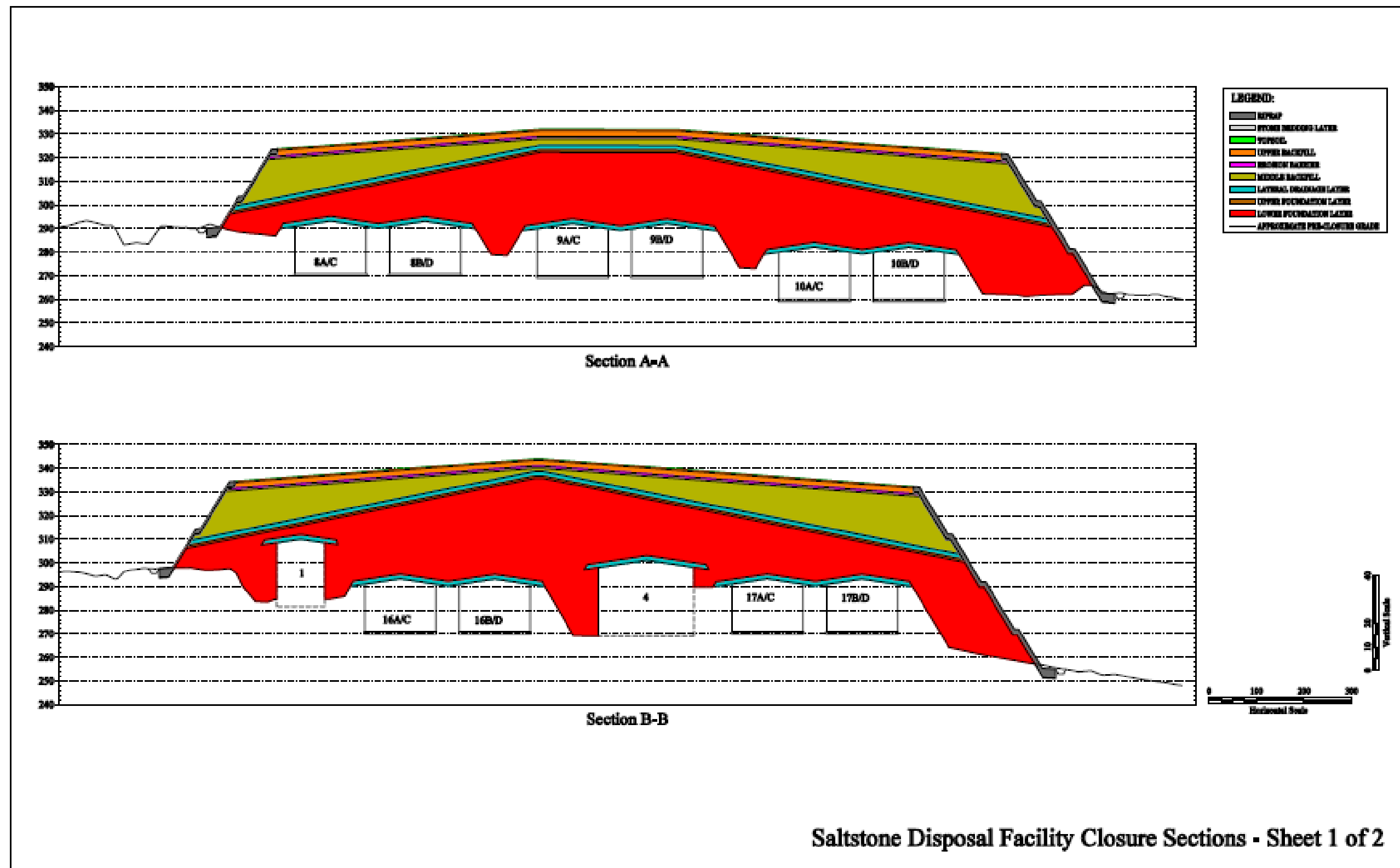
Figure 6.   SDF Anticipated Closure Cap Cross-Sections (1 of 2)

This page intentionally left blank.
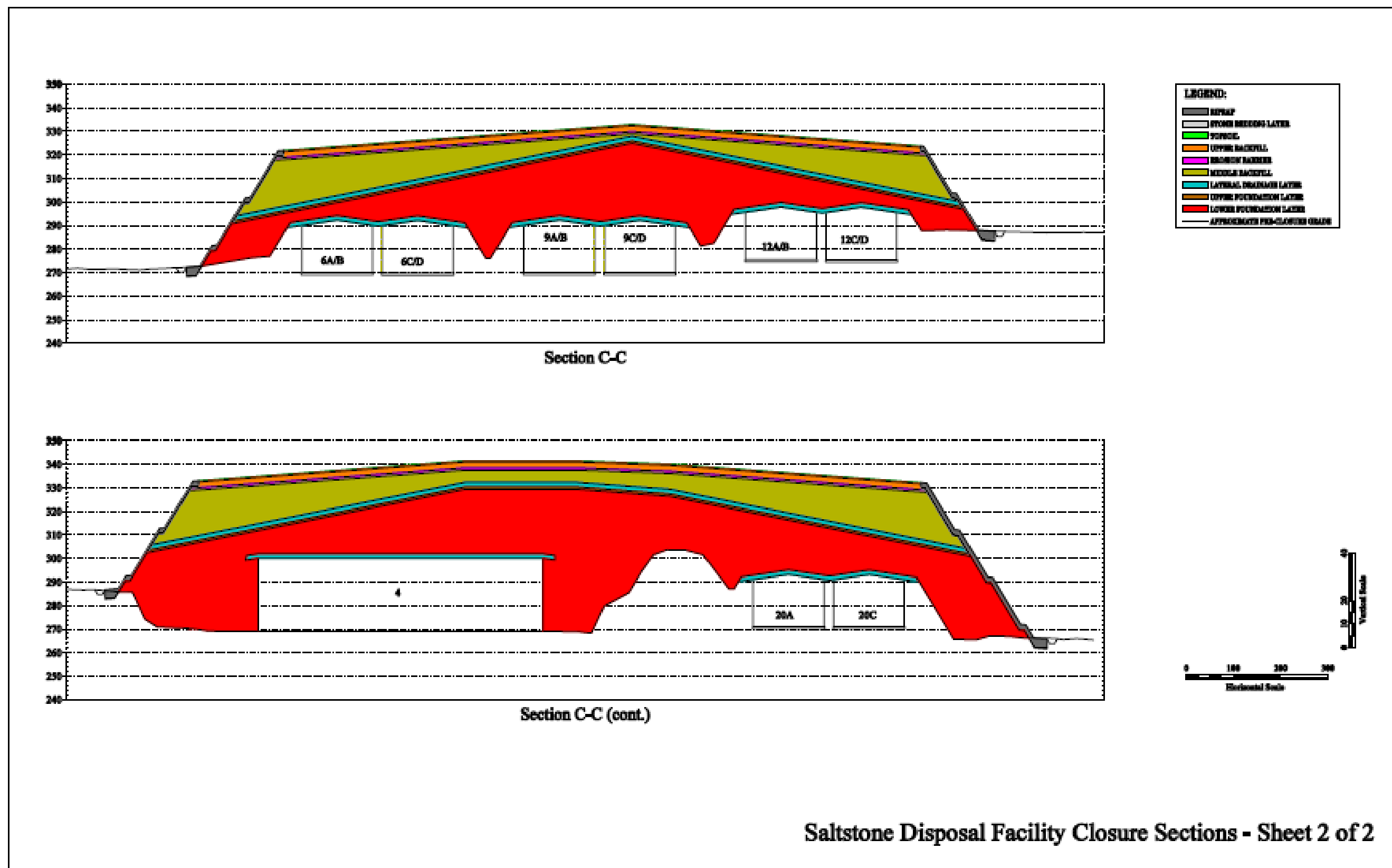
Figure 7. SDF Anticipated Cross-Sections (2 of 2)

This page intentionally left blank.

Typical Saltstone Disposal Facility Closure Cap

Note: Vertical Scale = 5 x Horizontal Scale
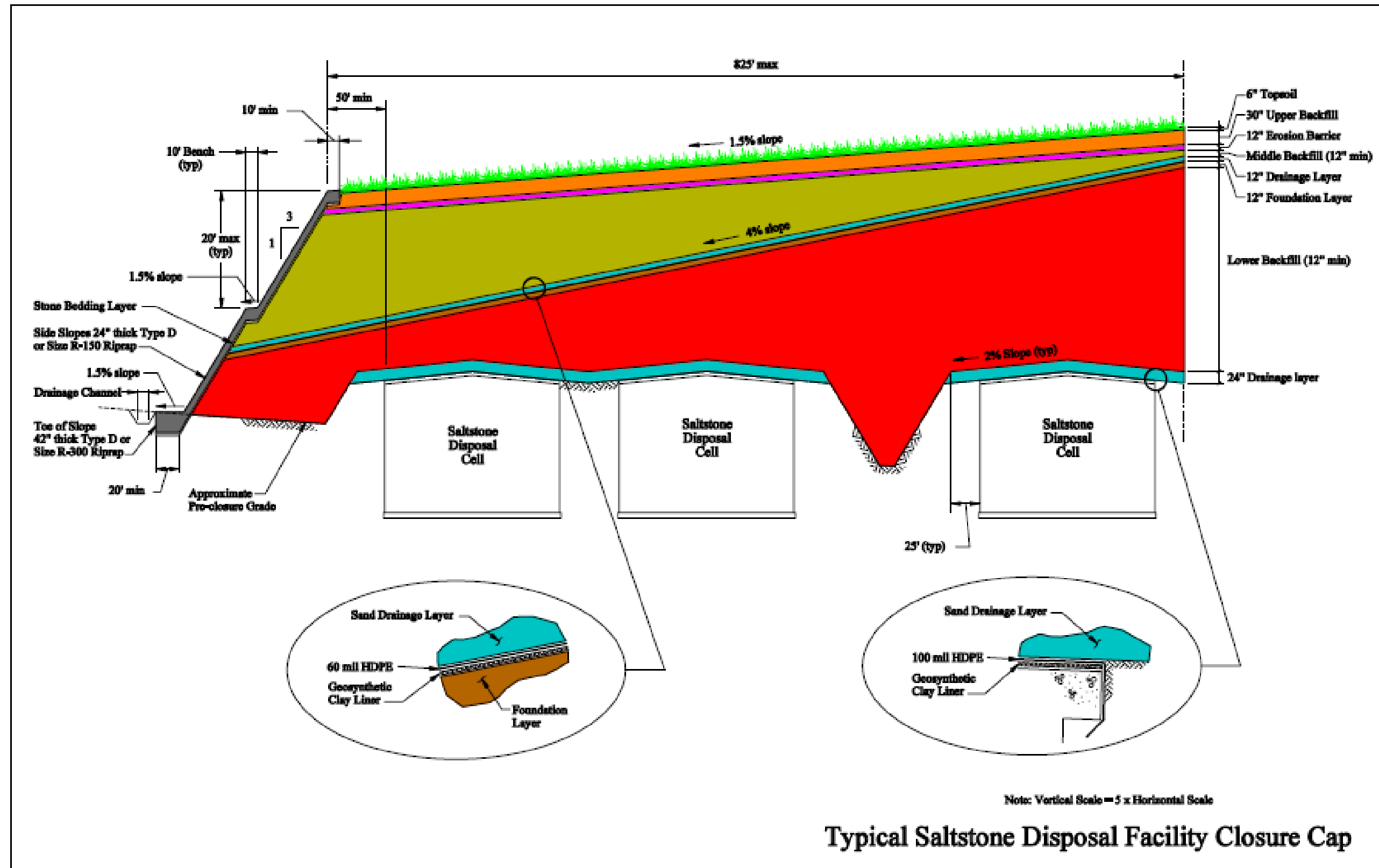
Figure 8. SDF Closure Cap Layers Configuration

This page intentionally left blank.

3.2 BACKGROUND WATER BALANCE AND INFILTRATION STUDIES

Numerous water balance and infiltration studies have been conducted in and around the Savannah River Site (SRS) by various organizations including the Savannah River Laboratory (SRL), the United States Geological Survey (USGS), the State University of New York at Brockport, the Pennsylvania State University, the University of Arizona, and the Desert Research Institute (DRI). Findings from eight such studies are reported in Phifer et al. (2007) and summarized below.

Eight water balance and infiltration studies were evaluated in Phifer et al. (2007). They included both field and modeling studies and ranged in scale from 55-gallon drum lysimeters to entire watersheds. Table 2 provides the nominal water balance and infiltration estimate produced from each of the eight studies based upon nominal or average precipitation. The table provides the median of the nominal water balance values of the eight Studies. As seen in Table 2, the nominal annual infiltration for background conditions (i.e., no closure cap) based upon nominal or average annual precipitation ranges from 9 to 16 inches per year on average.

Table 3 provides the range of values reported by Hubbard and Englehardt (1987) for precipitation ranging from 34.7 to 71.9 inches/year. As seen in Table precipitation is distributed, in decreasing order, into evapotranspiration, infiltration, and runoff. Precipitation is seen to range from 35 to 72 inches/year with a median of the eight studies nominal values of 47.8 inches/year. Evapotranspiration is seen to range from 29 to 36 inches/year with a median of the eight studies nominal values of 31.2 inches/year. Infiltration is seen to range from 5 to 32 inches/year with a median of the eight studies nominal values of 14.8 inches/year. Runoff constitutes very little of the water balance; it is seen to range from 0.1 to 4 inches/year with a median of the Eight studies nominal values of 1.6 inches/year. Clearly evapotranspiration dominates the water balance distribution of precipitation at the SRS.

Table 2. Nominal Water Balance and Infiltration Estimate Produced from each of Eight Studies [1]

Source	Nominal Annual Precipitation (inches/year)	Nominal Annual Runoff (inches/year)	Nominal Annual Evapotranspiration (inches/year)	Nominal Annual Infiltration (inches/year)
Cahill (1982)	46.62	0	31.62	15
Hubbard and Emslie (1984)	47	2	30	15
Hubbard (1986)	48	2	30	16
Parizek and Root (1986)	47.78	2	30.78	15
Hubbard and Englehardt (1987)	48.51	1.21	32.60	14.70
Dennehy and McMahon (1989)	47.8	0	33.5	14.3
Young and Pohlmann (2001)	10-year Augusta, GA data from 1977 to 1987	Assumed to be 0	Determined but not reported within the document [2]	9.1
Young and Pohlmann (2003)	10-year Augusta, GA data from 1977 to 1987	Assumed to be 0	Determined but not reported within the document [2]	11.7
Median of the eight Studies Nominal Values [3]	47.79	1.6	31.2	14.85

[1] All of these studies assumed that the change in water storage was a minor water budget component

[2] Based upon the infiltration estimates, the associated evapotranspiration estimates would have had to be relatively high (at least in the 30s of inches/year range).

[3] The median of the eight studies nominal values does not include precipitation, runoff, and evapotranspiration from Young and Pohlmann (2001 and 2003)

Table 3. Hubbard and Englehardt (1987) Water Balance Range

Parameter	Precipitation (inches/year)	Runoff (inches/year)	Evapotranspiration (inches/year)	Infiltration (inches/year)
Range	34.7 to 71.9	0.1 to 4.1	29.1 to 35.9	5.0 to 32.1

4.0 SDF CLOSURE CAP SCOPING LEVEL CONCEPT

The SDF closure cap is primarily intended to provide physical stabilization of the site, to minimize infiltration, and to provide an intruder deterrent. Final closure will consist of site preparation and construction of an integrated closure system composed of one or more closure caps installed over all the disposal cells, and construction of a drainage system at the end of the operational period. The closure cap design and installation will take into account disposal cell characteristics and location, disposition of non-disposal structures and utilities, site topography and hydrogeology, potential exposure scenarios, and lessons learned implementing other closure systems, including other SRS facilities and Uranium Mill Tailings sites.

The SDF is currently in the construction-operational period, during which the disposal cells will be constructed and waste will be placed. The operational period is anticipated to last through 2030 (WSRC 2007). The closure cap information provided herein is consistent with the level of detail associated with a scoping level concept. That is, this report provides sufficient information for planning purposes and to evaluate the closure cap configuration relative to its constructability and functionality, but it is not intended to constitute final design. Final design will not be performed until near the end of the operational period prior to actual installation of the closure cap. Technological advances in materials and closure cap design may necessitate that changes to the SDF closure cap concept discussed herein be made at the time of final design. Additionally as more material property data become available, the material property data used for modeling will be updated to be consistent with the advances in knowledge. Any such changes will be considered acceptable so long as the overall closure cap performance is equivalent to or better than that discussed herein in terms of site physical stabilization, infiltration minimization, and the provision of an intruder deterrent. An independent Professional Engineer will be retained by SRS to certify that the SDF closure system has been constructed in accordance with the approved closure plan and the final drawings, plans, and specifications at the time of closure.

4.1 SDF CLOSURE CAP SCOPING LEVEL LAYOUT

A scoping level evaluation of the SDF closure cap layout was conducted in order to determine the following: the maximum slope length that should be considered for the closure cap physical stability conceptualization and for determination of the infiltration through the closure cap.

4.1.1 Closure Cap Layout Scenario:

The initial closure cap layout evaluated was that of a "C"-shaped closure cap covering the northern and southern Disposal cell areas, with the hollow of the "C" in the process buildings area. The larger, northern area was used to determine that the most likely construction scenario, including a cap with longest slopes running to the northeast and southwest from a central northwest-southeast oriented peak. The longest cap surface-slopes were estimated at

825 ft. with the length of the peak, or cap apex, 1,380 ft (Figure 9). The cap for the southern Disposal cell area was not anticipated to be any larger than that of the northern area, so infiltration for a second cap would be expected to be no greater than the scenario modeled herein.

Upon completion of a detailed cap-configuration drawing based on the earlier C-shaped disposal cell configuration presented in Figure 9, it was determined that relocating some of the anticipated disposal cell locations would allow both the previously assumed maximum 825-ft surface slope length and a more functional drainage system.

Figure 9. Closure Cap Layout Scenario to Determine Slope Length[1]
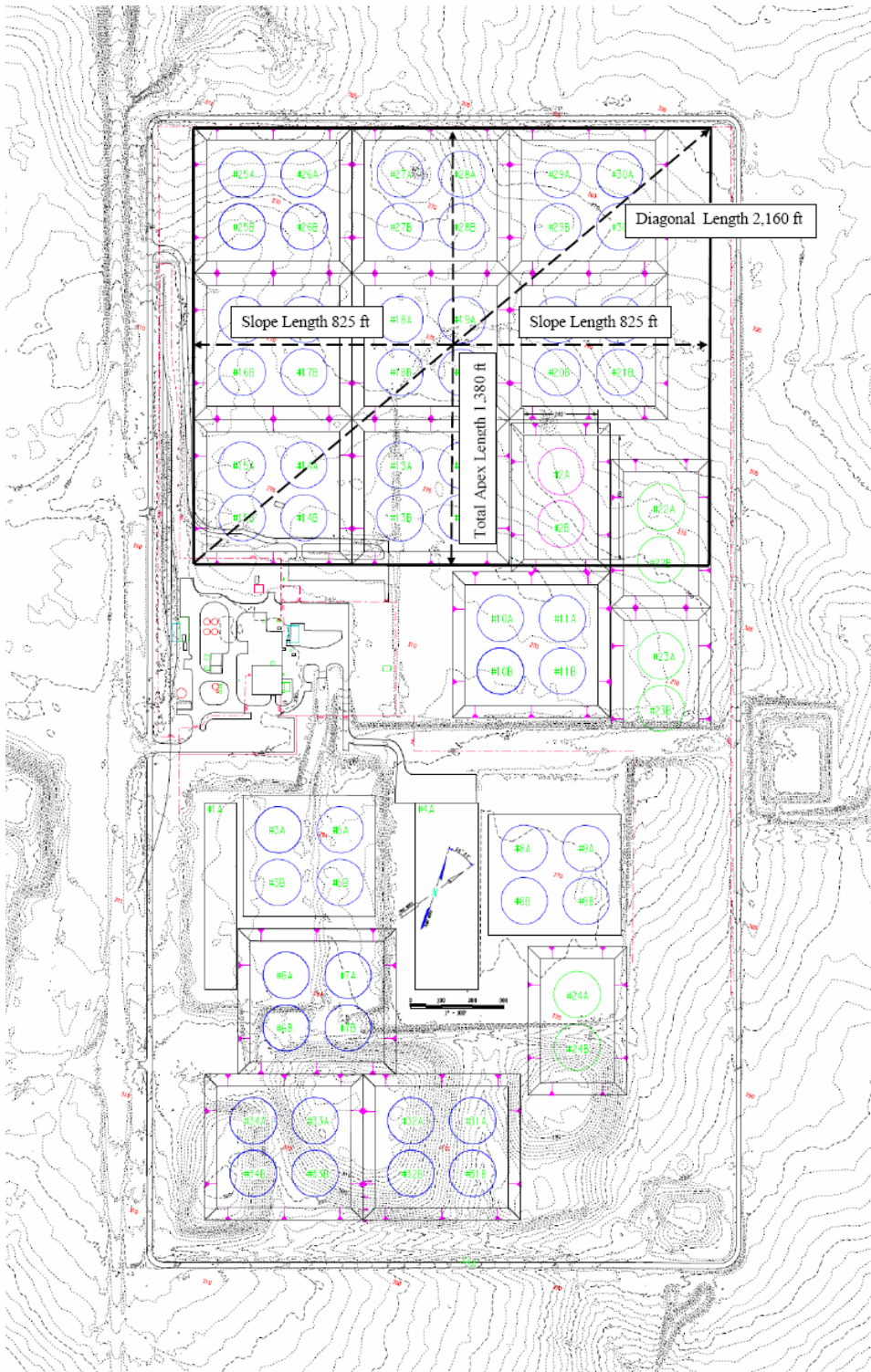
[1]Note this older layout has been modified. See Figure 5 for current layout.

4.2 SDF CLOSURE CAP SCOPING LEVEL PHYSICAL STABILITY REQUIREMENTS

Scoping level calculations have been made in order to determine closure cap requirements for physical stability. The calculations have been made consistent with Abt and Johnson (1991) and Johnson (2002) to assess physical stability requirements relative to erosion potential resulting from a SRS-specific probable maximum precipitation (PMP) event over a maximum 825-ft slope length (see Section 4.1). A PMP is defined as the theoretically greatest depth of precipitation for a given duration that is physically possible over a given storm size area at a particular geographic location. Stability calculations for the following key components of the closure cap are provided in detail in Appendix A:

- Vegetative soil cover
- Erosion barrier
- Side slope
- Toe of the side slope

As discussed in detail in Appendix A these calculations resulted in the following conclusions:

- A 1.5 percent slope over a 825-ft slope length for the vegetative soil cover is considered physically stable (i.e. prevents the initiation of gullying during a PMP event). Maximum acceptable slopes for portions of the closure cap with slope lengths less than 825 ft may be greater than 1.5 percent, if it is determined that they are physically stable during the actual closure cap design process.
- An erosion barrier consisting of 12-in thick riprap with a D_{50} (median size) of 2.5 in on a 825-ft long, 1.5 percent slope is considered physically stable (i.e. prevents any riprap movement during a PMP event). Based upon the D_{50} of 2.5 in, rock consistent with Type B riprap from Table F-3 of Johnson (2002) or Size R-20 riprap from Table 1 of ASTM (1997) is suitable for use in the erosion barrier.
- Side slope riprap that is 24 in thick with a D_{50} (median size) of 10.1 in on a 300-ft long, 33.3 percent slope receiving drainage from a 825-ft long, 1.5 percent slope is considered physically stable (i.e. prevents any riprap movement during a PMP event). Based upon the D_{50} of 10.1 in, rock consistent with Type D riprap from Table F-3 of Johnson (2002) or Size R-150 riprap from Table 1 of ASTM (1997) is suitable for use on the side slopes.
- Toe of the side slope riprap that is 42 in thick, extends out 20 ft from the side slope, and has a D_{50} (median size) of 12.82 in is considered physically stable (i.e., prevents any riprap movement due to receiving runoff from the 1.5 percent, 825-ft top slope and 33.3 percent, 300-ft side slope during a PMP event). Based upon the D_{50} of 112.82 in, rock consistent with Type D riprap from Table F-3 of Johnson (2002) or Size R-300 riprap from Table 1 of ASTM (1997) is suitable for use on the toe.

Erosion barrier, side slope, and toe riprap size may be smaller for portions of the closure cap with shorter slope lengths than those used to determine the requirements outlined above, if it is determined that the smaller sized riprap is stable versus a PMP event during the actual closure cap design process.

4.3 SDF CLOSURE CAP SCOPING LEVEL LAYERS AND FUNCTIONALITY

It is anticipated that the SDF closure cap will consist of the layers outlined in Table 4 from top to bottom. Table 5 provides an overview of the function of each of these layers. Figures 8 and 10 present scoping concepts for the cap layers. Figures 8 and 11 presents scoping concepts for side slopes and toes of the closure cap based upon Section 4.2.

Table 4. Generic SDF Closure Cap Layers

Layer [1]	Layer Thickness (in)
Vegetative Cover	Not applicable
Topsoil	6
Upper Backfill	30
Erosion Barrier	12
Geotextile Fabric	-
Middle Backfill	12 (minimum, will increase from cap apex to toe due to difference between surface slope and upper drainage layer slope)
Geotextile Filter Fabric	-
Upper Lateral Drainage Layer	12
Geotextile Fabric	-
High Density Polyethylene (HDPE) Geomembrane	0.06 (60 mil)
Geosynthetic Clay Liner (GCL)	0.2
Foundation Layer (backfill with bentonite admix)	12
Lower Backfill Layer	12 (minimum, will increase from cap toe to apex due to upper drainage layer slope)
Geotextile Filter Fabric	-
Lower Drainage Layer (above each disposal cell, extends approximately 25-ft from disposal cell)	24

Based upon Phifer and Nelson 2003 Table 4.7-1 with the addition of the HDPE geomembrane

[1] The layers are arranged in the table to reflect their order from top to bottom in the SDF Closure Cap. Detailed explanations of the layers are provided in the text.

Table 5. Function of the SDF Closure Cap Layers

Layer	Function
Vegetative Cover	The vegetative cover will be established to promote runoff, minimize erosion, and promote evapotranspiration. The initial vegetative cover will be a persistent grass such as Bahia. If it is determined that bamboo is a climax species that prevents or greatly slows the intrusion of pine trees, bamboo will be planted as the final vegetative cover at the end of the 100-year institutional control period.
Topsoil	The topsoil will be designed to support a vegetative cover, promote runoff, prevent the initiation of gullying, and provide water storage for the promotion of evapotranspiration.
Upper Backfill	The upper backfill will be designed to increase the elevation of the closure cap to that necessary for placement of the topsoil and to provide water storage for the promotion of evapotranspiration.
Erosion Barrier	The erosion barrier will be designed to prevent riprap movement during a PMP event and therefore form a barrier to further erosion and gully formation (i.e. provide closure cap physical stability). It will be used to maintain a minimum 10 ft of clean material above the disposal cells to act as an intruder deterrent. It will also act to preclude burrowing animals from access to underlying closure cap layers. It also provides minimal water storage for the promotion of evapotranspiration.
Geotextile Fabric	This geotextile fabric will be designed to prevent the penetration of erosion barrier stone into the underlying middle backfill and to prevent piping of the middle backfill through the erosion barrier voids.
Middle Backfill	The middle backfill will provide water storage for the promotion of evapotranspiration in the event that the topsoil and upper backfill are eroded away since the overlying erosion barrier provides only minimal such water storage.
Geotextile Filter Fabric	This geotextile fabric will be designed to provide filtration between the overlying middle backfill layer and the underlying lateral drainage layer. This filtration will allow water to freely flow from the middle backfill to the lateral drainage layer while preventing the migration of soil from the middle backfill to the lateral drainage layer.
Upper Lateral Drainage Layer	The upper lateral drainage layer will be a 1-ft thick coarse sand layer designed to: • Divert infiltrating water away from the underlying disposal cells and transport the water to the perimeter drainage system, in conjunction with the underlying composite hydraulic barrier (i.e., HDPE geomembrane and GCL), and • Provide the necessary confining pressures to allow the underlying GCL to hydrate properly.

Table 5.   Function of the SDF Closure Cap Layers **- continued**

Layer	Function
Geotextile Fabric	This geotextile fabric will be a nonwoven geotextile fabric designed to protect the underlying HDPE geomembrane from puncture or tear during placement of the overlying lateral drainage layer.
HDPE Geomembrane	The high density polyethylene (HDPE) geomembrane will form a composite hydraulic barrier in conjunction with the GCL. The composite hydraulic barrier will be designed to promote lateral drainage through the overlying lateral drainage layer and minimize infiltration to the disposal cells.
GCL	The Geosynthetic Clay Liner (GCL) will form a composite hydraulic barrier described above in conjunction with the HDPE geomembrane. As part of the composite hydraulic barrier the GCL is designed to hydraulically plug any holes that may develop in the HDPE geomembrane.
Foundation Layer	Provide structural support and required contours for slope of 4 percent for overlying layers. Provide relatively low-permeability layer directly above lower backfill.
Lower Backfill	The foundation layer will be designed to: • Provide structural support for the rest of the overlying closure cap, • Produce the required contours and produce a slope of 4 percent for the overlying layers, • Produce the maximum 3:1 side slopes of the closure cap, • Provide a suitable surface for installation of the GCL (i.e. a soil with a moderately low permeability and a smooth surface free from deleterious materials), • Promote drainage of infiltrating water away from and around the disposal cells, and • Contain utilities, facilities, etc. that are not removed from above current grade prior to installation of the closure cap.
Lower Drainage Layer	Located above each disposal cell and extending approximately 25 ft beyond each cell's roof edge, function is primarily to prevent buildup of hydraulic head on top of the disposal cells. The portion of this drainage layer extending beyond each disposal cell roof edge will be constructed atop backfill material.

Saltstone Closure Cap Configuration (not to scale)

Detail A

Multilayered Closure Cap System

Native Soil Backfill

Saltstone Disposal Cell

Saltstone Disposal Cell

Detail B

Undisturbed Native Soil

Detail C

100-mil HDPE

Minimum 8 inch thick concrete walls

Lean Concrete

Minimum 8 inch thick concrete floor slab

~0.2 inches Geosynthetic Clay Liner (not on vertical portion of wall)

Minimum 4 inch thick mudmat (same concrete as floor slab)

Minimum 6 inch thick mudmat

Detail C (not to scale)

Maximum Cap Surface Slope Length 825 feet; Slope 1.5%

Topsoil (6 inches)

Backfill (2.5 feet)

Erosion Barrier (1 foot)

Backfill (1 foot Min.), Thickening Outward

Sand Drainage Layer (1 foot), Slope 4%
HDPE 60 mil, Slope 4%
Geosynthetic Clay Layer (0.2 inches) Slope 4%

Foundation Layer (Backfill/Bentonite Blend, 1 foot)

Backfill (thickness varies, 1 foot Min.)

12 foot Min.

Sand Drainage Layer (2 foot), Slope 2% over Disposal Cell

Detail A (not to Scale)

~0.2 inches Geosynthetic Clay Liner

100-mil HDPE

Minimum 2% Slope

Minimum 8 inch thick concrete roof

Lean Concrete

Minimum 8 inch thick concrete walls

100-mil HDPE

Detail B (not to scale)

Figure 10.   Generic SDF Closure Cap and Disposal Cell Configuration

Vegetative Soil Cover on maximum 1.5% slope (3-foot thick)

10-foot (minimum)

Side Slope on maximum 3H:1V slope (benches not shown; 2-foot thick, Type D or Size R-150 riprap)

Toe of Side Slope (42-inches thick, Type D or Size R-300 riprap)

Stone Bedding Layer

Erosion Control Barrier on maximum 4% slope (1-foot thick, Type B or Size R-20 riprap)

20-foot (minimum)

Note: Not all closure cap layers are shown

NOT TO SCALE

Figure 11.   Generic Closure Cap Side Slope and Toe Configuration

4.4 SDF CLOSURE CAP SCOPING LEVEL DESIGN AND CONSTRUCTABILITY

Scoping level design and construction information associated with each of the Table 4 closure cap layers and for the side slopes and toes are provided in the following discussion.

Site preparation will be required to prepare the SDF area for installation of the closure cap. The exact nature of such site preparation has not yet been determined; however it will need to address the following:

- Above grade structures, utilities, etc. that could interfere with closure cap construction, and
- Existing surfaces (i.e. soils, asphalt, riprap, disposal cells, etc.) over which the closure cap will be constructed.
- Placement of GCL, HDPE, and geotextile fabric layers on each disposal cell prior to placement of lower drainage layer above each cell. The HDPE above each cell will be welded to the HDPE on that cell's sides

It is also anticipated that the Saltstone Production Facility, along with above grade structures, utilities, etc. that could interfere with closure cap construction will be removed from the SDF area prior to installation of the closure cap.

The existing surfaces (i.e., soils and riprap) over which the closure cap will be constructed must be prepared prior to closure cap construction. It is anticipated that existing soil surfaces will have 3 to 6 in of soil removed to eliminate any topsoil and vegetation present, will be rough graded to establish a base elevation, and compacted with a vibratory roller. Existing riprap is anticipated to be removed or the voids within the existing riprap surfaces will be filled to eliminate subsidence potential.

Preparation Above Each Disposal Cell
Each disposal cell will be prepared for placement of that cell's lower drainage layer by placing layers of GCL, HDPE, and geotextile fabric directly each disposal cell. The disposal cell tops will require all penetrations be sealed appropriately with material consistent with the Class 3 sulfate resistant concrete roof. Additionally, a smooth surface free of material which could be deleterious to the overlying GCL/HDPE will be required.

The GCL, HDPE, and geotextile fabric placed directly above each disposal cell are not contiguous across the closure cap, and therefore not part of the closure cap per se. They are described here because they are within the cap and exist to minimize infiltration to the disposal cell.

A GCL will be placed directly on top of each disposal cell. The GCL will form a composite hydraulic barrier in conjunction with an overlying HDPE geomembrane described below. The composite hydraulic barrier will be designed to promote lateral drainage through the overlying lower lateral drainage layer and to minimize infiltration to the underlying disposal cell. As part of the composite hydraulic barrier the GCL is designed to hydraulically plug any holes that may develop in the HDPE geomembrane. The GCL shall have a minimum dry weight of sodium bentonite of 0.75 lbs/ft^2 and a "maximum through plane" saturated hydraulic conductivity of 5.0E-9 cm/s. The GCL shall conform to the requirements of GRI 2005. The GCL shall be obtained from the manufacturer in rolls, which are on the order of 15 ft wide by 150 ft long. The GCL rolls shall be stored flat and kept dry. A separate GCL shall be placed directly on top of each disposal cell, which would have a smooth surface free from deleterious materials for GCL placement. Placement of the rolls of GCL shall consist of unrolling the GCL roll per the manufacturer's directions directly onto the surface of each disposal cell, producing a GCL panel.

An HDPE geomembrane will be placed directly on top of the GCL overlying each disposal cell. The HDPE geomembrane will form a composite hydraulic barrier in conjunction with the GCL described above. The composite hydraulic barrier will be designed to promote lateral drainage through the overlying lower lateral drainage layer and to minimize infiltration to the underlying disposal cell. The HDPE is considered the primary hydraulic barrier with the GCL acting as a secondary hydraulic barrier by plugging any holes that may develop in the geomembrane.

The geomembrane shall be 100-mils thick (minimum) and shall conform to the requirements of GRI (2003). The geomembrane shall be obtained from the manufacturer in rolls, which are on the order of 22 ft wide by 500 ft long or greater. The geomembrane rolls shall be stored flat; kept dry; protected from puncture, abrasions, and excessive dirt; and protected from ultraviolet light exposure. Each geomembrane roll shall be numbered and a panel placement plot plan shall be developed that minimizes the total length of field seaming required and maximizes the length of seams oriented down slope versus those across slope. Placement of the geomembrane rolls shall consist of unrolling the geomembrane roll down slope per the manufacturer's directions directly onto the surface of the GCL producing a geotextile panel. Adjacent geomembrane panels shall be overlapped a minimum of 6-in and seamed using either extrusion welding or hot wedge welding methods per the manufacturer's directions. A quality assurance plan shall be developed and implemented that incorporates the following: 100-percent visual inspection of all rolls as they are laid down and of all seams; appropriate wrinkle control measures as the rolls are laid down, seamed, and covered; 100-percent non-destructive field testing of all seams by vacuum testing (ASTM 2006a) and/or air pressure testing (ASTM 2006b); and destructive testing (ASTM 2006c) on a frequency consistent with GRI (1998). Any seam or non-seam area that has been identified as defective and any holes created for destructive testing shall be repaired and non-destructively tested prior to acceptance. The emplaced geomembrane panels shall be held down with sandbags or approved equivalent that will not damage the geomembrane until replaced with the overlying geotextile fabric and sand layer to prevent wind uplift of the geomembrane. (USEPA 1989; Koerner 1990) All work in association with placement of the geomembrane shall be performed in accordance with the approved drawings, plans, and specifications of the final design, which will be produced near the end of the operational period.

A nonwoven geotextile fabric will be placed directly on top of the HDPE geomembrane to protect it from puncture or tear during placement of the overlying 2-ft thick coarse sand, lower lateral drainage layer. The geotextile shall be selected primarily for its puncture and tear resistance and shall conform to the requirements of GRI (2002). The geotextile shall be obtained from the manufacturer in rolls, which are on the order of 15 ft wide by 300 ft long or greater. Placement of the rolls of geotextile shall consist of unrolling the geotextile roll down slope per the manufacturer's directions directly onto the surface of the HDPE geomembrane producing a geotextile panel. Adjacent geotextile panels shall be seamed using heat seaming or stitching methods per the manufacturer's directions in a manner that does not damage the underlying GCL and HDPE geomembrane. The emplaced geotextile panels shall be held down with sandbags or an approved equivalent until replaced with the overlying sand layer to prevent wind uplift of the geotextile. The emplaced geotextile panels shall not be exposed to direct sunlight for more than 7 days prior to placement of the overlying sand layer. The emplaced geotextile shall be inspected for rips, tears, wrinkling, and displacement prior to placement of the sand layer on top of it. Any rips, tears, wrinkling, and displacement shall be repaired per the manufacturer's directions prior to placement of the sand layer on top of it. The overlying sand layer shall be placed in a single 2-ft lift on top of the combined GCL, HDPE geomembrane, and geotextile fabric per the manufacturer's directions in order to avoiding damaging the GCL and HDPE geomembrane. No equipment used to place the sand shall come into direct contact with the GCL, HDPE geomembrane, or geotextile fabric. (Koerner 1990 Section 2.11; ASTM 1988)

All work in association with placement of this geotextile filter fabric shall be performed in accordance with the approved drawings, plans, and specifications of the final design, which will be produced near the end of the operational period.

The following pages provide detailed information regarding the purpose, design, and constructability of each of the SDF closure cap layers. Layers are discussed in order of their placement (i.e., from bottom to top of the closure cap) beginning with the foundation layer and ending with the vegetative cover.

4.4.1 Lower Drainage Layer Above Each Disposal Cell

A drainage layer will be placed over the combined GCL/HDPE geomembrane, and geotextile fabric overlying each disposal cell. This lower drainage layer will extend approximately 25-ft from each disposal cell, draining to the backfill material that will be placed adjacent to the disposal cells rather than "daylighting" and draining outside the closure cap. The lateral drainage layer will be designed to:

- Divert infiltrating water away from the underlying disposal cells and transport the water beyond each disposal cell perimeter in conjunction with the underlying composite hydraulic barrier (i.e., HDPE geomembrane and GCL), and
- Provide the necessary confining pressures to allow the underlying GCL to hydrate properly.

The lower lateral drainage layer will be sloped at the same slope as the disposal cell roof (i.e., 2 percent slope). The lower lateral drainage layer will be hydraulically connected to the foundation layer (lower backfill) in order to divert and transport as much infiltrating water as possible away from the underlying waste tanks. The lateral drainage layer shall consist of a 2-ft thick layer of coarse sand with a minimum saturated hydraulic conductivity of 5.0E-02 cm/s and that is free of any materials deleterious to the underlying GCL, HDPE geomembrane, and geotextile fabric or overlying geotextile fabric. The sand layer shall be placed in a single 2-ft lift on top of the GCL, HDPE geomembrane, and geotextile fabric per the GCL and HDPE geomembrane manufacturer's directions in order to avoiding damaging the GCL and HDPE geomembrane. The sand layer will be fine graded to the required contours. No equipment used to place the sand shall come into direct contact with the GCL, HDPE geomembrane, and geotextile fabric; the equipment used to place and fine grade the sand shall be low ground pressure equipment that is driven on top of the previously placed foot thick sand layer. No compaction effort shall be applied to the sand layer other than that provided by the equipment used to place and fine grade it. All work in association with placement of the drainage layer shall be performed in accordance with the approved drawings, plans, and specifications of the final design, which will be produced near the end of the operational period.

4.4.2 Lower Backfill

A lower backfill layer will be placed adjacent to and over the lower drainage layer associated with each disposal cell after site preparation (see Section 4.4). The lower backfill layer will be designed to:

- Provide structural support for the rest of the overlying closure cap,
- Produce the required contours and a slope of 4 percent for the overlying GCL, HDPE, and Upper Drainage Layer,
- Produce the maximum 3:1 side slopes of the closure cap,
- Provide a suitable surface for installation of the overlying GCL (i.e.,. a soil with a moderately low permeability and a smooth surface free from deleterious materials),
- Promote drainage of infiltrating water away from and around the disposal cells

The thickness of the lower backfill layer will vary (thickening inward from cap perimeter toward cap peaks), but in all cases it will have a minimum thickness of 1 ft (12 in) over all disposal cells.

4.4.3 Foundation Layer

The 1-ft thick foundation layer overlying the lower backfill layer will consist of soil with a moderately low permeability (i.e., ≤1.0E-06 cm/s) and a smooth surface free from deleterious materials suitable for installation of the GCL. It is anticipated that the foundation layer will consist of typical SRS backfill soil blended with a small weight percent bentonite to achieve the moderately low permeability (i.e., ≤1.0E-06 cm/s) and that it will be placed similar to that described for the middle backfill. The top lift of the foundation layer, upon which the GCL will be placed, shall be proof-rolled with a smooth drum roller to produce a surface satisfactory for placement of the GCL. It is anticipated that the foundation layer below the upper one foot will be control compacted backfill, placed similar to that described for the middle backfill, however the exact requirements for this portion of the layer, primarily in terms of its drainage, have not yet been determined. The maximum thickness of the foundation layer will be 1 ft.

4.4.4 Geosynthetic Clay Liner (GCL) Atop the Finished Foundation Layer

A GCL will be placed directly on top of the finished foundation layer (lower backfill) at a slope of 4 percent. The GCL will form a composite hydraulic barrier in conjunction with an overlying HDPE geomembrane described below. The composite hydraulic barrier will be designed to promote lateral drainage through the overlying lateral drainage layer and to minimize infiltration to the disposal cells. As part of the composite hydraulic barrier the GCL is designed to hydraulically plug any holes that may develop in the HDPE geomembrane. The GCL shall have a minimum dry weight of sodium bentonite of 0.75 lbs/ft^2 and a "maximum through plane" saturated hydraulic conductivity of 5.0E-9 cm/s. The GCL shall conform to the requirements of GRI 2005. The GCL shall be obtained from the manufacturer in rolls, which are on the order of 15-ft wide by 150-ft long. The GCL rolls shall be stored flat and kept dry. The GCL shall be placed directly on top of the foundation layer, which would have been appropriately prepared to produce a smooth surface free from deleterious materials for GCL placement. Placement of the rolls of GCL shall consist of unrolling the

GCL roll per the manufacturer's directions directly onto the surface of the foundation layer producing a GCL panel.

The GCL shall not be placed during periods of precipitation or under other conditions that could cause the bentonite to hydrate prematurely (i.e., prior to placement of the HDPE geomembrane and a minimum of 1 ft of sand on top of it). GCL panels shall be overlapped a minimum 12 in on panel edges and a minimum of 18 in on panel ends (Koerner and Koerner 2005). Only portions of the GCL containing bentonite shall be considered as part of the minimum required overlap. Portions of the GCL consisting of the geotextile only shall not be counted as part of the required minimum overlap. Loose granular bentonite shall be placed between overlapping panels at a rate of ¼ pound per linear foot. The GCL shall be inspected for rips, tears, displacement, and premature hydration prior to placement of the overlying HDPE geomembrane and sand. Any rips, tears, displacement, and premature hydration shall be repaired per the manufacturer's directions prior to placement of the HDPE geomembrane, geotextile fabric, and 1-ft coarse sand lateral drainage layer on top of it.

At the end of each working day, the uncovered edge of the GCL (i.e., that portion that does not have the sand on it) shall be protected with a waterproof sheet that is secured adequately with ballast to avoid premature hydration. (USEPA 2001; ASTM 2004a) All work in association with placement of the GCL shall be performed in accordance with the approved drawings, plans, and specifications of the final design, which will be produced near the end of the operational period.

4.4.5 High Density Polyethylene (HDPE) Geomembrane Atop the Foundation Layer

An HDPE geomembrane will be placed directly on top of the GCL at a slope of 4 percent. The HDPE geomembrane will form a composite hydraulic barrier in conjunction with the GCL described above. The composite hydraulic barrier will be designed to promote lateral drainage through the overlying lateral drainage layer and to minimize infiltration to the disposal cells. The HDPE is considered the primary hydraulic barrier with the GCL acting as a secondary hydraulic barrier by plugging any holes that may develop in the geomembrane.

The geomembrane shall be 60-mils thick (minimum) and shall conform to the requirements of GRI (2003). The geomembrane shall be obtained from the manufacturer in rolls, which are on the order of 22 ft wide by 500 ft long or greater. The geomembrane rolls shall be stored flat; kept dry; protected from puncture, abrasions, and excessive dirt; and protected from ultraviolet light exposure. Each geomembrane roll shall be numbered and a panel placement plot plan shall be developed that minimizes the total length of field seaming required and maximizes the length of seams oriented down slope versus those across slope. Placement of the geomembrane rolls shall consist of unrolling the geomembrane roll down slope per the manufacturer's directions directly onto the surface of the GCL producing a geotextile panel. Adjacent geomembrane panels shall be overlapped a minimum of 6-in and seamed using either extrusion welding or hot wedge welding methods per the manufacturer's directions. A quality assurance plan shall be developed and implemented that incorporates the following: 100-percent visual inspection of all rolls as they are laid down and of all seams; appropriate wrinkle control measures as the rolls are laid down, seamed, and covered; 100-percent non-destructive field testing of all seams by vacuum testing (ASTM 2006a) and/or air pressure

testing (ASTM 2006b); and destructive testing (ASTM 2006c) on a frequency consistent with GRI 1998. Any seam or non-seam area that has been identified as defective and any holes created for destructive testing shall be repaired and non-destructively tested prior to acceptance. The emplaced geomembrane panels shall be held down with sandbags or approved equivalent that will not damage the geomembrane until replaced with the overlying geotextile fabric and sand layer to prevent wind uplift of the geomembrane. (USEPA 1989; Koerner 1990) All work in association with placement of the geomembrane shall be performed in accordance with the approved drawings, plans, and specifications of the final design, which will be produced near the end of the operational period.

4.4.6 Geotextile Fabric

A nonwoven geotextile fabric will be placed directly on top of the HDPE geomembrane to protect it from puncture or tear during placement of the overlying 1-ft thick coarse sand lateral drainage layer. The geotextile shall be selected primarily for its puncture and tear resistance and shall conform to the requirements of GRI 2002. The geotextile shall be obtained from the manufacturer in rolls, which are on the order of 15 ft wide by 300 ft long or greater. Placement of the rolls of geotextile shall consist of unrolling the geotextile roll down slope per the manufacturer's directions directly onto the surface of the HDPE geomembrane producing a geotextile panel. Adjacent geotextile panels shall be seamed using heat seaming or stitching methods per the manufacturer's directions in a manner that does not damage the underlying GCL and HDPE geomembrane. The emplaced geotextile panels shall be held down with sandbags or an approved equivalent until replaced with the overlying sand layer to prevent wind uplift of the geotextile. The emplaced geotextile panels shall not be exposed to direct sunlight for more than 7 days prior to placement of the overlying sand layer. The emplaced geotextile shall be inspected for rips, tears, wrinkling, and displacement prior to placement of the sand layer on top of it. Any rips, tears, wrinkling, and displacement shall be repaired per the manufacturer's directions prior to placement of the sand layer on top of it. The overlying sand layer shall be placed in a single 1-ft lift on top of the combined GCL, HDPE geomembrane, and geotextile fabric per the manufacturer's directions in order to avoiding damaging the GCL and HDPE geomembrane. No equipment used to place the sand shall come into direct contact with the GCL, HDPE geomembrane, or geotextile fabric. (Koerner et al. 1990 Section 2.11; ASTM 1988)

All work in association with placement of this geotextile filter fabric shall be performed in accordance with the approved drawings, plans, and specifications of the final design, which will be produced near the end of the operational period.

4.4.7 Upper Lateral Drainage Layer

An upper lateral drainage layer will be placed over the combined GCL, HDPE geomembrane, and geotextile fabric. The lateral drainage layer will be designed to:

- Divert infiltrating water away from the underlying disposal cells and transport the water to the perimeter drainage system in conjunction with the underlying composite hydraulic barrier (i.e., HDPE geomembrane and GCL), and
- Provide the necessary confining pressures to allow the underlying GCL to hydrate properly.

The lateral drainage layer will be sloped at the same slope as the foundation layer (i.e., 4 percent slope). The lateral drainage layer will be hydraulically connected to the overall facility drainage system in order to divert and transport as much infiltrating water as possible through the lateral drainage layer to the facility drainage system and away from the underlying disposal cells. The lateral drainage layer shall consist of a 1-ft thick layer of coarse sand with a minimum saturated hydraulic conductivity of 5.0E-02 cm/s and that is free of any materials deleterious to the underlying GCL, HDPE geomembrane, and geotextile fabric or overlying geotextile fabric. The sand layer shall be placed in a single 1-ft lift on top of the GCL, HDPE geomembrane, and geotextile fabric per the GCL and HDPE geomembrane manufacturer's directions in order to avoiding damaging the GCL and HDPE geomembrane. The sand layer will be fine graded to the required contours. No equipment used to place the sand shall come into direct contact with the GCL, HDPE geomembrane, and geotextile fabric; the equipment used to place and fine grade the sand shall be low ground pressure equipment that is driven on top of the previously placed foot thick sand layer. No compaction effort shall be applied to the sand layer other than that provided by the equipment used to place and fine grade it. All work in association with placement of the drainage layer shall be performed in accordance with the approved drawings, plans, and specifications of the final design, which will be produced near the end of the operational period.

4.4.8 Geotextile Filter Fabric

An appropriate geotextile filter fabric shall be placed on top of the 1-ft thick coarse sand lateral drainage layer to provide filtration between the underlying sand layer and the overlying middle backfill. Koerner 1990 (page 120) defines filtration with a geotextile as:

> "The equilibrium fabric-to-soil system that allows for free liquid flow (but no soil loss) across the plane of the fabric over an indefinitely long period of time."

The geotextile filter fabric shall have a minimum thickness of 0.1 in, a minimum through plane saturated hydraulic conductivity of 0.1 cm/s, and an apparent opening size small enough to appropriately filter the overlaying backfill. The geotextile shall be obtained from the manufacturer in rolls, which are on the order of 15 ft wide by 300 ft long or greater. The geotextile rolls shall be stored flat, kept dry, protected from ultraviolet light exposure. The geotextile shall be placed directly on top of the sand layer, which would have been appropriately contoured and determined to be free of materials deleterious to the geotextile. Placement of the rolls of geotextile shall consist of unrolling the geotextile roll down slope per the manufacturer's directions directly onto the surface of the sand producing a geotextile panel.

Adjacent geotextile panels shall be seamed using heat seaming or stitching methods per the manufacturer's directions. The emplaced geotextile panels shall be held down with sandbags or an approved equivalent until replaced with the overlying middle backfill to prevent wind uplift of the geotextile. The emplaced geotextile panels shall not be exposed to direct sunlight for more than 7 days prior to placement of the overlying middle backfill. The emplaced geotextile shall be inspected for rips, tears, wrinkling, and displacement prior to placement of

the middle backfill on top of it. Any rips, tears, wrinkling, and displacement shall be repaired per the manufacturer's directions prior to placement of the middle backfill on top of it. The initial loose lift of the overlying middle backfill shall be placed in a single lift on top of the geotextile per the manufacturer's directions in order to avoid displacing or damaging the geotextile.

No equipment used to place the backfill shall come into direct contact with the geotextile. The feet of any compaction equipment used on the backfill shall be sized so that compaction of the backfill does not damage the geotextile. (Koerner et al. 1990 Section 2.11; ASTM 1988) All work in association with placement of this geotextile filter fabric shall be performed in accordance with the approved drawings, plans, and specifications of the final design, which will be produced near the end of the operational period.

4.4.9 Middle Backfill

A backfill layer will be placed over the upper lateral drainage layer and associated geotextile filter fabric. The middle backfill's surface and the overlying layers will slope at 1.5 percent, compared to the 4-percent slope of the lower backfill and upper drainage layer. This change in slope between the middle backfill and the underlying upper drainage layer will result in the middle backfill thickening from the cap apex toward the cap perimeter at a rate of 2.5 ft/100 ft. This could result in the middle backfill layer increasing from its minimum 1-ft thickness to as much as 20.6 ft thick at areas where the maximum slope length may be reached.

The middle backfill will provide water storage for the promotion of evapotranspiration in the event that the topsoil and upper backfill are eroded away, since the overlying erosion barrier provides only minimal such water storage. The middle backfill soils will be obtained from on site sources. Only on-site soil classified as SC (clayey sands) shall be used. Borrow areas will be pre-qualified prior to use. The middle backfill shall be placed in lifts not to exceed 9-inches in uncompacted thickness in areas where hand operated mechanical compaction equipment is used and not to exceed 12 inches in uncompacted thickness in areas where self propelled or towed mechanical compaction equipment is used. Each lift shall be compacted to at least 90% of the maximum dry density per the Modified Proctor Density Test (ASTM 2002b) or 95% per the Standard Proctor Density Test (ASTM 2000). Each lift shall also be placed within specified tolerances of the optimum moisture content.

If the surface of a lift is smooth drum rolled for protection prior to placement of a subsequent lift, that lift will be scarified prior to placement of the subsequent lift to ensure proper bonding between lifts. The top lift, upon which an overlying geotextile fabric will be placed, shall be proof-rolled with a smooth drum roller to produce a surface satisfactory for placement of the geotextile fabric and erosion barrier. All work in association with placement of the lower backfill shall be performed in accordance with the approved drawings, plans, and specifications of the final design, which will be produced near the end of the operational period.

4.4.10 Geotextile Fabric

An appropriate geotextile fabric shall be placed on top of the middle backfill and below the erosion barrier to prevent the erosion barrier stone from penetrating into the middle backfill primarily during construction and as an additional measure to prevent piping of the middle backfill through the erosion barrier voids. The geotextile fabric material shall conform to the requirements of ASTM (2002a), AASHTO (2005), and GRI (2004). Although this geotextile fabric has a different material requirement and a different function than the previous geotextiles, the placement method of this geotextile is essentially identical to that of the previous geotextile filter fabric placed on top of the sand layer. The overlying erosion barrier shall be placed in a single lift on top of the geotextile per the manufacturer's directions in order to avoid displacing or damaging the geotextile. No equipment used to place the erosion barrier shall come into direct contact with the geotextile. All work in association with placement of this geotextile shall be performed in accordance with the approved drawings, plans, and specifications of the final design, which will be produced near the end of the operational period.

4.4.11 Erosion Barrier

An erosion barrier will be placed over the middle backfill and associated geotextile fabric. The erosion barrier will be designed to prevent riprap movement during a PMP event and will therefore form a barrier to further erosion and gully formation (i.e., provide closure cap physical stability). It will also be designed to act as a barrier to burrowing animals. It will also be used to maintain a minimum 10 ft of clean material above the tanks and significant ancillary equipment to act as an intruder deterrent. It also provides minimal water storage for the promotion of evapotranspiration. The erosion barrier rock has been sized based upon the PMP and the methodology outlined by Abt and Johnson (1991) and Johnson (2002; see Appendix A for the calculations). Based upon these calculations a 1 ft thick layer of rock consistent with Type B riprap from Table F-3 of Johnson (2002) or Size R-20 riprap from Table 1 of ASTM (1997) has been determined to be suitable for use in the erosion barrier. The stone shall conform to one of these two stone gradations or equivalent. The exact gradation utilized shall be determined by availability and economics.

Quarries located near the SRS produce aggregate and rip rap consisting of granite, granite gneiss, gneiss, and mylonite (GDOT 2007). Granite aggregate and rip rap is typically utilized at SRS. However, the mylonitic quartzite reported available at an Augusta, Georgia quarry will be evaluated for durability versus the local granite. Consistent with the recommendations of Johnson (2002) and ASTM (1997), the rock utilized for the erosion barrier shall be angular, shall have a minimum specific gravity of 2.65, and shall be considered durable per the criteria outlined below.

- The rock shall be dense, sound, resistant to abrasion, free of clays, and free of cracks, seams, and other defects as determined by a petrographic examination (ASTM 2003a).

- Specific gravity (ASTM 2004b), absorption (ASTM 2004b), sodium sulfate soundness (ASTM 2005b), Los Angeles abrasion (ASTM 2003b), Schmidt Rebound Hardness-ISRM Method (Johnson 2002) tests shall be performed on the rock. Based upon these

tests and the scoring methodology outlined by Johnson 2002, the rock shall have a quality score of 80 or greater.

Rock production and associated Quality Assurance/Quality Control (QA/QC) will be coordinated with the supplying quarry to assure the requisite rock size and mineralogical types are procured. The general approach will be to identify the highest-percent quartz rock type by quarry. Within the identified quarry, highly fractured, obviously weathered, and relatively feldspar-rich rock will be avoided, while "whole", fresh, and relatively quartz-rich rock will be preferentially selected. Visual selection of optimal rock may be supported by supplementary information (e.g., sulfate analyses and abrasion testing) available from the supplier. The final closure cap design will include a comprehensive QA/QC plan for selection and installation of all materials used to construct the cap.

The stone shall be handled, loaded, transported, stockpiled, and placed consistent with the requirements outlined in ASTM (2002a) and Johnson (2002). In particular, the stone shall be handled, loaded, transported, stockpiled, and placed in a manner that prevents breakage and segregation of the stone into various sizes. The stone shall be placed in a single 1-ft lift on top of the middle backfill and overlying geotextile fabric by dumping and spreading with heavy equipment. The stone shall be placed in a manner that achieves a reasonably well-graded distribution of stones, a fairly consistent thickness (i.e., 0.9 to 1.25 ft), and a densely packed, wedged together, firmly interlocked layer. No equipment used to place the stone shall come into direct contact with the underlying geotextile; the equipment used to place the stone shall be low ground pressure equipment that is driven on top of the previously placed 1-ft thick stone. The only compaction effort applied to the stone shall be that provided by the equipment used to place it and a minimum of two passes of a Caterpillar D6 tracked bulldozer or equivalent.

Additionally as pointed out by NUREG (2006 and 1982) natural or archaeological analogs can be utilized to help demonstrate the long-term performance of closure cap materials. Prior to developing a final closure cap design, available literature and local natural or archaeological analogs for the erosion barrier stone will be researched and included as input for erosion barrier durability and degradation with time. As a starting point for the literature review, the literature review for long-term survivability of riprap presented in NUREG (1982) will be reviewed.

The rock utilized for the erosion barrier will be located below grade, while similar rock utilized for the side slopes (Section 4.4.16) and toe (Section 4.4.15) will be located above grade. Therefore the literature review and evaluation of local natural or archaeological analogs will include both those applicable to below grade and above grade weathering. Since the erosion barrier rock will likely be granite because of its durability, cost, and local availability, the following potential below grade local natural or archaeological analogs will be considered for evaluation:

- The Nature Conservancy's Heggie's Rock Preserve, located in Columbia County Georgia near the town of Appling, is a granite outcrop that is nearly 70 feet higher than the surrounding area (The Nature Conservancy 2007)

- Other granitic regoliths located in the southeastern United States
- Local granite quarries (GDOT 2007):
  - Martin Marietta Aggregates, Appling, Georgia
  - Rinker Materials, Dogwood Quarry, Appling, Georgia
- Granite quarries and manufacturing in Elberton, Georgia, which can be found through the Elberton Granite Association at www.egaonline.com/home/ (known as the "Granite Capital of the World" and located less than 100 miles from SRS).

In conjunction with the evaluation of below grade local natural or archaeological analogs for granite weathering, above grade analogs will also be evaluated for applicability to the side slope (Section 4.4.16) and toe (Section 4.4.15) rock:

- The Nature Conservancy's Heggie's Rock Preserve, located in Columbia county Georgia near the town of Appling, is a granite outcrop that is nearly 70 feet higher than the surrounding area (The Nature Conservancy 2007).
- Other granitic regoliths located in the southeastern United States
- Local granite quarries (GDOT 2007):
  - Martin Marietta Aggregates, Appling, Georgia
  - Rinker Materials, Dogwood Quarry, Appling, Georgia
- Granite quarries and manufacturing in Elberton, Georgia, which can be found through the Elberton Granite Association at www.egaonline.com/home/ (known as the "Granite Capital of the World" and located less than 100 miles from SRS).
- Elberton, Georgia High School facilities constructed of granite
- SRS and local area granite rip rap
- Local area granite head stones
- Georgia sites with petroglyphs including:
  - Forsyth County, Georgia granite boulder, which has been on display at the University of Georgia since 1963
  - Track Rock Gap, near Blairsville
  - The Reinhardt Rock, which originated near Keithsburg, Cherokee County, and is now on display at Reinhardt College

In addition to these local analogs for above grade granite, the National Institute of Standards and Technology (NIST) Stone Test Wall, located in Gaithersburg, MD (Stutzman 2001) will also be considered. This wall, constructed in 1948 as a cooperative study between the National Bureau of Standards and ASTM Committee C18 on Building Stone, contains 2,352 individual samples of over 30 distinct types of stone. The wall's purpose is to allow study of the performance of stone subjected to above-ground weathering. However, as of 1987, of the many stone types placed in the wall, "…only a few fossiliferous limestones permit a valid measurement of surface reduction in a polluted urban environment" (Winkler 1987). A web site (http://stonewall.nist.gov) is available for additional information (Stutzman 2001).

Based upon the results of the natural or archaeological analog evaluation, the required size of the emplaced stone and the thickness of the stone layer will be increased, if necessary, during final closure cap design to accommodate anticipated weathering in order to ensure closure

cap physical stability with regards to erosion over 10,000 years. Weathering is discussed further in Section 6.4.1.

In order to prevent the loss of overlying material into the erosion barrier the voids within the rock mass will be filled. The material to be used to fill the voids within the rock mass has yet to be selected. An evaluation of potential materials will be conducted and will include at a minimum the following potential fill materials:

- Controlled low-strength material (CLSM) or Flowable Fill infilling
- Gravel and/or sand infilling
- Bituminous material infilling
- Other cementitious material infilling and placement similar to roller-compacted concrete

After placement of the stone infilling with CLSM or Flowable Fill, gravel and/or sand, or bituminous material shall be applied on top of the stone in a manner that allows the material to penetrate into all the voids within the stone layer. The evaluation of materials to infill the stone will consider the following favorably during the selection process:

- No negative impact on the layer's ability to adequately perform as an erosion barrier
- No negative impact upon weathering or preferably tending to decrease the weathering rate,
- Its ability to facilitate the layer's ability to act as a barrier to burrowing animals
- Its ability to facilitate the layer's ability to hinder root penetration
- Its projected durability (i.e. longevity)
- No negative impact upon other SDF Closure Cap layers, particularly the lateral drainage layer and GCL

All work in association with placement of the erosion barrier shall be performed in accordance with the approved drawings, plans, and specifications of the final design, which will be produced near the end of the operational period.

4.4.12 Upper Backfill

A backfill layer will be placed over the erosion barrier. The upper backfill will be a minimum 2.5-ft thick layer used to bring the elevation of the closure cap up to that necessary for placement of the topsoil. The upper backfill will also provide water storage to promote evapotranspiration. The materials and placement method for the upper backfill is essentially identical to that of the middle backfill. The initial loose lift of the upper backfill shall be placed in a single lift on top of the erosion control barrier in order to avoiding damaging the erosion control barrier. No equipment used to place the upper backfill shall come into direct contact with the erosion control barrier. It shall be driven only on top of previously placed backfill. The feet of any compaction equipment used on the backfill shall be sized so that during compaction of the backfill the feet do not directly run on the erosion control barrier. The upper backfill will be fine graded to the required contours. All work in association with placement of the upper backfill shall be performed in accordance with the approved

drawings, plans, and specifications of the final design, which will be produced near the end of the operational period.

4.4.13 Topsoil

The upper most soil layer of the closure cap shall consist of minimum 6 inches of soils capable of supporting a vegetative cover (i.e., topsoil) obtained from onsite sources. It will be placed at a maximum 1.5 percent slope in order to promote runoff and to provide a stable slope that will prevent the initiation of gullying (see Appendix A for the calculations based upon the Probable Maximum Precipitation (PMP) and the methodology outlined by Johnson 2002). The topsoil in conjunction with the vegetative cover will store water and promote evapotranspiration. The topsoil shall be placed in a single 0.5-ft lift on top of the upper backfill. The equipment used to place and fine grade the topsoil shall be low ground pressure equipment. No compaction effort shall be applied to the topsoil other than that provided by the equipment used to place and fine grade it. Measures shall be taken to minimize erosion of the topsoil layer prior to the establishment of the vegetative cover. Any such erosion shall be repaired by the installation subcontractor until such time as the vegetative cover has been established and construction of the closure cap has been certified as complete. Certification of closure cap construction completion will be provided by a Professional Engineer who certifies that the closure cap has been constructed per the approved drawings, plans, and specifications. All work in association with placement of the topsoil shall be performed in accordance with the approved drawings, plans, and specifications of the final design, which will be produced near the end of the operational period.

4.4.14 Vegetative Cover

A vegetative cover will be established to promote runoff, minimize erosion, and promote evapotranspiration. The topsoil will be fertilized, seeded, and mulched to provide a vegetative cover. The initial vegetative cover shall be a persistent grass such as Bahia. During seeding and establishment of the initial grass, appropriate mulch, erosion control fabric, or similar substances will be used to protect the surface.

The area will be repaired through transplanting or replanting to ensure that a self maintaining cover is developed. If it is determined that bamboo is a climax species that prevents or greatly slows the intrusion of pine trees, it will be planted as the final vegetative cover at the end of the 100-year institutional control period. Pine trees are typically assumed to be the most deeply rooted naturally occurring climax plant species which will degrade the GCL through root penetration at SRS. In contrast, bamboo is a shallow-rooted species, which will not degrade the GCL. Additionally bamboo evapotranspires year-round in the SRS climate, minimizes erosion, and can sustain growth with minimal maintenance. A study conducted by the U.S. Department of Agriculture (USDA) Soil Conservation Service (SCS) has shown that two species of bamboo (Phyllostachys bissetii and Phyllostachys rubromarginata) will quickly establish a dense ground cover (Salvo and Cook 1993). All work in association with the vegetative cover shall be performed in accordance with the approved drawings, plans, and specifications of the final design, which will be produced near the end of the operational period.

4.4.15 Toe of Closure Cap Side Slopes

The toe of closure cap side slopes will consist of a riprap layer to stabilize the side slope rip rap, provide erosion protection at the toe, transition flow from the side slope to adjacent areas, and provide gully intrusion protection to the embankment. The toe riprap will extend from the toe of the side slope a minimum of 20 ft (Figure 11).

The toe riprap has been sized based upon the PMP and the methodology outlined by Johnson 2002 (see Appendix A for the calculations). Based upon these calculations, a 42-in thick layer of rock consistent with Type D riprap from Table F-3 of Johnson 2002 or Size R-300 riprap from Table 1 of ASTM (1997) has been determined to be suitable for use on the toe. The stone shall conform to one of these two stone gradations or equivalent. The exact gradation utilized shall be determined by availability and economics.

Quarries located near the SRS produce aggregate and rip rap consisting of granite, granite gneiss, gneiss, and mylonite (GDOT 2007). Granite aggregate and rip rap is typically utilized at SRS. However, the mylonitic quartzite reported available at an Augusta, Georgia quarry will be evaluated for durability versus the local granite. Consistent with the recommendations of Johnson (2002) and ASTM (1997), the toe riprap shall be angular, shall have a minimum specific gravity of 2.65, and shall be considered durable per the criteria outlined below:

- The rock shall be dense, sound, resistant to abrasion, free of clays, and free of cracks, seams, and other defects as determined by a petrographic examination (ASTM 2003a).

- Specific gravity (ASTM 2004b), absorption (ASTM 2004b), sodium sulfate soundness (ASTM 2005b), Los Angeles abrasion (ASTM 2003b), Schmidt Rebound Hardness-ISRM Method (Johnson 2002) tests shall be performed on the rock. Based upon these tests and the scoring methodology outlined by Johnson (2002), the rock shall have a quality score of 80 or greater.

Rock production and associated QA/QC will be coordinated with the supplying quarry to assure the requisite rock size and mineralogical types are procured. The general approach will be to identify the highest-percent quartz rock type by quarry. Within the identified quarry, highly fractured, obviously weathered, and relatively feldspar-rich rock will be avoided, while "whole", fresh, and relatively quartz-rich rock will be preferentially selected. Visual selection of optimal rock may be supported by supplementary information (e.g., sulfate analyses and abrasion testing) available from the supplier. The final closure cap design will include a comprehensive QA/QC plan for selection and installation of all materials used to construct the cap.

The toe riprap shall be handled, loaded, transported, stockpiled, and placed consistent with the requirements outlined in ASTM (2002a) and Johnson (2002). In particular, the riprap shall be handled, loaded, transported, stockpiled, and placed in a manner that prevents breakage and segregation of the stone into various sizes. The riprap shall be placed in a single 42-in lift by dumping and spreading with heavy equipment. The stone shall be placed in a manner that achieves a reasonably well-graded distribution of stones, a fairly consistent

thickness (i.e., 38 to 52 in.), and a densely packed, wedged together, firmly interlocked layer. The only compaction effort applied to the stone shall be that provided by the equipment used to place it and a minimum of two passes of a Caterpillar D6 tracked bulldozer or equivalent.

Weathering of the stone shall be considered as outlined in Sections 4.4.11 and 6.4.1. All work in association with placement of the toe riprap shall be performed in accordance with the approved drawings, plans, and specifications of the final design, which will be produced near the end of the operational period.

4.4.16 Closure Cap Side Slopes

The closure cap side slopes will be placed at a maximum 3 horizontal to 1 vertical (3H:1V, 33.3 percent, or 19.5 degrees) and have a riprap surface with an underlying gravel bedding layer to prevent gully formation on the side slopes and to provide long-term slope stability. The side slope riprap and underlying gravel bedding layer will extend from the toe of the side slope up the side slope to a minimum 10 ft onto the top slope (Figure 11). The stone bedding layer shall consist of a 6-in thick layer of well-graded crushed stone with either the gradation shown in Table F-4 of Johnson 2002 or that of Figure 8 of ASTM (1997; i.e., FS-2 filter/bedding stone). The side slope riprap has been sized based upon the PMP and the methodology outlined by Abt and Johnson (1991) and Johnson (2002; see Appendix A for the calculations). Based upon these calculations, a 24-in thick layer of rock consistent with Type D riprap from Table F-3 of Johnson 2002 or Size R-150 riprap from Table 1 of ASTM (1997) has been determined to be suitable for use on the side slopes. The stone shall conform to one of these two stone gradations or equivalent. The exact gradation utilized shall be determined by availability and economics.

Quarries located near the SRS produce aggregate and rip rap consisting of granite, granite gneiss, gneiss, and mylonite (GDOT 2007). Granite aggregate and rip rap is typically utilized at SRS. However, the mylonitic quartzite reported available at an Augusta, Georgia quarry will be evaluated for durability versus the local granite. Consistent with the recommendations of Johnson (2002) and ASTM (1997), both the bedding stone and riprap shall be angular, shall have a minimum specific gravity of 2.65, and shall be considered durable per the criteria outlined below:

- The rock shall be dense, sound, resistant to abrasion, free of clays, and free of cracks, seams, and other defects as determined by a petrographic examination (ASTM 2003a).

- Specific gravity (ASTM 2004b), absorption (ASTM 2004b), sodium sulfate soundness (ASTM 2005b), Los Angeles abrasion (ASTM 2003b), Schmidt Rebound Hardness-ISRM Method (Johnson 2002) tests shall be performed on the rock. Based upon these tests and the scoring methodology outlined by Johnson 2002, the rock shall have a quality score of 80 or greater.

Rock production and associated QA/QC will be coordinated with the supplying quarry to assure the requisite rock size and mineralogical types are procured. The general approach will be to identify the highest-percent quartz rock type by quarry. Within the identified

quarry, highly fractured, obviously weathered, and relatively feldspar-rich rock will be avoided, while "whole", fresh, and relatively quartz-rich rock will be preferentially selected. Visual selection of optimal rock may be supported by supplementary information (e.g., sulfate analyses and abrasion testing) available from the supplier. The final closure cap design will include a comprehensive QA/QC plan for selection and installation of all materials used to construct the cap.

Both the bedding stone and riprap shall be handled, loaded, transported, stockpiled, and placed consistent with the requirements outlined in ASTM (2002a) and Johnson (2002). In particular, the bedding stone and riprap shall be handled, loaded, transported, stockpiled, and placed in a manner that prevents breakage and segregation of the stone into various sizes. The bedding stone shall be placed in a single 6-in compacted lift on the side slope from the bottom of the slope up the side slope by dumping, spreading, and compacting with a rubber-tired or smooth drum roller. The riprap shall be placed in a single 2-ft lift on top of the bedding stone from the bottom of the slope up the side slope by dumping and spreading with heavy equipment. The stone shall be placed in a manner that achieves a reasonably well-graded distribution of stones, a fairly consistent thickness (i.e., 1.8 to 2.5 ft), and a densely packed, wedged together, firmly interlocked layer. The only compaction effort applied to the stone shall be that provided by the equipment used to place it and a minimum of two passes of a Caterpillar D6 tracked bulldozer or equivalent.

Weathering of the stone shall be considered as outlined in Sections 4.4.11 and 6.4.1. All work in association with placement of the side slope bedding stone and riprap shall be performed in accordance with the approved drawings, plans, and specifications of the final design, which will be produced near the end of the operational period.

4.4.17 Integrated Drainage System

An integrated drainage system will be designed and built to handle the runoff from the closure caps and drainage from the closure cap lateral drainage layers. The runoff and lateral drainage will be directed to a system of riprap lined ditches, which will be designed in accordance with Johnson 2002. The riprap lined ditches will direct the water away from the SDF closure cap as a whole and will be constructed around the perimeter of the SDF closure cap. The ditches will discharge into sedimentation basins as necessary for sediment control. The riprap for the ditches has not been sized yet since the SDF is currently in the initial phase operational period. Due to the early phase and lack of a detailed closure cap layout, a detailed drainage system cannot yet be designed. Therefore drainage areas and flows cannot be currently assigned in order to size the riprap for various sized ditches.

5.0 UNDEGRADED CAP INFILTRATION ESTIMATE METHOD

The undegraded cap infiltration estimate method for the SDF closure cap is described below. This infiltration is at Year 0 after construction. Section 7 presents infiltration estimates for future years incorporating parameter value changes due to degradation with time.

5.1 HELP MODEL USE AND DESCRIPTION

Within the SDF Performance Assessment (PA), the HELP Model is used to provide the upper boundary condition for a 2-dimensional PORFLOW vadose zone flow model. The upper boundary condition provided by the HELP Model consists of the average annual infiltration through the composite barrier layer (i.e., HDPE geomembrane overlaying a GCL) of the SDF Closure Cap (see Figures 8 and 10) at each time step modeled.

The HELP model is a quasi-two-dimensional water balance model designed to conduct landfill water balance analyses. The model requires the input of weather, soil, and closure cap design data. It provides estimates of runoff, evapotranspiration, lateral drainage, vertical percolation (i.e., infiltration), hydraulic head, and water storage for the evaluation of various landfill designs.

United States Army Corps of Engineers (USACE) personnel at the Waterways Experiment Station (WES) in Vicksburg, Mississippi, developed the HELP model, under an interagency agreement (DW21931425) with the U.S. Environmental Protection Agency (USEPA). As such the HELP model is a USEPA-sanctioned model for conducting landfill water balance analyses. HELP model version 3.07, issued on November 1, 1997, is the latest version of the model. It is public domain software available from the WES website at:

http://el.erdisposal cell.usace.army.mil/products.cfm?Topic=model&Type=landfill.

USEPA and the USACE have provided the following documentation associated with the HELP model:

- A user's guide (Schroeder et al. 1994a), which provides instructions for HELP model use.
- Engineering documentation (Schroeder et al. 1994b), which provides information on the source language used to write the code, the hardware necessary to operate the code, data generation methodologies available for use, and the methods of solution.
- Verification test reports comparing the model's drainage layer estimates to the results of large-scale physical models (Schroeder and Peyton 1987a) and comparing the model's water balance estimates to "field data from a total of 20 landfill cells at 7 sites in the United States" (Schroeder and Peyton 1987b).

The software quality assurance plan for the use of the HELP model in PAs is documented in Phifer (2006).

The National Research Council of the National Academies (NRC-NA 2007) conducted an assessment of waste barrier performance, which included information on the use of the HELP model. The NRC-NA concluded that the HELP model is probably the most widely used model to predict the water balance (infiltration in particular) of closure caps. They noted that the primary advantages of the HELP model over more sophisticated models for unsaturated flow (i.e., those solving Richard's equation and utilizing characteristic curves) are that the HELP model requires much less input data and requires significant less computational time. While the NRC-NA conceptually prefers the use of the more sophisticated models over the HELP model, their evaluation of the HELP model indicates that it over predicts infiltration in humid environments similar to that at SRS (see NRC-NA 2007 Table 5.5). Bonaparte, et al. (2002) came to conclusions consistent with the NRC-NA 2007 regarding the use of the HELP model. Bonaparte, et al. (2002) performed a literature review of the comparison of field derived landfill water balances to HELP model results. This evaluation concluded that "for a number of cases the HELP model analysis was shown to give reasonable predictions of cumulative longer-term water balances." In addition Bonaparte, et al. (2002) performed an evaluation of measured leachate collection and removal system flow rates for six landfill cells versus leachate generation rates estimated by HELP. Based upon this evaluation the authors concluded "that the HELP model can appropriately be employed as a tool to estimate long-term average leachate generation rates …"

Additional details for the Section 3.2 background SRS water balance and infiltration review are presented in Phifer et al. (2007). Phifer et al. (2007) concludes that the HELP model results compare very well with the background water balance and infiltration studies, indicating that the use of the HELP model produces reasonable and acceptable results. Based upon these evaluations, use of the HELP model to establish the upper boundary condition infiltration for a 2-dimensional PORFLOW vadose zone flow model seems appropriate.

The 2-dimensional PORFLOW vadose zone flow model, to which the HELP model infiltration results form the upper boundary condition, meets the preferred NRC-NA model requirements (i.e. solves Richard's equation and utilizing characteristic curves). The PORFLOW software package is a comprehensive mathematical model for simulating multi-phase fluid flow, heat transfer and mass transport in variably saturated porous and fractured media (Aleman 2007). It is a finite element code that solves Richard's equation utilizing characteristic curves to solve variably saturated flow problems. It can simulate transient or steady-state problems in Cartesian or cylindrical geometry. The porous medium may be anisotropic and heterogeneous and may contain discrete fractures or boreholes with the porous matrix. The theoretical models within the code provide a unified treatment of concepts relevant to fluid flow and transport.

The HELP and PORFLOW models will be used in conjunction for the SDF PA. The HELP model considers precipitation, runoff, evapotranspiration, and lateral drainage in estimating infiltration through the composite barrier layer (i.e., HDPE geomembrane overlaying a GCL) of the SDF Closure Cap (see Figures 8 and 10). This infiltration forms the upper boundary condition for a 2-dimensional PORFLOW SDF vadose zone flow model. This PORFLOW model solves Richard's equation utilizing characteristic curves to solve variably saturated

flow within the vadose zone consistent with the preferences of the NRC-NA. The combined use of the HELP and PORFLOW models appears reasonable.

However, as indicated in Section 7.7.1, the HELP model is not capable of appropriately considering the results of a probability based root penetration model which was developed as part of Phifer et al. (2007) to evaluate root penetration of the GCL through tensile stress cracks within the overlaying HDPE geomembrane. For this reason in the future other models will be evaluated as a replacement to the HELP model. The models to be considered may include but are not limited to FEHM, HYDRUS-2D, LEACHM, TOUGH-2, UNSAT-H, and VADOSE/W.

The initial infiltration estimate (i.e. at year 0) through the SDF closure cap configuration listed in Section 7.0 has been made using the HELP Model and the results are provided in Section 7.9. Additionally infiltration estimates which account for closure cap degradation have been made for SDF Closure Cap over 10,000 years are also presented in Section 7.9.

5.2 HELP MODEL WEATHER INPUT DATA

The HELP model requires the input of evapotranspiration, precipitation, temperature, and solar radiation data. There are several input options for each type of weather data required. In general the options available for weather data input include (Phifer and Nelson 2003):

- Historical records from specific cities ("default")
- Synthetically generated data based upon the statistical characteristics of historic data from specific cities
- Synthetically generated data modified with average monthly precipitation and temperature data from the site in question
- Manual data entry (Schroeder et al. 1994a and Schroeder et al. 1994b)

The default weather databases included in the HELP model are very limited in terms of the period of time and cities covered in the database. A complete set of historic weather data is not available for the SRS or Augusta, Georgia within the HELP model. However, the HELP model can generate synthetic weather data for up to a 100-year span and many more cities are included than in the default weather databases. In particular, synthetic weather data can be generated for Augusta; however it is not available for SRS. However average monthly data from SRS is available to modify the Augusta synthetically generated data. The manual input option requires data availability and placement of the data in a format acceptable to the HELP model, which is a very time consuming operation. Therefore for the purposes of this modeling, synthetic daily weather data for precipitation, temperature, and solar radiation over 100 years was generated based upon the HELP data for Augusta and modified with the SRS specific average monthly precipitation and temperature data. (Phifer and Nelson 2003)

The SRS collects meteorological data from a network of nine weather stations. The primary SRS precipitation data has been collected from the Savannah River National Laboratory (SRNL) (773-A) weather station between 1952 and 1995 and from the Central Climatology

Site (CLM) since 1995. However the closest weather station to the SDF is the 200-F weather station, from which daily precipitation data has been collected from a manual rain gauge from 1961 onward. Collection of temperature data at SRS began in 1968.

The primary SRS temperature data have been collected from the SRNL (773-A) weather station between 1968 and 1995 and from the CLM since 1995. Temperature data is not collected at the 200-F weather station where the manual rain gauge is located. (Hunter 2005).

SRS-specific monthly precipitation and average monthly temperature data from the combined SRNL/CLM weather stations and precipitation data from the 200-F weather station were obtained from the SRNL Atmospheric Technologies Group (ATG) web site located at http://shweather.srs.gov/servlet/idg.Weather.Weather (SRNL – ATG 2006). Table 6 provides the monthly precipitation for years 1952 to 2006 obtained from the combined SRNL/CLM weather stations and the average monthly precipitation over the entire time span. Table 7 provides the monthly precipitation for the years 1961 to 2006 obtained from the 200-F weather station and the average monthly precipitation over the entire time span. As noted in Table 7, there are some missing precipitation data associated with the 200-F weather station. Therefore the monthly 200-F precipitation data for each month that has any missing data has been replaced with the primary SRS precipitation data obtained from the combined SRNL/CLM weather stations, if the combined SRNL/CLM precipitation data for that month is greater than that of the 200-F weather station. The combined SRNL/CLM data result in an average precipitation of 48.53 in/yr over the 55-year monitoring period; whereas, the revised 200-F data results in an average precipitation of 49.04 in/yr over its 46 year monitoring period. Table 8 provides the average monthly temperature for the years 1968 to 2006 obtained from the combined SRNL/CLM weather stations and the monthly average over the entire time span. A 100 year synthetic daily weather database for precipitation, temperature, and solar radiation was generated based upon the HELP data for Augusta that was modified with the SRS specific average monthly precipitation and temperature for the entire time spans from Table 7 and Table 8, respectively.

To generate the evapotranspiration data, the default option for Augusta, Georgia was used, since it is available and is considered constant from year to year. Additionally, the user must specify two values, the evaporative zone depth and maximum leaf area index. The evaporative zone depth is the maximum depth to which the HELP model will allow evapotranspiration to occur. An evaporative zone depth of 22 inches was selected based upon HELP model guidance, which lists this depth as a "fair" depth for Augusta, Georgia. This is considered a conservative maximum evaporative zone depth due to the anticipated capillarity associated with the surficial soil types (i.e., topsoil and upper backfill) and the anticipated root depths (see Section 7.2). The maximum leaf area index is a measure of the maximum active biomass that the HELP model will allow to be present. The actual leaf area index utilized by the HELP model is modified from the maximum based upon daily temperature, daily solar radiation, and the beginning and ending dates of the growing season. A maximum leaf area index of 3.5 was selected based upon HELP model guidance, which lists this value for a "good" stand of grass (Schroeder et al. 1994b and Phifer and Nelson 2003). The HELP model methodology to estimate evapotranspiration is described in detail by Schroeder et al. (1994b). The methodology takes into consideration daily solar radiation, daily temperature,

Table 6. Combined SRNL/CLM Weather Stations Monthly and Annual Precipitation for Years 1952 to 2006

Year	Jan	Feb	March	April	May	June	July	August	Sept	October	Nov	Dec	Annual
1952	2.07	3.23	6.55	3.12	5.56	5.67	2.82	5.98	3.34	1.36	2.86	3.99	46.55
1953	2.69	5.48	3.83	2.96	4.42	5.38	3.63	3.61	8.53	0.11	1.04	7.51	49.19
1954	1.26	1.64	2.95	2.50	2.89	2.91	2.03	4.10	1.43	1.29	2.94	2.88	28.82
1955	4.75	2.62	2.21	5.57	4.53	3.31	3.94	5.07	3.42	1.32	2.93	0.46	40.13
1956	1.67	7.94	4.84	3.21	3.07	2.34	4.34	3.18	4.56	1.83	0.93	2.05	39.96
1957	2.05	1.58	4.29	2.75	8.02	4.17	3.51	2.41	5.04	6.12	6.46	2.24	48.64
1958	4.01	4.38	4.96	5.63	2.07	2.50	5.32	2.76	1.12	0.96	0.21	4.42	38.34
1959	3.54	6.06	6.44	2.03	3.81	4.06	5.80	2.93	8.71	10.86	1.97	3.54	59.75
1960	6.91	5.81	5.76	5.07	1.96	3.66	5.27	2.81	4.84	0.97	0.83	2.93	46.82
1961	3.59	5.76	7.23	8.20	3.88	3.01	3.09	7.15	1.00	0.07	1.83	6.60	51.41
1962	4.64	5.14	6.52	4.03	3.50	4.41	2.56	3.43	5.55	2.27	3.50	2.20	47.75
1963	5.96	3.64	3.34	3.70	2.98	8.42	3.18	1.04	5.37	0.00	3.68	4.47	45.78
1964	7.79	6.00	5.79	5.94	3.62	4.50	10.42	12.34	5.43	6.53	0.60	4.10	73.06
1965	1.83	6.19	10.18	2.81	1.63	5.14	9.57	1.29	2.36	2.95	1.99	1.69	47.63
1966	7.81	6.22	4.30	2.93	5.28	4.81	3.52	5.84	3.98	1.51	1.37	3.85	51.42
1967	3.91	4.43	7.54	2.60	5.94	4.06	7.23	8.48	0.99	0.31	2.81	3.37	51.67
1968	4.56	0.97	1.58	2.23	4.24	5.28	3.58	8.05	5.06	3.33	4.14	2.93	45.95
1969	2.20	2.47	3.42	4.71	2.57	4.26	1.94	4.38	4.05	2.00	0.40	4.42	36.82
1970	3.12	2.75	7.90	1.28	4.01	4.68	4.69	3.78	2.75	4.02	1.50	5.62	46.10
1971	5.01	3.80	9.71	2.57	3.62	4.81	13.71	9.98	4.74	5.27	2.16	2.79	68.17
1972	7.81	3.71	2.68	0.60	4.10	5.64	1.92	8.19	1.52	1.03	2.92	4.26	44.38
1973	5.50	4.47	6.67	4.55	4.91	12.97	6.86	3.90	4.38	1.72	0.98	3.99	60.90
1974	2.42	6.66	3.03	3.05	3.35	2.80	4.44	6.77	3.32	0.09	1.99	4.11	42.03
1975	4.98	6.64	5.92	4.42	5.15	3.83	8.55	3.83	5.18	1.74	3.41	2.03	55.68

Table 6. Combined SRNL/CLM Weather Stations Monthly and Annual Precipitation for Years 1952 to 2006 - continued

Year	Jan	Feb	March	April	May	June	July	August	Sept	October	Nov	Dec	Annual
1976	4.18	1.08	3.83	2.50	10.9	4.35	1.95	1.64	5.48	4.92	4.19	5.08	50.10
1977	3.72	1.62	6.86	1.27	1.79	2.47	3.42	7.30	5.50	4.27	1.63	3.86	43.71
1978	10.02	1.31	3.06	3.53	3.64	3.42	4.11	5.10	4.06	0.06	3.54	1.87	43.72
1979	3.59	7.74	3.09	6.49	8.94	1.54	7.85	2.12	6.13	1.35	3.95	2.17	54.96
1980	5.12	3.48	10.96	1.69	3.49	2.99	0.90	2.03	5.86	2.14	2.5	1.91	43.07
1981	0.89	5.02	4.72	2.07	6.90	4.29	3.96	5.79	0.54	2.81	1.00	9.55	47.54
1982	3.94	4.46	2.51	5.68	2.73	4.28	11.49	5.02	4.62	3.87	2.41	4.85	55.86
1983	3.75	7.22	6.62	5.77	1.67	6.57	4.85	6.32	3.56	1.92	5.39	4.15	57.79
1984	3.51	7.09	6.05	8.00	9.79	2.54	7.28	5.52	0.60	0.31	0.90	1.38	52.97
1985	3.01	6.92	1.31	0.84	1.70	4.62	8.10	4.38	0.49	6.34	6.36	2.48	46.55
1986	1.46	3.58	4.08	1.45	3.84	3.03	2.96	10.9	1.54	4.19	5.82	5.83	48.68
1987	7.39	7.55	4.97	0.70	3.57	5.64	4.87	4.93	3.56	0.29	2.74	1.42	47.63
1988	4.15	3.19	2.91	4.78	2.85	7.12	1.78	6.80	4.40	3.39	2.17	2.91	46.45
1989	1.42	3.59	5.52	4.89	2.60	6.67	11.46	3.27	4.87	3.36	3.00	4.41	55.06
1990	3.07	2.38	2.37	1.21	2.95	0.89	7.31	8.07	0.62	19.62	1.41	1.57	51.47
1991	7.03	1.84	7.89	4.73	3.06	2.17	7.89	9.26	4.40	0.99	1.55	3.32	54.13
1992	4.45	3.89	2.98	2.40	1.34	6.27	3.69	4.83	6.38	3.11	7.78	2.86	49.98
1993	7.45	3.62	8.37	1.74	1.43	3.27	3.12	2.23	7.29	0.99	1.87	1.81	43.19
1994	4.80	3.91	6.42	1.05	1.45	5.08	7.47	3.47	0.99	10.01	3.05	4.62	52.32
1995	6.96	7.97	0.92	1.28	1.77	8.15	5.71	6.92	5.75	2.64	2.38	4.47	54.92
1996	3.18	2.43	6.24	1.42	1.23	3.46	5.20	4.83	4.05	1.95	1.17	2.70	37.86
1997	4.42	5.35	2.88	3.05	2.23	9.58	6.00	4.00	5.59	3.90	4.76	7.91	59.67
1998	7.83	7.18	5.61	6.28	3.53	3.76	4.49	4.34	8.43	0.52	0.77	1.76	54.50
1999	5.71	2.75	2.55	1.66	2.82	5.21	4.97	3.86	5.02	2.38	1.04	1.47	39.44

Table 6.   Combined SRNL/CLM Weather Stations Monthly and Annual Precipitation for Years 1952 to 2006 - continued

Year	Jan	Feb	March	April	May	June	July	August	Sept	October	Nov	Dec	Annual
2000	6.53	0.61	3.84	1.43	0.20	4.86	2.49	5.11	7.82	0.00	3.50	1.94	38.33
2001	2.80	2.52	7.27	0.96	4.79	4.87	5.42	1.60	3.34	0.12	1.16	1.20	36.05
2002	2.97	2.23	3.88	2.10	2.87	3.25	3.92	4.59	3.88	2.62	4.73	4.32	41.36
2003	2.32	5.03	8.65	9.19	7.17	9.47	5.94	5.16	4.29	3.31	1.52	1.92	63.97
2004	3.79	6.28	1.44	1.94	2.50	8.71	4.66	2.74	8.72	0.66	4.74	1.72	47.9
2005	1.78	4.87	5.42	2.16	3.22	5.56	6.28	3.86	0.05	3.35	2.79	4.77	44.11
2006	2.94	2.83	2.90	2.98	1.60	7.23	2.59	2.54	2.43	3.48	2.61	5.03	39.16
Monthly Average Precip.	4.26	4.31	4.98	3.30	3.70	4.80	5.16	4.91	4.13	2.85	2.65	3.49	48.53

Notes to Table 6:

- All precipitation values in inches
- The 1952 through 1995 precipitation data has been collected from the SRNL (773-A) weather station and since 1995 it has been collected from the CLM
- The monthly data highlighted in grey represents months for which some precipitation data is missing from the 200-F weather station precipitation database. The Table 7 monthly 200-F precipitation data for each month that has any missing data has been replaced with the combined SRNL/CLM weather stations precipitation data, if the combined SRNL/CLM precipitation data for that month is greater than that of the 200-F weather station.

Table 7. 200-F Weather Station Monthly and Annual Precipitation for Years 1961 to 2006

Year	Jan	Feb	March	April	May	June	July	August	Sept	October	Nov	Dec	Annual
1961	3.55	5.53	7.57	7.23	4.21	2.00	2.94	8.55	0.56	0.02	1.80	6.20	50.16
1962	4.35	5.28	6.46	3.85	2.61	1.97	1.74	4.36	4.03	1.87	3.31	2.40	42.23
1963	6.05	3.59	3.15	3.18	2.37	7.04	2.00	1.54	5.05	0.00	3.24	4.11	41.32
1964	7.67	5.69	5.40	5.81	3.56	5.18	10.99	10.87	5.19	6.44	0.77	4.17	71.74
1965	2.12	6.24	8.13	2.45	1.70	4.28	9.63	1.75	2.11	3.00	2.18	1.31	44.90
1966	6.82	5.42	4.39	3.26	4.87	3.82	3.88	5.17	4.68	1.37	1.18	3.21	48.07
1967	3.56	3.71	7.54	2.60	4.56	2.13	6.28	7.31	1.02	0.53	2.37	2.83	44.44
1968	3.92	0.97	1.92	1.83	2.91	4.32	4.93	3.14	1.88	3.03	4.14	2.84	35.83
1969	1.85	2.13	3.43	4.20	3.41	4.36	1.99	5.43	5.96	1.96	0.34	3.83	38.89
1970	2.78	2.62	7.65	1.33	4.99	3.09	2.87	3.20	0.69	4.29	1.83	5.06	40.40
1971	5.01	3.97	8.70	2.85	2.03	6.73	11.52	9.40	2.33	4.91	2.16	3.03	62.64
1972	7.93	3.66	2.78	0.47	3.75	5.84	2.68	6.88	1.28	0.76	3.62	4.73	44.38
1973	5.31	4.82	6.48	4.97	5.17	8.52	4.50	5.83	3.22	1.22	0.35	4.69	55.08
1974	2.68	6.60	2.91	2.63	3.86	4.97	4.00	6.98	3.24	0.01	2.05	4.12	44.05
1975	5.45	6.19	5.97	3.98	5.48	3.24	7.65	3.95	7.86	1.00	4.43	4.00	59.20
1976	4.22	1.50	3.95	2.22	10.86	6.40	3.28	2.41	5.40	5.54	3.89	4.82	54.49
1977	3.86	2.20	7.90	1.02	2.61	3.79	4.02	8.43	4.66	5.44	2.07	5.14	51.14
1978	8.44	1.45	3.07	4.85	3.33	1.94	4.13	2.72	3.74	0.20	3.54	2.17	39.58
1979	3.41	9.31	3.95	5.37	7.44	1.55	7.55	9.14	7.77	1.38	7.34	2.29	66.50
1980	4.29	2.33	11.44	2.31	3.57	3.30	0.99	2.86	7.38	1.95	2.21	1.96	44.59
1981	0.93	3.91	3.87	2.71	4.51	5.05	4.39	5.92	0.85	2.88	0.91	8.45	44.38
1982	4.73	3.86	1.95	4.90	2.37	4.07	10.53	6.45	5.02	3.61	2.06	4.58	54.13
1983	4.00	8.06	5.49	4.71	3.00	2.77	3.71	6.21	3.52	2.21	4.98	3.66	52.32
1984	3.53	5.34	6.05	7.11	10.73	1.82	6.46	3.52	1.06	0.40	0.97	1.16	48.15
1985	2.98	6.36	1.06	0.83	3.49	4.88	9.82	2.90	0.90	3.77	7.51	2.74	47.24

Table7.   200-F Weather Station Monthly and Annual Precipitation for Years 1961 to 2006 - continued

Year	Jan	Feb	March	April	May	June	July	August	Sept	October	Nov	Dec	Annual
1986	1.18	3.05	2.75	0.96	3.47	2.60	2.61	8.59	0.80	3.05	5.76	4.94	39.76
1987	6.79	7.50	4.35	0.75	1.86	5.02	5.68	4.20	2.91	0.32	2.28	1.37	43.03
1988	3.74	1.03	2.48	4.88	0.97	6.67	2.24	2.98	4.79	3.50	1.92	1.66	36.86
1989	1.24	2.91	4.83	5.89	3.36	5.82	9.51	0.39	4.84	5.51	3.65	3.35	51.30
1990	2.91	1.84	1.88	0.94	2.16	3.87	7.65	10.65	0.50	17.84	1.25	2.55	54.04
1991	6.73	1.80	7.86	5.43	3.93	3.35	14.4	9.79	2.05	0.80	1.47	3.19	60.80
1992	3.63	5.32	2.93	2.74	1.54	8.28	5.18	8.70	2.42	6.21	8.57	2.96	58.48
1993	8.90	5.09	8.48	1.37	1.56	6.03	2.87	3.48	6.56	0.61	2.29	1.79	49.03
1994	4.81	3.38	6.68	0.98	1.20	4.80	5.54	5.29	1.48	10.5	2.56	4.91	52.13
1995	5.97	7.50	0.83	0.93	2.10	12.73	4.27	6.69	5.42	2.31	2.13	3.90	54.78
1996	3.08	2.08	6.81	1.69	2.40	4.59	5.55	10.58	3.14	2.09	1.46	2.97	46.44
1997	4.20	5.56	2.32	3.88	2.42	6.77	7.02	2.33	5.80	5.54	5.49	7.57	58.90
1998	8.42	6.59	6.48	5.97	3.63	3.74	4.79	3.63	8.30	0.78	0.76	1.90	54.99
1999	5.82	2.60	3.04	1.34	2.55	8.67	4.70	2.87	5.66	2.24	0.65	1.35	41.49
2000	5.80	1.06	3.06	2.08	2.27	6.02	2.90	5.84	6.47	0.02	3.86	2.02	41.40
2001	3.21	3.55	6.88	1.44	4.00	6.29	5.30	1.78	5.70	0.04	0.97	0.68	39.84
2002	2.07	2.13	3.50	2.19	1.54	2.75	4.76	6.02	3.87	3.34	5.64	4.20	42.01
2003	1.62	5.97	8.10	9.67	6.60	7.28	5.86	3.09	2.32	3.10	1.30	2.27	57.18
2004	4.63	6.81	0.99	1.69	2.47	8.49	3.01	4.21	10.54	3.32	4.11	3.81	54.08
2005	2.88	3.96	6.57	1.35	3.82	7.78	5.09	6.00	0.20	4.80	2.42	6.33	51.20
2006	3.47	3.37	2.45	3.22	1.53	7.73	5.88	1.49	2.34	2.53	3.25	5.12	42.38
Monthly Average Precip.	4.36	4.21	4.88	3.18	3.54	5.05	5.38	5.29	3.82	2.96	2.85	3.53	49.04

Notes to Table 7:
- All precipitation values in inches
- All precipitation data taken from the 200-F Weather Station, except that as noted below
- No 200-F Weather Station precipitation data is available for the following dates in the SRS ATG Climate Data database:
  - 3/30/1967 and 3/31/1967
  - 4/1/1967 through 4/18/1967
  - 11/4/1968
  - 10/31/1970
  - 1/24/1971
  - 11/27/1971
  - 10/31/1998
- The monthly data highlighted in grey represents months for which some precipitation data is missing from the 200-F weather station precipitation database. The monthly 200-F precipitation data for each month that has any missing data has been replaced with the Table 6 combined SRNL/CLM weather stations precipitation data, if the combined SRNL/CLM precipitation data for that month is greater than that of the 200-F weather station. The following denotes the replacement status of the monthly data highlighted in grey:
  - March 1967: The monthly 200-F precipitation data point of 5.29 inches was replaced with the monthly combined SRNL/CLM data point of 7.54 inches
  - April 1967: The monthly 200-F precipitation data point of 2.58 inches was replaced with the monthly combined SRNL/CLM data point of 2.6 inches
  - November 1968: The monthly 200-F precipitation data point of 2.89 inches was replaced with the monthly combined SRNL/CLM data point of 4.14 inches
  - October 1970: The monthly 200-F precipitation data point of 4.29 inches was not replaced with the monthly combined SRNL/CLM data point of 4.02 inches
  - January 1971: The monthly 200-F precipitation data point of 4.47 inches was replaced with the monthly combined SRNL/CLM data point of 5.01 inches
  - November 1971: The monthly 200-F precipitation data point of 1.75 inches was replaced with the monthly combined SRNL/CLM data point of 2.16 inches
  - October 1998: The monthly 200-F precipitation data point of 0.78 inches was not replaced with the monthly combined SRNL/CLM data point of 0.52 inches

Table 8. SRS Monthly and Annual Average Temperatures for Years 1968 to 2005

Year	Jan	Feb	March	April	May	June	July	August	Sept	October	Nov	Dec	Annual
1968	43.5	43.4	57.1	66.5	71.3	80.0	83.1	82.8	77.0	67.0	55.4	45.9	64.4
1969	46.5	46.6	51.5	64.5	70.5	80.3	83.3	77.6	72.8	66.1	52.1	45.4	63.1
1970	39.0	47.2	55.9	66.8	74.2	79.0	81.1	80.8	78.6	67.0	51.6	49.3	64.2
1971	44.6	46.4	49.5	63.4	70.7	81.3	80.7	80.4	75.2	70.2	55.5	56.9	64.6
1972	51.7	45.6	57.6	67.4	72.4	75.3	79.7	80.6	77.2	64.8	54.4	53.2	65.0
1973	46.1	45.9	60.7	61.9	70.5	77.7	79.1	74.5	70.5	62.4	59.0	50.3	63.2
1974	59.6	50.8	62.2	66.2	75.3	77.5	81.5	80.9	75.3	64.5	56.6	49.0	66.6
1975	51.4	53.2	55.8	63.9	75.6	79.1	79.7	82.4	75.7	68.7	59.3	48.5	66.1
1976	44.2	55.7	61.5	64.8	68.9	75.6	80.4	78.0	73.1	60.1	48.7	44.8	63.0
1977	35.3	47.1	60.0	66.9	73.3	80.6	83.6	80.6	77.9	62.1	58.2	46.7	64.4
1978	39.3	41.3	54.2	65.7	70.9	79.7	82.1	81.2	77.1	65.6	60.7	49.6	64.0
1979	42.1	44.6	57.5	64.5	71.3	75.1	79.6	80.5	73.4	64.8	57.4	47.4	63.2
1980	45.9	44.3	52.6	63.5	71.2	78.3	83.8	82.5	79.2	62.7	52.8	46.0	63.6
1981	40.4	48.5	53.0	67.0	68.6	81.3	81.3	76.3	74.0	62.1	54.4	43.2	62.5
1982	43.0	50.0	58.9	62.4	75.7	78.8	80.9	80.1	75.0	66.2	58.7	54.8	65.4
1983	43.3	48.0	55.3	59.4	66.8	76.7	84.3	83.9	74.8	67.2	56.4	45.8	63.5
1984	45.0	51.7	56.5	62.6	71.9	80.1	80.1	80.8	74.0	73.4	53.4	56.9	65.5
1985	42.9	49.5	60.2	67.5	74.5	80.8	81.1	79.7	75.7	70.8	65.5	45.4	66.1
1986	45.4	54.6	57.9	66.4	74.4	82.7	86.9	80.1	78.4	67.1	61.3	49.3	67.0
1987	46.2	48.6	56.5	62.3	74.5	79.9	82.8	83.8	76.6	60.7	59.1	52.9	65.3
1988	42.3	47.8	56.8	64.2	70.4	76.8	81.6	81.4	75.4	61.2	58.0	49.1	63.8
1989	52.2	52.0	58.3	64.2	70.6	79.8	81.4	80.9	75.3	67.3	52.4	44.2	64.9

Table 8.   SRS Monthly and Annual Average Temperatures for Years 1968 to 2005 - continued

Year	Jan	Feb	March	April	May	June	July	August	Sept	October	Nov	Dec	Annual
1990	54.9	57.5	60.0	64.0	72.9	80.5	83.7	83.8	79.0	69.4	59.9	54.6	68.4
1991	47.9	54.1	60.3	69.2	76.9	79.5	83.6	81.2	77.4	68.1	55.4	54.0	67.3
1992	49.5	54.1	57.2	65.0	71.2	78.9	83.7	80.7	76.9	65.0	57.1	48.0	65.6
1993	51.7	47.8	53.2	58.9	69.7	78.2	83.6	80.0	75.2	62.8	55.2	43.6	63.3
1994	41.5	50.1	60.2	68.0	71.2	82.3	81.8	81.2	77.4	67.2	62.3	53.3	66.4
1995	45.5	49.9	58.6	65.9	73.5	75.0	79.9	79.0	71.8	65.9	50.8	43.8	63.3
1996	44.6	50.1	50.6	61.6	72.9	76.5	79.3	76.0	72.7	62.1	51.6	48.8	62.2
1997	48.2	52.9	63.3	61.2	68.5	74.0	80.2	79.0	75.0	64.1	51.6	47.0	63.7
1998	49.7	51.1	53.6	62.7	74.6	82.1	82.6	80.3	75.8	66.9	60.5	53.6	66.1
1999	51.9	51.6	53.4	67.2	69.7	76.6	80.7	82.9	73.8	64.3	58.1	48.6	64.9
2000	44.4	50.2	58.5	60.7	75.1	78.0	79.9	77.6	71.7	62.5	53.1	38.2	62.5
2001	43.8	52.4	53.0	63.9	71.3	75.3	77.7	78.8	71.2	62.2	60.0	52.4	63.5
2002	47.3	48.0	57.6	68.1	70.2	77.5	80.5	78.4	75.4	66.7	51.7	44.5	63.8
2003	42.0	47.5	57.6	61.6	70.6	75.2	77.3	77.7	71.9	63.7	58.2	42.9	62.2
2004	43.7	45.2	58.5	63.4	74.0	77.7	80.1	77.3	73.2	66.2	56.1	45.8	63.4
2005	47.9	49.0	53.1	60.9	68.0	75.4	79.4	78.8	77.0	64.7	56.1	44.3	62.9
2006	50.8	47.3	55.3	66.3	70.1	76.2	80.3	80.5	72.9	62.4	53.6	50.6	63.8
Average Monthly Temp	46.0	49.3	56.8	64.4	71.9	78.3	81.3	80.1	75.1	65.3	56.2	48.4	64.4

Notes to Table 8:

- All temperatures in degree Fahrenheit (°F)
- Temperature data collected from the SRNL (773-A) weather station between 1968 and 1995 and from the CLM since 1995

humidity, wind speed, vegetation type, leaf area index, growing season, surface and soil water content, maximum evaporative depth, soil water transport, and soil capillarity. As outlined previously (see Section 4.4.14) the initial vegetative cover of the SDF Closure Cap shall be a persistent grass such as Bahia. Bamboo shall be used as the final vegetative cover only if it is determined that bamboo is a climax species that prevents or greatly slows the intrusion of pine trees onto the closure cap. Therefore at this time the HELP modeling of the SDF closure cap will be based upon the use of a grass vegetative cover rather than bamboo.

The HELP model weather data input files, which were utilized for all HELP model runs, are provided in the following appendices:

- Appendix B, Augusta Synthetic Precipitation Modified with SRS Specific Average Monthly Precipitation Data over 100 Years (file name: Fprec.d4)
- Appendix C, Augusta Synthetic Temperature Modified with SRS Specific Average Monthly Temperature Data over 100 Years (file name: Ftemp.d7)
- Appendix D, Augusta Synthetic Solar Radiation Data over 100 Years (file name: Fsolar.d13)
- Appendix E, Augusta Evapotranspiration Data (file name: Fevap.d11)

A statistical evaluation of the precipitation data set (file name: Fprec.d4) is provided in Table 9 and Table 10 as an aid to the interpretation of the HELP model infiltration results provided in subsequent sections. The precipitation data set utilized represents 100 years of synthetic daily precipitation data, developed as described. Table 9 provides a statistical evaluation of this precipitation data set in terms of both annual and daily precipitation. The annual precipitation within the data set ranges from 29.81 to 68.60 inches/ year; while the daily precipitation ranges from 0 to 6.72 inches/day. Table 10 provides the percentage frequency of daily precipitation events for the data set in 0.5 inch increments from 0 to 7.0 inches/day. No precipitation occurs on approximately 72.5 percent of the days, and on the days that precipitation does occur, the bulk of the precipitation (i.e.,
>99 percent) is in the 0 to 3 inch/day range.

Table 9.   Precipitation Data Set Annual and Daily Precipitation Statistics

Parameter	Annual Precipitation (inches/year)	Daily Precipitation (inches/day)
Maximum	68.60	6.72
Average	49.14	0.13
Median	48.83	0
Minimum	29.81	0
Standard Deviation	7.69	0.37

Table 10.   Precipitation Data Set Frequency of Daily Precipitation Events

Daily Precipitation Range (inches)	Percent of Total Days in Range	Cumulative Percent of Total Days	Percent of Days with Precipitation in Range	Cumulative Percent of Days with Precipitation
0	72.543	72.543	-	-
0 to 0.5	18.381	90.924	66.946	66.946
0.5 to 1.0	5.330	96.254	19.411	86.357
1.0 to 1.5	2.084	98.338	7.589	93.946
1.5 to 2.0	0.900	99.238	3.278	97.224
2.0 to 2.5	0.427	99.665	1.555	98.779
2.5 to 3.0	0.143	99.808	0.522	99.301
3.0 to 3.5	0.092	99.900	0.335	99.636
3.5 to 4.0	0.065	99.965	0.236	99.872
4.0 to 4.5	0.022	99.986	0.079	99.951
4.5 to 5.0	0.003	99.989	0.010	99.961
5.0 to 5.5	0.003	99.992	0.010	99.970
5.5 to 6.0	0.000	99.992	0.000	99.970
6.0 to 6.5	0.003	99.995	0.010	99.980
6.5 to 7.0	0.005	100.000	0.020	100.000

5.3 HELP MODEL GENERAL INPUT DATA

Table 11 provides a listing of the HELP model (Schroeder et al. 1994a and Schroeder et al. 1994b) general input parameters (i.e., HELP model query) and the associated values selected for the SDF Closure Cap. The reasoning for each of the selected values is discussed.

The closure cap area was based upon the maximum slope length of 825 feet as discussed in Section 4.1 and the 1-foot width as used in the Appendix A, Physical Stability Calculations. This results in a modeled landfill area of 0.0189 acres. The cap area is only used by the HELP model to estimate overall landfill water volumes associated with precipitation, runoff, evapotranspiration, lateral drainage, percolation, and change in water storage. This type of volume information is not used as input to subsequent models, therefore using the entire area of the SDF closure cap is not required.

As outlined in Section 4.1, it is assumed that the SDF Closure Cap is appropriately sloped so that 100 percent of the cap allows runoff to occur (i.e., there are no depressions).

Table 11. SDF Closure Cap HELP Model General Input Parameters and Values

Input Parameter (HELP Model Query)	Selected Input Parameter Value
Landfill area =	0.0189 acres
Percent of area where runoff is possible =	100%
Do you want to specify initial moisture storage? (Y/N)	Y
Amount of water or snow on surface =	0 in.

A "yes" response has been provided to the HELP model query, which asks, "Do you want to specify initial moisture storage? (Y/N)." Therefore the initial moisture storage has been specified for all soil layers. While the initial moisture storage is not a fixed value for all soil layers, a fixed method of selecting the initial moisture storage value has been utilized for consistency. The initial soil moisture storage value has been selected as follows:

- The initial moisture storage of soil layers designated as either a vertical percolation layer or a lateral drainage layer was set at the field capacity of the soil layer.
- The initial moisture storage of soil layers designated as a barrier soil liner was set at the porosity of the soil.

The amount of water or snow on the surface of the cap was assumed to be zero as the initial model condition.

5.4 HELP MODEL LAYER INPUT DATA

The HELP model requires the classification of each layer into one of the following classifications (Schroeder et al. 1994a; Schroeder et al. 1994b):

- Vertical Percolation Layer: Layers with this designation allow unsaturated downward water flux due to gravity and if the layer is within the evaporative zone depth of 22 inches as discussed in Section 5.2, upward water flux due to evapotranspiration.
- Lateral Drainage Layer: Layers with this designation allow unsaturated downward water flux due to gravity and saturated, down slope, lateral drainage due to the build up of positive head within the layer. A lateral drainage layer must be underlain by either a barrier soil liner or geomembrane liner.
- Barrier Soil Liner: Layers with this designation are those with lower saturated hydraulic conducitivites that are designed to restrict the downward flux of water. They are assumed to be saturated and allow saturated downward water flux due to positive head above the liner.
- Geomembrane Liner: Layers with this designation are synthetic membranes designed to restrict the downward flux of water. A saturated downward water flux due to positive head above the liner is allowed through these liners due to both holes in the liner and its saturated hydraulic conductivity.

Different HELP model inputs are required for each of the layer types as outlined in Table 12. Table 13 provides the thickness, maximum slope length, and top of layer slope associated with each of the SDF Closure Cap layers outlined in Sections 4.2 and 4.3 (Table 4). The four geotextile fabric layers outlined in Table 4 will not be included in the HELP modeling, since they act primarily to separate or protect layers rather than to perform a hydraulic function. Additionally, Table 13 provides the HELP model layer type associated with each layer. Development of the required inputs (Table 12) for each of the SDF Closure Cap layers modeled (Table 13) is discussed.

Note that the lower lateral drainage layer and the underlying disposal cell HDPE and GCL layers are not included in the HELP modeling. These layers do not extend across the cap and, therefore, cannot be handled by the HELP model. The HELP modeling provides infiltration input for the upper boundary on which to base PORFLOW modeling. Additionally, the lower drainage layer will not be included in the HELP modeling since it is two layers below the layer (i.e., GCL) through which infiltration information is desired and it has a higher saturated hydraulic conductivity than the layers (i.e., foundation layer and lower backfill layer) between it and the GCL.

5.4.1 Topsoil HELP Model Inputs

As indicated in Table 12, total porosity, field capacity, wilting point, and saturated hydraulic conductivity input values are required for the topsoil. SRS soils, utilized as top soils, would generally be classified as silty sand (SM) materials under the Unified Soil Classification System (USCS) or typically as loamy sand (LS) or sometimes as sandy loams (SL) in the United States Department of Agriculture (USDA) soil textural classification (i.e., textural

Table 12. HELP Model Required Input per Layer Type

Property	HELP Model Layer Type			
	Vertical Percolation Layer	Lateral Drainage Layer	Barrier Soil Liner	Geomembrane Liner
Thickness (in)	X	X	X	X
Total Porosity	X	X	X	na
Field Capacity [1]	X	X	X	na
Wilting Point [2]	X	X	X	na
Initial Moisture	X	X	X	na
Saturated Hydraulic Conductivity (cm/s)	X	X	X	X
Drainage Length (ft)	na	X	na	na
Drain Slope (%)	na	X	na	na
Geomembrane Pinhole Density (#/acre)	na	na	na	X
Geomembrane Installation Defects (#/acre)	na	na	na	X
Geomembrane Placement Quality	na	na	na	X

X = property input value required for that layer type

na = property input value is not applicable for that layer type

[1] The HELP model defines the field capacity as the volumetric water content (θ_v) at a soil suction head (Ψ) of 0.33 bars." (Schroeder et al. 1994a; Schroeder et al. 1994b) 0.33 bars ≈ 337 cm-H_2O (1 bar ≈ 1,020.7 cm-H_2O at 60°F)

[2] The HELP model defines the wilting point as the volumetric water content (θ_v) at a soil suction head (Ψ) of 15 bars." (Schroeder et al. 1994a; Schroeder et al. 1994b) 15 bars ≈ 15,310 cm-H_2O (1 bar ≈ 1,020.7 cm-H_2O at 60°F)

Table 13.   SDF Closure Cap LayerThickness, Slope Length, Slope and Layer Type

Layer	Thickness (inches)	Maximum Slope Length (ft)	Top of Layer Slope (%)	HELP Model Layer Type
Topsoil	6	825	2	1
Upper Backfill	30	825	2	1
Erosion Barrier	12	825	2	1
Middle Backfill	12 (minimum)	825	2	1
Lateral Drainage Layer	12	825	4	2
High Density Polyethylene (HDPE) Geomembrane	0.06 (60 mil)	825	4	4
Geosynthetic Clay Liner (GCL)	0.2	825	4	3
Foundation Layer	12	825	4	1
Lower Backfill	12 (minimum)	825	4	1

Within the HELP model the layer types are denoted by the following numeric designations:
1 = vertical percolation layer
2 = lateral drainage layer
3 = barrier soil liner
4 = geomembrane liner

triangle). Yu et al. 1993 provides total porosity, water retention (suction head versus saturation), and saturated hydraulic conductivity data for two samples of SRS topsoil.

Yu et al. (1993; page 1-5) provides the saturated hydraulic conductivity and porosity for two SRS topsoil samples. The average values of saturated hydraulic conductivity and porosity of the two SRS topsoil samples were used in the HELP modeling:

Sample ID	Saturated Hydraulic Conductivity, K_{sat} (cm/s)	Porosity, η (vol/vol)
Top Soil – 1	3.06E-03	0.405
Top Soil – 2	3.13E-03	0.388
Average	3.1E-03	0.396

See the notes from Table for the HELP model definition of field capacity and wilting point. Volumetric moisture content can be determined as follows (Hillel 1982):

$$\theta_v = \eta s , \quad \text{where } \theta_v = \text{volumetric moisture content; } \eta = \text{porosity; } s = \text{saturation}$$

The following information was obtained from the table on page 1-9 of Yu et al. (1993) for water retention (suction head versus saturation) testing of topsoil samples from which the

field capacity (volumetric water content at 0.33 bars or 337 cm-H_2O) can be derived by linear interpolation:

Sample ID	Applied Pressure	
	4 psi (281.2 cm-H_2O)	8 psi (562.5 cm-H_2O)
Top Soil – 1	0.298	0.257
Top Soil – 2	0.266	0.239
Average	0.282	0.248

All values are saturations (*s*) in vol/vol format
1 psi ≈ 70.3087 cm-H_2O at 4°C

The following provides the linear interpolation used to determine the top soil field capacity based upon the above top soil water retention data, which will be used in the HELP modeling:

Field capacity = θ_v at 337 cm-H_2O = $\eta \times s$ at 337 cm-H_2O =

$$0.396 \times \left(0.248 + \left[\left(\frac{562.5 - 337}{562.5 - 281.2} \right) (0.282 - 0.248) \right] \right) = 0.109$$

Site specific data are not available for the determination of SRS top soil wilting point. Therefore the wilting point from a HELP model default soil that closely resembles the SRS top soil will be utilized. Table 1 of Schroeder 1994b provides HELP model default soils. The HELP model default soil #4, with a wilting point of 0.047, that is classified as a SM material (USCS) and a LS material (USDA) is considered the closest HELP model default soil to the SRS top soil. Therefore the SRS top soil will be assigned a wilting point of 0.047 for the HELP modeling.

A comparison of the SRS top soil with HELP model default soil #4 is provided:

Material	Porosity, η (vol/vol)	Field Capacity (vol/vol)	Wilting Point (vol/vol)	Saturated Hydraulic Conductivity, K_{sat} (cm/s)
HELP model default soil #4 [1]	0.437	0.105	0.047	1.7E-03
SRS top soil	0.396	0.109	-	3.1E-03

[1] Schroeder 1994b Table 1

5.4.2 Upper, Middle, and Lower Middle Backfill HELP Model Inputs

As indicated in Table 12, total porosity, field capacity, wilting point, and saturated hydraulic conductivity input values are required for the upper backfill and middle backfill. Phifer et al. (2006) provides recommended values of total porosity, characteristic curves (suction head,

saturation, and relative permeability), and saturated hydraulic conductivity for control compacted backfill placed over the Old Radioactive Waste Burial Ground (643-G) and for remolded samples from Z-Area soils. The field capacity and wilting point can be derived from characteristic curve data. The 643-G and Z-Area materials represent typical SRS control compacted backfill, consisting of soils classified typically as clayey sands (SC) or sometimes silty sands (SM) materials under USCS or as sandy clay loam (SCL) in the USDA soil textural classification (i.e. textural triangle) that have been compacted to specified test standards.

From Table 5-18 of Phifer et al. (2006), the following recommended backfill property values were obtained, which will be utilized in the HELP modeling:

- Total porosity (η) = 0.35
- Vertical saturated hydraulic conductivity (K_{sat}) = 4.1E-05 cm/s

Use of the vertical saturated hydraulic conductivity within the HELP model for the backfill materials is considered appropriate, since the backfill has been designated as a vertical percolation layer within the model subject to vertical flow considerations only.

See the notes from Table for the HELP model definition of field capacity and wilting point. Volumetric moisture content can be determined as follows (Hillel 1982):

$$\theta_v = \eta s, \quad \text{where } \theta_v = \text{volumetric moisture content; } \eta = \text{porosity; } s = \text{saturation}$$

Backfill characteristic curve data was obtained from the Phifer et al. 2006, Table 5-21. From this data the field capacity (volumetric water content at 0.33 bars or 337 cm-H_2O) and wilting point (volumetric water content at 15 bars or 15,310 cm-H_2O) of the backfill were derived by linear interpolation:

Suction Head Ψ (cm-H_2O)	Saturation s (vol/vol)
331	0.721
381	0.711
14,400	0.519
16,600	0.513

The following provides the linear interpolation used to determine the backfill field capacity and wilting point, respectively, based upon the above backfill characteristic curve data, which will be used in the HELP modeling:

Field capacity = θ_v at 337 cm-H_2O = $\eta \times s$ at 337 cm-H_2O =

$$0.35 \times \left(0.711 + \left[\left(\frac{381 - 337}{381 - 331} \right) (0.721 - 0.711) \right] \right) = 0.252$$

Wilting point = θ_v at 15,310 cm-H$_2$O = $\eta \times s$ at 15,310 cm-H$_2$O =

$$0.35 \times \left(0.513 + \left[\left(\frac{16,600 - 15,310}{16,600 - 14,400} \right)(0.519 - 0.513) \right] \right) = 0.181$$

5.4.3 Erosion Barrier HELP Model Inputs

As indicated in Table , total porosity, field capacity, wilting point, and saturated hydraulic conductivity input values are required for the erosion barrier. As outlined within Section 4.4.11, the erosion barrier shall consist of rock consistent with Type B riprap from Table F-3 of Johnson (2002) or Size R-20 riprap from Table 1 of ASTM (1997) that is filled with a yet to be determined material (see Section 4.4.11) to prevent the loss of overlying material into the erosion barrier. The SDF configuration includes an erosion barrier infilled with a sandy soil.

This results in a combined material with the following properties:

Erosion Barrier Infill Material	Porosity, η (vol/vol)	Field Capacity (vol/vol)	Wilting Point (vol/vol)	Saturated Hydraulic Conductivity, K_{sat} (cm/s)
Erosion barrier with sandy soil infill	0.15	0.10	0.07	1.3E-04

See Appendix F for the calculations associated with the soil properties for the erosion barrier.

5.4.4 Upper Lateral Drainage Layer HELP Model Inputs

As indicated in Table 12, total porosity, field capacity, wilting point, and saturated hydraulic conductivity input values are required for the lateral drainage layer. As outlined within Section 4.4.7, the upper lateral drainage layer shall consist of a 1-foot thick layer of coarse sand. The sand utilized for the lateral drainage layer will be a procured material rather than a material obtained from a SRS borrow pit. Therefore a minimum saturated hydraulic conductivity of the sand will be a requirement in the specification for the procurement of the sand. Table 14 provides the saturated hydraulic conductivity of various sands. The saturated hydraulic conductivity of the natural sands in Table ranges from 1E-04 to 1 cm/s. The saturated hydraulic conductivity of the procured sands in Table 14 ranges from 5.0E-02 to 4.5E-01 cm/s. Based upon this information, a minimum saturated hydraulic conductivity of 5.0E-02 cm/s will be specified for the lateral drainage layer sand. The total porosity, field capacity, and wilting point for the HELP modeling will be taken as that of the HELP model default soil #1 (i.e., natural coarse sand (USDA) or poorly graded sand (USCS)) as shown below (Schroeder et al. 1994b):

- Total porosity (η) = 0.417
- Field capacity = 0.045
- Wilting point = 0.018

Table 14.   Sand Saturated Hydraulic Conductivity

Material	Saturated Hydraulic Conductivity, K_{sat} (cm/s)	Source
SRS water table aquifer at the TNX Terrace	2.1E-02	Phifer et al. 2001 Table 5
Natural deposit of clean sand	<1E-03 to 1	Freeze and Cherry 1979 Table 2.2
Clean sand or sand and gravel	1E-03 to 1	Bear 1972 Table 5.5.1
Various natural sands	1E-04 to 2.0E-01	Lamb and Whitman 1969 Figure 19.5
Sedimentary deposit of well-sorted sand, glacial outwash	1E-03 to 1E-01	Fetter 1988 Table 4.5
Sandy soils	1E-03 to 1E-02	Hillel 1982
HELP model default soil #1 [1]	1E-02	Schroeder et al. 1994b Table 1
Foster Dixianna FX-50 fine gravel pack	5.0E-02	Phifer et al. 2001 Table 7
Foster Dixianna FX-99 coarse gravel pack	4.5E-01	Phifer et al. 2001 Table 7
Fine gravel	1.5E-01	Phifer et al. 2006 Table 5-18 and Yu et al. 1993

Notes:

Materials in grey are natural sands and the other items are procured materials.

[1] HELP model default soil #1 is a natural coarse sand (USDA) or poorly graded sand (USCS)

5.4.5 HDPE Geomembrane HELP Model Inputs

As indicated in Table 12, saturated hydraulic conductivity, geomembrane pinhole density, geomembrane installation defects, and geomembrane placement quality input values are required for the HDPE geomembrane. The permeability of water through HDPE geomembranes is not a hydraulic conductivity through interconnected pore space, but rather it is a water vapor diffusional process (Rumer and Mitchell 1995). Therefore the water permeability of HDPE geomembranes is not determined by standard hydraulic conductivity tests performed for porous materials but by a water vapor transmission test (ASTM 2005a). A typical value of water vapor transmission through a 100 mil HDPE geomembrane is approximately 0.006 g/m^2-day, which equates to a saturated hydraulic conductivity of approximately 1.0E-13 cm/s (Koerner et al. 1990; Rumer and Mitchell 1995). Schroeder et al. 1994b Table 6 uses a saturated hydraulic conductivity of 2.0E-13 cm/s as the default value for HDPE geomembranes within the HELP model (HELP model default geosynthetic material #35). A saturated hydraulic conductivity of 2.0E-13 cm/s will be utilized for the 60 mil HDPE geomembrane within the HELP modeling, since it is the higher of those documented.

Layers designated as geomembrane liners (HELP model layer type #4) do not require the input of total porosity, field capacity, and wilting point as required for soil layers. However, geomembrane liners do require the additional input of geomembrane pinhole density (#/acre), geomembrane installation defects (#/acre), and geomembrane placement quality. Within the HELP model (Schroeder et al. 1994a; Schroeder et al. 1994b), geomembrane pinholes are defined as manufacturing defects such as polymerization deficiencies that result in holes estimated to be 1 mm in diameter (7.84E-03 cm^2).

The following is stated concerning pinholes (Schroeder et al. 1994b):

"… Pinhole flaws are more commonly associated with the original, less sophisticated, geomembrane manufacturing techniques. Current manufacturing and polymerization techniques have made pinhole flaws less common."

Schroeder et al. 1994a recommends that "typical geomembranes may have about 0.5 to 1 pinhole per acre from manufacturing defects." Based upon this guidance, the as-installed SDF Closure Cap HDPE geomembrane will be assumed to have 1 pinhole/acre.

Within the HELP model (Schroeder et al. 1994a; Schroeder et al. 1994b), geomembrane installation defects are defined as geomembrane damage resulting from seaming errors, abrasion, and punctures occurring during installation that result in holes estimated to be 1 cm^2 in area (1.13 cm in diameter). Schroeder et al. 1994b recommends an installation defect density of 1 defect per acre for intensively monitored projects and 10 defects per acre or more "when quality assurance is limited to spot checks or when environmental difficulties are encountered during construction". In summary Schroeder et al. 1994a provide the following installation defect densities based upon the quality of installation:

Installation Quality	Installation Defect Density (#/acre)	Frequency [1] (percent)
Excellent	Up to 1	10
Good	1 to 4	40
Fair	4 to 10	40
Poor	10 to 20	10

[1] Provides the frequency of landfill installation built to that particular level of quality assurance.

As outlined within Section 4.4.5, the HDPE geomembrane quality assurance plan shall be developed and implemented for 100-percent visual inspection of all rolls as they are laid down and of all seams; appropriate wrinkle control measures as the rolls are laid down, seamed, and covered; 100-percent non-destructive field testing of all seams by vacuum testing (ASTM 2006a) and/or air pressure testing (ASTM 2006b); and destructive testing (ASTM 2006c) on a frequency consistent with GRI (1998). Any seam or non-seam area that has been identified as defective and any holes created for destructive testing shall be repaired and non-destructively tested prior to acceptance. Additionally a nonwoven geotextile fabric will be placed directly on top of the HDPE geomembrane to protect it from puncture or tear during placement of the overlying 1-foot thick coarse sand lateral drainage layer.

Based upon these SDF Closure Cap requirements and the guidance provided by Schroeder et al. (1994a) and Schroeder et al. (1994b), the as-installed SDF Closure Cap HDPE geomembrane will be assumed to be installed with good quality assurance and will be assumed to have 4 installation defects/acre.

Within the HELP model (Schroeder et al. 1994a; Schroeder et al. 1994b), six geomembrane placement quality designations are provided. These geomembrane placement quality designations relate to the degree of contact between the geomembrane and the underlying soil and the potential for lateral flow along the boundary between the two layers. Schroeder et al. 1994b states the following regarding the geomembrane placement quality for geomembranes underlain by a GCL:

> "Excellent liner contact is achieved under three circumstances. Medium permeability soils and materials are typically cohesionless and therefore generally are able to conform to the geomembrane, providing excellent contact. The second circumstance is for very well prepared low permeability soil layer with exceptional geomembrane placement typically achievable in the laboratory, small lysimeters or small test plots. The third circumstance is by the use of a GCL adjacent to the geomembrane with a good foundation. The GCL, upon wetting, will swell to fill the gap between the geomembrane and the foundation, providing excellent contact."

Based upon the use of a GCL beneath the HDPE geomembrane for the SDF closure cap and the guidance provided by Schroeder et al. 1994a and Schroeder et al. 1994b, an "excellent" (HELP model numerical designation 2) geomembrane placement quality designation will be used.

5.4.6 GCL HELP Model Inputs

As indicated in Table 12 total porosity, field capacity, wilting point, and saturated hydraulic conductivity input values are required for the GCL. Schroeder et al. (1994a) Table 4 and Schroeder et al. (1994b) Table 2 provide the following default property values for bentonite mats (i.e. GCLs):

- Total porosity (η) = 0.750
- Field capacity = 0.747
- Wilting point = 0.400
- Saturated Hydraulic Conductivity (K_{sat}) = 3.0E-09 cm/s

GCL manufacturers typically list the maximum hydraulic conductivity of GCLs as 5.0E-09 cm/s. Dixon and Phifer (2006) reported the results of 9 saturated hydraulic conductivity measurements made on a GCL (BentoFix® Thermal Lock® NWL) manufactured by GSE Lining Technology, Inc., with simulated groundwater as the permeant. This GCL was utilized as part of the closure cap placed on the SRS Old Radioactive Waste Burial Ground (643-G).

The following provides the results of this testing:

GSE Lining Technology, Inc. BentoFix® Thermal Lock® NWL Saturated Hydraulic Conductivity		
GSE Specification	SRS Testing (Dixon and Phifer 2006)	
	Range	Average
5.0E-09 cm/s (maximum)	1.4E-09 to 4.1E-10 cm/s	6.81E-10 cm/s

All of the Dixon and Phifer (2006) saturated hydraulic conductivity values were well below the manufacture's specification of 5.0E-09 cm/s and the HELP model default value of 3.0E-09 cm/s. However, since the manufacturers typically list the maximum hydraulic conductivity of GCLs as 5.0E-09 cm/s, the manufacturers' value will be used for the SDF Closure Cap HELP modeling. The values of total porosity, field capacity, and wilting point recommended by Schroeder et al. (1994a) and Schroeder et al. (1994b) will also be used for the SDF Closure Cap HELP modeling.

5.4.7 Foundation Layer HELP Model Inputs

As outlined within Section 4.4.3, it is anticipated that one foot of material will consist of backfill soil with a moderately low permeability (i.e., ≤1.0E-06 cm/s) produced by blending typical SRS backfill with a small weight percent bentonite. Since it is anticipated that the foundation layer will consist of typical SRS backfill with a small weight percent bentonite, the porosity, field capacity, and wilting point of typical SRS backfill from Section 5.4.2 will be utilized for this portion of the foundation layer as shown below:

- Total porosity (η) = 0.35
- Field capacity = 0.252
- Wilting point = 0.181
- Saturated Hydraulic Conductivity (K_{sat}) = 1.0E-06 cm/s

5.4.8 HELP Model Layer Summary Input Data

Table 15 provides a summary of the initial intact HELP Model inputs for each of the SDF closure cap layers modeled.

Table 15.   Initial Intact HELP Model Input Summary for the SDF Closure Cap Layers

Layer	HELP Model Layer Type	Thickness (in)	Total Porosity	Field Capacity	Wilting Point	Initial Moisture [1]	Saturated Hydraulic Conductivity (cm/s)	Drainage Length (ft)	Drain Slope (%)
Topsoil	1	6	0.396	0.109	0.047	0.109	3.1E-03	na	na
Upper Backfill	1	30	0.35	0.252	0.181	0.252	4.1E-05	na	na
Erosion Barrier: (Assumes Sandy Soil Infill)	1	12	0.15	0.10	0.07	0.10	1.3E-04	na	na
Middle Backfill	1	12	0.35	0.252	0.181	0.252	4.1E-05	na	na
Lateral Drainage Layer	2	12	0.417	0.045	0.018	0.045	5.0E-02	825	4
HDPE Geomembrane	4	0.06 (60 mil)	na	na	na	na	2.0E-13	na	na
GCL	3	0.2	0.750	0.747	0.400	0.750	5.0E-09	na	na
Foundation Layer	1	12	0.35	0.252	0.181	0.252	1.0E-06	na	na
Lower Backfill Layer	1	72	0.457	0.131	0.058	0.131	1.0E-03	na	na

Layer	Geomembrane Pinhole Density (#/acre)		Geomembrane Installation Defects (#/acre)		Geomembrane Placement Quality	
HDPE Geomembrane	1		4		2	

[1] The initial soil moisture storage value has been selected as follows:

- The initial moisture storage of soil layers designated as either a vertical percolation layer or a lateral drainage layer was set at the field capacity of the soil layer.
- The initial moisture storage of soil layers designated as a barrier soil liner was set at the porosity of the soil.

5.5 HELP MODEL RUNOFF INPUT DATA

The Soil Conservation Service (SCS) runoff curve number (CN) is another required HELP model input parameter. The HELP model provides three options to specify the CN. The option that produces a HELP model computed curve number, based on surface slope and slope length, soil texture of the top layer, and vegetation, was utilized. Table 16 provides the input values of surface slope and slope length, soil texture of the top layer, and vegetation that were utilized to produce the HELP model computed curve number. The 1.5 percent slope at a maximum 825-foot slope length was derived within Section 4.2. The soil texture selected (i.e., HELP model default soil #4) was selected as outlined in Section 5.4.1 above as being the closest HELP model default soil to typical SRS top soil. The HELP model (Schroeder et al. 1994a; Schroeder et al. 1994b) provides the following entries for the vegetation for determination of the CN:

1. Bare ground
2. Poor stand of grass
3. Fair stand of grass
4. Good stand of grass
5. Excellent stand of grass

As outlined in Section 4.4.14, the SDF closure cap initial vegetative cover shall be established and maintained such that a persistent, self maintaining, grass cover is provided. Based upon this requirement a good stand of grass (i.e., HELP model designation 4) will be utilized in the modeling. Based upon these input parameter values the HELP model computed a CN of 46.2.

Table 16.   HELP Model Computed Curve Number Input Parameters

CN Input Parameter (HELP Model Query)	CN Input Parameter Value
Slope =	1.5%
Slope length =	825 ft
Soil Texture =	4 (HELP model default soil texture)
Vegetation =	4 (i.e., a good stand of grass)
HELP Model Computed Curve Number = 46.2	

6.0 POTENTIAL SDF CLOSURE CAP DEGRADATION MECHANISMS

Potential SDF closure cap degradation mechanisms presented in this section are discussed in context of the base case land use scenario (i.e., institutional control to pine forest, land use scenario). This scenario assumes a 100-year institutional control period following SDF closure cap construction during which the closure cap is maintained (see Section 2.0). At the end of institutional control, it is assumed that a pine forest succeeds the cap's original vegetative cover. This discussion has been adapted for the SDF closure cap from Phifer et al. (2007).

Table 17 provides a list of potential SDF closure cap degradation mechanisms that were taken into consideration for the estimation of infiltration through the closure cap over time. The table lists the potential degradation mechanisms associated with each of the major SDF closure cap layers, other than backfill layers located below the erosion barrier. Waste Layer subsidence is not considered an applicable degradation mechanism to the SDF closure cap, since the disposal cells will be filled with Saltstone. Additionally, chemical degradation from contact with waste leachate is generally not applicable to closure caps, since they are located above the waste layer. For the SDF closure cap, waste is contained within disposal cells located a minimum of seven feet below any closure cap layer that could be significantly affected by leachate. Therefore chemical degradation of the SDF closure cap by leachate is not considered applicable.

Finally, degradation of sand layers due to mineral precipitation and microbial growth are primarily degradation mechanisms associated with leachate collection layers rather than closure cap lateral drainage layers. Leachate collection layers receive leachate containing both organic and inorganic degradation products from the waste; whereas closure cap lateral drainage layers only receive non-contaminated water from infiltration (in the case of SRS, infiltrating water is very low in both mineral and organic content). Therefore mineral precipitation and microbial growth within the lateral drainage layer is not considered an applicable degradation mechanism. Since waste layer subsidence, chemical (waste leachate) degradation, and mineral precipitation and microbial growth within the lateral drainage layer are not applicable to the SDF closure cap, they will not receive further consideration. Subsequent sections will discuss the other potential SDF closure cap degradation mechanisms outlined in Table 17.

Table 17. Potential SDF Closure Cap Degradation Mechanisms

Affected Layer	Potential Degradation Mechanism
All	• Static loading induced settlement • Seismic induced liquefaction and subsequent settlement • Seismic induced slope instability • Seismic induced lateral spread • Seismic induced direct rupture due to faulting • Waste Layer Subsidence [1]
Vegetative cover	• Succession • Stressors (droughts, disease, fire, and biological)
Soil above the erosion barrier	• Erosion • Desiccation (wet-dry cycles)
Erosion barrier	• Weathering (Dissolution) • Biological (root penetration, burrowing animals) • Chemical (waste leachate) [2]
Lateral drainage layers	• Silting-in • Biological (root penetration; upper drainage layer only) • Mineral precipitation and microbial growth[3]
High density polyethylene (HDPE) geomembrane	• Ultraviolet (UV) radiation • Antioxidant depletion • Thermal oxidation • High energy irradiation • Tensile stress cracking • Biological (microbial, root penetration, burrowing animals) • Chemical (waste leachate) [2]
Geosynthetic clay liner (GCL)	• Slope stability • Freeze-thaw cycles • Dissolution • Divalent cations (Ca^{+2}, Mg^{+2}, etc.) • Desiccation (wet-dry cycles) • Biological (root penetration, burrowing animals) • Chemical (waste leachate) [2]

[1] Waste Layer subsidence is not considered applicable to the SDF Closure Cap since the Disposal cells will be filled with grout.

[2] Chemical degradation of the erosion barrier, HDPE, geomembrane, and GCL from leachate associated within the disposal cells is not considered applicable to the SDF Closure Cap, since the erosion barrier, HDPE geomembrane, and GCL will be located above the disposal cells.

[3]Mineral precipitation and microbial growth within the lateral drainage layers is not considered applicable to the SDF closure cap, since infiltrating SRS water is very low in both mineral and organic content and the layers will not contact waste leachate.

6.1 POTENTIAL STATIC LOADING AND SEISMIC INDUCED DEGRADATION

As outlined in Table 17, the following five, potential static loading and seismic induced degradation mechanisms will be considered versus their impact upon the overall closure cap:

- Static loading induced settlement
- Seismic induced liquefaction and subsequent settlement
- Seismic induced slope instability
- Seismic induced lateral spread
- Seismic induced direct rupture due to faulting

At the SRS, the first three potential degradation mechanisms above require attention during design. The latter two are of no consequence as the conditions at the SRS are not conducive to lateral spreading (at least not at the locations of the postulated cover system) and surface faulting is non-existent in the Southeast United States.

Settlement will occur due to two phenomena: first settlement due to the static load of the cap system itself, and second settlement due to seismic shaking (liquefaction or partial liquefaction). The current SDF closure cap concept indicates that the thickness of the cover system will be on the order of 25-ft to 45-ft over the disposal cell tops. It is expected that static settlement due to this load (approximately 4.200 psf) would be less than 2 to 3 inches, based on previous analyses in nearby F-Area. This amount of settlement would be expected to occur uniformly over the entire area of the cap, thus differential settlement would be negligible assuming the subsurface conditions are relatively uniform.

Settlement due to liquefaction or partial liquefaction is a result of the dissipation of excess porewater pressures that have been elevated due to a seismic event. Previous studies in F-Area (for PC-3 seismic events, return period of 2,500 years, peak ground acceleration (PGA) of 0.16 g, and a repeat of the 1886 Charleston event) indicate these settlements should be on the order of a few inches, and that they too should be rather uniform.

The stability of the SDF closure cap will depend on the final geometry of the system and the strength of the materials used. Given the types of soils used for construction of these systems global slope stability should not be an issue. Side slopes would vary probably between 3 horizontal (h) and 1 vertical (1) to 5 h to 1 v depending on the actual strength of the compacted soil, the final height of the embankment, the seismic coefficient used (for seismic design), and the actual subsurface conditions beneath the cover system.

Interface stability can actually control the design of the system, particularly under seismic conditions. Interface stability refers to the stability between interfaces of various geosynthetic materials and between geosynthetic materials and soil. This can be a key issue and depends heavily on environmental conditions.

In both cases it is fully expected that a stable design can be achieved with reasonable slopes and grades given the known subsurface conditions and the types of fill materials that would be used.

Since seismic induced lateral spreading and surface faulting are of no consequence at SRS they will not be considered as a SDF closure cap degradation mechanism for modeling purposes. The final design of the SDF closure cap will appropriately consider and handle static loading induced settlement, seismic induced liquefaction and subsequent settlement, and seismic induced slope instability, so that they are designed out as SDF closure cap degradation mechanisms; therefore they will not be considered as a SDF closure cap degradation mechanism for modeling purposes.

6.2 POTENTIAL VEGETATIVE COVER DEGRADATION MECHANISMS

As presented in Table 5 and Section 4.4.14, a vegetative cover will be established on the SDF closure cap to promote runoff, minimize erosion, and promote evapotranspiration. The initial vegetative cover shall be a persistent turf grass consisting predominately of bahia (*Paspalum notatum*). As discussed in Section 2.0, it is assumed that a 100-year institutional control period will begin after installation of the closure cap, during which active SDF facility maintenance will be conducted. This active maintenance will sustain a self maintaining, healthy, vigorous cover of the bahia grass throughout the 100-year institutional control period. As part of the maintenance conducted during the institutional control period, an area of 400-feet surrounding the SDF closure cap will be maintained in grass and the establishment of trees within this area will be prevented. Based upon this maintenance it will be assumed that mature pine trees exist at the edge of the maintenance boundary but that no pine trees exist within the area at the end of institutional control. This will result in the nearest mature pine tree stand being at least 400 feet from the SDF closure cap at the end of institutional control. After the institutional control period, it is assumed that a 10,000-year post-closure compliance period will begin, during which no active SDF facility maintenance will be conducted.

As outlined in Table 17 the following five potential degradation mechanisms will be considered for the vegetative cover:

- Succession
- Droughts
- Disease
- Fire
- Biological

The following provides a discussion of possible vegetation transition (succession) and stressors (droughts, disease, fire, and biological), based on typical events occurring in the SRS region, that are likely to occur after active SDF facility maintenance has ceased. The vegetative transition discussed is basically one from an old field community into an upland pine community (Odum 1960; Pinder 1975).

Bahia is a very hardy species in this region, and will continue to be a dominant ground cover for many years after active maintenance has ceased (McCarty 2003). However, without active maintenance, the pattern of vegetation on the cap will begin to change over time. Because of the location of the closure cap relative to the surrounding landscape and the top soils routinely used in capping projects (see Section 6.3.2), the site is expected to not be extremely moist or fertile. The scenarios discussed reflect this aspect of the microenvironment that the cap provides.

After active maintenance ceases, over time there will likely be some deterioration of the bahia cover, from many possible disturbances. Bahia is a low-growing creeping perennial species of grass with stolons and stout rhizomes. The stolons typically grow along the ground, have short innernodes, and root freely from the nodes, thus forming a dense sod. The species is deeply rooted and contains thick branching rhizomes. Most roots occur in the top 6 inches, but some may extent to 12 inches in non-compact soils (Gates et al. 1999). The species is very drought hardy and does not require frequent fertilization, although it does benefit from applications. It will remain a primary component of the community after maintenance stops until it begins to be reduced due to light competition.

During this transition period, numerous biotic and abiotic factors will influence the exact nature and timing of succession. These could include drought, insects, diseases, fire, etc. The basic biology and ecology of bahia and many of the early invaders will typically be altered only slightly due to biotic factors. This can result in a minimum lengthening of the time sequence of advancement. The possible exception is the occurrence of fire during the early successional years. This would tend to delay the advancement of the shrub and pine community until an interval after the last fire occurrence. When the interval between fires is long enough for the encroaching pine saplings to become tall enough to withstand fire disturbance and survive, the successional pattern to a pine dominated stand will proceed. This is the normal successional pattern for the SRS region.

During the first 10 years after active maintenance ceases, a number of early successional herbaceous species will begin to colonize the site, as well as other grass species (Odum 1960). Typical of the new herbaceous species are horseweed (*Erigeron canadense*), yellow aster (*Haplopappus divaricatus*), and sheep sorrel (*Rumex acetosella*), and the grass broomsedge (*Andropogon* spp.). Also expected to begin invasion during this early transitional period are blackberry (*Rubus* spp.) and loblolly pine (*Pinus taeda*) (Golley 1965; Golley and Gentry 1966). The herbaceous and vine species that are early invaders typically have well developed root systems to take advantage of the soil resource, but rarely extend beyond 18 inches.

The closure cap will be an upland, better drained site due to cap construction techniques and become somewhat less diverse than mixed species upland hardwood sites. Loblolly pine is expected to become the dominant species over time. This will be a progression over time and produce a mixed age pine stand that will become self perpetuating. There will be a small component of mixed hardwoods in the understory and sapling layers of the forest, and would include turkey oak (*Quercus laevis*), sweetgum (*Liquidambar styraciflua*), and black cherry (*Prunus serotina*).

These species will not become dominant or co-dominant trees and will remain suppressed in the understory. They typically have more evenly distributed root patterns and will not extent the six feet to the HDPE geomembrane in this community structure (Zutter et al. 1999). Shrubs and vines typical of this community type would also be present and would include sparkleberry (*Vaccinium* spp.), poison ivy (*Rhus radicans*), green briar (*Smilax* spp.) and grape (*Vitis* spp.; Jones et al. 1981). As previously mentioned, the vine species can produce large root and tuber mass below ground, but typically do not extend more than 18 to 24 inches into the soil. Loblolly pine has a much deeper root system as described below that could potentially damage the composite hydraulic barrier of the SDF Closure Cap. Due to the potential closure cap damage caused by loblolly pine roots, the succession of pine trees is discussed in detail. Encroachment by loblolly pine would begin initially along the edges of the maintained area and progressively work towards the closure cap and eventually cover the cap.

Seed production of loblolly pine in the South East region is typically good to heavy, but can vary by individual year. Individual trees as young as 10 years old have produced viable seed, but the seed production typically increases from 30 to 50 years of age (40 years is taken as representative for this discussion) for dominant and co-dominant trees at an individual site (Fowells 1965). Production continues at this maximum rate throughout the remaining life of the tree. Seed production can vary between 18,000 and 300,000 seeds per acre in natural stands.

Loblolly pine has a winged seed that is typically dispersed and disseminated by wind. The cones and seeds ripen to maturity during early October and seeds are released as the cones open in the upper portion of the canopy. When natural stands are cut, seed dispersal from the remaining edge of the forest generally results in 85% of the subsequent seeds being released falling within 200 feet of the boundary (Pomeroy and Korstian 1949). Migration into old fields, where dispersal of seed is less restricted, establishment of less than 1000 seedlings per acre at 330 feet from the seed source have been noted (McQuilkin 1940). Prevailing wind direction at the SDF closure site during the month of October is from the southwest, as recorded in historic SRS meteorological data base. According to the planned closure scenario, the distance from the nearest seed source to the southwest will be approximately 400 feet. This prevailing southwest wind direction will result in seedlings being established in a direction perpendicular to the long axis of the closure cap, over a cap-width distance of approximately 1,400 ft. The other nearby seed sources are at least 400 feet distant, and not in the appropriate wind direction pathway for dispersal toward to closure cap.

According to the expected seed sources and dispersal of the seed, movement of loblolly pine across grassed areas towards the closure cap will be a sequential process. Seedlings will become established in harvested areas as institutional control is removed at a conservative rate of 400 feet the first seed dispersal event. These trees would subsequently mature and produce seed after 40 years.

Because the closure cap will be approximately 30 to 70 feet taller than the surrounding landscape, this will present an additional barrier to the wind dispersal of loblolly pine seeds. Individual trees that provide the initial seeds upon the actual closure cap will have to be tall enough that the gravity/wind movement will allow them to fall on the cap itself. After active

maintenance is ceased it is anticipated that at least 2 cycles of 40 years will be required begin establishment of pine seedlings on top of the closure cap. The distance over the cap in the predominant wind direction (from southwest to northeast) ranges from about 1,350 ft to 1,600 ft. A conservative distance of 1,400 ft will be used to estimate time of seed dispersal/tree growth over the cap (conservative because this shorter distance is covered more quickly than a longer or even average distance). Once the seedlings become established on the closure cap, the migration to disperse seed over the entire cap area would probably be accomplished in the succeeding seven 40-year periods (i.e., over the entire 1,400 –foot cap width in 7 periods covering 200-ft each; requiring 360 years from the end of institutional control for establishment of mature pine over the entire closure cap). At this point, the natural pattern of pine forest cycling detailed below will become the norm.

The long-term continuance of a pine forest community on a closure cap has been previous discussed and referenced (Phifer and Nelson 2003), and the relevant aspects are repeated here with appropriate modifications (Bohm (1979), Burns and Hondala (1990), Ludovici et al. (2002), Taylor (1974), Ulrich et al. (1981), Walkinshaw (1999), and Wilcox (1968)). Because of the age structure difference from edge to center and across the cap due to age of the overstory individuals, the second generation, and subsequent ones, will also probably be variable across the cap. Decline of individual loblolly trees will begin around 100 years of age. After the second establishment, the new seedlings will be established as "gaps" occur in the overstory, either through the decline or death of a dominant tree, or through abiotic occurrences (wind throw, lightning strikes, fire, insect outbreak, tornado, etc.). This will tend towards making the entire acreage an uneven age, constantly re-establishing forest. In this region, fire may be quite important in the long-term ecology of the cap. Fire will reduce the smaller understory individuals and seedlings, but will have minimal impact on the dominant individuals.

It is anticipated that tree density will remain fairly constant. For a natural regeneration stand over a 100-year period, the tree density is assumed to be approximately 550 dominant and co-dominant trees per acre with approximately 400 mature (i.e., 40 to 125 years old) trees per acre. It is assumed that complete turnover of the 400 mature trees per acre occurs every 100 years (i.e. 400 mature trees per acre die every 100 years in a staggered manner). Smaller trees will be suppressed and die.

It is assumed that mature pine will have 5 deep roots, mainly near the center of the tree spread (i.e., concentrated near main trunk). Of these 5 deep roots, four go to a depth of 6 feet and one to 12 feet. It is assumed that it takes approximately 30 years for the tap roots to reach a 6-foot depth and the remainder of the tree's life (i.e., 70 years) for the root to go its full depth. Deep roots have a diameter of 3 inches in the top foot of soil and taper with depth to 0.25 inches at depth. These roots will be maintained over the life of the tree and exhibit little turnover prior to death. They will enlarge with yearly growth, similar to branches, although anatomically different and at a slower rate. Smaller trees, which are suppressed and die, will not establish deep roots in excess of 4 to 5 feet, and primarily only 1 or 2 such roots. Hard layers and water-saturated layers will slow root penetration. A continuous water surface will stop elongation. Hard natural layers will eventually be penetrated. HDPE geomembranes can only be penetrated by root in locations of existing cracks or holes (Phifer et al. 2007). GCLs are freely penetrated by roots (Phifer et al. 2007).

Decomposition of roots near the ground surface should occur fairly quickly due to better microclimate for microbial populations than at depth. Decomposition of roots at depth will be fairly slow, depending on the soil environment and aeration. It is assumed that it will take 25 years for the decomposition of intermediate depth roots and 30 years at depth due to the soil environment. Some shrinkage of the deep roots may occur at depth and provide a channel for water or sediment movement along the surface. Very rapid yearly turnover of fine roots and feeder roots occurs in the soil, although these are primarily in the top 18 inches of soil and will not go vertically with any intensity or longevity.

Based upon the above discussion, vegetation transition (succession) from a bahia grass field to a pine forest will be considered as a SDF closure cap degradation mechanism for modeling purposes. Primarily such a succession will result in the deep roots of the pine tree penetrating various SDF closure cap layers resulting in degradation particularly of the uppercomposite hydraulic barrier. The lower composite hydraulic barrier located on top of the SDF Disposal cells should not be impacted by pine tree roots due to the maintenance of a minimum of 12 ft of soil materials above these barriers. Vegetative stressors (droughts, disease, fire, and biological) primarily impact the SDF closure cap in terms of the rate of succession rather than as any long term degradation mechanism on their own. Therefore these vegetative stressors will not be considered as a SDF closure cap degradation mechanism for modeling purposes.

The following assumptions are made relative to the succession of a bahia grass field to a pine forest for this evaluation:

- A 100-year institutional control period begins after closure cap installation during which the initial bahia grass vegetative cover is maintained and pine trees are excluded.
- 40 years after the end of institutional control it is conservatively assumed that pine trees will be established over the entire 400-ft, clear-cut buffer area surrounding the cap.
- 80 years after the end of institutional control it is assumed that the establishment of pine seedlings on top of the closure cap will begin. The 40-yr delay is assumed to result due to the 30 ft to 70 ft elevation increase from the surrounding landscape to the cap surface.
- It will take approximately 30 years for the tap roots to reach a 6-foot depth and the remainder of the tree's life (i.e. 70 years) for the root to go its full depth.
- The distance across the cap in the predominant wind direction (southwest to northeast) ranges from about 1,350 to 1,600 ft. It is conservatively assumed the distance is 1,400 ft. Therefore, it will take approximately 7 cycles of pine seedling to mature pine trees (i.e. approximately 200 ft in each 40-year cycle) to establish mature pine over the entire cap
- 360 years after the end of institutional control it is assumed that the entire cap is dominated by mature loblolly pine.
- Complete turnover of the 400 mature trees per acre occurs every 100 years (i.e. 400 mature trees per acre die every 100 years in a staggered manner).
- Each mature tree has 4 tap roots to 6 feet and 1 tap root to 12 feet. The roots are 3 inches in diameter at a depth of 1 foot and 0.25 inches in diameter at either 6 or 12 feet, whichever is applicable.
- Deep roots will freely penetrate the erosion barrier and the geosynthetic clay liner (Phifer et al. 2007).

- Deep roots will be unable to penetrate the intact HDPE geomembrane; roots that reach the HDPE geomembrane will only be able to penetrate in locations where holes in the geomembrane have already formed due to HDPE degradation (Phifer et al. 2007).
- No roots will penetrate sufficiently deep to encounter the lower hydraulic barrier layers located directly atop the Disposal cells.

Loblolly pine seedling development is very dependent on the availability of light for growth. These scenarios are for migration of pine across a grass landscape which allows for sufficient light to the developing seedling. If an alternative cap vegetation strategy is pursued to reduce the availability of light to the seedlings, such as use of bamboo as the final vegetation cover, the rate of migration and establishment of pine on the closure cap would be retarded. Preliminary reports indicate that pine succession can be markedly inhibited by dense bamboo cover at SRS in a natural landscape (Nelson 2005).

6.3 POTENTIAL SOIL ABOVE THE EROSION BARRIER DEGRADATION MECHANISMS

As presented in Table 5 and Sections 4.4.12 and 4.4.13, a 2.5-foot thick upper backfill to provide water storage for the promotion of evapotranspiration and a 6-inch thick topsoil capable of supporting a vegetative cover and promote evapotranspiration will be located above an erosion barrier in the SDF Closure Cap. As outlined in Table 17 the following two potential degradation mechanisms will be considered for this soil located above the erosion barrier:

- Erosion
- Desiccation (wet-dry cycles)

6.3.1 Erosion

As outlined in Section 4.2 the SDF closure cap vegetative soil cover (i.e., topsoil and upper backfill), erosion barrier, side slope, and toe of the side slope have been designed to be physically stable relative to erosion potential resulting from a SRS-specific PMP event consistent with Abt and Johnson 1991 and Johnson 2002. A 1.5-percent slope over an 825-ft slope length for the vegetative soil cover is considered physically stable (i.e., prevents the initiation of gullying during a PMP event). An erosion barrier consisting of 12-in thick riprap with a D_{50} (median size) of 2.5 in on an 825-ft long, 1.5-percent slope is considered physically stable (i.e., prevents any riprap movement during a PMP event).

While the slope and slope length of topsoil and upper backfill layers have been specified to prevent the initiation of gullying during a PMP event, these layers are subject to erosion, since they are located above the erosion barrier. The erosion barrier has been designed to preclude further erosion into the SDF closure cap profile (see Section 4.2 and associated Appendix A). Therefore layers located below the erosion barrier are not subject to erosion. Since the soil layers located above the erosion barrier are subject to erosion, erosion of these layers will be considered as a SDF closure cap degradation mechanism for modeling purposes.

6.3.2 Desiccation (wet-dry cycles)

As outlined in Sections 4.4.13 and 5.4.1, the soil used as topsoil will be obtained from an on-site source and would typically be classified as silty sand (SM) materials under the Unified Soil Classification System (USCS) or as loamy sand (LS) or sandy loam (SL) in the USDA soil textural classification (i.e., textural triangle). As outlined in Sections 4.4.9, 4.4.12, and 5.4.2, only onsite soil classified as clayey sands (SC) under USCS or as sandy clay loam (SCL) in the USDA soil textural classification (i.e., textural triangle) will be used for the upper backfill. Table 18 presents the grain size distribution for typical SRS backfill from Phifer et al. (2006). As seen on average SRS backfill consists of 3% gravel, 61% sand, 10% silt, and 26% clay.

The surficial soils at SRS are highly leached and weathered. Looney et al. (1990) conducted a SRS soils geochemical and physical property investigation. Samples of unimpacted soil were obtained from six soil series considered representative of the 29 soil series at SRS. Table 19 presents a summary of the SRS soil mineralogy/composition as determined by Looney et al. (1990) for the 32 samples analyzed for mineralogy by x-ray diffraction (XRD). The samples were taken in intervals from the ground surface to a depth of 10 feet. As seen in Table 19 the soil mineralogy is dominated by quartz at an average of 93 wt%. The clay fraction is dominated by kaolinite at an average of 84 wt%. Kaolinite is one of the most stable phases in the weathering zone. The organic content of the soil is very low at an average of 0.22 wt%. Iron oxide minerals are also present in many of the SRS soils and give them their distinctive red coloration; however the iron oxide levels were below the XRD detection limits and are therefore not reported in Table 19. In summary SRS surficial soils are highly leached and consist predominately of quartz and kaolinite with a low organic and iron oxide content.

Table 18. Typical SRS Backfill Grain Size Distribution (Phifer et al. 2006)

Statistical Parameter	% +3"	% Gravel	% Sand	% Silt	% Clay
Minimum	0.00	0.00	36.90	2.70	15.60
Average	0.00	3.38	60.73	9.42	26.46
Standard Deviation	0.00	6.98	9.02	3.67	4.52
Median	0.00	1.00	62.80	8.90	26.80
Maximum	0.00	34.90	73.90	18.30	35.90

Grain size distribution definitions: gravel > 4.45 mm; 4.45 mm < sand > 0.074 mm; 0.074 mm < silt > 0.005 mm; clay < 0.005

Table 19. SRS Soil Mineralogy/Composition (Looney et al. 1990)

Statistical Parameter	Quartz (wt%)	Clay (wt%)	TOC (wt%)	Total Quartz, Clay, & TOC (wt%)	Clay Mineralogy (wt%)		
					Vermiculite	Illite	Kaolinite
Minimum	82.00	0.00	0.02	89.03	0.70	0.00	62.60
Average	93.06	5.06	0.22	98.34	14.92	1.51	83.57
Standard Deviation	4.53	4.22	0.31	3.13	9.32	1.99	9.68
Median	94.00	3.50	0.09	99.08	15.60	0.90	83.05
Maximum	100.00	17.00	1.31	101.11	34.30	7.10	98.80

The potential for shrinkage of soils upon drying, which results in cracking of the soil, is influenced by the following (Dinauer 1977; Phifer et al. 1993; Chien et al. 2006):

- The type of clay present in the soil. Smectite clays (montmorillonite or bentonite) have an extremely high shrink/swell capacity. When such clays are present in the soil in a large fraction, it can lead to cracking of the soil upon drying. In general clay with a high cation exchange capacity, a high specific surface area, and monovalent exchangeable ions such as sodium are more likely to cause a soil to crack upon drying.
- Soils containing a large clay fraction are more likely to exhibit cracking upon drying, whereas soils containing a small clay fraction will likely not exhibit cracking upon drying.
- Soils that include a significant fraction of granular soils (sand and silts) are less likely to crack upon drying.
- Soils that have undergone greater compaction are less likely to crack upon drying, than those that have not undergone significant compaction.

As outlined above typical SRS topsoil consists predominately of sand with a very small clay fraction and would be classified as loamy sand (LS) or sandy loam (SL) per USDA. Typical SRS backfill consists predominately of sand with a smaller fraction of clay and would be classified as clayey sand (SC) under USCS or as sandy clay loam (SCL) under USDA. As shown in Table 19, the predominate clay mineral in SRS topsoil and backfill is kaolinite. Kaolinite is low plasticity clay with a low shrink/swell capacity, low cation exchange capacity (3 to 15 meq/100g) and a low specific surface area (10 to 20 m^2/g) (Lambe and Whitman 1969; Mitchell 1993; Phifer et al. 1993). Additionally since SRS soils are highly leached the presence of significant amounts of monovalent exchangeable ions such as sodium are highly unlikely. Finally, as outlined in Sections 4.4.9 and 4.4.12, the backfill will be controlled compacted backfill. For all these reasons significant shrinkage of SRS topsoil and backfill upon drying that could lead to significant cracking is highly unlikely and will therefore not be considered as a SDF Closure Cap degradation mechanism for modeling purposes.

6.4 POTENTIAL EROSION BARRIER DEGRADATION MECHANISMS

As outlined within Section 4.4.11 the erosion barrier will be designed to form a barrier to erosion and gully formation and as a barrier to burrowing animals. It is likely that granite will be utilized for the stone within the erosion barrier due to its durability, cost, and local availability. Other potential rock types available locally include granite gneiss, gneiss, and mylonite (GDOT 2007). As outlined in Table 17, the following two potential degradation mechanisms will be considered for the erosion barrier:

- Weathering (Dissolution)
- Biological (root penetration, burrowing animals)

6.4.1 Weathering (Dissolution)

In humid environments, such as the southeastern United States, silicate rocks are more resistant to both mechanical and chemical weathering than are carbonates and many sandstones and mudstones. Studies have evaluated weathering rates for various silicate rocks. Granite is the most chemically durable plutonic silicate rock type, and pure quartzite is the most chemically durable metamorphic silicate rock type (Lindsey et al. 1982). Briefly, mineral weathering rates in granitic alluvium occur in the following decreasing order: hornblende > plagioclase > K-feldspar > quartz, with these minerals' loss resulting in increasing authigenic kaolinite and residual quartz (White et al. 1996). So, rocks containing relatively higher percentages of quartz (such as granite and quartzite) are desirable for resistance to chemical weathering. Well known examples of granite durability in the humid southeast include granitic monadnocks such as Stone Mountain, near Atlanta, Georgia, and Heggie's Rock, near Appling, Georgia.

As mentioned in Section 4.4.11, the likely material to be used for both the closure cap's erosion barrier and side slopes and toe is granite from nearby Georgia quarries. Another option may be a mylonitic quartzite from a nearby Georgia quarry. The rock used for the erosion barrier will be located below grade, while similar rock utilized for the side slopes (Section 4.4.16) and toe (Section 4.4.15) will be located above grade. Therefore, both below grade and above grade weathering will be considered.

Below Grade Weathering

The most appropriate below grade analogs identified to date include the weathering of granitic regoliths. White et al. (1996) also indicate that changes in bulk density and volume occur with granitic soil age, with significant density increase and volume decrease taking place well beyond the 10,000-year timeframe. From granitic regoliths in the southeastern United States, White et al. (2000) identify weathering front propagation rates of $7 \text{ m}/10^6$ yr for the Panola regolith in Georgia, and $4 \text{ m}/10^6$ yr for the Davis Run regolith in Virginia. Using the faster rate yields a weathering front propagation of 0.07 m/10,000 yr (7 cm/10,000 yr or 2.8 in/10,000 yr). Other below-ground analogs will be evaluated as they are identified as outlined in Section 4.4.11. However, because granite weathers so slowly in the humid southeast compared to rocks such as carbonates, it is expected that natural analogs will provide the most reliable data for the 10,000-yr timeframe.

Above Grade Weathering

As indicated in Section 4.4.11 sites with petroglyphs can provide above grade archaeological examples of granite weathering. A 5th to 6th century mining site at Bir Umm Fawakhir in the Eastern Desert of Egypt (Meyer 1997) has "ancient graffiti scratched on granite boulders". The Lake Onega petroglyph, now on display at the State Hermitage Museum in Russia has an estimated age of 5,000 to 6,000 years (web site reference - www.hermitagemuseum.org/html_En/03/hm3_2_2c.html). Even older petroglyph ages are reported in Bednarik (2002), for locations in the Pilbara region of western Australia. Ages dating as old as just under 20,000 years are reported for openly exposed quartz monzonite rock (a granitic rock) using "microerosion analysis" for the Woodstock adamellite petroglyph. In a web site (http://mc2.vicnet.net.au/home/cognit/shared_files/cupules.pdf) article "Cupules – The Oldest Surviving Rock Art", the same author, Robert G. Bednarik, summarizes peer reviewed works citing minimum ages of Middle Paleolithic (200,000 – 150,000 years ago) and, arguably, even Lower Paleolithic age for cupules (simple anthropogenic indentations made on rock surfaces) from quartzite rocks in Auditorium Cave, located in central India. These oldest, simple petroglyphs provide context for maximum petroglyph age, but since they are from environments protected from the weather, provide limited information on weathering rates for the rock. Possible examples from the United States include Native American granite petroglyphs located in Grapevine Canyon, near Las Vegas, Nevada; in Picture Canyon, near Needles, California; or in the Coso Rock Art District National Historic Landmark in China Lake, California (though, per the National Park Service web site http://www.nps.gov/archeology/rockArt/arch1.htm, the latter site primarily has petroglyphs on basalt rocks and few on granite). In the humid southeastern United States, limestone stelae petroglyphs thought to be 2,100 years old can be found at Crystal River State Park, Florida (web site reference - http://www.public.asu.edu/~rexweeks/Public_Access_RA_Sites.htm). Closer to the SRS, granite petroglyphs are reported on a boulder that originated in Forsyth County, Georgia and has been on display at the University of Georgia in 1963. The petroglyphs may be over 800 years old (web site reference - http://abob.libs.uga.edu/bobk/rockpet.html). Other Georgia petroglyph sites include Track Rock Gap, near Blairsville, and the Reinhardt Rock, which originated near Keithsburg, Cherokee County, and is now on display at Reinhardt College. The Sprayberry Rock, on display at the Wachovia Bank, Sandy Plains Road, Marietta, is a soapstone source-rock with petroglyphs overlying soapstone bowl-removal scars, and an estimated age no earlier than Late Archaic (3,600 to 3,000 years; (Loubser et al. 2003). Overall, Georgia petroglyphs suggest ages between the Late Woodland (1,500 to 1,000 years ago) to Middle Mississippian (800 to 600 years ago) periods (Loubser et al. 2003). The evidence from above grade petroglyphs suggests very slow weathering rates for above grade granite, even in the humid southeast.

As indicated in Section 4.4.11, above grade weathering results from the NIST Stone Test Wall, located in Gaithersburg, MD (Stutzman 2001), will also be considered as they become available. Over a 40 year period ending in 1987 only a few limestones have had measurable weathering.

Additionally new information regarding rock weathering through efforts by the Weathering System Science Consortium (WSSC; recently proposed to be renamed the Critical Zone Exploration Network) may be available by the time final design for the closure cap is underway. WSSC has proposed an initiative to, "…predict how weathering rates… respond to climatic, tectonic, and anthropogenic forces over all temporal and spatial scales". WSSC is a coalition of geochemists, geomorpologists, soil scientists, and ecologists with the objective of developing integrated weathering research, including human impacts on and resulting from weathering (Anderson et al. 2004). The WSSC plans to develop three highly-instrumented "node" sites to investigate weathering at the soil profile and catchment scales, and also to establish a network of "backbone" soil sites to be measured for standard weathering parameters over a range of depths. The fourth of the four "Driving Questions" for the WSSC is, "…how do weathering processes change and evolve over human time scales and over geologic time, and what approaches are useful in predicting the temporal evolution of weathering products and elemental fluxes?" (Anderson et al. 2004). If WSSC is successful in integrating weathering research, new information pertinent to closure cap design may be forthcoming.   More information regarding WSSC is available at http://www.wssc.psu.edu/index.html and at http://www.czen.org/wssc.

As outlined in Section 4.4.11 available literature and local natural or archaeological analogs for the erosion barrier and side-slope and toe stone will be researched and included as input for erosion barrier durability and degradation with time. Based upon these results, the required size of the emplaced stone and the thickness of the stone layer will be increased, if necessary, during final closure cap design to accommodate anticipated weathering in order to ensure closure cap physical stability with regards to erosion over 10,000 years. Additionally as discussed in Section 4.4.11 the voids within the erosion barrier rock mass will be filled with a yet-to-be determine materials in order to prevent the loss of overlying material into the erosion barrier. Selection of the material to infill the voids will consider the impact of the material upon weathering of the stone. A material which has either no impact upon weathering or preferably tends to decrease the weathering rate will be favored in the selection process. Based upon appropriate consideration of stone weathering during the final design phase of the SDF closure cap, weathering of the erosion barrier stone will not be considered as a SDF closure cap degradation mechanism for modeling purposes.

6.4.2 Biological (root penetration, burrowing animals)

Potential biological degradation mechanisms include plant root penetration and burrowing animals. As discussed in Section 6.2 it is anticipated that a pine forest will eventually succeed the initial bahia grass vegetative cover, and that pine trees will produce roots 6 to 12 feet deep, which will eventually penetrate hard layers such as the erosion barrier. As discussed in Section 4.4.10 one criterion for the selection of the material which will be used to infill the voids of the erosion barrier stone mass will be its ability to facilitate the layer's ability to hinder root penetration. However for modeling purposes, the erosion barrier will be assumed to not hinder root penetration and root penetration will be considered as a SDF closure cap degradation mechanism for modeling purposes for both the erosion barrier and underlying layers as appropriate.

The SDF closure cap model configuration includes an erosion barrier whose stone is infilled with a sand as outlined in Section 5.4.3, resulting in an erosion barrier with a fairly high saturated hydraulic conductivity as shown in Table 15. While it is assumed that roots can freely penetrate the erosion barrier, such penetration will not impact the layer's ability to function as an erosion barrier, since the roots will only minimally displace the stones. Additionally such root penetration will only minimally impact the saturated hydraulic conductivity of the sand infilled erosion barrier for the following reasons:

- Living tap roots will form an essentially impermeable barrier. However such roots will constitute a very small area of the erosion barrier resulting in very little impact to the overall saturated hydraulic conductivity. Ignoring this tends to be conservative, since considering it would tend to lower the saturated hydraulic conductivity of the erosion barrier resulting in lower infiltration through it.
- As tap roots die and decay over a 25 to 30 year period (see Section 6.2) the sand of the erosion barrier will tend to flow back into the void left by the slowly decaying roots. The sand will have very little cohesion to keep it in place.
- There is very little difference between the saturated hydraulic conductivity of the erosion barrier and the overlying and underlying backfill (i.e., a factor of 3 between the erosion barrier conductivity of 1.3E-04 cm/s versus that of the backfill at 4.1E-05 cm/s). Even if the overlying backfill were to fall into void created by slowly decaying roots, such non-densified accumulation would cause its saturated hydraulic conductivity to increase to near that of the sand (i.e., 3.3E-04 cm/s (see Appendix F)) of the erosion barrier.

For these reasons, although tap roots will be assumed to freely penetrate the erosion barrier and impact the hydraulic properties of underlying layers, the hydraulic properties of the erosion barrier will not be assumed to be appreciably impacted by root penetration.

Another consideration, in association with plant root penetration, is the potential impact on the erosion barrier of wind-thrown trees that have been uprooted. This is not considered a significant degradation mechanism in relation to the functionality of the erosion barrier due to the following reasons:

- The instances of uprooted wind-thrown trees tend to be isolated and infrequent and will therefore have minimal impact on the erosion barrier as a whole. If uprooted wind-thrown trees did result in localized damage to the erosion barrier, adjacent intact portions of the erosion barrier would still ensure the overall functionality of the erosion barrier. That is erosion in the localized damaged area could not proceed below the depth of the adjacent intact portions of the erosion barrier. This indicates that uprooted wind-thrown trees are not a significant degradation mechanism for the erosion barrier.

- As outlined in Section 4.3, three feet of soil will initially exist over the erosion barrier. Additionally as outlined in Section 4.2, the slope of the three feet of soil above the erosion barrier has been selected to promote physical stability (i.e. to prevent the initiation of gully erosion during a PMP event) consistent with Abt and Johnson 1991 and Johnson (2002; i.e., per NRC guidance). Due to this shallow slope, erosion of the soil above the erosion barrier should proceed very slowly (see Section 7.2 for anticipated erosion rates). Finally as outlined in Section 6.2 the bulk of pine tree roots which could potentially hold and displace rocks from the erosion barrier are located in the upper 18 inches of the soil, well above the erosion barrier. There are an insufficient number of tap roots to hold and displace rocks from the erosion barrier. For these reasons uprooted wind-thrown trees are not considered an applicable degradation mechanism for the erosion barrier prior to the occurrence of significant erosion.
- As currently conceived the erosion barrier consists of 0.5 to 7.5 inch diameter rock infilled with sandy soil. Such a configuration provides no cohesion between the individual particles of rock or sand, which will severely limit the ability of even the roots in the upper 18 inches of soil to hold and displace rocks from the erosion barrier. That is the finer material will quickly slip from the roots and more coarse material will tend to subsequently slip from the roots as openings become larger with the removal of finer materials. For these reasons uprooted wind-thrown trees are not considered a significant degradation mechanism for the erosion barrier.
- Finally the roots of uprooted wind-thrown trees rot more quickly than the rest of the tree and any material held in the roots tends to subsequently fall back into the hole from which it originated, tending to negate any lasting impacts on the erosion barrier (i.e., it is not a significant degradation mechanism for the erosion barrier).

Since root penetration has minimal impact on the erosion barrier either hydraulically or due to uprooted wind-thrown trees, root penetration of the erosion barrier will not be considered an SDF closure cap degradation mechanism for modeling purposes.

At SRS, burrowing animals include: old field mouse (*Peromyscus polionotus*); short tail shrew (*Blarine brevicauda*); eastern mole (*Scalopus aquiticus*); harvester ant (*Pogonomyrmex badius*); pyramid ant (*Dorymyrmex pyramicus*); imported red fire ant (Solenopsis invicta); and earthworms (Mcdowell-Boyer et al. 2000). As discussed in Section 4.4.11 the erosion barrier will be designed to act as a barrier to burrowing animals. Also as discussed selection of the material used to infill the stone will consider its ability to facilitate the layer's ability to act as a barrier to burrowing animals. The use of rock layers to preclude burrowing animals is discussed in Jacobs (1988), Koerner (1990), IAEA (2001), and Link et al., (1995). Therefore, animal burrowing into and below the erosion barrier will not be considered as a SDF closure cap degradation mechanism for modeling purposes.

6.5 POTENTIAL LATERAL DRAINAGE LAYER DEGRADATION MECHANISMS

As outlined in Table 5 and Section 4.4.7 a one-foot thick upper lateral drainage layer with a minimum saturated hydraulic conductivity of 5.0E-02 cm/s will be provided in conjunction with a composite hydraulic barrier to divert infiltrating water away from the underlying Saltstone vaults and disposal cells. A lateral drainage layer with the same hydraulic properties will also be constructed atop each disposal cell. As outlined in Table 17 the following two potential degradation mechanisms will be considered for the lateral drainage layers:

- Silting-in (both upper drainage layer and drainage layer atop disposal cells)
- Biological (i.e., root penetration; upper drainage layer only)

6.5.1 Silting-in

As outlined in Table and Sections 4.4.7 and 4.4.8 the lateral drainage layers will be overlain with a geotextile filter fabric to prevent the migration of soil from the overlying backfill into the lateral drainage layers. As outlined in Section 4.4.8 the apparent opening size of this filter fabric will be appropriately designed to provide filtration between the underlying sand drainage layers and the overlying backfill (i.e., free liquid flow but no soil loss). Sufficient data is not currently available to estimate the service life of the filter fabric. However it will degrade due to oxidation and root penetration, both of which will tend to increase its already high through plane saturated hydraulic conductivity. It is unlikely that the filter fabric will become clogged, since there is very little organic matter in SRS soils to promote the formation of a biofilm and since SRS soils consist predominately of quartz and non-swelling clays (see Section 6.3.2). Any potential clogging of the filter fabric will be more than compensated for by the formation of root penetrations over time. Therefore for modeling purposes the presence of the filter fabric will be ignored.

Since such a fabric will degrade over time and is unlikely to completely preclude the migration of colloidal clay, the lateral drainage layers will be assumed to silt-up over time with colloidal clay that migrates from the overlying backfill as an SDF closure cap degradation mechanism for modeling purposes. It will be assumed that colloidal clay migrates from the overlying backfill and accumulates in the lateral drainage layers reducing their saturated hydraulic conductivity over time. The clay minerals (in order of predominance) at SRS are shown in Table 20 along with the average clay mineral fraction and typical range in particle size for each. Colloids can be mineral grains such as clays, which have particle sizes between 0.01 and 10 µm (Looney and Falta 2000). Colloidal clay can exist in groundwater in concentrations up to 63 mg/L as measured by suspended solids (Puls and Powell 1992). Based upon this information and the previous assumption, it will be assumed that water flux driven colloidal clay migration at a concentration of 63 mg/L occurs from the overlying backfill layers to the lateral drainage layers (i.e., both the upper drainage layer and the drainage layers overlying each disposal cell).

Table 20. SRS Soil Clay Minerals

Clay Mineral	SRS Soil Average Clay Mineral Fraction [1] (%)	Typical Particle Size Range [2] (μm)
Kaolinite	83.57	0.1 to 4
Vermiculite	14.92	0.1 to 2
Illite	1.51	0.1 to 2

[1] See Table 23 (Looney et al. 1990)
[2] Mitchell (1993)

It is conservatively assumed that all colloidal clay migrating from the backfill layers to the underlying lateral drainage layers remains in the drainage layer. This is a conservative assumption because there are reasons to believe that if colloidal clay enters the drainage layers, all or some of it will continue to move through and exit the drainage layers. One reason is because the hydraulic conductivity of the drainage layers is, by design, much higher than that of the backfill material (5.0E-2 cm/sec compared to 4.1E-5 cm/sec). So, sufficient flux through the backfill to move colloidal clay would certainly provide sufficient flux through the drainage layer to continue moving the colloidal clay to exit the drainage layer. Another reason is that a natural "filter pack" is expected to develop between the backfill and the drainage layer, not unlike the outward-to-inward increasing grain size filter that develops along the perimeter of a water well's borehole filter pack. At SRS, relatively clean sand layers are seen lying directly beneath clayey layers in natural geologic units ten's of millions of years old, showing it is possible for high hydraulic conductivity sand units to have well over a 10,000 year lifetime.

Because the middle backfill varies from a minimum of 1 ft to 20+ ft in thickness, and the lower backfill varies from approximately 5 ft to 30 ft in thickness, they will be regarded as providing a limitless volume of colloidal clay to the 1-ft thick drainage layer while maintaining the same hydraulic conductivity, porosity, and other soil parameters. It will be assumed that the clay migrates out of the backfill layers into the lateral drainage layer with the water flux containing 63 mg/L of colloidal clay. It will also be assumed that the time to achieve the endpoint conditions will be based upon the estimated water flux into the lateral drainage layers. This water-flux driven clay accumulates in the drainage layers from the bottom up, filling the void space with clay at a density of 1.1 g/cm^3 (Hillel 1982). These assumptions are analogous to the formation of the B soil horizon as documented in the soil science literature. Clay translocation is a very slow process where discrete clay particles are washed out in slightly acidic conditions and deposited lower in the soil profile (McRae 1988). Evidence has been found that the B-horizon where the translocated clay is deposited may form at a rate of 10 inches per 5,000 years (Buol et al. 1973).

The hydraulic conductivity of the clay-filled drainage layers is reduced from 5.0E-02 cm/s to that of the overlying backfill, 4.1E-05 cm/s. The hydraulic conductivity of the upper, non-clay-filled portion of the drainage layer remains at 5.0E-02 cm/s. The thickness of the clay-filled portion increases with time, while the thickness of the non-filled portion decreases with time, resulting in an overall decrease in hydraulic conductivity for the lower drainage layer.

6.5.2 Biological (root penetration)

As discussed in Section 6.2, it is anticipated that a pine forest will eventually succeed the initial bahia grass vegetative cover. The closure cap is anticipated to eventually be covered with approximately 400 mature trees per acre over a 100-year period, each with five deep roots that can penetrate through the one foot thick lateral drainage layer (i.e., deep roots). The bulk of the roots associated with the closure cap vegetation will be located within 24 inches of the ground surface (see Section 6.2) and therefore cannot impact the lateral drainage layer, since the erosion barrier will always maintain at least 24 inches of material between the top of the lateral drainage layer and the ground surface. Deep roots will be maintained and enlarge with yearly growth over the life of the tree.

Trees are expected to die at approximately 100 years of age, and it is anticipated that decomposition of deep roots will occur over a 30 year period. Prior to decomposition the roots represent an impermeable volume within the lateral drainage layer. The presence of roots within the lateral drainage layer will be considered as a SDF closure cap degradation mechanism for modeling purposes.

6.6 POTENTIAL HDPE GEOMEMBRANE DEGRADATION MECHANISMS

HDPE is one of the most common polymers utilized in the production of geomembranes (Koerner 1998). HDPE geomembranes consist of 95-98% resin, 2-3% carbon black, and 0.25-1% antioxidants. HDPE geomembranes have a minimum sheet density of 0.940 g/cm^3 (GRI 2003; Koerner and Hsuan 2003; Needham et al. 2004). It has an extremely low permeability (2.0E-13 cm/s) (Schroeder et al. 1994a; Schroeder et al. 1994b) and an extremely low water vapor diffusional flux (~0.006 g/m^2-day) (Rumer and Mitchell 1995). Rumer and Mitchell (1995) report that "diffusion of water or solvent through HDPE geomembranes can only occur in a vapor state".

As outlined Table 5 and Sections 4.4.4 and 4.4.5, a HDPE geomembrane will be used in conjunction with a GCL to form a composite hydraulic barrier to infiltration. The potential HDPE geomembrane degradation mechanism discussion presented below was primarily extracted from Phifer (2005). HDPE geomembranes can degrade over time through the following mechanisms (also see Table 17), which are discussed in detail in the succeeding sections (Koerner 1998; Needham et al. 2004; Rowe 2004):

- Ultraviolet (UV) radiation
- Antioxidant Depletion
- Thermal Oxidation
- High Energy Irradiation
- Tensile Stress Cracking
- Biological (root penetration, burrowing animals)

6.6.1 Ultraviolet (UV) Degradation

HDPE geomembrane degradation due to short-wavelength ultraviolet (UV) radiation (i.e. sunlight) exposure has been extensively studied both in the laboratory and field (Koerner

1998; Koerner and Hsuan 2003). Exposure to UV radiation and subsequent penetration of UV radiation into the polymer structure causes polymer degradation by chain scission and bond breaking. Additionally, photo-oxidation due to UV radiation and atmospheric exposure causes significantly faster antioxidant depletion than thermal oxidation (Needham et al. 2004).

However current HDPE geomembrane formulations typically contain 2 to 3% carbon black and may contain other ultraviolet chemical stabilizers to minimize ultraviolet degradation. Due to carbon black usage, UV radiation is not considered a significant degradation mechanism for short-term exposures associated with construction, where the geomembrane is covered in a timely manner. Typically exposures of less than several years is not considered a concern, since manufacturers' warranties for up to 20 years are available for exposed geomembranes. (Koerner 1998; Needham et al. 2004) Additionally UV degradation is not autocatalytic, that is after burial UV degradation does not continue to occur (Bonaparte et al. 2002). Therefore UV degradation of the HDPE geomembrane will not be considered as a SDF closure cap degradation mechanism for modeling purposes.

6.6.2 Antioxidant Depletion

Antioxidants are added to HDPE geomembranes primarily to prevent thermal oxidative degradation (see Section 6.6.3). As long as significant antioxidants are present within a HDPE geomembrane, as measured by Oxidative Induction Time (OIT) tests, thermal oxidative degradation will be prevented and the mechanical properties of the geomembrane will remain essentially unchanged. However after the antioxidants have been depleted, thermal oxidation of the geomembrane can begin. Typical antioxidants packages consist of a phosphite and a hindered phenol at 0.1 to 1.0 weight percent of the geomembrane. Phosphites are most effective at higher temperatures and are used as manufacturing process stabilizers, whereas hindered phenols are effective over a wide temperature range and are used as long-term field stabilizers. (Koerner 1998; Hsuan and Koerner 1998; Sangam and Rowe 2002; Mueller and Jakob 2003; Rowe 2004; Needham et al. 2004)

The OIT time determined from OIT tests is related to the quantity and type of antioxidants in the polymer. OIT tests use a differential scanning calorimeter with a special testing cell capable of sustaining pressure. In the standard OIT test (ASTM 2007) a 5 mg specimen is brought to a temperature of 200°C and a pressure of 35 kPa under a nitrogen atmosphere. Oxygen is then introduced and the test is terminated when an exothermal peak is reached. The OIT time is the time from oxygen introduction to the exothermal peak. The high pressure OIT (HP-OIT) test (ASTM 2006d) is conducted similar to the standard test except it is conducted at a temperature of 150°C and a pressure of 3,500 kPa are used.

Three major antioxidant depletion studies have been performed: Hsuan and Koerner (1998); Sangam and Rowe (2002); and Mueller and Jakob (2003). Each of these studies is discussed in the succeeding sections.

6.6.2.1 Hsuan and Koerner (1998) Antioxidant Depletion Study

Hsuan and Koerner (1998) reported on twenty-four months of HDPE geomembrane antioxidant depletion testing. The HDPE geomembrane tested was taken from a single roll of commercially available 60 mil thick HDPE. The primary antioxidants in this geomembrane

were probably phosphites and hindered phenols (Hsuan and Guan 1997). OIT tests, which provide a relative measure of the total antioxidants within the geomembrane, were initially performed.

The following were the initial OIT measurements for this geomembrane:
- Standard-OIT = 80.5 min (The Std-OIT value for pure unstabilized (no antioxidants) HDPE resin was found to be 0.5 min)
- High Pressure-OIT = 210 min (The HP-OIT value for pure unstabilized (no antioxidants) HDPE resin was found to be 20 min)

Four sets of five columns for a total of twenty were maintained at elevated temperatures of 85, 75, 65, and 55°C and under a static normal load of 260 kPa and a 300 mm head of tap water. The top surface of the HDPE was saturated sand and the bottom surface was dry sand vented to the atmosphere. Samples were retrieved at various time intervals over a two year period and analyzed for numerous physical, mechanical, and chemical properties including OIT.

Although the OIT value decreased with time, the testing was not conducted to antioxidant depletion. Therefore no significant changes in physical and mechanical properties (i.e., density, melt flow index, yield stress, yield strain, break stress, and break strain) were noted over the 24 month period, since these properties remain unchanged as long as antioxidants exist in the geomembrane (i.e., OIT values greater than that of unstabilized HDPE resin).

Hsuan and Koerner (1998) plotted both the standard and high pressure OIT data for each of the four test temperatures as the natural logarithm of OIT versus incubation time. This produced a linear response for each test temperature for each OIT methodology, where the OIT depletion rate for each temperature is the slope of its respective line and the y-intercept is the natural logarithm of the initial geomembrane OIT value.

The equation for the line then becomes:

$\ln(OIT) = \ln(P) - St$, where OIT = OIT (minutes); S = OIT depletion rate (minutes/month);
$\qquad$ t = incubation time (months); and
$\qquad$ P = the initial geomembrane OIT value (i.e., a constant)

Based upon these plots Hsuan and Koerner (1998) determined the antioxidant depletion rates for each OIT methodology for each test temperature as shown in Table 21.

Table 21.   Hsuan and Koerner (1998) Antioxidant Depletion Rates

Temperature (^{o}C)	S $_{Std-OIT}$ (min/month)	S $_{HP-OIT}$ (min/month)
85	0.1404	0.0661
75	0.0798	0.0387
65	0.0589	0.0284
55	0.0217	0.0097

Hsuan and Koerner (1998) then used the Arrhenius equation to extrapolate the OIT depletion rate to lower temperatures more representative of typical field condition. The Arrhenius equation can be use to expressed by:

$$S = Ae^{-E/RT}$$
$$\ln(S) = \ln(A) + (-E_a / R)(1/T),$$ where S = OIT depletion rate (see Table); E_a = activation energy of the antioxidant depletion reaction (kJ/mol); R = universal gas constant (8.31 j/mol); T = test temperature in absolute Kelvin (K); and A = constant.

A plot of ln(S) versus 1/T results in a linear plot as shown in Figure 12. The activation energy of the antioxidant depletion reaction is obtained from the slope of the line. From the Arrhenius plot Hsuan and Koerner (1998) determined the Arrhenius equation associated with each OIT test method and the associated activation energy as shown in Table 22. Table 22 equations were utilized to determine the OIT depletion rate (S) associated with various temperatures (see Table). Then the time to antioxidant depletion was determined for select temperatures (see Table) using the following equation:

$$\ln(OIT) = \ln(P) - St,$$ where OIT = antioxidant depleted OIT value (minutes) taken as the OIT value of pure unstabilized (no antioxidants) HDPE resin; S = OIT depletion rate (minutes/month) (see Table); t = time to antioxidant depletion (months); and P = the original value of OIT of the geomembrane (i.e. a constant)
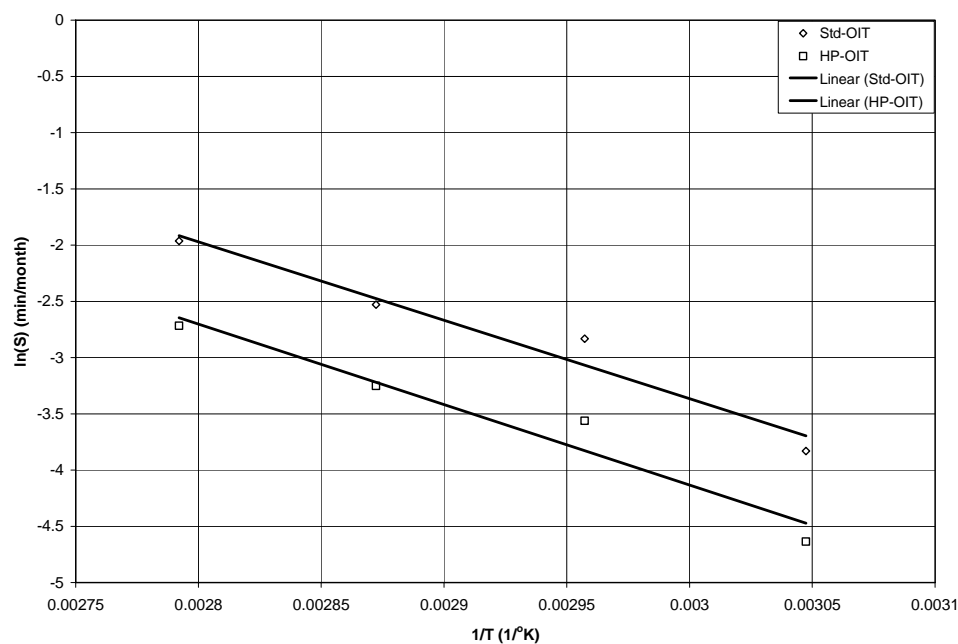
Figure 12.   Hsuan and Koerner (1998) Arrhenius Plot

Table 22. Hsuan and Koerner (1998) Arrhenius Equations and Activation Energy

OIT Test Method	Arrhenius equation	E_a (kJ/mol)
Std-OIT	$Ln(S) = 17.045 - 6798/T$	56
HP-OIT	$Ln(S) = 16.850 - 6989/T$	58

Table 23. Hsuan and Koerner (1998) OIT depletion Rate (S) and Time to Antioxidant Depletion

Temperature (^{o}C)	$S_{std-OIT}$ (minute/month)	$t_{std-OIT}$ (yrs)	S_{HP-OIT} (minute/month)	t_{HP-OIT} (yrs)
13	0.0012	348.1	0.0005	381.6
15	0.0014	295.2	0.0006	322.1
20	0.0021	197.4	0.0009	213.0
25	0.0032	133.8	0.0014	142.8
33	0.0057	73.7	0.0025	77.4
40	0.0094	44.9	0.0042	46.5

Based upon their 24 months of testing, Hsuan and Koerner (1998) postulated that HDPE degradation due to thermal oxidation occurs in the following three stages:

- Stage A: Antioxidant depletion period
- Stage B: Induction period
- Stage C: Polymer thermal oxidation period

After 24 months of testing, the HDPE degradation was still in the antioxidant depletion period, based upon this data Hsuan and Koerner (1998) estimated that the antioxidant depletion period would last approximately 200 years at a temperature of 20 °C. Koerner (1998) has additionally estimated that the induction period (i.e., the time between antioxidant depletion and onset of thermal oxidation) would last from 20 to 30 years based upon the examination of exhumed HDPE milk containers at the bottom of a landfill. Thus in a buried environment at 20 °C, they estimate a time span of approximately 220 years with essentially no degradation of physical and mechanical properties.

6.6.2.2 Sangam and Rowe (2002) Antioxidant Depletion Study

Sangam and Rowe (2002) reported on approximately thirty-three months of HDPE geomembrane antioxidant depletion testing. The HDPE geomembrane tested was a GSE Lining Technology, Inc. 80-mil thick smooth HDPE manufactured from a copolymer resin with a density of 0.940 g/cm^3, a carbon black content of 2.54%, and an initial standard OIT of 133 minutes. It was assumed that the primary antioxidants in this geomembrane were phosphites and hindered phenols based upon the previous work of Hsuan and Guan (1997).

HDPE coupons were immersed in air, tap water, and synthetic landfill leachate (i.e., exposed on both sides), each at temperatures of 22 ± 2, 40, 55, 70, and 85°C. Samples were retrieved at various time intervals over a 33-month period and analyzed for primarily standard OIT.

The synthetic landfill leachate consisted of approximately 15,000 mg/L inorganic ions, 7,500 mg/L volatile fatty acids, 5000 mg/L of a surfactant, and less than 10 mg/L trace heavy metals.

Sangam and Rowe (2002) plotted the standard OIT data for each of the immersion medium (i.e., air, tap water, and synthetic landfill leachate) at each of the five test temperatures as the natural logarithm of OIT versus incubation time. This produced a straight line for each test exposure condition (i.e., immersion medium and temperature) suggesting that the antioxidant depletion follows first-order decay, with the OIT depletion rate represented by the slope of the line. At any time (t), the OIT value which represents the remaining amount of antioxidants the geomembrane can be expressed as:

$$OIT(t) = OIT_0\, e^{-St},$$ where OIT(t) = OIT at any time, t, in minutes; OIT_0 = initial OIT in minutes; S = rate of antioxidant depletion in month^{-1}.; t = time in months

This resulted in the inferred depletion rates provided in Table 24.

Table 24. Sangam and Rowe (2002) Inferred Depletion Rates (S = month^{-1})

Temperature (°C)	Air	Water	Leachate
85	0.1094	0.1746	0.4074
70	0.0497	0.1050	-
55	0.0226	0.0470	0.1504
40	0.0152	0.0362	0.0886
22	0.0023	0.0043	0.0188

The Table 24 depletion rates determined at elevated temperatures can be extrapolated to typical field temperatures using the Arrhenius equation (a time-temperature superposition principal) in order to estimate the field service life.

$$S = A\, e^{-E_a / RT}$$
$$\ln(S) = \ln(A) + (-E_a / R)(1/T),$$ S = OIT depletion rate (see Table); E_a = activation energy in J/mol; R = 8.314 J/mol K (universal gas constant); T = absolute temperature in K; A = constant (collisional factor)

A plot of ln(S) versus 1/T results in a linear plot as shown in Figure 13. The activation energy of the antioxidant depletion reaction is obtained from the slope of the line. From the Arrhenius plot Sangam and Rowe (2002) determined the Arrhenius equation associated with each immersion medium (i.e., air, water, and leachate) and the associated activation energy. However Sangam and Rowe (2002) appear to have made a mistake in their calculations. Rather than using the temperature 40°C in their calculations they appeared to have used 50 °C. Making this correction, the derived Arrhenius equation and the inferred activation energy (E_a) for each immersion medium are summarized in Table 25.
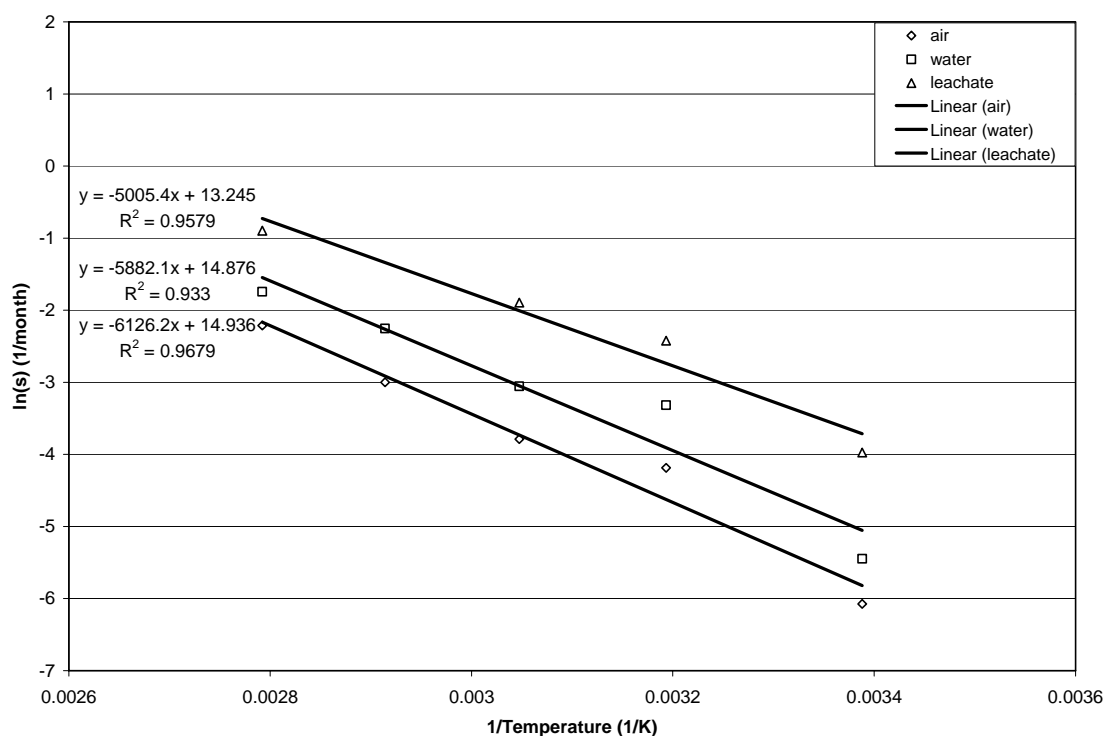
Figure 13. Sangam and Rowe (2002) Arrhenius Plot

The Table 25 equations were utilized to determine the OIT depletion rate (S) associated with various temperatures (see Table 26). Then the time to antioxidant depletion was determined for select temperatures (see Table 26) using the following equation and assuming the OIT of an unstabilized HDPE to be 0.5 minute:

$$\ln(OIT_D) = \ln(OIT_o) - St ,$$ where OIT_D = antioxidant depleted OIT value of 0.5 minutes;
S = OIT depletion rate (minutes/month) (see Table);
t = time to antioxidant depletion (months); and P = the original value of OIT of the geomembrane (i.e., a constant)

Table 25. Sangam and Rowe (2002) Arrhenius Equations and Activation Energy

Exposure Medium	Arrhenius equation ($S = month^{-1}$; $T = month$)	E_a (kJ/mol)	R^2
Air	Ln(s) = 14.936 – 6126.2/T	50.93	0.9679
Water	Ln(s) = 14.876 – 5882.1/T	48.90	0.933
Leachate	Ln(s) = 13.245 – 5005.4/T	41.61	0.9579

Table 26. **Sangam and Rowe (2002) OIT Depletion Rate (S) and Time to Antioxidant Depletion**

Temp. (°C)	S (month^{-1})	Air (yrs)	S (month^{-1})	Water (yrs)	S (month^{-1})	Leachate (yrs)
13	0.0015	301.3	0.0034	136.3	0.0143	32.5
15	0.0018	259.7	0.0039	118.2	0.0162	28.8
20	0.0026	180.7	0.0056	83.4	0.0217	21.4
25	0.0037	127.3	0.0078	59.6	0.0289	16.1
33	0.0063	74.4	0.0131	35.6	0.0448	10.4
40	0.0098	47.6	0.0201	23.2	0.0646	7.2

As seen in Table 26, antioxidant depletion for the range of temperatures 13 to 33°C is estimated to be approximately twice as fast in tap water than in air and four times faster in high organic content leachate than in tap water. Sangam and Rowe (2002) state that the following regarding these estimates of antioxidant depletion:

- The Table 26 time to antioxidant depletion estimates represent a lower bound to the time and the time in the field would be expected to be longer under these exposure conditions.

- The Table 26 time to antioxidant depletion estimates are based upon having the immersion medium on both sides of the geomembrane and must be adjusted for actual field conditions (i.e., leachate is not typically located on both sides of the membrane).

6.6.2.3 Mueller and Jakob (2003) Antioxidant Depletion Study

Mueller and Jakob (2003) report on 13.6 years of HDPE geomembrane antioxidant depletion testing for immersion in air and 6 years for immersion in de-ionized water. The HDPE geomembranes tested by Mueller and Jakob (2003) consisted of nine commercially available HDPE geomembranes made by five different manufacturers from seven different resins. The geomembranes were 100-mil thick, had densities ranging from 0.940 to 0.950 g/cm^3, contained 2 to 2.5 weight percent carbon black and a few thousand ppm phenolic and phosphite antioxidants, and had an initial OIT (Al-pan at 200°C) from 11 to 138 min.

HDPE samples were immersed in air and de-ionized water (i.e., exposed on both sides) at 80°C. The samples immersed in air were in an oven with substantially less than 10 air changes per hour. The samples were immersed in water in glass flasks, which were opened and shook every four weeks. The water was completely changed every three months. At various times samples were removed and tested for OIT and tensile strength and elongation.

During accelerated aging in heated air, the OIT slowly decreased in a steady, exponential-like, fashion. After 13.6 years of accelerated aging in heated air, no significant changes in mechanical properties due to oxidation were detected. For aging in heated air it was found that "the relative OIT values (i.e., OIT/OIT$_{intial}$) showed roughly a common decline as a function of aging time, independent of the resin or the OIT testing temperature".

During accelerated aging in heated water, the OIT decreased rapidly at first and then leveled off. Mueller and Jakob (2003) looked at this as a two step exponential decline with a short-term high antioxidant depletion rate and a long-term low antioxidant depletion rate. After 6 years of accelerated aging in heated water, it was found that most samples approached very

low OIT values after 200 days (i.e. the antioxidant depletion rate was initially fairly high), that the antioxidant depletion rate decreased significantly after 200 days, and that oxidation of the polymer itself started after 5 years, and that deterioration proceeded quite rapidly after oxidation began at the elevated test temperature (80°C). Since the phosphite stabilizer substantially determines the initial OIT and since it constitutes the bulk of the stabilizer in the HDPE geomembranes, Mueller and Jakob (2003) assume that depletion especially of the phosphite component is seen in the initial rapid OIT decrease. "The long-term antioxidant depletion time would then be determined by the migration of the remaining phenolic stabilizer. Therefore, a high initial OIT does not necessarily correlate with good long-term oxidation stability."

Short-term antioxidant depletion rates were estimated at 0.15 to 0.3 minute/month (approximately 0.2) in water at 80°C (100-200 days) and long-term antioxidant depletion rates at 0.015 to 0.03 minute/month (1000-2000 days). Most of the data appeared to be in the 0.15 minute/month (200 days) range for the short-term antioxidant depletion rate and 0.015 minute/month (2000 days) for long-term antioxidant depletion rate.

Mueller and Jakob (2003) could not estimate the antioxidant depletion time (i.e., time it takes to deplete the antioxidants and begin oxidation) at typical field temperatures using the Arrhenius equation, since they did not perform their testing at multiple temperature as required for use of the Arrhenius equation. Therefore they utilized the van't Hoff rule for the temperature dependence of antioxidant depletion time, their measured antioxidant depletion time of 5 years for HDPE GMs immersed in 80°C de-ionized water, and assumed activation energies from other studies.

$$t_1(T) = t_1(T') \, e^{\frac{E_a}{R}\left[\frac{1}{T} - \frac{1}{T'}\right]},$$ where $t_1(T)$ = antioxidant depletion period in years at the ambient temperature of the HDPE; $t_1(T')$ = antioxidant depletion period in years at test temperature of 80°C (i.e., 5 years); E_a = depletion process activation energy; R = universal gas constant (8.319 J/mol K); T = ambient temperature of the HDPE in K (K = 273.15 + °C); T' = test temperature in K = 273.15 + 80°C = 353.15

Table 27 provides various antioxidant depletion process activation energies that have been determined by others. These activation energies have been utilized with the van't Hoff rule to calculate estimated antioxidant depletion times per Mueller and Jakob's (2003) methodology (see Table 28). As seen in Table 28 the estimated antioxidant depletion time varies widely with the assumed activation energy. At a temperature of 33°C the antioxidant depletion time varies from 45 to 930 years with the utilization of activation energies of 42 and 100 kJ/mol, respectively.

Mueller and Jakob (2003) believe that an activation energy of 60 kJ/mol is a very low activation energy which is expected to represent the lower limit of antioxidant depletion time. At a temperature of 33°C and an activation energy of 60 kJ/mol the antioxidant depletion time would be approximately 103.6 years.

Table 27. Antioxidant Depletion Process Activation Energies

Source	Media	E_a (kJ/mol)	Comment
Hsuan-Koerner (1998)	Sand-water-air	56	Using Std-OIT test; didn't take test out to antioxidant depletion
		58	Using HP-OIT test; didn't take test out to antioxidant depletion
Sangam-Rowe (2002)	Air	51	Using Std-OIT test; didn't take test out to antioxidant depletion
	Water	49	
	Synthetic Leachate	42	
Smith et al. (1992)	Water	100	-

Table 28. Estimated Antioxidant Depletion Times (Mueller and Jakob 2003)

Temperature (^{o}C)	E_a = 42 kJ/mol Antioxidant Depletion Time (years)	E_a = 49 kJ/mol Antioxidant Depletion Time (years)	E_a = 51 kJ/mol Antioxidant Depletion Time (years)
13	142.1	248.3	291.2
15	125.8	215.2	251.0
20	93.3	151.9	174.6
25	69.9	108.4	123.0
33	44.9	64.7	71.8
40	31.0	42.1	45.9
Temperature (^{o}C)	E_a = 56 kJ/mol Antioxidant Depletion Time (years)	E_a = 58 kJ/mol Antioxidant Depletion Time (years)	E_a = 100 kJ/mol Antioxidant Depletion Time (years)
13	433.8	508.8	14,462.3
15	368.4	429.6	10,804.6
20	247.4	284.3	5,303.9
25	168.3	190.8	2,666.5
33	93.3	103.6	929.8
40	57.1	62.3	386.6

Mueller and Jakob (2003) determined that antioxidant depletion occurs due to diffusion out of the HDPE geomembrane and oxidative consumption. It was also determined that under conditions of low temperature and low oxygen levels, diffusion is the predominant antioxidant depletion mechanism as with typical field conditions. The diffusion rate is higher with immersion in water rather than in air. Oxidative consumption is the predominant mechanism, under conditions of high temperature and high oxygen levels. Additionally, Mueller and Jakob (2003) determined that the mechanical properties of HDPE geomembrane are not significantly degraded as long as a significant OIT value is measurable.

6.6.2.4 Summary of Antioxidant Depletion Studies

Both Hsuan and Koerner (1998) and Mueller and Jakob (2003) determined that no significant changes in physical and mechanical properties of the HDPE geomembrane occur until the antioxidants are essentially depleted. Sangam and Rowe (2002) and Mueller and Jakob (2003) determined that the antioxidant depletion rate is dependent upon the medium within which the HDPE geomembrane is immersed. Sangam and Rowe (2002) determined that the antioxidant depletion rate increases in order with immersion in the following media: air, tap water, and high organic content leachate. Mueller and Jakob (2003) confirmed that the antioxidant depletion rate is greater with immersion in water than with air. Both Sangam and Rowe (2002) and Mueller and Jakob (2003) immersed their HDPE geomembrane samples in the immersion medium such that both side of the samples were in contact with the medium.

Mueller and Jakob (2003) observed a two-stage antioxidant depletion process with immersion in water. The two-stage process was seen to consist of initial short-term antioxidant depletion at a high rate followed by long-term antioxidant depletion at a low rate. They assume that the initial short-term depletion during their testing at 80°C was the phosphite stabilizer, which constitutes the bulk of the antioxidant, diffusing out over 200 days at a rate of 0.15 minute/month as determined by OIT measurement. They further assume that the long-term depletion during their testing at 80°C was the hindered phenols diffusing out over 2000 days at a rate of 0.015 minute/month as determined by OIT measurement. They further observed that oxidation of the polymer itself started after 5 years and that deterioration proceeded quite rapidly after oxidation began at the elevated test temperature (80°C). This was not observed in the testing conducted by Hsuan and Koerner (1998) nor Sangam and Rowe (2002), since their testing was of a much shorter duration than that of Mueller and Jakob (2003). Additionally testing by Hsuan and Koerner (1998) nor Sangam and Rowe (2002) were not conducted to antioxidant depletion as with Mueller and Jakob (2003); therefore they did not observe oxidative degradation and associated degradation of the physical and mechanical properties.

Mueller and Jakob (2003) determined that antioxidant depletion occurs over time due to diffusion out of the HDPE geomembrane and oxidative consumption within the geomembrane. It was also determined that under conditions of low temperature and low oxygen levels, diffusion is the predominant antioxidant depletion mechanism as with typical field conditions. Oxidative consumption is the predominant mechanism, under conditions of high temperature and high oxygen levels.

Hsuan and Koerner (1998) postulated that HDPE degradation due to thermal oxidation occurs in the following three stages:
- Stage A: Antioxidant depletion period
- Stage B: Induction period
- Stage C: Polymer thermal oxidation period

Koerner (1998) has additionally estimated that the induction period (i.e., the time between antioxidant depletion and onset of thermal oxidation) would last from 20 to 30 years based upon the examination of exhumed HDPE milk containers at the bottom of a landfill.

Table 29 presents the estimated antioxidant depletion times at temperatures of 33 and 40°C based upon the testing by Hsuan and Koerner (1998) and Sangam and Rowe (2002). Additionally the times based upon the methodology of Mueller and Jakob (2003) are provided utilizing the corresponding activation energies determined by Hsuan and Koerner (1998) and Sangam and Rowe (2002). In general the antioxidant depletion times estimated by the methodology of Mueller and Jakob (2003) are greater than those determined by Hsuan and Koerner (1998) and Sangam and Rowe (2002) for the same activation energies. It is likely that the antioxidant depletion times provided in Table 29 are low (i.e., conservative), since they are probably based upon activation energies associated with the initial short-term depletion of the phosphite stabilizer rather than the long-term depletion of the hindered phenols.

Table 29.   Summary of Estimated Antioxidant Depletion Times

Temperature (°C)	Hsuan and Koerner (1998) Water/Air/Sand (yrs)	Mueller and Jakob (2003) E_a = 56 kJ/mol Antioxidant Depletion Time (years)	Sangam and Rowe (2002) Air (yrs)	Mueller and Jakob (2003) E_a = 51 kJ/mol Antioxidant Depletion Time (years)
33	73.7	93.3	74.4	71.8
40	44.9	57.1	47.6	45.9
Temperature (°C)	Sangam and Rowe (2002) Water (yrs)	Mueller and Jakob (2003) E_a = 49 kJ/mol Antioxidant Depletion Time (years)	Sangam and Rowe (2002) Leachate (yrs)	Mueller and Jakob (2003) E_a = 42 kJ/mol Antioxidant Depletion Time (years)
33	35.6	64.7	10.4	44.9
40	23.2	42.1	7.2	31.0

A final item of note is the fact that the studies utilized different HDPE geomembranes with potentially different antioxidant packages. All three studies assumed that the antioxidant packages of the HDPE geomembranes they tested included phosphites and hindered phenols, however the quantity of each was unknown. The antioxidant packages are typically treated as proprietary information, by the HDPE geomembrane manufacturers, and therefore the information is not generally available to the public. Differences in the makeup of the antioxidant packages could have a significant impact on the on the estimated antioxidant depletion times derived from each study.

Needham et al. (2004) performed an extensive review of these studies and came to the following primary conclusions:

- The antioxidant depletion times of HDPE geomembranes may be significantly longer than that estimated by Hsuan and Koerner (1998) and Sangam and Rowe (2002), based upon the two-stage depletion seen by Mueller and Jakob (2003). Additionally it may also be longer due to the following:

- The leachate strength in testing by Sangam and Rowe (2002) remained constant, whereas it will likely decrease with time and the rate of antioxidant depletion will probably also decrease with time,
- The presence of soil particles in contact with the geomembrane in the field reduces its contact area with air, water, and/or leachate.
- Antioxidant depletion due to oxidative consumption would be low, since only limited oxygen levels would be present due to the partially saturated or saturated surrounding materials and the reducing conditions often associated with landfills.

- Mueller and Jakob (2003) took samples for OIT measurement from the center of the geomembrane thickness, whereas Hsuan and Koerner (1998) and Sangam and Rowe (2002) tested the entire geomembrane thickness. This could have had an impact on the antioxidant depletion times estimated, since a greater concentration of antioxidants should be located in the center than at the surface over time.

- "The activation energy reflects the necessary minimum energy of the antioxidant depletion process and will depend on the characteristics of the polyethylene resin, the antioxidant package, and the exposure conditions in which the antioxidant loss is occurring." The rate of antioxidant depletion is exponentially dependent upon the activation energy. "It is tentatively inferred that the lower activation energies found by Hsuan and Koerner (1998) and Sangam and Rowe (2002) reflect faster diffusion of more easily depleted antioxidants, rather than slower diffusion of the residual antioxidants, which provide the very long-term antioxidant protection." "Values of activation energy of 60-75 kJ/mol appear a reasonable, conservative estimate."

- "As noted by Mueller and Jakob (2003), the overall rate of antioxidant loss from a geosynthetic is proportional to its surface area and the total amount of stabilizer in the geosynthetic is proportional to its volume. Thus, the antioxidant depletion time should be proportional to the thickness of the material." However due to the limited available data sets, it is not yet possible to draw quantitative conclusions with regard to geomembrane thickness.

- High initial OIT values do not necessarily result in long-term oxidation stability. For example, phosphites can produce high initial OIT values but do not greatly contribute to long-term oxidative stability at typical field temperatures. Therefore HDPE geomembrane specifications should not only stipulate an initial OIT value.

- Needham et al. (2004) believe that a reasonable estimation of the antioxidant depletion time can be derived from the following:
  - Slow long-term OIT depletion rates from Mueller and Jakob (2003),
  - Increased rate of depletion for leachate exposure found by Sangam and Rowe (2002),
  - Effects of a confined sample under compressive stress sandwiched between saturated sand and dry sand, as investigated by Hsuan and Koerner (1998), and
  - Measuring durability of the geomembrane in terms of the tensile test (but not service life as a hydraulic barrier).

Based upon the above discussion antioxidant depletion of the HDPE geomembrane will be considered as a SDF Closure Cap degradation mechanism for modeling purposes using the Needham et al. (2004) model discussed in Section 6.6.7.

6.6.3 Thermal Oxidative Degradation

Thermal oxidative degradation is the principal degradation mechanism for HDPE geomembranes in landfills (Rowe 2004). Thermal oxidative degradation of a HDPE geomembrane can begin only after the antioxidants have been depleted and only if oxygen is available. (Koerner 1998; Mueller and Jakob 2003; Needham et al. 2004). Thermal oxidative degradation is initiated with the production of free radicals ($R^\bullet$) within the polymer structure due to elevated temperatures, high energy irradiation, etc (Koerner 1998; Needham et al. 2004). If oxygen is available the free radicals rapidly combine with oxygen producing peroxide free radicals ($ROO^\bullet$). These peroxide free radicals can then react with intact portions of the polymer to form additional free radicals and hydroperoxides (i.e., oxidized polymer chains (ROOH)).

The hydroperoxides can then decompose to produce additional free radicals. This progression leads to accelerated polymer chain reactions, resulting in polymeric main chain scission (i.e., breakage of covalent bonds within the polymer structure) (Koerner 1998; Koerner and Hsuan 2003; Needham et al. 2004). The following are the primary thermal oxidative degradation reactions:

$$RH + energy \ R^\bullet + H^\bullet$$
$$R^\bullet + O_2 \rightarrow ROO^\bullet$$
$$ROO^\bullet + RH + energy \rightarrow ROOH + R^\bullet,$$

where RH = polymer chain, $R^\bullet$ = free radical, $ROO^\bullet$ = peroxide free radical; ROOH = hydroperoxides (i.e. oxidized polymer chains)
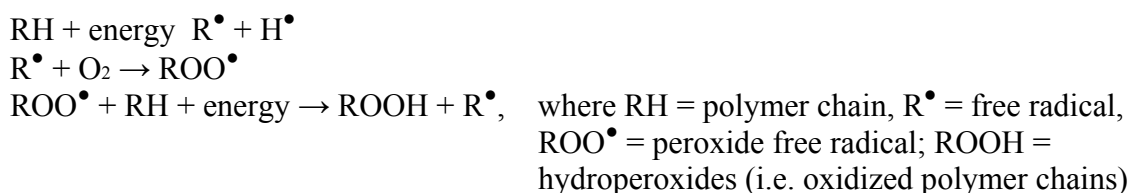
Polymeric main chain scission caused by oxidation results in embrittlement of the HDPE geomembrane and degradation of its mechanical properties (Koerner and Hsuan 2003; Mueller and Jakob 2003). However, even after the HDPE geomembrane becomes brittle it remains intact and can withstand high pressure (Mueller and Jakob 2003). Oxidation only occurs in amorphous regions of an HDPE geomembrane, since oxygen can not enter the crystalline regions. Therefore the overall rate of oxidation is inversely proportional to the degree of crystallinity (Needham et al. 2004). Elevated temperatures and the presence of transition metals (e.g. manganese, copper, aluminum, and iron) increase the rate of oxidation (Needham et al. 2004). However complete oxidation of a HDPE geomembrane will take an extended period of time. It has been estimated by Albertsson and Banhidi (1980) that a 60-mil thick HDPE geomembrane would take 10,000,000 years for complete oxidation based upon a mass loss of 0.00001% per year once oxidation starts (Needham et al. 2004).

However if oxygen is not available, the production of free radicals ($R^\bullet$) leads to polymer cross linking (i.e., combining polymer molecules) rather than polymer chain scission. Polymer cross linking up to a point in general improves the mechanical properties of the HDPE geomembrane (Kresser 1957; Frados 1976; Schnabel 1981; Sangster 1993; Koerner 1998).

Based upon this information it has been concluded (Koerner 1998; Needham et al. 2004) that HDPE geomembranes in landfill service will slowly degrade by thermal oxidation. Oxidation will generally be limited by the availability of oxygen within the subsurface, and such slow oxidative degradation will not result in the disintegration or disappearance of the

geomembrane within a timeframe of interest (i.e., 10,000 years). Thermal oxidative degradation is of no concern where oxygen has been removed from the surface of the geomembrane.

Based upon the above discussion thermal oxidative degradation of the HDPE geomembrane in conjunction with tensile stress cracking degradation (see Section 6.6.5) will be considered as a SDF Closure Cap degradation mechanism for modeling purposes using the Needham et al. (2004) model discussed in Section 6.6.7.

6.6.4 High Energy Irradiation Degradation

HDPE degradation by high energy irradiation can be similar to degradation by UV radiation (Needham et al. 2004). It has often been cited that the basic mechanical properties of a typical polymer start to change due to irradiation degradation by main chain scission at a total dose greater than 1 to 10 Mrad (Phillips 1988; Koerner et al., 1990; Koerner 1998; Nimitz et al. 2001; Needham et al., 2004). However, as discussed below, the impact of irradiation on polymers, and on HDPE in particular, is determined primarily by the total absorbed dose and the presence or absence of oxygen.

The absorption of high energy ionizing radiation such as gamma rays (γ-rays) by polymers primarily results in the production of free cation radicals and the ejection of electrons within the polymer. The ejected electrons can induce additional ionizations or produce electronic excitation in surrounding molecules. Secondary reactions can include the production of ions (both cations and anions) and free anion radicals. These products of radiation absorption are unstable and are reactive toward surrounding intact molecules resulting in both cross linking (combining polymer molecules) and main-chain scission (breakage of polymer molecules). For polyethylene the extent of irradiation induced cross linking or main chain scission appears to be independent of the type of radiation within a factor of 2 (i.e., alpha particles, beta particles, gamma-rays, X-rays, protons). Cross linking predominates in the absence of oxygen and main chain scission predominates in the presence of oxygen. (Schnabel 1981; Sangster 1993; Harper 1996; Kudoh et al. 1996)

Irradiation of polyethylene in the absence of oxygen at relatively low doses (i.e. less than 10 Mrad) primarily results in cross linking, which improves temperature and chemical resistance, increases the elastic modulus, tensile strength, and hardness, reduces the solubility, and improves the weatherability of the polyethylene (Kresser 1957; Frados 1976; Schnabel 1981; Sangster 1993). However, at high absorbed doses polyethylene becomes very hard and brittle (Kresser 1957; Kane and Widmayer 1989; Sangster 1993). For HDPE, the ultimate strength half-dose value in vacuum has been measured at greater than 5000 Mrad and the ultimate elongation half-dose value in vacuum has been measured at between 10 to 30 Mrad (Brandrup and Immergut 1989). The half-dose value is the absorbed dose required to reduce a particular mechanical property of the polymer by half under a defined environment (Brandrup and Immergut 1989). (Schnabel 1981)

However during irradiation in the presence of oxygen (i.e., in the presence of air) polyethylene undergoes predominately main-chain scission, which results in a rapid deterioration and subsequent deleterious impact upon mechanical properties. Main-chain scission can occur during reactions involving peroxyl and oxyl radicals. Since the oxidation

of free cation radicals, produced during irradiation, results in peroxyl and oxyl radicals, the presence of oxygen during irradiation results in the occurrence of more main-chain scission. Additionally oxygen can react with lateral macroradicals, which would otherwise crosslink, thus reducing the occurrence of cross linking. Finally radiation can provide the activation energy necessary for oxidation to occur, if oxygen is available. (Schnabel 1981; Sangster 1993; Sun et al. 1996; Badu-Tweneboah et al. 1999)

In the absence of oxygen the dose rate does not appear to influence the impact of irradiation on polyethylene (Brandrup et al. 1999). However in the presence of oxygen the following are two apparent dose rate effects (Schnabel 1981; Brandrup and Immergut 1989):

- High dose rates can result in the rapid depletion of oxygen within a polymer. This can result in further polymer deterioration, due to the combined effect of irradiation and oxidation which produces main-chain scission, being limited by oxygen diffusion into the polymer. In the case of polyethylene this can actually lead to increased cross linking due to further irradiation once the interior oxygen has been depleted and an actual improvement in mechanical properties. In this case main-chain scission only occurs at the surface of the polymer where oxygen is available. This, therefore, produces an apparent dose rate effect upon polymer deterioration at high dose rates. (Brandrup et al. 1999). At low dose rates polymer deterioration due to main-chain scission produced by irradiation and oxidation is not limited by oxygen diffusion into the polymer. Therefore at these low dose rates the full impact of combined irradiation and oxidation is realized. Therefore at lower dose rates, dose rate does not appear to impact degradation due to irradiation but it appears to be dependent upon total dose and the presence of oxygen. Polymer thickness also impacts the influence of oxygen on the polymer, since the thicker the polymer the longer the diffusion path for oxygen diffusion into the polymer (Brandrup et al. 1999). Figure 14 and Table 30 provide the impact of dose rate on the half-dose values for ultimate strength and ultimate elongation of HDPE in air (Brandrup and Immergut 1989). From Figure 14 it is seen that dose rates above about 5000 Rad/hr have an apparent dose rate effect while dose rates below 5000 Rad/hr do not.
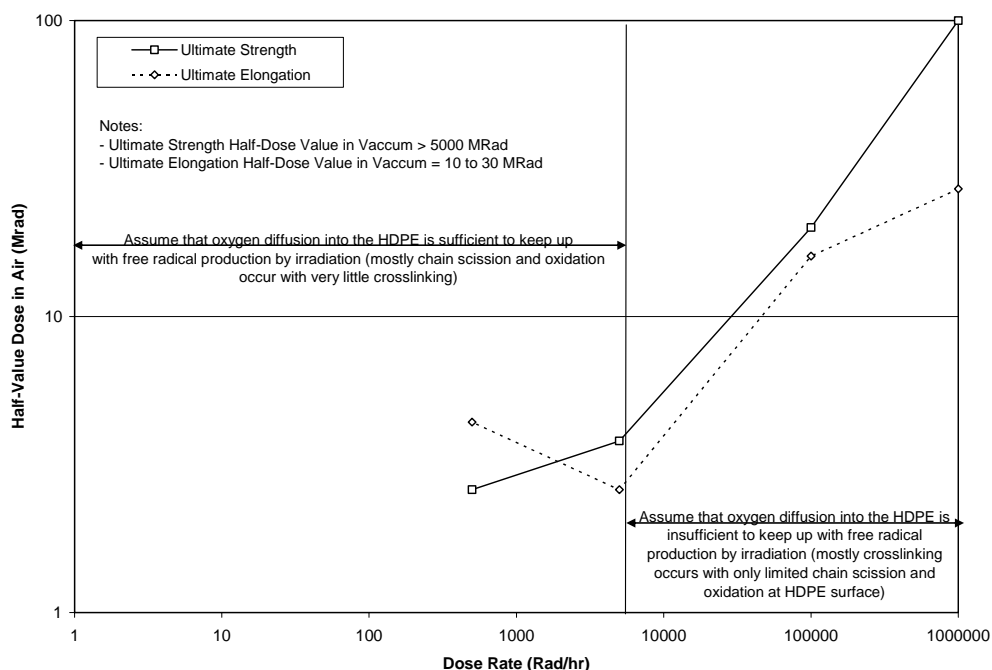
Figure 14. Dose Rate Impact on HDPE Ultimate Strength and Elongation Half-Value Dose in Air (Brandrup and Immergut 1989)

Table 30. Dose Rate Impact on HDPE Ultimate Strength and Elongation Half-Value Dose in Air (Brandrup and Immergut 1989)

Dose Rate (Rad/hr)	Ultimate Strength Half-Value Dose in Air (Mrad)	Ultimate Elongation Half-Value Dose in Air (Mrad)
1000000	100	27
100000	20	16
5000	3.8	2.6
500	2.6	4.4

- High dose rates can also result in an increase in the polymer's temperature. Many chemical reactions have fairly high activation energies, which can be overcome with the irradiation induced temperature increase and lead to reactions which might not otherwise occur (Brandrup et al. 1999).

Mechanical stress combined with irradiation is also known to accelerate radiation-induced degradation. (Hamilton et al. 1996).

6.6.4.1 Mitigating Irradiation Impacts on HDPE

The impacts of irradiation on HDPE can be mitigated by one or a combination of the following:

- The radiation dose rate can be lowered through the use of shielding to reduce the total dose absorbed by the HDPE over the period of concern,
- The level of oxygen to which the HDPE is exposed over the period of concern can be lowered so that the level and rate of degradation is oxygen dependent,
- Antioxidants (prevents oxidative chain reactions and scavenges free radicals) and carbon black (acts as an energy sink) can be incorporated into the HDPE to lower the impact of the presence of oxygen and radiation (Schnabel 1981; Brandrup et al. 1999),
- Thicker HDPE, such as 100 mil (2.5 mm) rather than 60 mil (1.5 mm), can be utilized to limit degradation to the surface of the sheet rather than to its interior, and/or
- Tensile stress on the HDPE can be minimized.

In most cases it is recommended that all of the mitigation means be employed.

6.6.4.2 Nuclear Regulatory Commission Recommendations

Staff from the Nuclear Regulatory Commission (NRC) recommended the following within Kane and Widmayer 1989:

"To compensate for the uncertainties associated with the long-term performance of geosynthetics, and to provide the level of confidence that is required by federal regulations, the use of geosynthetics alone (e.g., as a low-permeability geomembrane or as a geotextile filter fabric) is not recommended by the NRC staff. However, the use of geosynthetics to complement and improve the performance of natural soils and rocks or other proven construction materials is recommended by the staff."

A "100 Mrad regulatory guideline was established to promote selection of polyethylene materials with extremely low risk of degradation under the exposure conditions expected in the high integrity containers." (Badu-Tweneboah et al. 1999)

6.6.4.3 HDPE Irradiation Examples

Several HDPE irradiation examples are provided below particularly those dealing with its use in low-level radioactive waste disposal service:

- Whyatt and Fansworth (1990) evaluated a 60-mil HDPE geomembrane in simulated short-term (up to 120 days) chemical compatible tests with a high pH (~14) inorganic solution at 90°C and subjected them to radiation doses ranging from 0.6 to 38.9 Mrad. The solution consisted predominately of the following in descending order: sodium, nitrite, nitrate, aluminum, potassium, and sulfate. With immersion in the solution and an applied radiation dose, the break strength and elongation decreased (i.e. properties degraded), while yield and puncture strengths and their associated elongations all increased (i.e., properties improved). The 38.9 dose was slightly greater than the break elongation half-dose value (see Section 6.6.4 for the definition of the half-dose value) of the HDPE geomembrane under the conditions tested. No other properties tested were near the half-dose value.

- Badu-Tweneboah et al. 1999 performed an evaluation that demonstrated that the polyethylene components of a low-level radioactive waste disposal landfill in Barnwell South Carolina would perform their intended function of containment during at least the 500-year design period. The two polyethylene components were a 60 mil HDPE geomembrane in the cover system and 3/8 inch thick Linear Medium Density Polyethylene (LMDPE) inner liners within concrete high integrity containers for the disposal of low-level radioactive waste.
- Compatibility testing was performed on the 60-mil smooth HDPE geomembrane planned for the Hanford Grout facility. HDPE samples were exposed to a dose rate of 740,000 rads per hour until a total radiation dose of 16 Mrad or 37 Mrad was reached. The total dose of 37 Mrad resulted in a greater than 25% decrease in geomembrane strength and elasticity. Then the HDPE was immersed in a 194°F solution with a pH of 9.2 and a concentration of inorganics of 368,336 mg/L. It was stated that under these conditions the HDPE showed no unacceptable effects. (INEEL 2004)
- Traditional radiation sterilization of polymers for medical implants is performed to a dose of 2.5 Mrad (Deng et al. 1996).

6.6.4.4 High Energy Irradiation Degradation Applicability to SDF Closure Cap HDPE Geomembrane

Rosenberger (2007) has determined that the dose rate to the SDF closure cap HDPE geomembrane would be less than 0.1 mR/hr and that the total dose over 10,000 years would be less than 9,000 rad. This dose rate is significantly below the 5000 Rad/hr dose rate above which an apparent dose rate effect in HDPE is seen (see Section 6.6.4). Therefore the irradiation impact upon the HDPE geomembrane is assumed to be due to only total dose and not dose rate. From Table 30 the HDPE ultimate strength half-value dose in air at a dose rate of 500 Rad/hr was 2.6 Mrad (Brandrup and Immergut 1989). The basic mechanical properties of a typical polymer start to change due to irradiation degradation at a total dose greater than 1 to 10 Mrad (Phillips 1988; Koerner et al., 1990; Koerner 1998; Nimitz et al. 2001; Needham et al., 2004), with levels as high as 100 Mrad being listed as acceptable (Badu-Tweneboah et al. 1999). Therefore a total dose of 2.6 Mrad appears to be a reasonable limit for total dose to the HDPE geomembrane utilized as part of the SDF closure cap. This limit of 2.6 Mrad is approximately 290 times greater than the maximum dose of 9,000 rad over 10,000 years to which the SDF closure cap geomembrane could potentially be exposed. Based upon this discussion, high energy irradiation of the SDF closure cap HDPE geomembrane is considered an insignificant degradation mechanism.

6.6.5 Tensile Stress Cracking Degradation

After the antioxidants in a HDPE geomembrane have been depleted, thermal oxidation of the geomembrane commences if oxygen is present causing embrittlement and degradation of mechanical properties over time. However the geomembrane will remain an effective hydraulic barrier unless it is physically damaged or develops holes or cracks. Holes or cracks can develop from the following two types of tensile stress cracking in a HDPE geomembrane (Needham et al. 2004):

- Ductile tensile failure is a ductile failure where the applied tensile stress exceeds the short-term tensile break strength of the geomembrane

- Brittle stress cracking is a brittle failure where the applied long-term tensile stress is less than the short-term tensile break strength of the geomembrane

In general, HDPE geomembrane installations should be designed so that the short-term tensile break strength of the geomembrane is not exceeded. However subgrade settlement and geomembrane downdrag by waste settlement on the side slopes can occur and cause exceedance of the geomembrane's tensile break strength. (Needham et al. 2004)

Brittle stress cracking, on the other hand, can occur as oxidation of the HDPE geomembrane proceeds and causes increased embrittlement and degradation of its mechanical properties over time. As thermal oxidation proceeds brittle stress cracking will occur where the geomembrane is under stress at lower and lower stresses over time. However as cracking occurs stresses are relieved thus reducing the likelihood of further cracking. Brittle stress cracking can be exasperated by elevated temperatures and contact with agents such as detergents, alcohols (e.g., methanol, ethanol, and propanol), acids and chlorinated solvents (i.e., environmental stress cracking).

The extent of brittle stress cracking is dependent upon the geomembrane stress crack resistance (SCR), the local and global stress over the geomembrane, the geomembrane temperature, the fluid in contact with the geomembrane, and the extent of thermal oxidative degradation. However as long as the geomembrane is not subjected to tensile or shear stresses, it should not fragment and disintegrate, but it should remain intact, for practical considerations, indefinitely. (Needham et al. 2004)

Based upon the above discussion tensile stress cracking degradation of the HDPE geomembrane in conjunction with thermal oxidative degradation (see Section 6.6.3) will be considered as a SDF Closure Cap degradation mechanism for modeling purposes using the Needham et al. (2004) model discussed in Section 6.6.7.

6.6.6 Biological Degradation (microbial, root penetration, burrowing animals)

Biological degradation of HDPE geomembranes could potentially be caused by microbial biodegradation, root penetration, or burrowing animals. Limited investigations have been performed relative to the microbial degradation of HDPE geomembranes. Koerner (1998) stated that the high-molecular-weight polymers used for geomembranes are judged insensitive to microbial (i.e., fungi or bacteria) biodegradation.

Information regarding root penetration of HDPE geomembranes is present in the literature. Available references, including field experience at SRS, indicate HDPE membranes of the thickness used for landfill liners typically preclude root penetration and cause roots to follow laterally atop the geomembrane surface. Landreth (1991) describes a USEPA test using four membranes "that might be used in waste management facilities for landfill cover systems", including polyethylene. The results were that although root mass achieved maximum density atop the membranes, "there was no evidence of root penetration". Badu-Tweneboah et al. (1999) confirm this with their statement that roots are not likely to penetrate an intact geomembrane, they are likely to develop laterally above the geomembrane, and they are not known to enlarge existing geomembrane defects. Additionally Carson (2001) indicated that roots do not penetrate geomembranes. An investigation conducted by Serrato (2004) at SRS

showed that roots from overlying pine trees turned horizontally and followed along the top of the geomembrane upon reaching a HDPE geomembrane without damaging or penetrating it. Newman et al. (2004) describe the thirty-year durability of a 20-mil thick polyvinylchloride (PVC) geomembrane used as an aquaculture pond liner. They interpreted the lack of holes to indicate resistance to both microorganisms and root penetration from the dense stand of cattails, trees, and other vegetation. In general, polymer sheets such as polyethylene, polypropylene, and PVC are impervious to roots, and are commercially marketed as root barriers. For example, the Henry Company markets various polypropylene root barrier sheets for "green roofs" and other horticultural applications. "Root Stop HD (Heavy Duty)" is a commercially available 27-mil thick HDPE root barrier distributed by Hydrotech, Inc., also designed for rooftop gardens.

Based upon this information, it will be assumed that roots reaching intact portions of the HDPE geomembrane will be unable to penetrate it. Such roots upon reaching intact portions of the HDPE geomembrane will instead turn and continue growth laterally along the top of the geomembrane in a down slope direction. Roots that reach the HDPE geomembrane will only be able to penetrate it in locations where holes in the geomembrane have already formed due to HDPE degradation. Such root penetration through existing holes within the HDPE geomembrane and subsequent penetration of the underlying GCL (see Section 6.7.7) will be considered as a SDF Closure Cap degradation mechanism for modeling purposes.

Very little information is available relative to the potential for geomembrane damage due to burrowing animals. A geomembrane would have to be harder than the burrowing animals' teeth or claws to avoid the potential for damage. Therefore geomembranes are potentially vulnerable to burrowing animals. Logically it is assumed that stronger, harder, and thicker geomembranes are more resistant to burrowing animals. (Koerner 1998) While burrowing animals can potentially damage unprotected HDPE geomembranes in general, damage of the SDF Closure Cap HDPE geomembrane is not considered a threat due to the presence of the overlying erosion barrier, which will be designed to preclude burrowing animals (see Table 5 and Section 4.4.11) from reaching the HDPE geomembrane. Therefore burrowing animals will not be considered as a SDF Closure Cap HDPE geomembrane degradation mechanism for modeling purposes.

6.6.7 Environment Agency Degradation Model

Based upon an extensive literature of HDPE geomembrane degradation mechanisms, Needham et al. (2004) has produced a long-term degradation HDPE geomembrane degradation model for use by the Environment Agency of England and Wales in the preparation of Performance Assessments (PAs) for landfills. Needham et al. (2004) tie all degradation mechanisms to the generation of holes or cracks in the HDPE geomembrane through time. From this they have produced a six-stage model for generation of holes over time. They take generation of holes from initial installation of the geomembrane to long-term generation of holes as the geomembrane becomes increasingly more susceptible to brittle stress cracking. The following are the six stages considered by Needham et al. (2004):

- Stage 1 is the period of disposal facility construction and considers the holes produced by construction.
- Stage 2 is the operational period and considers the holes produced by waste placement.

- Stage 3 is a 10 to 50 year period immediately following closure cap construction during which no additional holes are assumed to be produced.
- Stage 4 is a combination of the antioxidant depletion and induction periods during which holes are assumed to be produced at low rates relative to subsequent stages due to tensile stresses.
- Stage 5 is the oxidation stage, which is assumed to last 50 years, during which embrittlement and further stress cracking will occur relatively rapidly due to any significant remaining tensile stress.
- Stage 6 is the terminal stage, during which it is assumed that the total number of holes present at the end of Stage 5 are reproduced as new holes every 100 years.

For each of the stages Needham et al. (2004) the generation of holes is divided into an excellent, good, and fair case with the number of holes produced increasing from the excellent to fair case. They also provide different hole sizes divided into the categories of pin holes, holes, tears, and cracks. The model produced by Needham et al. (2004) is based upon the most current research conducted concerning HDPE geomembrane degradation. They have converted that research into a form (i.e., generation of holes over time) that can be utilized in PA contaminant transport modeling.

This model will be used for the consideration of antioxidant depletion (Section 6.6.2), thermal oxidation (Section 6.6.3), and tensile stress cracking (Section 6.6.5) as a SDF closure cap degradation mechanism for modeling purposes.

6.7 POTENTIAL GCL DEGRADATION MECHANISMS

A geosynthetic clay liner GCL consists of "bentonite sandwiched between two geotextiles" (USEPA 2001) or bentonite mixed with an adhesive and attached to a geomembrane (Bonaparte et al. 2002). Bentonite, the hydraulically functional portion of a GCL, is a mixture of minerals typically dominated by swelling-type montmorillonite clays, which is formed as the stable alteration product of volcanic ash (Worrall 1975). The bentonite used is generally sodium or calcium bentonite. Sodium bentonite is used more frequently because of its superior swelling capacity and lower initial permeability. Calcium bentonite has a smaller swelling capacity and a somewhat higher initial hydraulic conductivity (Witt and Siegmund 2001). The following is the definition of a Geotextile GCL as defined by the Environmental Protection Agency (USEPA 2001):

> A Geotextile GCL "is a relatively thin layer of processed" bentonite … "fixed between two sheets of geotextile. … A geotextile is a woven or nonwoven sheet material … resistant to penetration." … "Adhesives, stitchbonding, needlepunching, or a combination of the three" are used to affix the bentonite to the geotextile. "Although stitchbonding and needlepunching create small holes in the geotextile, these holes are sealed when the installed GCL's clay layer hydrates."

A GCL was first used in a landfill in 1986 (Bonaparte et al. 2002). Major advantages of GCLs over compacted clay liners (CCL) include an extremely low hydraulic conductivity (1 to 5E-09 cm/s), low infiltration rate, ability to withstand differential settlement and

assimilate deformations, ability to self-heal after desiccation, resistance to the potentially damaging effects of freezing temperatures, relatively low cost, simple and quick construction, and its thinness (Benson 1999; Bonaparte et al. 2002; Witt and Siegmund 2001). GCLs, which have not been hydrated, are on the order of 0.2 inches thick, much thinner than the typical 2-foot CCL. Some primary potential disadvantages associated with GCLs relative to CCL are related to the thinness of GCLs. These include increased thinning due to excessive or unevenly applied pressure such as that resulting from overlying gravel intrusion (Chien et al. 2006), increased vulnerability to puncture from construction equipment, less capacity to adsorb and attenuate chemicals, and less resistance to chemical diffusion (Bonaparte et al. 2002). For the SDF closure cap these potential disadvantages relative to CCLs are mitigated by the following:

- It will be immediately overlain (from bottom to top) by a 60-mil HDPE geomembrane (see Section 4.4.5), a geotextile fabric (see Section 4.4.6), and a sand drainage layer (see Section 4.4.7); all of which will tend to produce even application of the overburden pressure on the GCL. Therefore potential thinning due to excessive or unevenly applied pressure will be mitigated.
- The GCL will be overlain by a 60-mil HDPE geomembrane (see Section 4.4.5) and a geotextile fabric (see Section 4.4.6) which will provide GCL protection from puncture.
- As outlined in Section 6.0 the GCL will be located in the SDF closure cap above the disposal cells and is therefore not subject to chemical degradation from leachate. Therefore the GCL is not designed to attenuate chemicals or provide resistance to chemical diffusion from any such leachate as it might be if it were located in a bottom liner.

These items will receive no further consideration as potential GCL degradation mechanisms based upon the above discussion.

As outlined Table 5 and Sections 4.4.4 and 4.4.5, a GCL will be utilized in conjunction with a HDPE geomembrane to form a composite hydraulic barrier to infiltration. As outlined in Table 17, the following potential degradation mechanisms will be considered for the GCL:

- Slope stability
- Freeze-thaw cycles
- Dissolution
- Divalent cations (Ca^{+2}, Mg^{+2}, etc.)
- Desiccation (wet-dry cycles)
- Biological (root penetration, burrowing animals)

6.7.1 Slope Stability

Hydrated sodium bentonite within GCLs has both low shear strength and bearing capacity. Fully hydrated sodium bentonite may have internal friction angles as low as 4 to 10° (Benson 1999; Bonaparte et al. 2002). GCLs can generally be safely placed on slopes of 10H:1V (5.7° or 10%) or flatter without the need for internal reinforcement or slope stability analysis (Bonaparte et al. 2002). Internally-reinforced GCLs can be safely placed on greater than 10% slopes. Bonaparte et al. (2002) report on slope stability monitoring of final cover system test plots that include internally-reinforced GCLs. The results demonstrate acceptable

performance on 3H:1V (33%) slopes but not on 2H:1V (50%) slopes. The failures were due to inadequate interface strength and not inadequate internal shear strength, clearly indicating that proper characterization of GCL interface shear strength is an important design step.

As outlined in Section 4.4.4, the GCL will be placed at a 4% slope and it is not anticipated that the GCL would be placed on the side-slopes. This is well below the 10% to 33% slopes upon which GCLs can be safely placed. Therefore slope failure due to the GCL on a 4% will not be considered as a SDF closure cap degradation mechanism for modeling purposes.

6.7.2 Freeze-Thaw Cycles

Field studies indicate that GCLs are resistant to damage from freezing temperatures, are undamaged by freeze-thaw cycling, and do not need to be protected from frost (Benson 1999: Bonaparte et al. 2002). These studies "indicate that GCLs are not damaged by frost because the hydrated bentonite is soft, and readily consolidates around ice lenses and other defects during thawing" (Benson 1999).

DeGaetano and Wilks (2001) produced a map of extreme-value maximum soil freezing depths for the United States (see Figure 15). As seen in the figure most of South Carolina has a maximum frost depth of between 0 and 25 cm (0 and 10 inches). Interpolation to SRS yields a maximum frost depth of approximately 5 inches, which is much shallower than the SDF closure cap's GCL depth of burial (i.e., 6 feet or greater) thereby precluding freeze-thaw cycles as a degradation mechanism. Therefore freeze-thaw will not be considered as a SDF Closure Cap GCL degradation mechanism for modeling purposes.
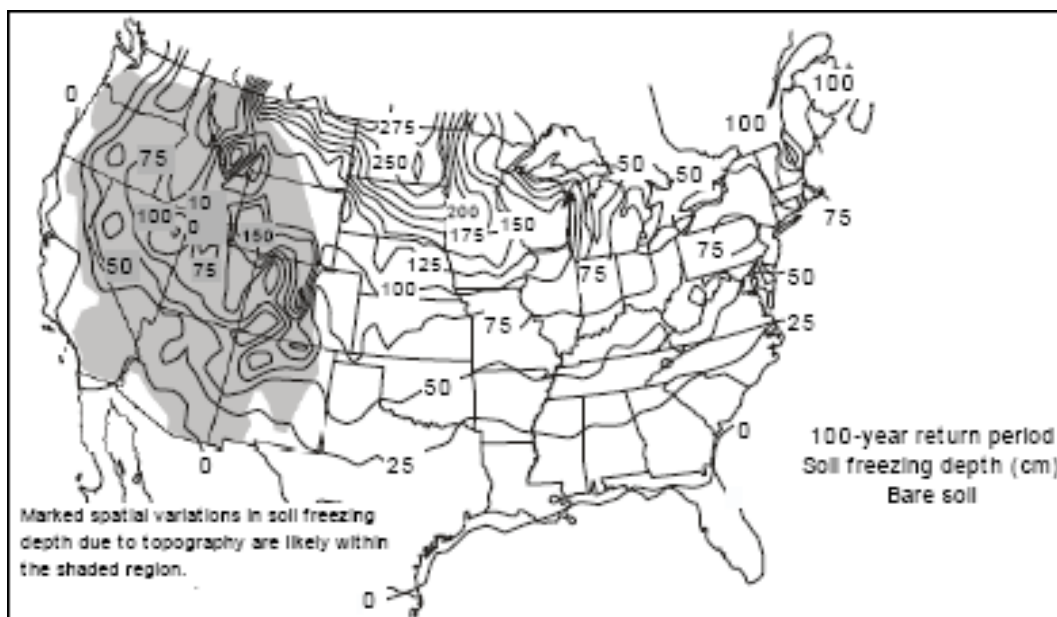
Figure 15.   United States Extreme-Value Maximum Soil Freezing Depth Map

6.7.3 Dissolution

Bentonite is a mixture of minerals typically dominated by montmorillonite clays, with sodium-bentonite dominated by sodium-montmorillonite. Thus, degradation of sodium - bentonite depends on how sodium-montmorillonite degrades. As with many clay minerals,

sodium-montmorillonite has a variable formula. For the purposes of this discussion and selection of thermodynamic data the formula will be assumed to be:

$Na_{0.33}Mg_{0.33}Al_{1.67}Si_4O_{10}(OH)_2$, where Na is the interlayer, easily exchangeable cation and Mg substitutes for Al in octahedral sheets.
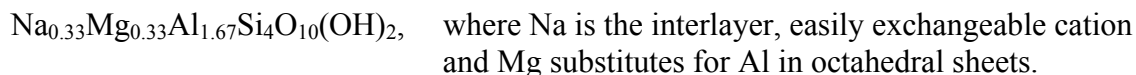
Sodium-montmorillonite dissolves incongruently. If it is assumed that all Na and Mg stays in solution, the dissolution reaction can be written as:

Sodium-montmorillonite + $0.99H^+$ + $0.175H_2O$ = $0.33Mg^{+2}$ + $0.33Na^+$ + 0.835 Kaolinite + 2.33 Quartz,
where kaolinite and quartz are the products.
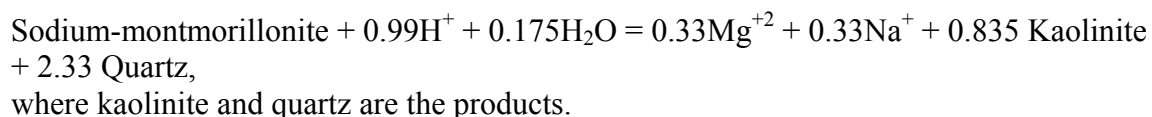
Based on a log K of 6.12 for this reaction (Bethke, 2005), 1.8×10^{-5} moles of sodium-montmorillonite would dissolve in 1 liter of relatively clean water under equilibrium conditions (i.e., assuming no kinetic limitations). For a bentonite quantity of 0.75 lbs/ft^2 and assuming the bentonite consists of 90% sodium-montmorillonite, 46,364 liters of water would have to pass through a square foot to dissolve all of the bentonite under equilibrium conditions. The infiltration rate through a closure cap without the composite hydraulic barrier, lateral drainage layer, and erosion control layer) of 16.45 in/yr) can be used to represent the infiltration rate at complete failure of the closure cap.

Assuming this complete closure cap failure infiltration rate of 16.45 in/yr, it would take approximately 1,200 years to completely convert the sodium-montmorillonite to kaolinite and quartz. Under slowly degrading closure cap conditions, it would take significantly longer for the conversion to occur. Additionally while montmorillonite can weather directly to kaolinite and quartz (Borchardt, 1977), it more commonly weathers through a series of predominately clay minerals. The low solubility of sodium-montmorillonite, the large volume of water and extended time required to convert it to kaolinite and quartz under equilibrium conditions, and the fact that it more commonly weathers through a series of clays suggest that sodium-bentonite dissolution is probably not its predominate degradation mechanism versus infiltration. Therefore dissolution of the bentonite in the GCL will not be considered as a major SDF closure cap degradation mechanism over a 10,000 year period and will therefore not be modeled.

6.7.4 Divalent Cations (Ca^{+2}, Mg^{+2}, etc.)

The bentonite used in GCLs is generally sodium or calcium bentonite. Sodium bentonite is used more frequently than calcium bentonite because of its superior swelling capacity and lower initial permeability (Witt and Siegmund 2001). However within closure caps, sodium bentonite GCLs that are not protected by an overlying geomembrane are susceptible to exchange of sodium with divalent cations such as calcium and magnesium particularly when calcium and magnesium rich soils overly the GCL (Benson 1999; Bonaparte et al. 2002; Egloffstein 2001). The conversion of hydrated sodium bentonite to calcium bentonite results in a decrease in the swell potential or potential volume of water bound to the mineral surface (i.e., immobile water) and a subsequent increase in the saturated hydraulic conductivity of the GCL particularly under conditions of low confining or overburden stress such as found in closure caps (Bonaparte et al. 2002; Egloffstein 2001; Jo et al. 2005).

The free swell index (ASTM 2006e) of sodium bentonite is typically greater than 24 ml/2 g (GSE 2006a), while that of calcium bentonite is on the order of 12 ml/2 g (CIMBAR 2001). Studies and case histories have shown that permeation of a sodium bentonite GCL with solutions containing a large fraction of divalent cations can cause the hydraulic conductivity of the GCL to increase 1 order of magnitude or more (Benson 1999; Jo et al. 2005).

One of the most comprehensive studies regarding the impact of divalent cation solutions on sodium bentonite GCLs has been conducted by Jo et al. (2005). Jo et al. (2005) permeated sodium bentonite GCL samples with deionized water, 100 mM sodium chloride (NaCl) and potassium chloride (KCl) solutions, and calcium chloride ($CaCl_2$) solutions ranging from 5 to 500 mM until further changes in saturated hydraulic conductivity were not detected (in some cases this took more than 2.5 years and up to 686 pore volumes). Table 31 presents a summary of the results from Jo et al. (2005). The following are the primary conclusions drawn by Jo et al. (2005):

- Permeation of the sodium bentonite GCL with DI water from a practical perspective resulted in essentially no change in the saturated hydraulic conductivity of approximately 3.0E-09 cm/s (see Table 31).
- Permeation of the sodium bentonite GCL with either NaCl or KCl solutions from a practical perspective resulted in essentially no change in the saturated hydraulic conductivity (i.e., within a factor of 2 of those obtained using DI water) even though Na and K have different hydrated radii.
- Permeation of the sodium bentonite GCL with weak divalent solutions (i.e., $CaCl_2 \leq 20$ mM), resulted in an initially low saturated hydraulic conductivity (~2.0E−09 cm/s), which did not change for some time. Subsequently, the saturated hydraulic conductivity gradually increased by approximately one order of magnitude (~2.0E−08 cm/s). Measurements of the exchange complex after testing showed that exchange of Ca^{+2} for Na^+ was essentially complete regardless of which weak divalent solution was used.
- Permeation of the sodium bentonite GCL with strong divalent solutions ($CaCl_2 \geq 50$ mM) resulted in an almost immediate (<1 day) increase in saturated hydraulic conductivity of approximately 3 orders of magnitude (~1.0E−06 cm/s) than that of GCLs permeated with DI water. The high Ca^{+2} concentration resulted in rapid Na^+ exchange and saturated hydraulic conductivity increase.
- $CaCl_2$ solutions should be representative of the behavior of sodium bentonite GCLs to solutions containing divalent cations in general.

Based upon the above literature concerning the impact of the exchangeable cations on the saturated hydraulic conductivity of sodium bentonite, geochemical simulations using Geochemist's Workbench® (Bethke, 2005) have been performed to evaluate the potential changes to the sodium bentonite from likely SRS permeants. The following two potential SRS permeants were modeled: 1) rainwater equilibrated with SRS soil; 2) rainwater equilibrated with portlandite ($Ca(OH)_2$).

Table 31. **GCL Average Saturated Hydraulic Conductivity from Jo et al. (2005)**

Permeant	DI Water		5 to 20 mM CaCl$_2$ [1]		50 to 500 mM CaCl$_2$ [2]	
Period	Initial	Final	Initial	Final	Initial	Final
K$_{sat}$ (cm/s)	2.1E-09	3.0E-09	2.3E-09	1.8E-08	1.2E-06	1.3E-06
K$_{sat}$ / Initial DI Water K$_{sat}$	1	1.4	1.1	8.6	571	619

Source: Jo et al. (2005) Table 2
Samples were under either an effective stress of 2.3 or 3.4 psi
[1] 209 to 848 mg/L Ca^{+2}
[2] 1,985 to 19,400 mg/L Ca^{+2}

The composition of rainwater equilibrated with SRS soil used in the simulation was taken as that of uncontaminated SRS background monitoring well (P27D) in the vicinity of the General Separations Area (Strom and Kaback, 1992). The well is screened in the water table aquifer and is assumed to be an approximation of rainwater equilibrated with SRS soil. The composition of rainwater equilibrated with portlandite (Ca(OH)$_2$) is an approximation of the composition of infiltration passing through typical CLSM containing portland cement.

The compositions of the two waters used in the simulations are shown in Table 32. Reaction of the infiltrating water with an initial 306 grams of sodium-montmorillonite was simulated. This is the estimated mass in a sodium-bentonite composed of 90 wt% sodium-montmorillonite and incorporated into the GCL at 0.75 lbs/ft^2. Thus, the simulations are for liters of infiltrating water that pass through this hypothetical square foot of GCL. Figure shows the geochemical simulation of sodium-montmorillonite degradation with infiltrating water representing rainwater equilibrated with SRS soil. Figure 17 shows the geochemical simulation of sodium-montmorillonite degradation with infiltrating water representing rainwater equilibrated with a typical CLSM (i.e., portlandite (Ca(OH)$_2$))

Table 32. **Chemical Compositions of Infiltrating Water used for Sodium-Montmorillonite Degradation Geochemical Simulations**

Constituent	P27D Groundwater	Water Equilibrated with Portlandite
pH	5.4	12.3
Ca	2.5 mg/L	641 mg/L
Mg	0.4 mg/L	99.6 mg/L
Na	1.0 mg/L	1.0 mg/L
Cl	3.3 mg/L	3.3 mg/L
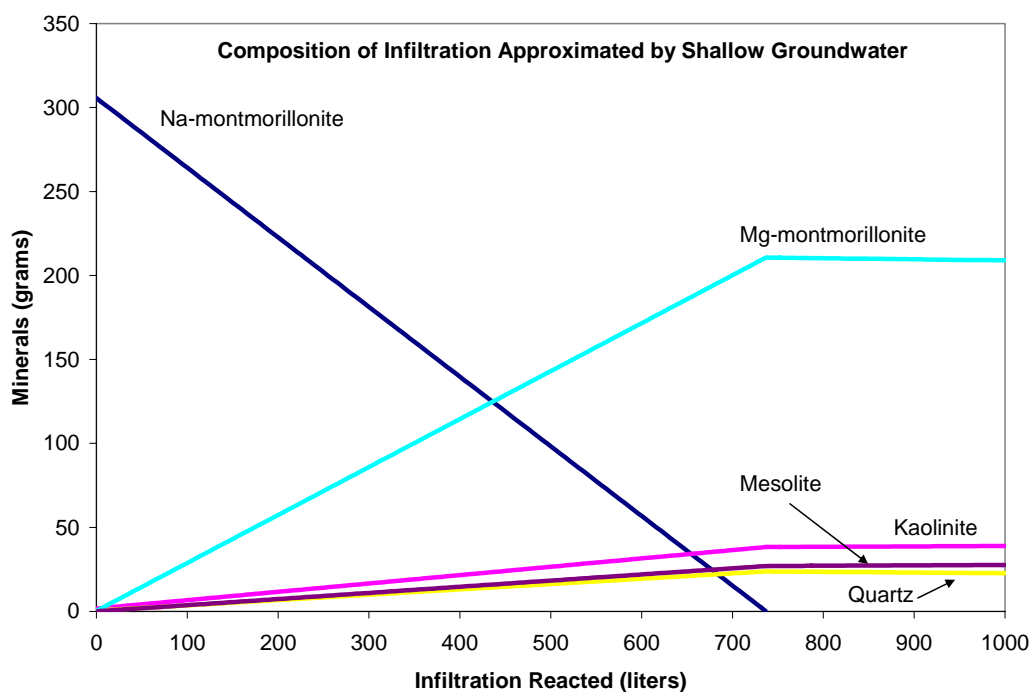
Figure 16. **Geochemical Simulation of the Alteration of Sodium-Montmorillonite by Infiltrating Water Equilibrated with SRS Soil**
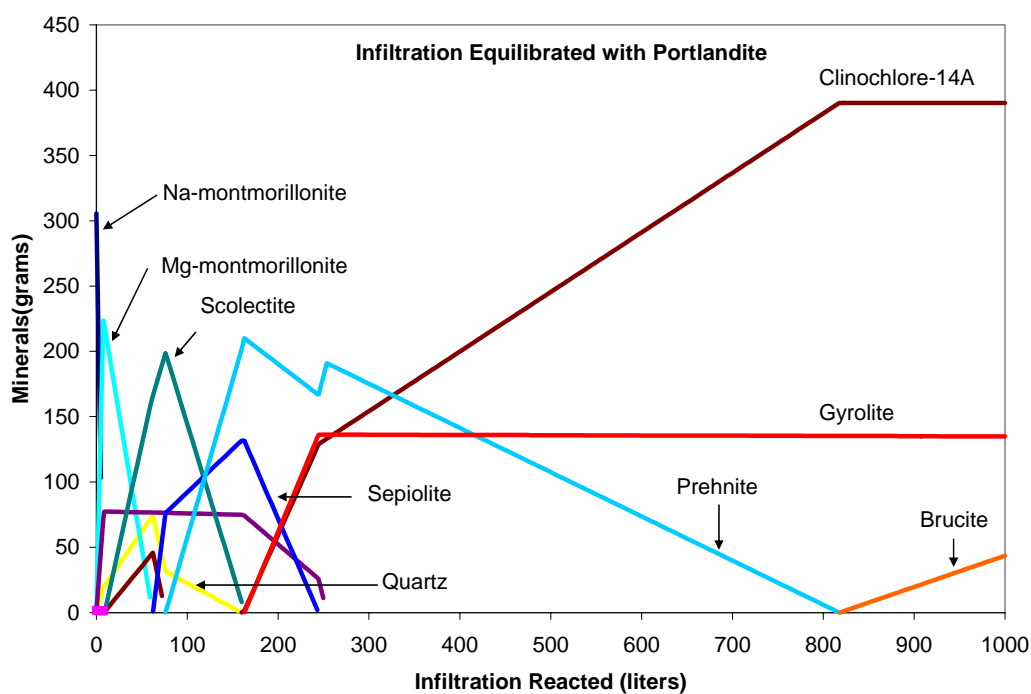
Figure 17. **Geochemical Simulation of the Alteration of Sodium-Montmorillonite by Infiltrating Water Equilibrated with Typical CLSM**

For infiltration equilibrated with SRS soil, sodium-montmorillonite completely degrades to magnesium-montmorillonite after passage of about 740 liters of water through a square foot containing 0.75 lbs of bentonite. Between 740 and 1000 liters the assemblage of minerals replacing sodium-montmorillonite is magnesium-montmorillonite, kaolinite, mesolite (a calcium zeolite), and quartz.

Infiltration equilibrated with portlandite has a much higher pH and concentrations of Ca and Mg (for these simulations the Mg/Ca ratio was assumed to be the same in both waters). This causes much quicker and more complicated degradation of sodium-montmorillonite. The sodium-montmorillonite is initially converted to magnesium-montmorillonite after fewer than 5 liters of infiltration have passed. This is followed by alteration of the magnesium-montmorillonite to various clays, zeolites, and other minerals. At 1000 liters of infiltration the mineral assemblage is clinochlore-14A (a chlorite clay), gyrolite (a Ca silicate), and brucite ($Mg(OH)_2$).

The different mechanisms and environments of degradation result in very different rates of sodium-montmorillonite removal. The fastest rate is when infiltration has equilibrated with portlandite. In none of these cases is the mineral layer in the GCL completely removed, rather it is altered to different minerals.

Some information on long-term degradation rates of bentonite has been garnered from study of bentonites in their natural settings. Ohe et al. (1998) concluded that the alteration rate of a Japanese sodium-bentonite to calcium-magnesium-bentonite for a layer below the water table was about 1 cm/1000 years. Based on study of another Japanese bentonite, Kamei et al. (2005) concluded that if this material was used in a geologic storage system complete conversion to illite would require greater than 10,000 years. While these studies do not allow a prediction of the life-time of a GCL in the closure cap, they do suggest the processes of bentonite degradation are slow.

Based upon this discussion, it will be assumed that if a sodium bentonite GCL with a saturated hydraulic conductivity of 5.0E-09 cm/s (see Section 5.4.6) is used, it will be eventually converted to a calcium or magnesium bentonite with a saturated hydraulic conductivity one order of magnitude lower (i.e. 5.0E-08 cm/s). Additionally if it is determined that a sodium bentonite GCL will be utilized, selection of the material utilized to fill the voids in the erosion barrier stone will consider its impact upon the sodium bentonite GCL. In particular materials such as CLSM, which typically contain cement with significant calcium content, would likely not be utilized.

Use of a calcium bentonite GCL or bagged calcium bentonite as a substitute for a sodium bentonite GCL will be evaluated. If calcium bentonite is utilized a saturated hydraulic conductivity of 5.0E-08 cm/s will also be assigned to this layer at this time pending further investigation. This is considered conservative relative to the information provided in Section 6.7.5 concerning the saturated hydraulic conductivity of 4.0E-09 cm/s determined for a 45 year old calcium bentonite field installation at SRS (Serrato 2007). Therefore degradation of the bentonite GCL by cation exchange will be considered as a SDF closure cap degradation mechanism for modeling purposes, with the assignment of a degraded saturated hydraulic conductivity of 5.0E-08 cm/s whether sodium or calcium bentonite is utilized for the GCL.

Since it is currently difficult to assign timing to conversion of sodium bentonite to calcium or magnesium bentonite, it will be assumed that during the 100-year institutional period that the GCL has a saturated hydraulic conductivity of 5.0E-09 cm/s and thereafter it has a saturated hydraulic conductivity of 5.0E-08 cm/s for modeling purposes.

6.7.5 Desiccation (wet-dry cycles)

One often reported advantage of GCLs over compacted clay liners (CCL) is the ability of GCLs to self-heal after desiccation (Boardman and Daniel 1996; Carson 2001; Egloffstein 2001; Witt and Siegmund 2001). However the following must be taken into consideration in relation to the potential desiccation self-healing properties of GCLs:

- After desiccation and subsequent cracking of a GCL, it can take a significant period of time (i.e., potentially days) upon rewetting to seal the cracks and re-achieve the initially low saturated hydraulic conductivity. This delay in crack sealing can allow preferential saturated flow through the cracks rather than through the GCL matrix during the resealing period (Bonaparte et al. 2002; Witt and Siegmund 2001).
- The alteration of sodium-bentonite to calcium-magnesium-bentonite can potentially reduce the swell potential of the bentonite to such an extent that cracks formed during desiccation can not completely swell shut upon rewetting thus increasing the saturated hydraulic conductivity of the GCL by several orders of magnitude (Benson 1999; Chien et al. 2006; Egloffstein 2001; Lin and Benson 2000; Witt and Siegmund 2001).

The following can preclude or reduce the impact of GCL desiccation and desiccation combined with the alteration of sodium-bentonite to calcium-magnesium-bentonite on the saturated hydraulic conductivity of the GCL and potential infiltration:

- A sufficient thickness of soil overlying the GCL can be provided to prevent desiccation and maintain constant water content. The thicker the overlying soil, the less likely desiccation cracks will form within the GCL. There is little danger of desiccation at all for GCLs overlain by 6 feet or more of soil and located in humid environments with a relatively uniform annual precipitation. (Egloffstein 2001; Witt and Siegmund 2001)
- The GCL can be overlain by both a geomembrane and a minimum of several feet of soil to prevent desiccation, maintain constant water content, and preclude or reduce the rate of alteration of sodium-bentonite to calcium-magnesium-bentonite (Benson 1999; GSE 2006b; Lin and Benson, 2000). Benson 1999 takes this further by stating that "GCLs should not be used without being overlain by a geomembrane."
- The soil overlying the GCL should not contain an abnormally high concentration of soluble salts containing divalent cations such as Ca^{+2} or Mg^{+2} (GSE 2006b; Jo et al. 2005).
- Calcium bentonite can be used rather than sodium bentonite. While calcium bentonite has a smaller swelling capacity and a somewhat higher initial hydraulic conductivity, it more resistance to degradation due to exchange with external cations and therefore will maintain its self-healing capacity and a more constant saturated hydraulic conductivity (Egloffstein 2001; Witt and Siegmund 2001).

Hawkins (1962) reports on a series of laboratory to field scale tests to investigate the use of bentonite at SRS to limit soil moisture movement into buried radioactive waste. The bentonite utilized was a southeastern calcium bentonite (American Colloid Company Panther Creek bentonite (Serrato 2006)). The tests included an evaluation of the impact of desiccation on the bentonite. Hawkins (1962) reported the following concerning the tests conducted at SRS:

- A laboratory saturated hydraulic conductivity of 3.0E-08 cm/s was determined for the bentonite.
- A laboratory test was conducted where dry bentonite was placed between two 4-inch layers of clayey sand, the bentonite was hydrated, the system was allowed to dry under atmospheric conditions for three weeks, and then the system was rewetted. During the drying phase cracks completely penetrating the bentonite developed which were rapidly (<1 hour) resealed upon rewetting. It was estimated that approximately 5% of the rewetting water past through the cracked bentonite before it resealed.
- Lysimeter testing in the field was conducted from November 1960 through March 1962, during which a 3-month drought occurred in the fall of 1961. The lysimeters consisted of bentonite layers overlain by 1 or 2 feet of soil in addition to soils only lysimeters. A total rainfall of 74.71 inches was recorded during this period. No percolation occurred through any of the lysimeters with bentonite, whereas an average of 27.51 inches of percolation was recorded through the soils-only lysimeters. Noticeable settling of the surface soil of the lysimeters containing bentonite overlain by 1-foot of soil was observed after the 3-month drought; this was not observed in the lysimeters containing bentonite overlain by 2-foot of soil. It was concluded that cracking of the bentonite overlain by only 1-foot of soil resulted in the settling; however the bentonite subsequently resealed upon rewetting.
- Based upon the previous testing, a 50-foot by 50-foot field test area (Test Facility – Bentonite Umbrella Test (TFBUT)) was completed in November 1961 that consisted of 3 to 4 inches of dry calcium bentonite (Serrato 2006) overlain by 2-feet of soil. Active maintenance of the field test site to maintain natural grasses and prevent the establishment of trees was conducted until 1989. Since 1989 no active maintenance of the area has been conducted.

In 2006 (45 years after installation) a Shelby tube sample of the bentonite within TFBUT was taken and the saturated hydraulic conductivity of the bentonite layer was determined to be 4.0E-09 cm/s (Serrato 2007). This is a lower saturated hydraulic conductivity than that determined by Hawkins (1962); indicating that no degradation of the bentonite in relation to the saturated hydraulic conductivity of the matrix is evident after 45 years.

As outlined in Table 4, the SDF Closure Cap GCL will be overlain by a 60-mil HDPE geomembrane (see Section 6.7.6 below for information on the benefits of composite hydraulic barriers) and 6-feet of soil materials. This conforms to the requirements laid out by Benson (1999), Egloffstein (2001), GSE (2006b), Lin and Benson (2000), and Witt and Siegmund (2001) for closure cap systems that preclude desiccation damage of the GCL.

Additionally as outlined in Section 6.7.4 if it is determined that a sodium bentonite GCL will be utilized, selection of the material utilized to fill the voids in the erosion barrier stone will consider its impact upon the sodium bentonite GCL. In particular materials such as CLSM, which typically contain cement with significant calcium content, would likely not be utilized. Use of a calcium bentonite GCL or bagged calcium bentonite as a substitute for a sodium bentonite GCL will also be evaluated. Therefore GCL desiccation damage will not be considered as a SDF Closure Cap degradation mechanism for modeling purposes.

6.7.6 Composite Hydraulic Barriers versus Divalent Cations and Desiccation

Composite hydraulic barriers typically consist of a GCL or compacted clay liner (CCL) overlain by a geomembrane. The use of a GCL or CCL as the sole hydraulic barrier results in infiltration through the barrier over its entire surface area when subjected to a positive hydraulic head. Additionally experience has shown that closure caps that rely solely on GCLs and particularly CCLs as the hydraulic barrier are prone to failure, whereas composite barriers appear to function extremely well. The use of a geomembrane as the sole hydraulic barrier placed over a permeable soil results in flow through any geomembrane holes that "can approach the rate of flow through a similarly-sized orifice".

Whereas, since geomembranes are nearly impervious, the use of a composite hydraulic barrier results in percolation essentially only occurring at the location of geomembrane holes, where such leakage is subsequently impeded by the presence of the GCL or CCL (i.e., flow will be much slower than flow through an orifice). In particular, experimentation has shown that when water migrates through a geomembrane hole in a geomembrane/GCL composite that interface flow between the geomembrane and GCL is of only minor consequence, while it may be more important with a geomembrane/CCL composite. While GCLs, CCLs, or geomembranes can be used as a sole hydraulic barrier, the combination of components in a composite hydraulic barrier has proven (both theoretically and through field performance) to be most effective in terms of minimizing percolation (i.e. infiltration) through the barrier. (Benson 1999; Bonaparte et al. 2002; Chien et al. 2006)

Benson 1999 reported on several field studies that evaluated the performance of geomembrane/CCL composite hydraulic barriers in closure cap situations and made the following observations:

- At a site in Hamburg, Germany a closure cap profile consisting of from top to bottom a 2-foot vegetative soil layer, a 1-foot sand drainage layer, and a composite hydraulic barrier consisting of a 60-mil HDPE geomembrane overlying a 2-foot compacted clay liner (CCL) was tested. Percolation through this closure cap with a composite hydraulic barrier leveled off between 0.08 and 0.12 in/yr. This percolation was nearly two orders of magnitude less than percolation through a closure cap profile with a CCL as the sole hydraulic barrier at the same location (~ 8 in/yr). "Test pits excavated in the composite cover test sections showed that the geomembrane prevented desiccation cracking of the clay. The compacted clay beneath the geomembrane was moist, pliable, and homogeneous even after the cover had been exposed to drought." (Benson 1999)

- At the Kettleman Hills hazardous waste landfill in southern California (semi-arid climate) a closure cap profile consisting of from top to bottom a 2-foot vegetative soil layer and a composite hydraulic barrier consisting of a 60-mil HDPE geomembrane overlying a 3-foot compacted clay liner (CCL) constructed with highly plastic clay was evaluated. "After six months of exposure to ambient conditions, test pits were excavated to examine the condition of the clay in each test pad. The compacted clay barrier in the composite cover was devoid of cracks. The clay was moist, soft, and pliable as if it had just been placed." (Benson 1999)
- At a site in Steamboat Springs, Colorado test pits were dug three years after construction into a closure cap profile with a composite hydraulic barrier. The compacted clay in the composite cover was still moist and un-cracked. (Benson 1999)

Based upon concerns with the potential impacts of divalent cation exchange and desiccation on sodium bentonite GCLs and the favorable field experience of CCLs overlain with geomembranes, Benson (1999) concludes that "GCLs should not be used without being overlain by a geomembrane."

As outlined in Sections 4.4.3, 4.4.4, and 6.7.5, the SDF closure cap includes a composite hydraulic barrier consisting of a GCL overlain by a HDPE geomembrane, both beneath a minimum of 6-feet of soil materials. This conforms to the best practices to limit divalent cation and desiccation damage to the GCL.

6.7.7 Biological (root penetration, burrowing animals)

Plant roots can freely penetrate unprotected GCLs and results in increases in the hydraulic conductivity of the GCL (Bonaparte et al. 2002; Carson 2001; Witt and Siegmund 2001). Since plant roots can freely penetrate GCLs but not HDPE geomembranes except in locations of existing holes within the HDPE geomembrane (see Section 6.6.6), root penetration of the GCL in locations of existing holes within the HDPE geomembrane will be considered as a SDF Closure Cap degradation mechanism for future modeling purposes.

While burrowing animals can potentially damage unprotected GCLs in general, damage of the SDF Closure Cap GCL is not considered a threat due to the presence of the overlying erosion barrier, which will be designed to preclude burrowing animals (see Table 17 and Section 4.4.11) from reaching the GCL. Therefore burrowing animals will not be considered as a SDF Closure Cap GCL degradation mechanism for modeling purposes.

6.8 SDF CLOSURE CAP DEGRADATION MECHANISM SUMMARY

A summary of the applicability of the potential degradation mechanisms from Table 17 to the SDF closure cap is provided in Table 33. Table 33 lists the potential degradation mechanisms per closure cap layer, provides the section which discusses the potential degradation mechanism and its applicability to the SDF closure cap, and provides a summary statement concerning its applicability. The summary statement of each potential degradation mechanism's applicability lists the mechanisms in one or more of the following categories:

- **Not applicable**: for the reason(s) provided the potential degradation mechanism has been deemed not applicable to the SDF closure cap. Therefore it will not be considered a SDF closure cap degradation mechanism for modeling purposes.
- **Not significant**: for the reason(s) provided the potential degradation mechanism has been deemed not a significant degradation mechanism for the SDF closure cap. Therefore it will not be considered a SDF closure cap degradation mechanism for modeling purposes.
- **Incorporate in system design**: for the potential degradation mechanism sufficient design measures exist and will be taken as necessary to preclude that mechanism from being a SDF closure cap degradation mechanism. Therefore it will not be considered a SDF closure cap degradation mechanism for modeling purposes.
- **Applicable**: this potential degradation mechanism is considered a significant SDF closure cap degradation mechanism that will be taken into account during modeling.

Table 34 provides a listing of open issues related to the SDF closure cap concept particularly in regard to potential degradation mechanisms.

Table 33. SDF Closure Cap Degradation Mechanism Summary

Affected Layer	Potential Degradation Mechanism	Section	Summary of the Applicability to the SDF Closure Cap
All	Static loading induced settlement	6.1	**Not significant**: Settlement due static loading is anticipated to be on the order of 2 to 3 inches and expected to occur uniformly over the entire area of the cap. Differential settlement, from which degradation could result, is anticipated to be negligible.
	Seismic induced liquefaction and subsequent settlement	6.1	**Not significant**: Settlement due to seismic loading and resulting liquefaction is anticipated to be on the order of a few inches and expected to occur uniformly over the entire area of the cap. Differential settlement, from which degradation could result, is anticipated to be negligible.
	Seismic induced slope instability	6.1	**Incorporate in system design**: The side-slopes will be designed for seismic stability.
	Seismic induced lateral spread	6.1	**Not applicable**: Conditions at SRS are not conducive to lateral spreading.
	Seismic induced direct rupture due to faulting	6.1	**Not applicable**: Surface faulting is non-existent in the Southeast United States.
	Waste Layer Subsidence	6.1	**Not applicable**: Waste Layer subsidence is not considered applicable to the closure cap, since the disposal cells will be filled with saltstone.
Vegetative cover	Succession	6.2	**Applicable**: Vegetation succession from a bahia grass field to a pine forest will be considered a closure cap degradation mechanism, resulting in deep pine tree roots penetrating various closure cap layers resulting in degradation particularly of the composite hydraulic barrier.
	Stressors (droughts, disease, fire, and biological)	6.2	**Not significant**: Vegetative stressors (droughts, disease, fire, and biological) primarily impact the closure cap in terms of the rate of succession rather than as any long term degradation mechanism on their own.

Table 33.   SDF Closure Cap Degradation Mechanism Summary **- continued**

Affected Layer	Potential Degradation Mechanism	Section	Applicability to the SDF Closure Cap
Soil above the erosion barrier	Erosion	6.3.1	**Applicable**: Erosion of the soil layers above the erosion barrier will be considered a closure cap degradation mechanism.
	Desiccation (wet-dry cycles)	6.3.2	**Not significant**: Significant cracking of SRS topsoil and backfill upon drying is highly unlikely since the soils consist predominately of quartz sand, the clay content is predominately kaolinite, SRS soils are highly leached, and the backfill is compacted.
Erosion barrier	Weathering (Dissolution)	6.4.1	**Incorporate in system design**: The erosion barrier stone size will be designed considering the applicable weathering rate over 10,000 years. materials used to infill the stone voids will be selected such that it has either no impact upon weathering or preferably tends to decrease the weathering rate of the stone.
	Biological: – Root penetration – Burrowing animals	6.4.2	**Applicable**: It is assumed that deep pine tree roots will penetrate the erosion barrier. **Incorporate in system design**: The erosion barrier will be designed to act as a barrier to burrowing animals.
	Chemical (waste leachate)	6.0	**Not applicable**: Chemical degradation of the erosion barrier from leachate associated with the disposal cells is not considered applicable, since the erosion barrier will be located above the disposal cells.
Lateral drainage layer	Silting-in	6.5.1	**Applicable**: It will be assumed that the lateral drainage layer silts up over time with colloidal clay that migrates from the overlying middle backfill.
	Biological (root penetration)	6.5.2	**Applicable**: It is assumed that deep pine tree roots will penetrate into the lateral drainage layer and act as an impermeable volume until they decay.

Table 33.   SDF Closure Cap Degradation Mechanism Summary **- continued**

Affected Layer	Potential Degradation Mechanism	Section	Applicability to the SDF Closure Cap
HDPE geomembrane	Ultraviolet (UV) radiation	6.6.1	**Incorporate in system design**: The HDPE geomembrane will contain carbon black which acts as a UV stabilizer and HDPE geomembrane exposure to sunlight during closure cap construction will be limited in duration.
	Antioxidant depletion	6.6.2	**Applicable**: Antioxidant depletion of the HDPE geomembrane will occur through oxidation of the antioxidants and diffusion out of the geomembrane.
	Thermal oxidation	6.6.3	**Applicable**: Thermal oxidation of the HDPE geomembrane will occur after depletion of the antioxidants and it is assumed in conjunction with tensile stress cracking will cause degradation of the geomembrane.
	High energy irradiation	6.6.4	**Not significant**: high energy irradiation of the SDF Closure Cap HDPE geomembrane is considered an insignificant degradation mechanism
	Tensile stress cracking	6.6.5	**Applicable**: It is assumed that tensile stress cracking of the HDPE geomembrane will occur in conjunction with thermal oxidation.
	Biological: – Microbial – Root penetration – Burrowing animals	6.6.6	**Not significant**: The high-molecular-weight polymers used for geomembranes seem insensitive to microbial biodegradation **Applicable**: Intact HDPE geomembranes preclude root penetration and cause the roots to follow laterally atop the geomembrane surface; however it will be assumed that roots can penetrate the geomembrane in locations where holes have already formed due to other degradation mechanisms. **Incorporate in system design**: The overlying erosion barrier will be designed to act as a barrier to burrowing animals and preclude their reaching the HDPE geomembrane.
	Chemical (waste leachate)	6.0	**Not applicable**: Chemical degradation of the HDPE geomembrane from leachate associated with the disposal cells is not considered applicable, since the HDPE geomembrane will be located above the disposal cells.

Table 33.   SDF Closure Cap Degradation Mechanism Summary **- continued**

Affected Layer	Potential Degradation Mechanism	Section	Applicability to the SDF Closure Cap
GCL	Slope stability	6.7.1	**Incorporate in system design**: The GCL will be placed at a 4% slope and it is not anticipated that the GCL would be placed on the side-slopes. This is well below the 10% to 33% slopes upon which GCLs can be safely placed.
	Freeze-thaw cycles	6.7.2	**Incorporate in system design**: GCLs are resistant to damage from freeze-thaw cycling and the closure cap GCL will be well below the SRS maximum frost depth of approximately 5 inches.
	Dissolution	6.7.3	**Not significant**: Sodium-montmorillonite has a low solubility and a large volume of water and extended time are required to weather it through a series of clays.
	Divalent cations (Ca^{+2}, Mg^{+2}, etc.)	6.7.4	**Applicable**: It will be assumed that sodium bentonite is converted to calcium-magnesium-bentonite, resulting in an order of magnitude increase in saturated hydraulic conductivity
	Desiccation (wet-dry cycles)	6.7.5	**Incorporate in system design**: The GCL will be located beneath a 60-mil HDPE geomembrane and a minimum 6-feet of soil materials in order to preclude desiccation damage. Additionally the material utilized to fill the stone voids of the erosion barrier will be selected so that it does not negatively impact the underlying GCL.
	Biological: – Root penetration – Burrowing animals	6.7.7	**Applicable**: The GCL will be overlain by a HDPE geomembrane. Intact HDPE geomembranes preclude root penetration; however it will be assumed that roots can penetrate the GCL in locations where holes have already formed in the HDPE geomembrane due to other degradation mechanisms. **Incorporate in system design**: The overlying erosion barrier will be designed to act as a barrier to burrowing animals and preclude their reaching the GCL.
	Chemical (waste leachate)	6.0	**Not applicable**: Chemical degradation of the GCL from leachate associated with the disposal cells is not considered applicable, since the GCL will be located above the disposal cells.

Table 34. SDF Closure Cap Concept Open Design Issues Not Affecting Modeling

Issue #	Section(s)	Open Design Issues
1	2.0 4.4.13 6.2	Is bamboo a climax species that prevents or greatly slows the intrusion of pine trees?
2	4.4.2 5.4.7	What are the requirements for the lower backfill layer particularly in terms of its ability to drain water away from and around the disposal cells?
3	4.4.10 4.4.14 4.4.15 5.4.3 6.4.1	What is the estimated weathering rate of the erosion barrier, toe of side slopes, and side slopes stone (assumed granite) based upon natural or archaeological analogs and available literature?
4	4.4.10 5.4.3 6.4.1 6.4.2 Appendix F	What material should be used to fill the stone voids of the erosion barrier to prevent loss of overlying material into the erosion barrier?
5	6.7.4 6.7.5	Should a sodium bentonite or calcium bentonite GCL be utilized?
6	4.1	Is the 50-foot extension of the closure cap beyond the sides of the disposal cells sufficient to prevent infiltration at the side-slopes, the perimeter drainage system, or the natural surrounding land surface from impacting contaminant transport out of the tanks?
7	4.3 4.4.6 4.4.15	The final design must allow the free transport of water out of the lateral drainage layer into the side-slope rip rap, while at the same time preventing sand movement from the lateral drainage layer into the side-slope rip rap.
8	4.4.3 6.6 7.5	The final design will consider the practicality and benefit of conducting an electrical leak detection survey of the HDPE geomembrane as an additional QA/QC measure.

7.0 SDF CLOSURE CAP DEGRADATION AND INFILTRATION MODELING

As outlined in Section 5, SDF closure cap has been modeled for infiltration over time. SDF closure cap configuration is described in Table 4, Table 13, and Figures 8 and 10. Potential SDF closure cap degradation mechanisms are discussed in detail in Section 6. Section 6 culminates with Table 33, which lists all the degradation mechanisms evaluated and provides an evaluation of the applicability and significance of each degradation mechanism to the SDF closure cap.

Based upon the Section 6 evaluation of degradation mechanisms, the degradation mechanisms and affected closure cap layers selected for modeling along with a brief description of the method of modeling are provided in Table 35. The following sections (Sections 7.1 through 7.7) discuss the application of degradation mechanisms in more detail and the development of HELP model inputs based upon the impact of the degradation mechanisms on the various closure cap layers. Root penetration of the erosion barrier receives no further discussion than that provided in previous Section 6.4.2 and Table . Root penetration of the HDPE geomembrane and underlying GCL has been considered together as together they form a composite hydraulic barrier. Appendix I provides the associated SDF closure cap degraded property value calculations. Based upon the development of generally conservative degraded HELP model inputs, an estimate of SDF closure cap Infiltration over 10,000 years has been made.

Table 35. SDF Closure Cap Degradation Mechanisms Applicable to Infiltration Modeling

Affected Layer	Applicable Degradation Mechanism	Method of Modeling
Vegetative cover	Succession	Vegetation succession from a bahia grass field to a pine forest will be assumed to begin at the end of the 100-year institutional control period as outlined in Section 6.2
Soil above the erosion barrier	Erosion	Erosion of the soil layers above the erosion barrier will be assumed to begin immediately following closure cap construction as outlined in Section 6.3.1
Erosion barrier	Root penetration	Pine tree roots will be assumed to freely penetrate the erosion barrier consistent with the rate of root production as outlined in Section 6.2, however such penetration will be assumed to have no impact on the hydraulic properties of the erosion barrier as outlined in Section 6.4.2
Upper Lateral drainage layer	Silting-in	Upon closure cap construction accumulation of colloidal clay, which migrates from the middle backfill into the underlying lateral drainage layer, will be assumed to begin and reduce the saturated hydraulic conductivity of the drainage layer over time as outlined in Section 6.5.1
	Root penetration	Pine tree roots will be assumed to freely penetrate the erosion barrier consistent with the rate of root production as outlined in Section 6.2 and to reduce the saturated hydraulic conductivity of the layer as outlined in Section 6.5.2
High density polyethylene (HDPE) geomembrane	Antioxidant depletion, thermal oxidation, & tensile stress cracking	The Mueller and Jakob (2003) methodology (see Section 6.6.2.3) for antioxidant depletion and the Needham et al. (2004) methodology (see Section 6.6.7) for combining these degradation mechanisms into hole generation over time will be used
	Root penetration	It will be assumed that every HDPE geomembrane hole generated over time is penetrated by a root that subsequently penetrates the GCL, once significant roots are available to penetrate
Geosynthetic clay liner (GCL)	Divalent cations (Ca^{+2}, Mg^{+2}, etc.)	It will be assumed that the GCL consists of sodium bentonite with a saturated hydraulic conductivity of 5.0E-09 cm/s during the 100-year institutional control period and that it consists of calcium bentonite with a conductivity of 5.0E-08 cm/s thereafter
	Root penetration	It will be assumed that every HDPE geomembrane hole generated over time is penetrated by a root that subsequently penetrates the GCL, once significant roots are available to penetrate

7.1 PINE TREE SUCCESSION OF THE VEGETATIVE COVER

As outlined in Section 6.2 and Table 35 vegetation succession from a bahia grass field to a pine forest is assumed to be a degradation mechanism that is both applicable and significant to degradation of the SDF closure cap.

Pine Tree Succession of the Vegetative Cover

The following assumptions associated with pine tree succession discussed in Section 6.2 affect the timing of pine tree succession on the SDF closure cap:

- A 100-year institutional control period begins after closure cap installation during which the initial bahia grass vegetative cover is maintained and pine trees are excluded.
- 40 years after the end of institutional control it is conservatively assumed that pine trees will be established over the entire 400-ft, clear-cut buffer area surrounding the cap.
- 80 years after the end of institutional control it is assumed that the establishment of pine seedlings on top of the closure cap will begin. The 40-yr delay is assumed to result due to the 30 ft to 70 ft elevation increase from the surrounding landscape to the cap surface.
- It will take approximately 30 years for the tap roots to reach a 6-foot depth and the remainder of the tree's life (i.e. 70 years) for the root to go its full depth.
- The distance across the entire cap in the predominant wind direction (southwest to northeast) ranges from about 1,350 to 1,600 ft. It is conservatively assumed the distance is 1,400 ft. Therefore, it will take approximately 7 cycles of pine seedling to mature pine trees (i.e. approximately 200 ft in each 40-year cycle) to establish mature pine over the entire cap
- 360 years after the end of institutional control it is assumed that the entire cap is dominated by mature loblolly pine.
- Complete turnover of the 400 mature trees per acre occurs every 100 years (i.e. 400 mature trees per acre die every 100 years in a staggered manner).

The pine tree succession assumptions result in the vegetative cover pine tree succession timeline presented in Table 36. Along with the Table 36 vegetative cover pine tree succession timeline, the assumption that there are 400 mature trees per acre with 4 roots to 6 feet and 1 root to 12 feet as discussed in Section 6.2 impact the number of pine roots at any one time and the cumulative number of roots produced over time. Within Appendix I, the Table 36 timeline has been converted into an accounting of pine root accumulation over time as shown in Figure 18.

Table 36.   Vegetative Cover Pine Tree Succession Timeline

Year	Occurrence
0	Construction of SDF Closure Cap
100	End of 100-year institutional control period
140	Pine tree seedlings established along the SDF Closure Cap perimeter
180	Pine tree roots first established on the SDF Closure Cap
210	Pine tree roots first reach 6 ft depth on SDF Closure Cap
220	Mature pine trees established over one-seventh of the SDF Closure Cap.
260	Mature pine trees established over two-sevenths of the SDF Closure Cap
300	Mature pine trees established over three-sevenths of the SDF Closure Cap.
340	Mature pine trees established over four-sevenths of the SDF Closure Cap
380	Mature pine trees established over five-sevenths of the SDF Closure Cap
420	Mature pine trees established over six-sevenths of the SDF Closure Cap
460	Mature pine trees established over the entire SDF Closure Cap
460 to 10,000	Complete turnover of mature trees occurs every 100 years

Saltstone Closure Cap Cumulative Roots Over Time

Figure 18.   Pine Root Accumulation over Time

7.2 EROSION OF THE SOIL ABOVE THE EROSION BARRIER

As outlined in Section 6.3.1 and Table 35, erosion of the soil layers above the erosion barrier (i.e. topsoil and upper backfill) is assumed to be a degradation mechanism that is both applicable and significant to degradation of the SDF closure cap. For this institutional control to pine forest land use scenario, it is assumed that the closure cap will be vegetated with bahia grass during the institutional control period (see Sections 4.4.14 and 6.2), with a combination of bahia and pine trees for a period immediately following the institutional control period, and with a pine forest thereafter.

The projected erosion rate for both the topsoil and upper backfill layers has been determined utilizing the Universal Soil Loss Equation (Goldman et al. 1986) for both vegetative cover conditions (i.e. bahia grass and pine forest) within Appendix I. Table 37 provides a summary of the estimated SDF Closure Cap vegetative soil cover (i.e. topsoil and upper backfill) soil losses due to erosion. In order to maximize the erosion rate utilized, the bahia grass erosion rate, which is higher, will be used until the projected time that mature pine trees are assumed to cover the entire closure cap (i.e., at year 460 per Table 36). Based upon these erosion rates, the thickness of the topsoil and upper backfill layers over time was calculated within Appendix I. The summary Appendix I results are provided in Table 38.

Table 37. Estimated SDF Closure Cap Vegetative Soil Cover Soil Losses

Soil-Vegetation Condition	Estimated Soil Loss (tons/acre/year)	Estimated Soil Loss (inches/year)
Topsoil with a bahia grass vegetative cover	0.084	4.5E-04
Topsoil with a pine forest	0.021	1.1E-04
Backfill with a bahia grass vegetative cover	0.060	3.1E-04
Backfill with a pine forest	0.015	7.7E-05

Table 38. Topsoil and Upper Backfill Thickness over Time

Year	Topsoil Thickness (inches)	Upper Backfill Thickness (inches)
0	6.00	30
100	5.96	30
180	5.92	30
220	5.90	30
300	5.87	30
380	5.83	30
460	5.79	30
560	5.78	30
1,000	5.73	30
1,800	5.64	30
3,200	5.49	30
5,412	5.25	30
5,600	5.23	30
10,000	4.74	30

7.3 SILTING-IN OF THE UPPER LATERAL DRAINAGE LAYER

As outlined in Section 6.5.1 and Table 35, silting-in of the upper lateral drainage layer is assumed to be a degradation mechanism that is both applicable and significant to degradation of the SDF closure cap. As outlined in Section 6.5.1 silting-in of the lateral drainage layer is assumed to occur as follows:

- Over time colloidal clay migrates with the water flux from the middle backfill to the underlying 1-foot-thick lateral drainage layer at a concentration of 63 mg of colloidal clay per liter of water flux.
- This water-flux driven clay accumulates in the lower drainage layer from the bottom up. The hydraulic conductivity of the clay-filled portion of the drainage layer is reduced from 5.0E-02 cm/s to that of the overlying backfill, 4.1E-05 cm/s. The hydraulic conductivity of the upper, non-clay-filled portion of the drainage layer remains at 5.0E-02 cm/s. The thickness of the clay-filled portion increases with time, while the thickness of the non-filled portion decreases with time, resulting in an overall decrease in hydraulic conductivity for the drainage layer. The hydraulic conductivity of the backfill is assumed not to change, since its thickness is significantly greater than that of the drainage layer.

Based upon these assumptions, the hydraulic properties of the middle backfill and lateral drainage layer were calculated within Appendix I. Table 39 provides the Appendix I calculated values of saturated hydraulic conductivity, porosity, field capacity, and wilting point for the upper lateral drainage, respectively, based upon the above silting-in assumptions.

Table 39. Upper Lateral Drainage Layer Saturated Hydraulic Conductivity, Porosity, Field Capacity, and Wilting Point

Year	Saturated Hydraulic Conductivity (cm/s)	Porosity	Field Capacity	Wilting Point
0	5.00E-02	0.417	0.045	0.018
100	4.91E-02	0.414	0.0484	0.0215
180	4.84E-02	0.411	0.0513	0.0243
220	4.80E-02	0.410	0.0528	0.0259
300	4.73E-02	0.407	0.0555	0.0286
380	4.65E-02	0.405	0.0584	0.0314
460	4.58E-02	0.402	0.0612	0.0343
560	4.49E-02	0.399	0.0647	0.0378
1,000	4.08E-02	0.384	0.0803	0.0535
1,800	3.34E-02	0.358	0.1086	0.0819
3,200	2.05E-02	0.312	0.1579	0.1315
5,412	4.10E-05	0.240	0.236	0.210
5,600	4.10E-05	0.240	0.236	0.210
10,000	4.10E-05	0.240	0.236	0.210

7.4 ROOT PENETRATION OF THE UPPER LATERAL DRAINAGE LAYER

As outlined in Section 6.5.2 and Table 35 root penetration of the upper lateral drainage layer is assumed to be a degradation mechanism that is both applicable and significant to degradation of the SDF closure cap. For this institutional control to pine forest land use scenario, it is assumed that the closure cap will be vegetated with bahia grass during the institutional control period (see Sections 4.4.14 and 6.2), with a combination of bahia and pine trees for a period immediately following the institutional control period, and with a pine forest thereafter. From the calculations above, it is assumed that mature pine trees will be established over one-seventh of the SDF closure cap by year 220; over two-sevenths of the cap by year 260; over three-sevenths of the cap by year 300, over four-sevenths of the cap by year 340, over five-sevenths of the cap by year 380, over six-sevenths of the cap by year 420, and over the entire cap by year 460. As discussed in Section 6.5.2, roots will represent an impermeable volume within the upper lateral drainage layer prior to their decomposition.

From Section 6.2, the following assumptions were made relative to the establishment of a pine forest on the closure cap that results in root penetration through the lateral drainage layer and a subsequent impermeable volume in the layer due to roots:
- The closure cap will eventually be covered with approximately 400 mature trees per acre.
- Each mature tree will have 4 roots to 6 feet and 1 root to 12 feet. The roots are 3 inches in diameter at a depth of 1 foot and 0.25 inches in diameter at either 6 or 12 feet, whichever is applicable.
- Deep roots will be maintained and enlarge with yearly growth over the life of the tree.
- Trees are expected to die at approximately 100 years, and it is anticipated that decomposition of deep roots will occur over a 30 year period.

- Prior to decomposition the roots represent an impermeable volume within the lateral drainage layer

Based upon these assumptions, the impermeable volume that roots represent within the upper lateral drainage layer was calculated within Appendix I. Based upon the Appendix I calculations the roots within the lateral drainage layer will represent an impermeable volume at any time that ranges from 0.032 to 0.17 percent, depending upon the extent of erosion above the erosion barrier. In order to compensate for the presence of the roots within the upper lateral drainage layer the saturated hydraulic conductivity of the layer will be reduced by multiplying by 0.998 once the pine forest has been established on the closure cap. The conductivity will be reduced at year 300 when three-sevenths of the SDF closure cap is anticipated to be covered in mature pine trees (roughly the percent of closure cap with middle backfill thin enough to allow root penetration to the upper drainage layer). This factor is based upon the worse case percent volume of roots in the layer (i.e., approximately 0.2 percent). Table 40 provides the resulting saturated hydraulic conductivity of the lateral drainage layer over time based upon the use of this factor.

Table 40. Lateral Drainage Layer Saturated Hydraulic Conductivity Modification due to Root Penetration

Year	Table Saturated Hydraulic Conductivity (cm/s)	Modified Saturated Hydraulic Conductivity (cm/s)
0	5.00E-02	5.00E-02
100	4.91E-02	4.91E-02
180	4.84E-02	4.84E-02
220	4.80E-02	4.80E-02
300	4.73E-02	4.72E-02
380	4.65E-02	4.64E-02
460	4.58E-02	4.57E-02
560	4.49E-02	4.48E-02
1,000	4.08E-02	4.07E-02
1,800	3.34E-02	3.33E-02
3,200	2.05E-02	2.05E-02
5,412	4.10E-05	4.09E-05
5,600	4.10E-05	4.09E-05
10,000	4.10E-05	4.09E-05

7.5 ANTIOXIDANT DEPLETION, THERMAL OXIDATION, AND TENSILE STRESS CRACKING OF THE HDPE

As outlined in Table 35, antioxidant depletion (see Section 6.6.2), thermal oxidation (see Section 6.6.3), and tensile stress cracking (see Section 6.6.5) of the HDPE geomembrane are assumed to be degradation mechanisms that are both applicable and significant to degradation of the SDF closure cap. These HDPE geomembrane degradation mechanisms have been equated to geomembrane hole generation over time within Appendix I utilizing the Mueller and Jakob (2003) methodology (see Section 6.6.2.3) for antioxidant depletion and the Needham et al. (2004) methodology (see Section 6.6.7) for combining these degradation mechanisms into hole generation over time. The resulting HDPE geomembrane hole generation summary is provided in Table 41 and depicted in Figure 19.

Table 41. Summary HDPE Geomembrane Hole Generation over Time

Year	Total Cumulative # of Holes (#/acre)	Total Cumulative Hole Size (cm^2/acre)
0	12	4
100	26	50
180	39	90
220	45	109
300	63	170
380	158	479
460	253	760
560	370	1115
1,000	886	2669
1,800	1825	5496
3,200	3468	10442
5,412	6064	18257
5,600	6285	18921
10,000	11448	34466

Geomembrane Hole Generation Over Time

Figure 19.   Summary HDPE Geomembrane Hole Generation over Time

7.6 DIVALENT CATION DEGRADATION OF THE GCL

As outlined in Section 6.7.4 and Table 35, divalent cation degradation of the GCL is assumed to be a degradation mechanism that is both applicable and significant to degradation of the SDF closure cap. As outlined in Section 6.7.4, it will be assumed that the sodium bentonite GCL is converted to calcium-magnesium-bentonite GCL, resulting in an order of magnitude increase in saturated hydraulic conductivity. During the 100-year institutional period, it will be assumed the GCL consists of sodium bentonite with a saturated hydraulic conductivity of 5.0E-09 cm/s. After the 100-year institutional period, it will be assumed the GCL consists of calcium-magnesium-bentonite with a saturated hydraulic conductivity of 5.0E-08 cm/s.

7.7 ROOT PENETRATION OF THE COMPOSITE HYDRAULIC BARRIER

As outlined in Table root penetration of the HDPE geomembrane (see Section 6.6.6), and GCL (see Section 6.7.7) are assumed to be degradation mechanisms that are both applicable and significant to degradation of the SDF closure cap. The HDPE geomembrane and immediately underlying GCL together form a composite hydraulic barrier. For conservatism it will be assumed that every HDPE geomembrane hole generated over time is penetrated by a root that subsequently penetrates the GCL, once significant roots are available to penetrate. As with the drainage layer (see Section 7.4), it will be assumed that significant roots are

available for penetration at year 300 and beyond (at year 300 a third of the closure cap is assumed to be covered by mature trees).

Figure provides a comparison of the number of pine tree roots (see Section 7.1 and Figure 18) versus the number of holes in the HDPE geomembrane (see Section 7.5 and Figure 19) over time as derived from Appendix I. As seen there are significantly more pine tree roots than HDPE geomembrane holes. The HELP model allows the input of up to 999,999 one square centimeter installation defects per acre for a geomembrane liner; therefore the total cumulative hole size provided in Table 41 for each year to be modeled will be used as the number of one square centimeter installation defects per acre for input into the HELP model. This results in more holes than determined but maintains the area of holes determined.

Since the HELP model can not handle holes in a barrier soil liner (i.e., the GCL), the GCL must either be ignored in the HELP modeling or combined with the HDPE geomembrane for all cases at year 300 and beyond. Due to this the HELP model will be run with the following representations of the composite hydraulic barrier (i.e., combined HDPE geomembrane and GCL) as determined in Appendix I:

- At or before year 100, the HDPE geomembrane and GCL will be modeled as separate layers with holes in the HDPE geomembrane and an intact GCL with a Ksat = 5.0E-09 cm/s.
- After year 100 but before year 300, the HDPE geomembrane and GCL will be modeled as separate layers with holes in the HDPE geomembrane and an intact GCL with a Ksat = 5.0E-08 cm/s.
- At and beyond year 300, the HDPE geomembrane and GCL will be modeled as a combined layer with holes all the way through and with a Ksat = 8.7E-13 cm/s and a thickness of 0.260" for intact portions

The conservative nature of the above method of considering root penetration of the composite hydraulic barrier is further discussed in Sections 7.7.1 and 7.7.2.
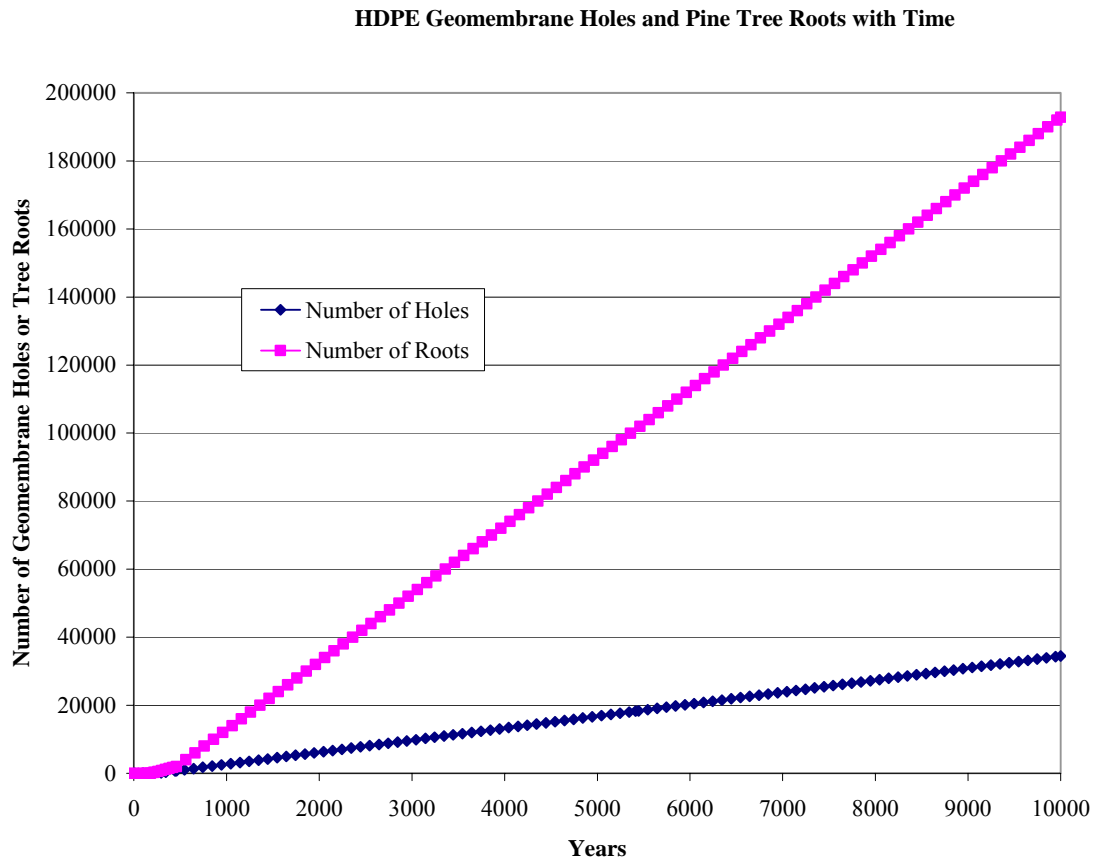
Figure 20.   Pine Tree Roots Versus HDPE Geomembrane Holes

7.7.1 Probability Based Root Penetration Model

Shine (2007) documents a root-penetration model to estimate the probability of pine tree roots penetrating cracks in the HDPE geomembrane and subsequently producing a hole in the underlying GCL for SRS' F-Area Tank Farm (FTF) closure cap modeling. This probability model demonstrates the conservative nature of infiltration estimates produced under the assumption that every HDPE geomembrane hole generated over time is penetrated by a root that subsequently penetrates the GCL, once significant roots are available to penetrate.

In the FTF probability model, thirty-three probability based simulations of root penetration through the HDPE/GCL composite barrier were run with the probability model, resulting in the root/hole averages for the years of interest shown in Table 42. Figure and Figure provide the average results of the root penetration probability model graphically. Figure provides the number of pine tree roots, HDPE geomembrane cracks, and GCL penetrations over time, and Figure provides a close-up to better see the number of HDPE geomembrane cracks and GCL penetrations over time. As seen in Table 42, no roots penetrate the FTF HDPE geomembrane holes (and subsequently the underlying GCL) until year 560. As seen in Table and Figure the number of FTF GCL penetrations is significantly less

Table 42. FTF Root Penetration Probability Simulation Average

Year	Cumulative Number of Tap Roots (# / acre)	Total Number of HDPE Geomembrane Holes (# / acre)	Total Number of Live Tap Roots in HDPE Geomembrane Holes (# / acre)	Total Number of Dead Tap Roots in HDPE Geomembrane Holes (# / acre)	Total Number of HDPE Geomembrane Holes without Roots (# / acre)
0	0	12	0	0	12
100	0	26	0	0	26
180 [1]	0	39	0	0	39
290 [2]	665	56	0	0	56
300	665	63	0	0	63
340	1335	111	0	0	111
380	2000	158	0	0	157
560	5600	370	0	2	367
1000	14400	886	2	15	870
1800	30400	1825	4	64	1758
3200	58400	3468	8	234	3227
5600	106400	6285	12	738	5535
10000	194400	11449 [3]	20	2272	9157

[1] HDPE geomembrane hole values for year 180 interpolated from years 175 and 182:

175	0	38	0	0	38
182	0	39	0	0	39

[2] HDPE geomembrane hole values for year 290 interpolated from years 289 and 291; and cumulative number of tap roots taken as that of year 291.

289	0	56	0	0	56
291	665	56	0	0	56

[3] The previously determined total cumulative number of holes per acre in the HDPE geomembrane at 10,000 years was 11448, which is one less than the value of 11449 produced by the probability based root penetration model simulations.
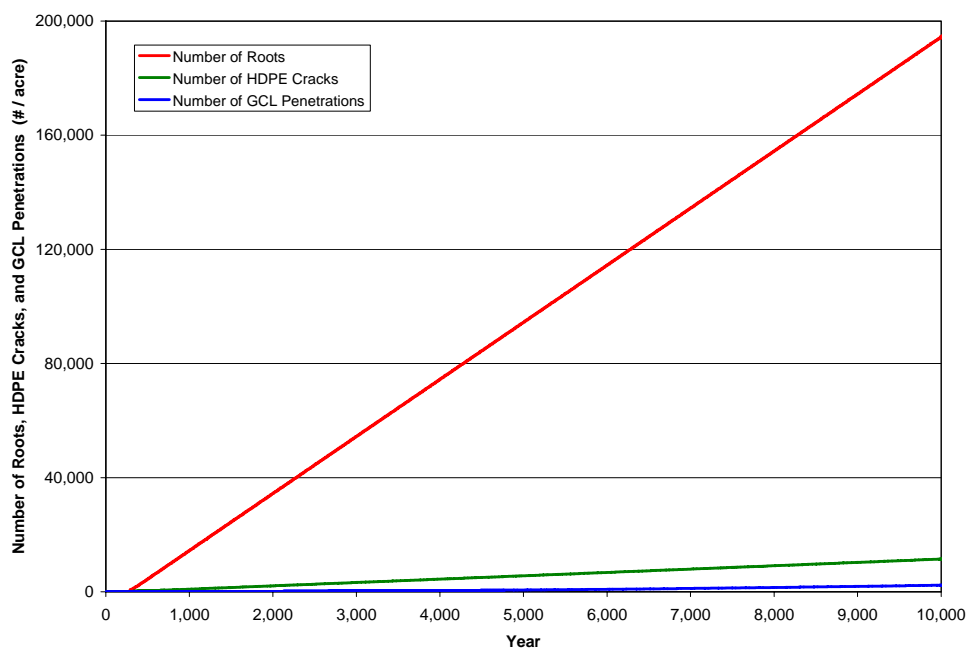
Figure 21. FTF Root Penetration Probability Simulation Average (Roots, Cracks, and Penetrations)
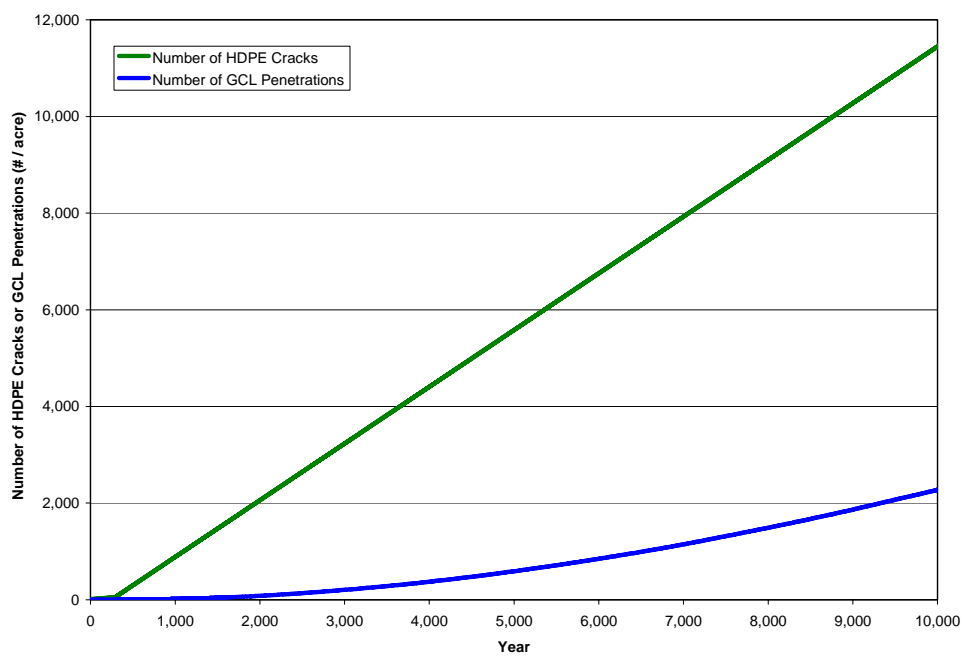
Figure 22. FTF Root Penetration Probability Simulation Average (Cracks and Penetrations)

than the number of HDPE geomembrane cracks over time, demonstrating the conservative nature of infiltration estimates made with the assumptions outlined in Section 6.7.

The simulations of root penetration through the composite barrier results in the following four areas of consideration for the composite barrier:

- Areas comprised of both intact HDPE geomembrane and intact GCL
- Areas comprised of holes in the HDPE geomembranes and intact GCL
- Areas comprised of holes in both the HDPE geomembrane and GCL with a live root in the hole
- Areas comprised of holes in both the HDPE geomembrane and GCL with a dead root which is assumed to immediately disappear upon death of the tree

The HELP model is capable of handling the first two types of areas outlined above, but it is not capable of handling all four of these conditions together. The HELP model does not allow holes in barrier soil liners such as the GCL, and it does not allow the placement of two geomembrane liners, which can have holes, directly on top of one another. Due to this, the HELP model is not suitable to appropriately incorporate the results of such a root penetration probability model, and the modeling conservatively assumes that all composite barrier holes are penetrated by roots.

7.7.2 Thickness of Soil Overlying Composite Hydraulic Barrier

As discussed in Sections 4.4.7 and 7.9, and in Appendix I, the middle backfill layer will thicken outward from each SDF closure cap apex. Because root penetration is not considered possible below a depth of 12 ft, less than one-half of the HELP-modeled closure cap area can have an upper drainage layer, GCL, or HDPE subject to pine root penetration. However, the HELP model is not designed to assign different properties to any single layer (e.g., assign a root-affected permeability to the topographically upper-280 ft of the Upper Drainage Layer and a non-root affected permeability to the lower-545 ft of the Upper Drainage Layer). So, the upper drainage layer, GCL, and HDPE layers will be conservatively modeled as being at the minimum depth, with each entire layer subject to root contact.

7.8 SUMMARY HELP MODEL INPUT

The HELP model runs are to provide infiltration through the GCL. These values provide upper boundary conditions to be used in PORFLOW modeling and to develop degradation conditions for the Lower Drainage Layer atop the individual disposal cells and water available for infiltration into the disposal cells. Development of the HELP model weather data input files were discussed in Section 5.2, and the files, which were utilized for all HELP model runs, are provided in the following appendices:

- Appendix B, Augusta Synthetic Precipitation Modified with SRS Specific Average Monthly Precipitation Data over 100 Years (file name: Fprec.d4)
- Appendix C, Augusta Synthetic Temperature Modified with SRS Specific Average Monthly Temperature Data over 100 Years (file name: Ftemp.d7)
- Appendix D, Augusta Synthetic Solar Radiation Data over 100 Years (file name: Fsolar.d13)
- Appendix E, Augusta Evapotranspiration Data (file name: Fevap.d11)

Development of the HELP model general input data and runoff input data were discussed in Sections 5.3 and 5.5, respectively. Both the general and runoff input data developed in these sections is applicable to both the initial, intact and the degraded SDF closure cap conditions. Development of initial, intact HELP model layer input data were discussed in Section 5.4. Table 15 of Section 5.4.8 provides a summary of the initial, intact HELP model input for the SDF closure cap layers. Sections 7.1 through 7.7 discuss the application of closure cap degradation mechanisms and the development of HELP model inputs based upon the impact of the degradation mechanisms on the various closure cap layers. Appendix I provides the associated SDF closure cap degraded property value calculations. The following tables provide the degraded HELP model inputs used to produce, an estimate of SDF closure cap Infiltration over 10,000 years (except as noted in the tables below, the HELP model input is the same as that of the initial intact conditions in Table 15):

- Table 43 provides the reduction in topsoil thickness over time.
- Table 45 provides the change in the lateral drainage layer's hydraulic properties over time.
- Table 46 provides the change in the saturated hydraulic conductivity and number of holes over time in the composite hydraulic barrier (i.e., combined HDPE geomembrane and underlying GCL).

The degraded HELP model inputs presented in Table 43 through Table 46 along with the initial, intact HELP model inputs presented in Table 15 were used to develop the Appendix J HELP model inputs for the SDF Closure Cap for each year modeled.

Table 43.   Topsoil Thickness over Time

Year	Topsoil Thickness (inches)
0	6.00
100	5.96
180	5.92
220	5.90
300	5.87
380	5.83
460	5.79
560	5.78
1,000	5.73
1,800	5.64
3,200	5.49
5,412	5.25
5,600	5.23
10,000	4.74

Table 44.   Upper Lateral Drainage Layer Saturated Hydraulic Conductivity, Porosity, Field Capacity, and Wilting Point

Year	Hydraulic Conductivity (cm/s)	Porosity	Field Capacity	Wilting Point
0	5.00E-02	0.417	0.0450	0.0180
100	4.91E-02	0.414	0.0484	0.0215
180	4.84E-02	0.411	0.0513	0.0243
220	4.80E-02	0.410	0.0528	0.0259
300	4.72E-02	0.407	0.0555	0.0286
380	4.64E-02	0.405	0.0584	0.0314
460	4.57E-02	0.402	0.0612	0.0343
560	4.48E-02	0.399	0.0647	0.0378
1,000	4.07E-02	0.384	0.0803	0.0535
1,800	3.33E-02	0.358	0.1086	0.0819
3,200	2.05E-02	0.312	0.1579	0.1315
5,412	4.09E-05	0.240	0.2360	0.2100
5,600	4.09E-05	0.240	0.2360	0.2100
10,000	4.09E-05	0.240	0.2360	0.2100

Table 45. Composite Barrier Saturated Hydraulic Conductivity and Number of Holes

Year	GCL [1] Saturated Hydraulic Conductivity (cm/s)	HDPE Geomembrane [2]		Composite Barrier [3] (i.e., combined GCL and HDPE geomembrane)	
		Saturated Hydraulic Conductivity (cm/s)	Number of One cm^2 Holes (#/acre)	Saturated Hydraulic Conductivity (cm/s)	Number of One cm^2 Holes (#/acre)
0	5.0E-09	2.0E-13	4	na	Na
100	5.0E-09	2.0E-13	50	na	Na
180	5.0E-08	2.0E-13	90	na	Na
220	5.0E-08	2.0E-13	111	na	Na
300	na	na	Na	8.7E-13	170
380	na	na	Na	8.7E-13	479
460	na	na	Na	8.7E-13	760
560	na	na	Na	8.7E-13	1115
1,000	na	na	Na	8.7E-13	2669
1,800	na	na	Na	8.7E-13	5496
3,200	na	na	Na	8.7E-13	10442
5,412	na	na	Na	8.7E-13	18257
5,600	na	na	Na	8.7E-13	18921
10,000	na	na	Na	8.7E-13	34466

na = not applicable
[1] The thickness of the GCL alone is taken as 0.20 inches
[2] The thickness of the HDPE geomembrane alone is taken as 0.060 inches
[3] The thickness of the composite barrier is taken as 0.260 inches

7.9 SUMMARY HELP MODEL RESULTS

HELP Modeling Assumptions
The following are measures, which have been taken ensure to conservative tending HELP Model infiltration results:

- The precipitation data included significant pulses of water, not just average values, by utilizing a range of daily precipitation from 0 inches up to 6.7 inches, and an annual range from 29.8 inches to 68.6 inches.
- The use of bamboo to preclude or delay pine forest succession is not currently considered, even though current research indicates that the use of bamboo would be beneficial in this regard.
- Physical stability of the top surface of the closure cap is obtained by both the use of an erosion barrier designed to preclude any movement due to a PMP event and surficial soil designed to preclude gully erosion due to a PMP event. Such design could be considered redundant, and the use of a surficial slope greater than 1.5 percent would result in greater runoff.
- The maximum slope length of the closure cap (i.e., 825 feet) was used to determine both runoff and lateral drainage for the entire cap. A significant portion of the cap will have slope lengths less than 825 ft.

- An evaporative zone depth of 22 inches was selected based upon HELP model guidance, which lists this depth as a "fair" depth for Augusta, Georgia. This is considered a conservative maximum evaporative zone depth due to the anticipated capillarity associated with the surficial soil types (i.e., topsoil and upper backfill) and the anticipated root depths.
- The erosion barrier is assumed to be infilled with a sandy soil; the use of a less permeable infill would reduce infiltration.
- No lateral drainage is assumed to occur over the erosion barrier; however such lateral drainage could occur particularly if a low permeable infill were used.
- The initial saturated hydraulic conductivity of the sand used for the lateral drainage layer was taken as 5.0E-02 cm/s, which is well below the maximum (1 cm/s) in the range of values presented in the literature for various grain-size sands.
- Silting-in of the upper lateral drainage layer is assumed to begin immediately upon construction; it is assumed to result from the migration of elevated levels of colloidal clay within infiltrating water; the use of the overlying filter fabric is assumed not to reduce colloidal clay movement; and all colloidal clay that enters the layer is assumed to remain in the layer (i.e., not be flushed from the drainage layer) thus reducing its hydraulic conductivity. Silting-in may not occur, or may occur on a much-reduced scale compared to the scenario modeled.
- The upper lateral drainage layer slope is increased over that of the cap surface (4 percent vs. 1.5 percent). This will result in more effective and rapid drainage. It will also cause the middle backfill layer to increase in thickness from the cap peaks toward the cap perimeter, which will cause the surface-to-HDPE/GCL thickness under much of the cap to exceed the maximum root depth. Even though much of the cap HDPE/GCL will be at too great a depth to be contacted by roots, the modeling conservatively assumes the entire HDPE/GCL layer is subject to root penetration.
- A saturated hydraulic conductivity was assigned to the intact portions of the HDPE geomembrane even though water transport through HDPE is a vapor diffusional process.
- The HDPE geomembrane antioxidant depletion time has been calculated using a conservative estimate of activation energy (i.e. 60 kJ/mol). Literature activation energies range from 42 to 100 kJ/mol (see Section 6.6.2.3).
- The production of holes in the HDPE geomembrane over time has been estimated using both the "fair" and "good" cases outlined by Needham et al. (2004). The "fair" case results in more holes than either the "good" or "excellent" cases. Since installation of the closure cap over the SDF will undergo a high level of QA/QC and the HDPE geomembrane will be under relative low stress conditions (i.e. emplaced on a 4 percent slope), the applicability of the "good" case and possibly the "excellent" case could potentially be supported.
- Every HDPE geomembrane hole generated over time is assumed to be penetrated by a pine root that subsequently penetrates the GCL. However the results of the probability based root penetration model demonstrate that this is not the case and that most of the HDPE geomembrane holes are not penetrated by roots over the time period of interest. Additionally, less than one-half of the HELP-modeled closure cap area can have the composite hydraulic barrier subject to pine root penetration due to the increase in thickness of the overlying middle backfill from the cap peaks toward the cap perimeter.
- The initial saturated hydraulic conductivity of the GCL was taken as 5.0E-09 cm/s even though test results indicate that the value could be significantly lower.

- It has been assumed that the GCL saturated hydraulic conductivity increases to 5.0E-08 cm/s at the end of the 100-year institutional control period. This is not likely since infiltrating water at SRS should be very low in dissolved calcium and other divalent cations.
- The saturated hydraulic conductivity of the Upper Foundation Layer, which will be a soil-bentonite blend, was taken as 1.0E-06 cm/s even though significantly lower conductivities can be obtained with soil-bentonite blends.

Appendix J provides the HELP model input for each of the years modeled. The post-closure years modeled (0, 100, 180, 220, 300, 380, 460, 560, 1,000, 1,800, 3,200, 5,412, 5,600, and 10,000) were run in the HELP model in order to produce an estimate of SDF Closure Cap GCL infiltration over 10,000 years. Table 46 provides input and output files names for each of the years modeled. For each year, the HELP model runs one hundred HELP model simulations, with precipitation ranging from 29.8 to 68.6 inches/year, to produce an average annual value. The detailed simulation-produced water balance data for each of the years modeled are provided in Appendix K. Within Appendix K, at the end of each year's 100-simulation data table is a summary of statistics (count, maximum value, average value, median value, minimum value, and standard deviation) for each parameter (precipitation, runoff, evapotranspiration, lateral drainage, infiltration through the GCL, and change in water storage) for that modeled year.

Table 46. HELP Model Input and Output File Names

Year	HELP Model Input File	HELP Model Output File
0	SSYr0.D10	SSYr0.OUT
100	SSYr100.D10	SSYr100.OUT
180	SSYr180.D10	SSYr180.OUT
220	SSYr220.D10	SSYr220.OUT
300	SSYr300.D10	SSYr300.OUT
380	SSYr380.D10	SSYr380.OUT
460	SSYr460.D10	SSYr460.OUT
560	SSYr560.D10	SSYr560.OUT
1,000	SSYr1000.D10	SSYr1000.OUT
1,800	SSYr1800.D10	SSYr1800.OUT
3,200	SSYr3200.D10	SSYr3200.OUT
5,412	SSYr5412.D10	SSYr5412.OUT
5,600	SSYr5600.D10	SSYr5600.OUT
10,000	SSY10000.D10	SSY10000.OUT

HELP Modeling Results by Year

Year 0 – Intact Conditions
Intact conditions at year 0 result in an average infiltration of 0.00042 inches/year through the GCL. The water balance for precipitation falling on the cap at year 0 (see Figure 23 for illustration of water balance pathways) is dominated by evapotranspiration (average 32.57 inches/year) and lateral drainage (average 16.18 inches/year).

Year 100

Precipitation falling on the closure cap under degraded conditions at year 100 results in an average infiltration of 0.00333 inches/year through the GCL. The water balance for precipitation falling on the cap at year 100 is dominated by evapotranspiration (average 32.57 inches/year) and lateral drainage (average 16.17 inches/year).

Figure 23. Saltstone Closure Cap Year 0 (intact) Average Water Balance
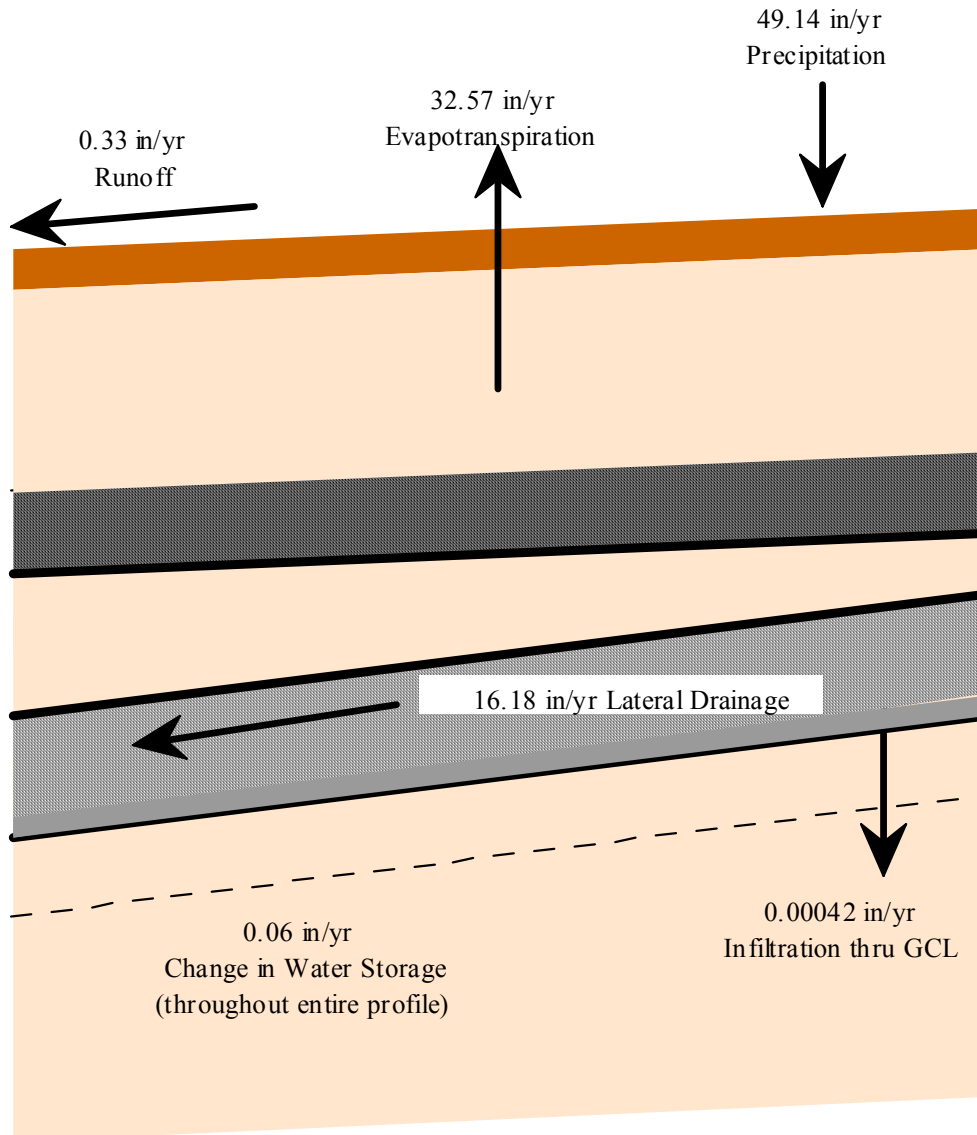
Year 180

Precipitation falling on the closure cap under degraded conditions at year 180 results in an average infiltration of 0.04520 inches/year through the GCL. The water balance for

precipitation falling on the cap at year 180 is dominated by evapotranspiration (average 32.56 inches/year) and lateral drainage (average 16.13 inches/year).

Year 220
Precipitation falling on the closure cap under degraded conditions at year 220 results in an average infiltration of 0.05676 inches/year through the GCL. The water balance for precipitation falling on the cap at year 220 is dominated by evapotranspiration (average 32.56 inches/year) and lateral drainage (average 16.12 inches/year).

Year 300
Precipitation falling on the closure cap under degraded conditions at year 300 results in an average infiltration of 0.17110 inches/year through the GCL. The water balance for precipitation falling on the cap at year 300 is dominated by evapotranspiration (average 32.55 inches/year) and lateral drainage (average16.01 inches/year).

Year 380
Precipitation falling on the closure cap under degraded conditions at year 380 results in an average infiltration of 0.47236 inches/year through the GCL. The water balance for precipitation falling on the cap at year 380 is dominated by evapotranspiration (average 32.55 inches/year) and lateral drainage (average 15.71 inches/year).

Year 460
Precipitation falling on the closure cap under degraded conditions at year 460 results in an average infiltration of 0.72342 inches/year through the GCL. The water balance for precipitation falling on the cap at year 460 is dominated by evapotranspiration (average 32.54 inches/year), and lateral drainage (average 15.46 inches/year).

Year560
Precipitation falling on the closure cap under degraded conditions at year 560 results in an average infiltration of 1.0211 inches/year through the GCL. The water balance for precipitation falling on the cap at year 560 is dominated by evapotranspiration (average 32.54 inches/year), lateral drainage (average 15.16 inches/year), and infiltration through the GCL (average 1.0211 inches/year).

Year 1,000
Precipitation falling on a the closure cap under degraded conditions at year 1,000 results in an average infiltration of 2.2638 inches/year through the GCL. The water balance for precipitation falling on the cap at year 1,000 is dominated by evapotranspiration (average32.53 inches/year), lateral drainage (average 13.91 inches/year), and infiltration through the GCL (average 2.2638 inches/year).

Year 1,800
Precipitation falling on the closure cap under degraded conditions at year 1,800 results in an average infiltration of 4.340 inches/year though the GCL. The water balance for precipitation falling on the cap at year 1,800 is dominated by evapotranspiration (average 32.52 inches/year), lateral drainage (average 11.79 inches/year), and infiltration through the GCL (average 4.340 inches/year).

Year 3,200

Precipitation falling on the closure cap under degraded conditions at year 3,200 results in an average infiltration of 6.795 inches/year through the GCL. The water balance for precipitation falling on the cap at year 3,200 is dominated by evapotranspiration (average 32.53 inches/year), lateral drainage (average 8.99 inches/year), and infiltration through the GCL (average 6.795 inches/year).

Year 5,412

Precipitation falling on the closure cap under degraded conditions at year 5,412 results in an average infiltration of 10.6 inches/year through the GCL. The water balance for precipitation falling on the cap at year 5,412 is dominated by evapotranspiration (average 33.62 inches/year), infiltration through the GCL (average 10.6 inches/year) and runoff (4.42 inches/year).

Year 5,600

Precipitation falling on the cap under degraded conditions at year 5,600 results in an average infiltration of 10.6 inches/year through the GCL. The water balance for precipitation falling on the cap at year 5,600 is dominated by evapotranspiration (average 33.62 inches/year), infiltration through the GCL (average 10.6 inches/year), and runoff (average 4.43 inches/year).

Year 10,000

Precipitation falling on the closure cap under degraded conditions at year 10,000 results in an average infiltration of 10.6 inches/year through the GCL. The water balance for precipitation falling on the cap at year 10,000 is dominated by evapotranspiration (average 33.57 inches/year), infiltration through the GCL (average of 10.6 inches/year), and runoff (average 4.54 inches/year).

Figure 24 provides a comparison of the 100 annual infiltration simulations with linear regressions for annual precipitation versus infiltration through the GCL for several modeled years across the 10,000 timeframe. The plot demonstrates that the modeling approach was conservative in including precipitation values well over the measured SRS average (about 49 inches/year). The plot also shows that infiltration increases with time of closure cap degradation. Under initial, intact conditions (i.e., year 0) very little infiltration occurs, however as closure cap degradation proceeds, the infiltration increases until at year 5,412 and thereafter the infiltration appears to stabilize at an approximate average of 10.6 inches/year.

As outlined in Section 5.2, the precipitation data set used to produce the 100 annual simulations for each year modeled ranged from 29.8 to 68.6 inches/year with daily precipitation ranging from 0 to 6.7 inches/year. No precipitation occurs on approximately 72.5 percent of the days. On days that precipitation does occur (i.e., approximately 100 days per year), the range in daily precipitation consisted of 86.4 percent (i.e., approximately 86 days per year) ranging from 0.01 to 1.0 inches/day; 12.9 percent (i.e., approximately 13 days per year) ranging from 1.0 to 3.0 inches/day; and 0.7 percent (i.e., approximately 1 day per year) ranging from 3.0 to 7.0 inches/day. Based upon the precipitation data set used to

produce the 100 annual simulation for each year modeled, it is evident that the modeling took into account large pulses of precipitation.

A previous evaluation (WSRC 2005), which looked at the relationship between daily precipitation ranging from 0 to 6.9 inches/day and daily infiltration through a closure cap drew the following conclusions:

Annual Precipitation vs. Annual Infiltration Through GCL (Linear Regression Overlies Each Year's One-Hundred Annual Simulation Values)
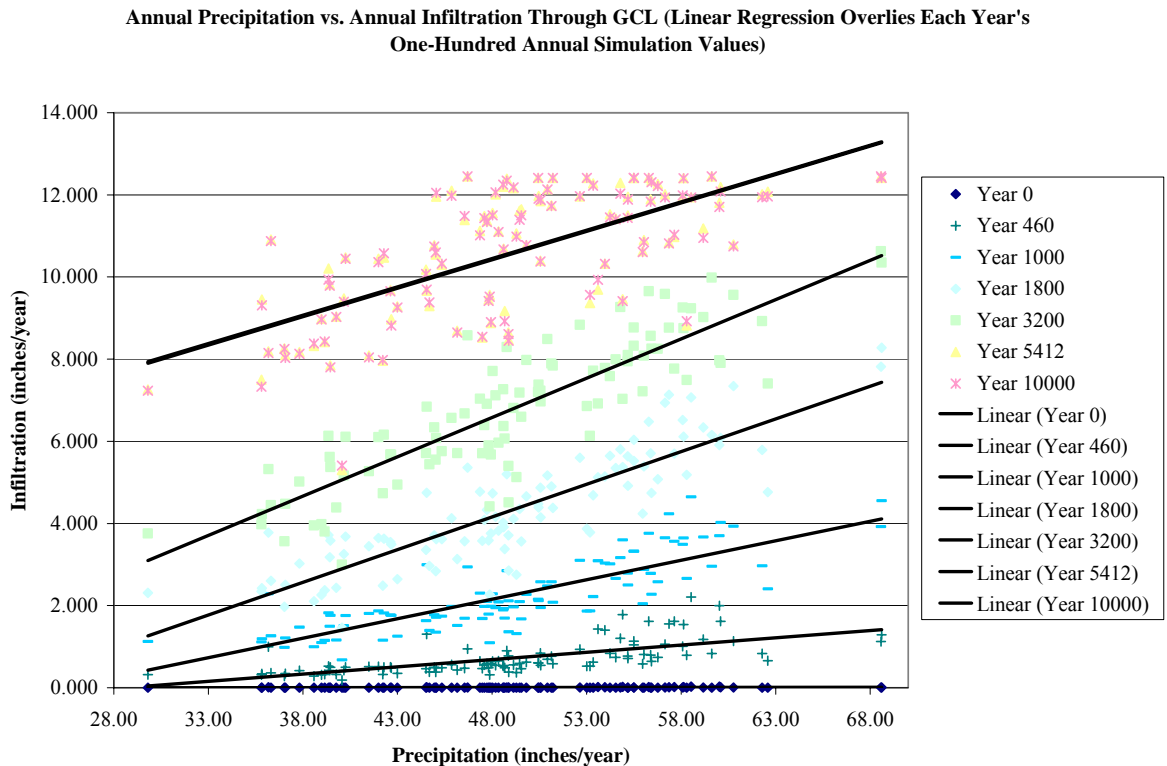
Figure 24. Annual Precipitation vs. Annual Infiltration Through GCL (Linear Regression Overlies Each Year's One-Hundred Annual Simulation Values)

- "No discernable functional relationship could be established between precipitation and infiltration on a daily basis, as could be determined on an annual basis, due to the many processes which are very dynamic on a daily basis as compared to an annual basis."
- Infiltration increases "with daily precipitation events greater than about one inch and/or multiple consecutive days of precipitation".

Additionally it is evident from WSRC 2005 that under intact closure cap conditions the infiltration variations produced by variations in precipitation remain fairly small even with large pulses of precipitation up to 6.9 inches/day. Under intact conditions the closure cap lateral drainage layer and barrier layer can effectively remove even large pulses of precipitation with very little increases in infiltration. However under degraded conditions the infiltration variations produced by variations in precipitation are larger. The infiltration under such conditions is still much less than the precipitation (i.e. muted), since increased runoff

- 153 -

and soil water storage occur under conditions of heavy precipitation. It is evident that while large pulses of precipitation do impact daily infiltration, there is little impact under intact closure cap conditions, and the daily infiltration is much less than precipitation, even under degraded closure cap conditions. Therefore using average annual infiltration rates based upon the precipitation data set is considered appropriate.

Table 47 and Figure 25 provide a comparison of the average water balance for SDF Closure Cap for all the modeled years. As seen for an average annual precipitation of 49.14 inches/year the average water balance changes as follows with closure cap degradation:

- Evapotranspiration remains fairly constant over time at an average ranging from 32.57 to 33.62 inches/year.
- Lateral drainage starts out at 16.18 inches/year under initial, intact conditions and decreases to less than 0.5 inches/year at year 5,412 and thereafter as the lateral layer silts-in.
- Runoff starts out at 0.33 inches/year under initial, intact conditions and increases to about 4.4 inches/year at year 5,412 and thereafter as pluggage of the lateral drainage layer results in somewhat slower soil water drainage in the overlying soil layers.
- Infiltration through the GCL starts out at 0.00042 inches/year under initial, intact conditions and increases to about 10.6 inches/year at year 5,412 and thereafter as increasing holes through the composite hydraulic barrier (HDPE geomembrane and underlying GCL) result in increased infiltration through the GCL.

The average annual infiltration through the GCL, which will be utilized as an upper boundary condition for the SDF PorFlow vadose zone modeling are provided in Table 48. For sensitivity and uncertainty purposes, the average infiltration through the GCL could be assumed to fall within the range of 9 inches/year to 16 inches/year after year 5,412. Prior to that year (wherein essentially complete closure degradation is reached), this range of infiltration is not applicable. This range is based upon background conditions (i.e., no closure cap), and should therefore be conservative in application to a degraded closure cap. See Section 3.2 for a summary of background water balance and infiltration studies.

The closure cap design and infiltration information provided herein is preliminary and conceptual in nature, being consistent with a scoping level concept. In other words, it provides sufficient information for planning purposes, to evaluate the closure cap configuration relative to its constructability and functionality, and to estimate infiltration over time through modeling. It is not intended to constitute final design. Final design and a re-evaluation of infiltration will be performed near the end of the operational period. Technological advances, increased knowledge, and improved modeling capabilities are all likely and will result in improvements in both the closure cap design and infiltration estimates.

Table 47.   Comparison of Modeled Time Steps - Average Water Balance

Year	Precipitation (inch/yr)	Runoff (inch/yr)	Evapotrans-piration (inch/yr)	Lateral Drainage (inch/yr)	Infiltration thru GCL (inch/yr)	Change in Water Storage (inch/yr)
0	49.14	0.33	32.57	16.18	0.00042	0.06
100	49.14	0.34	32.57	16.17	0.00333	0.06
180	49.14	0.35	32.56	16.13	0.04520	0.06
220	49.14	0.35	32.56	16.12	0.05676	0.06
300	49.14	0.36	32.55	16.01	0.17110	0.07
380	49.14	0.35	32.55	15.71	0.47236	0.07
460	49.14	0.36	32.54	15.46	0.72342	0.08
560	49.14	0.36	32.54	15.16	1.0211	0.08
1,000	49.14	0.38	32.53	13.91	2.2638	0.08
1,800	49.14	0.44	32.52	11.79	4.340	0.09
3,200	49.14	0.77	32.53	8.99	6.795	0.09
5,412	49.14	4.42	33.62	0.43	10.6	0.10
5,600	49.14	4.43	33.62	0.43	10.6	0.10
10,000	49.14	4.54	33.57	0.40	10.6	0.10

Comparison of Modeled Time Steps - Average Water Balance
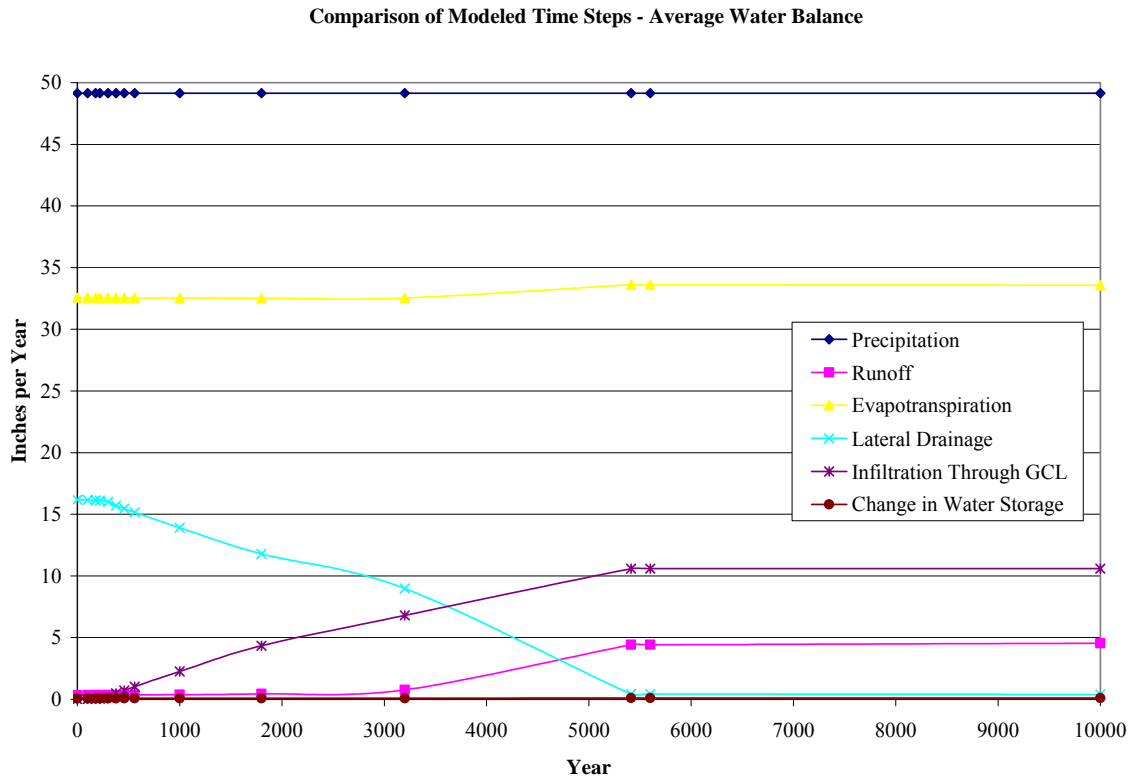
Figure 25.   Comparison of Modeled Time Steps - Average Water Balance

Table 48.   PorFlow Model Upper Boundary Condition Input

Year	Average Annual Infiltration thru the GCL (in/yr)
0	0.00042
100	0.00333
180	0.04520
220	0.05676
300	0.17110
380	0.47236
460	0.72342
560	1.0211
1,000	2.2638
1,800	4.340
3,200	6.795
5,412	10.6
5,600	10.6
10,000	10.6

8.0 ADDITIONAL DEGRADATION VALUES FOR PORFLOW MODELING

8.1 LOWER DRAINAGE LAYER DEGRADATION

The HDPE and GCL covering each disposal cell will be overlain by a 2-ft-thick lateral drainage layer. The lower drainage layer will not "daylight", i.e. extend to the cap perimeter to drain outside the cap, rather it will terminate approximately 25 ft from the individual disposal cell perimeter. This design will facilitate drainage off the disposal cell top to the backfill material between and outside disposal cell groups, while not requiring a contiguous drainage layer across varying disposal cell-top elevations.

Lower Drainage Layer Silting-In
As outlined in Section 6.5.1 silting-in of the lower lateral drainage layer is assumed to occur similar to that of the upper lateral drainage layer (Section 7.3):
- Over time colloidal clay migrates with the water flux from the lower backfill to the underlying 2-foot-thick lower lateral drainage layer at a concentration of 63 mg of colloidal clay per liter of water flux.
- This water-flux driven clay accumulates in the lower drainage layer from the bottom up. The hydraulic conductivity of the clay-filled portion of the drainage layer is reduced from 5.0E-02 cm/s to that of the overlying backfill, 4.1E-05 cm/s. The hydraulic conductivity of the upper, non-clay-filled portion of the drainage layer remains at 5.0E-02 cm/s. The thickness of the clay-filled portion increases with time, while the thickness of the non-filled portion decreases with time, resulting in an overall decrease in hydraulic conductivity for the drainage layer.
- The hydraulic conductivity of the backfill is assumed not to change, since its thickness is significantly greater than that of the drainage layer.
- Since the minimum depth to the lower drainage layer is 13 ft and root penetration is assumed to not exceed 13 ft, root penetration is not an issue for the drainage layer overlying each disposal cell as it is for the upper drainage layer (see Section 7.4 and Appendix I).

A summary of lower drainage layer hydraulic properties with time is presented in Table 49. Calculations for determining the hydraulic properties are presented in Appendix I.

Table 49. SDF Lower Drainage Layer Hydraulic Properties With Time

Lower Drainage Layer Hydraulic Properties With Time				
Year After Cap Construction	Hydraulic Conductivity (cm/s)	Porosity (vol/vol)	Field Capacity (vol/vol)	Wilting Point (vol/vol)
0	5.000E-02	0.417	0.045	0.018
100	5.000E-02	0.417	0.045	0.018
180	5.000E-02	0.417	0.045	0.018
220	5.000E-02	0.417	0.045	0.018
300	5.000E-02	0.417	0.045	0.018
380	4.999E-02	0.417	0.045	0.018
460	4.998E-02	0.417	0.045	0.018
560	4.995E-02	0.417	0.045	0.018
1,000	4.974E-02	0.417	0.046	0.019
1,800	4.899E-02	0.416	0.049	0.021
3,200	4.676E-02	0.413	0.058	0.029
5,412	4.126E-02	0.405	0.081	0.047
5,600	4.069E-02	0.405	0.084	0.048
10,000	2.736E-02	0.387	0.139	0.092

8.2 DEGRADATION OF HDPE ENCASING DISPOSAL CELLS

HDPE will be placed over and around individual disposal cells (see Figure 8). Degradation of this 100-mil thick HDPE is evaluated following the methods outlined in Phifer (2005). Degradation is expressed in terms of the fraction or percentage area of HDPE geomembrane consisting of holes over time. A summary of the cumulative area of holes is presented in the Table 50. See Appendix I for calculation details.

Table 50. Cumulative Area of Holes in HDPE Encasing Disposal Cells

Interpolated Cumulative Area of Holes[1]			
Year	Total Cumulative Hole Size[2] (mm2/Hectare)	Fraction of HDPE Membrane with Holes[3]	Percentage of HDPE Membrane with Holes[4]
0	550	5.50E-08	5.50E-06
100	46500	4.65E-06	4.65E-04
180	122220	1.22E-05	1.22E-03
220	157140	1.57E-05	1.57E-03
300	226980	2.27E-05	2.27E-03
380	296820	2.97E-05	2.97E-03
460	366660	3.67E-05	3.67E-03
560	453960	4.54E-05	4.54E-03
1000	838080	8.38E-05	8.38E-03
1800	1536480	1.54E-04	1.54E-02
3200	2758680	2.76E-04	2.76E-02
5412	4689756	4.69E-04	4.69E-02
5600	4853880	4.85E-04	4.85E-02
10000	8695080	8.70E-04	8.70E-02
[1]Using Phifer 2005, page D-6 [2]Total Cumulative Hole Size = earlier year hole size + (year interpolated - earlier year) / (later year - earlier year) * (later year hole size - earlier year hole size) [3]Fraction of HDPE geomembrane with holes = Total cumulative hole size/10,000,000,000 mm²/Hectare [4]Percentage with holes = Fraction with Holes x 100			

8.3 DEGRADATION OF GCL OVERLYING AND UNDERLYING DISPOSAL CELLS

The Saltstone disposal cell design includes a 0.2-inch thick sodium bentonite GCL on the top and bottom of each cell in conjunction with the HDPE geomembrane as a hydraulic/diffusional barrier to contaminant migration from the Saltstone disposal cell. The GCL will be placed on the disposal cell concrete roof with an overlying HDPE geomembrane. It will also be placed on the disposal cell concrete mud mat with an overlying HDPE geomembrane. Bentonite is a swelling-type, monmorillonite clay, with very low hydraulic conductivity. Its purpose in being coupled with the HDPE is to fill any holes or tears in the HDPE, providing a redundant and "HDPE healing" low-permeability layer.

Swelling of bentonite clays results from an increase in the thickness of the electrostatic double layer, a term used to describe the diffuse layer of cations held in solution by the attractive forces of the negatively charged clay particles. The thickness of the double-layer can be impacted by both the electrolyte concentration and valence of the cations comprising

the hydrating solution. As salt concentration or cation valence increases in the ambient solution, the double-layer thickness decreases (Dixon and Phifer 2006).

Dixon and Phifer (2006) reports the results of permeability testing on a sodium bentonite GCL exposed to three different solutions: simulated groundwater, simulated Saltstone leachate, and simulated Saltstone pore fluid. The average saturated hydraulic conductivity of GCL samples permeated with simulated groundwater is 6.8E-10 cm/sec. The average saturated hydraulic conductivity for GCL samples permeated with Saltstone leachate is similar to that of GCL permeated with simulated groundwater, 9.1E-10 cm/sec. The average saturated hydraulic conductivity for GCL samples permeated with Saltstone pore fluid is 8.5E-8 cm/sec.

All of these values are well below the typical Resource Conservation and Recovery Act 1.0E-7 cm/sec barrier performance expectation, indicating that a GCL can be appropriately used in conjunction with an HDPE geomembrane as a hydraulic/diffusional barrier to contaminant migration from Saltstone disposal cells.

Since the GCL used in association with Saltstone disposal cells will be in contact with concrete and could be exposed to a Ca^{+2}–containing salt solution, it will be assigned the following conservative saturated hydraulic conductivities based upon the data provided by Dixon and Phifer (2006):
- 0 to 100 years – 5E-09 cm/s
- beyond 100 years – 1.0E-07 cm/s

9.0 REFERENCES

Note to references: These references also include those cited in the appendices.

AASHTO (American Association of State Highway and Transportation Officials). 2005. Geotextile Specifications for Highway Applications. AASHTO M 288-05. American Association of State Highway and Transportation Officials, Washington DISPOSAL CELL. 2005

Abt, S. R. and Johnson, T. L. 1991. Riprap Design for Overtopping Flow. Journal of Hydraulic Engineering, Volume 117, Number 8, pp. 959-972. August 1991.

Albertsson and Banhidi (1980). Microbial and oxidative effects in degradation of polyethylene. Albertsson, A. C. and Banhidi, Z. G. Journal Applied Polymer Science, John Wiley & sons, New York, vol. 25, pp. 1655-1671.

Aleman, S. E. 2007. PORFLOW Testing and Verification Document, WSRC-STI-2007-00150, revision 0. Washington Savannah River Company, Aiken, SC. June 2007.

Anderson, S., Blum, J., Brantley, S. L., Chadwick, O., Chorover, J., Derry, L. A., Drever, J. I., Hering, J. G., Kirchner, J. W., Kump, L. R., Richter, D., and White, A. F. 2004. *Proposed Initiative Would Study Earth's Weathering Engine*, EOS, Transactions, American Geophysical Union, Vol. 85, No. 28, July 2004, pages 265-272.

ASTM International. 1988. *Standard Guide for Identification, Storage, and Handling of Geotextiles*. ASTM D-4873-88. ASTM International, West Conshohocken, PA. November 25, 1988.

ASTM International. 1997. *Standard Practice for Specifying Standard Sizes of Stone for Erosion Control*. ASTM D-6092-97. ASTM International, West Conshohocken, PA. March 10, 1997.

ASTM International. 2000. *Standard Test Methods for Laboratory Compaction Characteristics of Soil Using Standard Effort* (12,400 ft-lbf/ft^3 (600 kN-m/m^3)). ASTM D-698-00. ASTM International, West Conshohocken, PA. June 10, 2000.

ASTM International. 2002a. *Standard Guide for Placement of Riprap Revetments*. ASTM D-6825-02. ASTM International, West Conshohocken, PA. August 10, 2002.

ASTM International. 2002b. *Standard Test Methods for Laboratory Compaction Characteristics of Soil Using Modified Effort* (56,000 ft-lbf/ft^3 (2,700 kN-m/m^3)). ASTM D-1557-02. ASTM International, West Conshohocken, PA. November 10, 2002.

ASTM International. 2003a. *Standard Guide for Petrographic examination of Aggregates for Concrete*. ASTM C-295-03. ASTM International, West Conshohocken, PA. January 10, 2003.

ASTM International. 2003b. *Standard Test Method for Resistance to Degradation of Small-Size Coarse Aggregate by Abrasion and Impact in the Los Angeles Machine.* ASTM C-131-03. American Society of Testing and Materials, West Conshohocken, PA. March 10, 2003.

ASTM International. 2004a. *Standard Guide for Installation of Geosynthetic Clay Liners*, ASTM D-6102-04. ASTM International, West Conshohocken, PA. 2004.

ASTM International. 2004b. *Standard Test Method for Density, Relative Density (Specific Gravity), and Absorption of Coarse Aggregate*. ASTM C-127-04. ASTM International, West Conshohocken, PA. August 1, 2004.

ASTM International. 2005a. *Standard Test Methods for Water Vapor Transmission of Materials*. ASTM E-96/E 96M-05. ASTM International, West Conshohocken, PA. June 2005.

ASTM International. 2005b. *Standard Test Method for Soundness of Aggregates by Use of Sodium Sulfate or Magnesium Sulfate*. ASTM C-88-05. ASTM International, West Conshohocken, PA. July 15, 2005.

ASTM International. 2006a. *Standard Practice for Geomembrane Seam Evaluation by Vacuum Chamber*. ASTM D-5641-94 (Reapproved 2006). ASTM International, West Conshohocken, PA. June 2006.

ASTM International. 2006b. *Standard Practice for Pressurized Air Channel Evaluation of Dual Seamed Geomembranes.* ASTM D-5820-95 (Reapproved 2006). ASTM International, West Conshohocken, PA. June 2006.

ASTM International. 2006c. *Standard Test Method for Determining the Integrity of Nonreinforced Geomembrane Seams Produced Using Thermo-Fusion Methods*. ASTM D-6392-99 (Reapproved 2006) ASTM International, West Conshohocken, PA. June 2006.

ASTM International. 2006d. *Standard Test Method for Oxidative Induction Time of Polyolefin Geosynthetics by High-Pressure Differential Scanning Calorimetry*. ASTM D 5885-06. ASTM International, West Conshohocken, PA. November 2006.

ASTM International. 2006e. *Standard Test Method for Swell Index of Clay Mineral Component of Geosynthetic Clay Liners*. ASTM D 5890-06. ASTM International, West Conshohocken, PA. February 2006.

ASTM International. 2007. *Standard Test Method for Oxidative-Induction Time of Polyolefins by Differential Scanning Calorimetry.* ASTM-D 3895-07. ASTM International, West Conshohocken, PA. April 2007.

Badu-Tweneboah, K., Tisinger, L.G., Giroud, J. P., Smith, B. S., 1999. Assessment of the Long-Term Performance of Polyethylene Geomembrane and Containers in a Low-Level Radioactive Waste Disposal Landfill, Geosynthetics '99 Conference Proceedings, Vol. 2, pp. 1055-1070, Industrial Fabrics Association International, Roseville, MN, 55113.

Bear, J. 1972. Dynamics of Fluids in Porous Media. Dover Publications, Inc., New York.

Bednarik, R. G. 2002. *First Dating of Pilbara Petroglyphs*, Records of the Western Australian Museum, Vol. 20, pages 414-429.

Benson, C. H. 1999. Final Covers for Waste Containment Systems: A North American Perspective. XVII Conference of Geotechnics of Torino: "Control and Management of Subsoil Pollutants". Torino, Italy. November 23-25, 1999.

Bethke, C.M., 2005, The Geochemist's Workbench®, Release 6.0. University of Illinois, Urbana, IL.

Bohm, W. 1979. Methods of Studying Root Systems, Springer-Verlag, page 188.

Boardman, B.T. and Daniel, D.E. 1996. Hydraulic Conductivity of Desiccated Geosynthetic Clay Liners, Journal of Geotechnical Engineering, Volume 122, No. 3, pp 204-208.

Bonaparte, R., Daniel, D. E., and Koerner, R. M. 2002. Assessment and Recommendations for Improving the Performance of Waste Containment Systems. EPA/600/R-02/099, United States Environmental Protection Agency, Office of Research and Development, Cincinnati, OH. December 2002.

Borchardt, G.A., 1977, Montmorillonite and Other Smectite Minerals. In Minerals in Soil Environments, J.B. Dixon and S.B. Weed editors. Soil Science Society of America, Madison, WI.

Brandrup and Immergut (1989). Polymer Handbook, 3rd edition, Brandrup, J., and Immergut, E. H. (editors). John Wiley & Sons, Inc., New York.

Brandrup et al. (1999). Polymer Handbook, 4th edition, Brandrup, J., Immergut, E. H., and Grulke, E. A. (editors). John Wiley & Sons, Inc., New York.

Buol, S. W., Hole, F. D., and McCracken, R. J. 1973. Soil Genesis and Classification. The Iowa University Press, Ames.

Burns, R. M., and B. H. Hondala (Technical Coordinators). 1990. Silvics of North America, Volume 1. Conifers, Agriculture Handbook 654, USDA.

Cahill, J. M., 1982, Hydrology of the Low-Level Radioactive-Solid-Waste Burial Site and Vicinity near Barnwell, South Carolina, Open-File Report 82-863: Columbia, South Carolina, U. S. Geological Survey, 101 p.

Carson, D. A. 2001. Geosynthetic Clay Liners in Waste Containment. Presentation found at www.epa.gov/tio/tsp/download/2001_meet/prez/carson.pdf. Office of Research and Development, US Environmental Protection Agency, Cincinnati, OH.

Chien C. C., Inyang, H. I., and Everett, L. G. (editors). 2006. Barrier Systems for Environmental Contaminant Containment and Treatment. CRC Press, Taylor & Francis Group, LLC, Boca Raton, FL.

CIMBAR 2001. Cal-Ben[TM] (Calcium Bentonite). CIMBAR Performance Minerals, www.cimbar.com. June 2001.

DeGaetano, A.T. and Wilks, D.S. 2001. Extreme-value climatology of maximum soil freezing depths in the United States, Journal of Cold Regions Engineering, Vol. 16, pp. 51-71.

Deng et al. (1996). Effects of Gamma-ray Irradiation on Thermal and Tensile Properties of Ultrahigh-Molecular-Weight Polyethylene Systems. Deng, M., Johnson, R. A., Latour, Jr., R. A., Shalaby, S. W. Irradiation of Polymers – Fundamentals and Technological Applications. Clough R. L. and Shalaby, S. W. (editors). ACS Symposium Series 620, pp 293-301. American Chemical Society, Washington, DISPOSAL CELL.

Dennehy, K. F. and McMahon, P. B. 1989. Water Movement in the Unsaturated Zone at a Low-Level Radioactive-Waste Burial Site near Barnwell, South Carolina, United States Geological Survey Water-Supply Paper 2345: Denver, Colorado, U. S. Geological Survey, United States Government Printing Office, 40 p.

Dinauer, R. C. (managing editor). 1977. Mineral in Soil Environments. Soil Science Society of America, Madison, Wisconsin.

Dixon, K. L. and Phifer, M. A. 2006. Geosynthetic Clay Liner Compatibility with Saltstone Leachate, WSRC-STI-2006-00018, Revision 0. Washington Savannah River Company, Aiken, SC. September 2006.

Egloffstein, T. A. 2001. Natural bentonites—influence of the ion exchange and partial desiccation on permeability and self-healing capacity of bentonites used in GCLs. Geotextiles and Geomembranes, Volume 19, Issue 7, September 2001, Pages 427-444.

Fetter, C. W. 1988. Applied Hydrogeology, second edition. Macmillan Publishing Company, New York.

Fowells, H. A. 1965. Silvics of forest trees of the United States. USDA, Forest Service. Ag. Handbook No. 271, 762 p.

Frados (1976). Plastics Engineering Handbook of the Society of the Plastics Industry, Inc., 4th edition, Frados, J. (ed.). Van Nostrand Reinhold Company, New York.

Freeze, R. A. and Cherry, J. A. 1979. Groundwater. Prentice-Hall, Inc., Englewood Cliffs, New Hersey.

Gates, R. N., G. M. Hill and G.W. Burton. 1999. Response of selected and unselected bahia grass populations to defoliation. Agron. J. 91:787-795.

GDOT 2007. Qualified Products List – APL-2 – Coarse Aggregate Sources – Section A "Standard Sources List". Pits and Quarry Control Branch, Office of Materials and Research, Georgia Department of Transportation, Forest Park, GA. May 2, 2007. (http://www.dot.state.ga.us/dot/construction/materials-research/qpl-catlist.shtml)

Glover, T. J. 2001.Pocket Ref. Sequoia Publishing, Inc. Littleton, CO. June 2001.

Goldman, S. J., Jackson, K., and Bursztynsky, T. A. 1986. Erosion and Sediment Control Handbook, McGraw-Hill Publishing Company, New York.

Golley, F. B. 1965. Structure and function of an old-field broomsedge community. Ecol. Monogr 35:113-131.

Golley, F. B. and J. B. Gentry. 1966. A comparison of variety and standing crop of vegetation on a one-year and twelve-year abandoned field. Oikos 15:185-199.

GRI 1998. Selecting Variable Intervals for Taking Geomembrane Destructive Seam Samples Using the Method of Attributes, GRI Test Method GM14, Geosynthetic Research Institute, Folsom, PA. March 27, 1998.

GRI 2002. Test Methods and Properties for Geotextiles Used as Protection (or Cushioning Materials, GRI Test Method GT12(a) - ASTM Version, Geosynthetic Research Institute, Folsom, PA. February 18, 2002.

GRI 2003. Test Properties, Testing Frequency and Recommended Warranty for High Density Polyethylene (HDPE) Smooth and Textured Geomembranes, GRI Test Method GM13, Geosynthetic Research Institute, Folsom, PA. June 23, 2003.

GRI 2004. Test Methods and Properties for Nonwoven Geotextiles Used as Separation between Subgrade Soil and Aggregate, GRI Test Method GT13, Geosynthetic Research Institute, Folsom, PA. March 10, 2004.

GRI 2005. Test Methods, Required Properties, and Testing Frequencies of Geosynthetic Clay Liners (GCLs), GRI-GCL3. Geosynthetic Research Institute, Folsom, PA. May 16, 2005.

GSE 2006a. Product Data Sheet: GSE GundSeal GCL (Smooth HDPE). GSE Lining Technology, Inc., www.gseworld.com. 03/09/06

GSE 2006b. Technical Note: Bentofix[®] GCL Resistance to Cation Exchange. GSE Lining Technology, Inc., www.gseworld.com. 03/16/06.

Hamilton et al. (1996). Anisotropic Properties in Ultrahigh-Molecular-Weight Polyethylene after Cobalt-60 Irradiation. Hamilton, J. V., Greer, K. W., Ostiguy, P., and Pai, P. N. Irradiation of Polymers – Fundamentals and Technological Applications. Clough R. L. and Shalaby, S. W. (editors). ACS Symposium Series 620, pp 81-93. American Chemical Society, Washington, DISPOSAL CELL.

Hansen, E. M., Schreiner, L. C. and Miller, J. F. 1982. Application of Probable Maximum Precipitation Estimates, United States East of the 105th Meridian, Hydrometeorological Report 52. National Oceanic and Atmospheric Administration, National Weather Service, Office of Hydrology, Hydrometeorological Branch and U.S. Army Corps of Engineers. 168 p.

Harper (1996). Handbook of Plastics, Elastomers, and Composites, 3rd edition, Harper, C. A. (ed.). McGraw-Hill, New York.

Hawkins, R. H. 1962. Bentonite as a Protective Cover for Buried Radioactive Waste, DPSPU 62-30-3A, E. I. du Pont de Nemours and Company, Aiken, SC. May 1962.

Hillel, D. 1982. Introduction to Soil Physics. Academic Press, Inc., San Diego, California.

Horton, J. H. and Wilhite, E. L. 1978. Estimated Erosion Rate at the SRP Burial Ground, DP-1493, E. I. du Pont de Nemours and Company, Aiken, South Carolina. April 1978.

Hubbard, J. E. and Emslie, R. H. 1984. Water Budget for SRP Burial Ground Area, DPST-83-742. E. I. du Pont de Nemours and Company, Savannah River Plant, Aiken, South Carolina, March 19, 1984.

Hubbard, J. E. 1986. An Update on the SRP Burial Ground Area Water Balance and Hydrology, DPST-85-958. E. I. du Pont de Nemours and Company, Savannah River Plant, Aiken, South Carolina, January 9, 1986.

Hubbard, J. E. and Englehardt M. 1987. Calculation of Groundwater Recharge at the old SRP Burial Ground Using the CREAMS Model (1961-1986), State University of New York, Brockport, New York, Summer 1987 (report prepared for E. I. du Pont de Nemours and Company, Savannah River Plant, Aiken, South Carolina and given DuPont document number DP-MS-87-126)

Hsuan and Guan (1997). Evaluation of the Oxidation Behavior of Polyethylene Geomembranes Using Oxidative Induction Time Tests. Hsuan, Y. G. and Guan, Z. Oxidative Behavior of Materials by Thermal analytical Techniques, ASTM STP 1326, Riga, A. T. and Patterson, G. H. (editors). American Society of Testing and Materials (ASTM), Philadelphia, PA, pp. 76-90.

Hsuan and Koerner (1998). Antioxidant depletion lifetime in high density polyethylene geomembranes. Hsuan, Y. G. and Koerner, R. M. Journal of Geotechnical and Geoenvironmental Engineering, ASCE, Vol. 124, No. 6, pp. 532-541.

Hunter, C. H. 2005. Probable Maximum Precipitation for the Z-area Saltstone Facility. SRNL-ATG-2005-00022, Westinghouse Savannah River Company, Aiken, South Carolina. September 2005.

IAEA, (2001). Procedures and Techniques for Closure of Near Surface Disposal Facilities for Radioactive Waste, IAEA-TECDOC-1260, International Atomic Energy Agency, Vienna, Austria, December 2001.

INEEL (2004). Engineering Design File Project No. 23350 Liner/Leachate Compatibility Study. EDF-ER-278, Revision 2, Idaho National Engineering and Environmental Laboratory (INEEL), 6/18/04.

Jacobs, 1988. Special Study on Vegetative Covers, final report for vegetative cover special study for UMTRA Project Office by Jacobs Engineering Group, November 1998, Albuquerque, NM,

Jo, H. Y., Benson, C. H., Shackelford, C. D., Lee, J., and Edil, T. E. 2005. Long-Term Hydraulic Conductivity of a Geosynthetic Clay Liner Permeated with Inorganic Salt Solutions. Journal of Geotechnical and Geoenvironmental Engineering, Vol. 131, No. 4, pp. 405-417, April 2005.

Johnson, T. L. 2002. Design of Erosion Protection for Long-Term Stabilization, NUREG-1623. U.S. Nuclear Regulatory Commission, Washington, DISPOSAL CELL. 139 p.

Jones, S. M., D. H. VanLear, and S. K. Cox. 1981. Major forest community types of the Savannah River Plant: A field guide. SRO-NERP-9, Savannah River National Environmental Research Park Program, Aiken, SC, 79 p.

Kamei, G., M.S. Mitsui, K. Futakuchi, S. Hashimoto, and Y. Sakuramoto, 2005, Kinetics of long-term illitization of montmorillonite – a natural analogue of thermal alteration of bentonite in the radioactive waste disposal system, *Journal of Physics and Chemistry of Solids*, 66, 612-614.

Kane and Widmayer (1989). Consideration for the Long-Term Performance of Geosynthetics at Radioactive Waste Disposal Facilities. Durability and Aging of Geosynthetics, ed. R. M. Koerner, London: Elsevier, 1989, pp. 13-27.

Koerner, R. M. 1990. *Designing with Geosynthetics, Second Edition*. Prentice Hall, Englewood Cliffs, New Jersey. 1990.

Koerner et al. (1990). Long-Term Durability and Aging of Geomembranes. Koerner, R. M., Halse, Y. H., and Lord, Jr., A. E. Waste Containment Systems: Construction, Regulation, and Performance, Bonaparte R. (editor), Geotechnical Special Publication No. 26, American Society of Civil Engineers, San Francisco, CA. pp. 106-134.

Koerner, R. M. 1998. Designing with Geosythetics, 4th edition. Prentice Hall, Upper Saddle River, New Jersey.

Koerner and Hsuan 2003. Lifetime Prediction of Polymeric Geomembranes Used in New Dam Construction and Dam Rehabilitation. Koerner, R. M. and Hsuan, Y. G. Proceedings of the Association of State Dam Safety Officials Conference, Lake Harmony, Pennsylvania, June 4-6, 2003.

Koerner, R. M. and Koerner, G. R. 2005. In-Situ Separation of GCL Panels Beneath Exposed Geomembranes, GRI White Paper #5. Geosynthetic Institute, Folsom, PA. April 15, 2005.

Kresser (1957). Reinhold Plastics Application Series 1. Polyethylene. Kresser, T. O. J. Reinhold Publishing Corporation, New York.

Kudoh et al. (1996). High-Energy Ion Irradiation Effects on Polymer Materials. Kudoh, H., Sasuga, T., and Seguchi, T. Irradiation of Polymers – Fundamentals and Technological Applications. Clough R. L. and Shalaby, S. W. (editors). ACS Symposium Series 620, pp 2-10. American Chemical Society, Washington, DISPOSAL CELL.

Lamb, T. W. and Whitman, R. V. 1969. Soil Mechanics. John Wiley & Sons, New York.

Landreth, R. E., 1991. The Resistance of Membranes in Cover Systems to Root Penetration by Grass and Trees, EPA/600/A-92/202, presented at Geosynthetics '91 Conference, Atlanta, GA.

Lin, L. and Benson, C. H. 2000. Effect of Wet-Dry Cycling on Swelling and Hydraulic Conductivity of GCLs. Journal of Geotechnical and Geoenvironmental Engineering, Vol. 126, No. 1, January 2000, pp. 40-49.

Lindsey, C. G., Long, L. W., Begej, C. W. 1982. *Long-Term Survivability of Riprap for Armoring Uranium Mill Tailings and Covers: A Literature Review*, prepared for U. S. Nuclear Regulatory Commission, Pacific Northwest Laboratory, Richland, WA 99352.

Link, S. O., Cadwell, L. L., Petersen, K. L., Sackschewsky, M. R., and Landeen, D. S., 1995. The role of Plants and Animals in Isolation Barriers at Hanford, Washington, PNL-10788, Pacific Northwest Laboratory, Richland, WA 99352.

Looney, B. B., Eddy, C. A., Ramdeen, M., Pickett, J., Rogers, V., Scott, M. T., and Shirley, P. A. 1990. Geochemical and Physical Properties of Soils and Shallow Sediments at the Savannah River Site (U), WSRC-RP-90-1031, Westinghouse Savannah River Company, Aiken, South Carolina. August 31, 1990.

Looney, B. B. and Falta, R. W. 2000. Vadose Zone Science and Technology Solutions, Volume II, Battelle Press, Columbus, Ohio. pp. 852-853.

Loubser, J., Hudson, T., and Greiner, T. 2003. *The Recent Recording of Petroglyphs in Georgia*, in The Profile, The Newsletter of the Society for Georgia Archaeology, No. 117, Winter 2002-2003, pages 3-5.

Ludovici, K. H., S. J. Zarnoch, and D. D. Richter. 2002. "Modeling In-situ Pine Root Decomposition Using Data from a 60-year Chronosequence", Can. J. For. Res. 32:1675-1684.

McCarty, B. (Ed.). 2003. Southern lawns: best management practices for the selection, establishment and maintenance of southern lawngrasses. EC 707, Clemson University, Clemson, SC, 566 p.

McDowell-Boyer, L., Yu, A. D., Cook, J. R., Kocher, D. C., Wilhite, E. L., Holmes-Burns, H., and Young, K. E. 2000. Radiological Performance Assessment for the E-Area Low-Level Waste Facility, Revision 1, WSRC-RP-94-218. Westinghouse Savannah River Company, Aiken, South Carolina. January 31, 2000.

McQuilkin, W. E. 1940. The natural establishment of pine in abandoned fields in the Piedmont Plateau region. Ecology 21:135-147.

McRae, S. G. 1988. Practical Pedology Studying Soils in the Field, Halsted Press: a division of John Wiley & Sons, New York.

Meyer, C. 1997. Bir Umm Fawakhir: Insights Into Ancient Egyptian Mining, Journal of the Minerals, Metals and Materials Society, Vol. 49, No. 3, 1997, pages 64-68.

Mitchell, J. K. 1993. Fundamentals of Soil Behavior, Second Edition. John Wiley & Sons, Inc. New York.

Mueller and Jakob (2003). Oxidative resistance of High-Density Polyethylene Geomembranes. Mueller, W. and Jakob, I. Polymer Degradation and Stability, Elsevier Science Ltd. Vol. 79 (2003) pp. 161-172.

Needham et al. (2004). The likely medium to long-term generation of defects in geomembrane liners. Needham, A., Gallagher, E., Peggs, I., Howe, G, and Norris, J. R&D Technical Report P1-500/1/TR, Environment Agency, Bristol, England.

Nelson, E. A. 2005. Assessment of the biological basis of bamboo as the final vegetation option for closure caps at SRS. WSRC-TR-2005-00424, Savannah River National Laboratory, 22p.

Nelson, J. D., Abt, S. R., Volpe, R. L., van Zyl, D., Hinkle, N. E., and Staub, W. P. 1986. Methodologies for Evaluating Long-Term Stabilization Designs of Uranium Mill Tailing Impoundments, NUREG/CR-4620, U.S. Nuclear Regulatory Commission, Washington, D.C. June 1986.

Newman, E. J., Stark, T. D., Rohe, F. P., and Diebel, P., 2004. Thirty-Year Durability of a 20-mil PVC Geomembrane, Journal of Vinyl and Additive Technology, V. 10, Issue 4, pp. 168-173.

Nimitz et al. (2001). Chemical Compatibility Testing Final Report Including Test Plan and Procedures. Nimitz, J. S., Allred, R. E., and Gordon, B. W. SAND2001-1988, Sandia National Laboratories.

NRC-NA 2007. Assessment of the Performance of Engineered Waste Containment Barriers. Prepublication Copy. National Research Council of the National Academies (NRC-NA), The National Academies Press, Washington, D.C.

Odum, E. P. 1960. Organic production and turnover in old field succession. Ecology 41:34-49.

Ohe, T., M. Itoh, T. Ishii, H. Nakashima, Y. Hirata, and H. Yoshida. 1998. The long-term alteration rate of Na-smectite in natural bentonite formation, *Journal of Contaminant Hydrology*, 35, 285-294.

NCSU (North Carolina State University). 1991. *Erosion and Sediment Control – Field Manual*, State of North Carolina. February 1991.

NUREG 1982. *Long-Term Survivability of Riprap for Armoring Uranium-Mill Tailings and Covers: A Literature Review,* NUREG/CR-2642, U. S. Nuclear Regulatory Commission, Washington, D. C. 20555-0001.

NUREG 2006. *Consolidated Decommissioning Guidance Characterization, Survey and Determination of Radiological Criteria,* Final Report, NUREG-1757, Vol. 2, Rev. 1, U. S. Nuclear Regulatory Commission, Washington, D. C. 20555-0001.

Parizek, R. R. and Root, R. W. 1986. Development of a Ground-Water Velocity Model for the Radioactive Waste Management Facility Savannah River Plant, South Carolina, The Pennsylvania State University, University Park, Pennsylvania, June 1986 (report prepared for E. I. du Pont de Nemours and Company, Savannah River Plant, Aiken, South Carolina and given DuPont document number DPST-86-658)

Phifer, M. A., Drumm, E. C., and Wilson, G. V. 1993. Effects of Post Compaction Water Content Variation on Saturated Conductivity, *Hydraulic Conductivity and Waste Contaminant Transport in Soils, ASTM STP 1142*, David E. Daniel and Stephen J. Trautwein, Eds., American Society for Testing and Materials, Philadelphia, PA.

Phifer, M. A., Nichols, R. L., Sappington, F. C., Steimke, J. L., and Jones, W. E. 2001. TNX GeoSiphon^{TM} Summary Report (U), WSRC-TR-2001-00015, Revision 0. Westinghouse Savannah River Company, Aiken, SC. January 19, 2001.

Phifer, M. A. and Nelson, E. A. 2003. Saltstone Disposal Facility Closure Cap Configuration and Degradation Base Case: Institutional Control to Pine Forest Scenario (U), WSRC-TR-2003-00436, Revision 0. Westinghouse Savannah River Company, Aiken, SC. September 22, 2003.

Phifer, M. A., Milllings, M. R., and Flach, G. P. 2006. Hydraulic Property Data Package for the E-Area and Z-Area Soils, Cementitious Materials, and Waste Zones, WSRC-STI-2006-00198, Revision 0. Washington Savannah River Company, Aiken, SC. September 2006.

Phifer, M. A., Jones, W. E., Nelson, E. A., Denham, M. E., Lewis, M. R., and Shine, E. P. 2007. FTF Closure Cap Concept and Infiltration Estimates, WSRC-STI-2007-00184, Revision 2. Washington Savannah River Company, Aiken, SC. October 2007.

Phifer, M. A. 2005. Scoping Study: High Density Polyethylene (HDPE) in Saltstone Service, WSRC-TR-2005-00101, Revision 0. Westinghouse Savannah River Company, Aiken, SC. February 2005.

Phifer, M. A. 2006. Software Quality Assurance Plan for the Hydrologic Evaluation of Landfill Performance (HELP) Model, Q-SQA-A-00005, Revision 0. Washington Savannah River Company, Aiken, SC. October 2006.

Phillips (1988). Effects of Radiation on Polymers. Phillips, D. C. Materials Science and Technology, Vol. 4, pp. 85-91.

Pinder, J. E. III. 1975. Effects of species removal on an old-field plant community. Ecology 56:747-751.

Pomeroy, K. B. and C. F. Korstian. 1949. Further results of loblolly pine seed production and dispersal. J. Forestry 47:968-970.

Puls, R. S. and Powell, R. M. 1992. "Chapter 4, Surface-Charge Repulsive Effects on the Mobility of Inorganic Colloids in Subsurface System", Sabatini, D. A. and Knox, R. C. (editors), Transport and Remediation of Subsurface Contaminants Colloidal, Interfacial, and Surfactant Phenomena, American Chemical Society, Washington, DISPOSAL CELL.

Rosenberger, K. 2007. Subject: Potential Dose to F-Tank Farm Closure Cap Geomembrane, SRS-REG-2007-00001. Washington Savannah River Company, Aiken, SC. June 1, 2007.

Rowe (2004). Resolving Some of the Outstanding Issues in Landfill Barrier Design. Rowe, R. K. 3rd Asian Regional Conference on Geosynthetics.

Rumer, R. R. and Mitchell, J. K. (editors). 1995. Assessment of Barrier Containment Technologies A Comprehensive Treatment for Environmental Remediation Applications. International Containment Technology Workshop, Baltimore, Maryland. August 29-31, 1995.

Salvo and Cook 1993. Selection and Cultivation of Final Vegetative Cover for Closed Waste Sites at the Savannah River Site, SC (WSRC-MS-92-513). Salvo, S. K. and Cook, J. R. Westinghouse Savannah River Company, Aiken, South Carolina, 1993.

Sangam and Rowe (2002). Effects of exposure conditions on the depletion of antioxidants from HDPE geomembranes. Sangam, H. P. and Rowe, R. K. Canadian Geotechnical Journal, National Research Council Canada, Vol. 39, No. 6, pp. 1221-1230.

Sangster (1993). Applications of Radiation Treatment of Ultradrawn Polyethylene. Sangster, D. F. Irradiation of Polymeric Materials – Processes, Mechanisms, and Applications. Reichmanis, E., Frank, C. W., and O'Donnell, J. H. (editors). ACS Symposium Series 527, pp 95-101. American Chemical Society, Washington, DISPOSAL CELL.

Sappington, F. C., Phifer, M. A., Denham, M. E., Millings, M. R., Turick, C. E., and McKinsey, P. C. 2005. D-Area Sulfate Reduction Study Comprehensive Final Report (U), WSRC-TR-2005-00017. Westinghouse Savannah River Company, Aiken, SC. February 11, 2005.

Schnabel (1981). Polymer Degradation Principles and Practical Applications. Schnabel, W. Hanser International, Germany (distributed by Macmillan Publishing Co., Inc., New York)

Schreiner, L. C. and Riedel, J. T. 1978. Probable Maximum Precipitation Estimates, United States East of the 105th Meridian, Hydrometeorological Report 51. National Oceanic and Atmospheric Administration, National Weather Service, Office of Hydrology, Hydrometeorological Branch and U.S. Army Corps of Engineers. 87 p.

Schroeder, P. R. and Peyton, R. L. 1987a. Verification of the Lateral Drainage Component of the HELP Model Using Physical Models. EPA/600/2-87/049. Office of Research and Development, United States Environmental Protection Agency (EPA), Cincinnati, Ohio. July 1987.

Schroeder, P. R. and Peyton, R. L. 1987b. Verification of the Hydrologic Evaluation of Landfill Performance (HELP) Model Using Field Data. EPA/600/2-87/050. Office of Research and Development, United States Environmental Protection Agency (EPA), Cincinnati, Ohio. July 1987.

Schroeder, P. R., Lloyd, C. M., Zappi, P. A., and Aziz, N. M. 1994a. The Hydrologic Evaluation of Landfill Performance (HELP) Model User's Guide for Version 3. EPA/600/R-94/168a. Office of Research and Development, United States Environmental Protection Agency (EPA), Cincinnati, Ohio. September 1994.

Schroeder, P. R., Dozier, T. S., Zappi, P. A., McEnroe, B. M., Sjostrom, J. W., and Peyton, R. L. 1994b. The Hydrologic Evaluation of Landfill Performance (HELP) Engineering Documentation for Version 3. EPA/600/R-94/168b. Office of Research and Development, United States Environmental Protection Agency (EPA), Cincinnati, Ohio. September 1994.

SCS (Soil Conservation Service). 1984. Engineering Field Manual, fourth printing, U.S. Department of Agriculture, Soil Conservation Service. 1984.

Serrato, M. G., 2004. Field Observation Summary for Tree Extractions at the SRS E-Area Test Pads (U), SRNL-2004-00063, Westinghouse Savannah River Company, Aiken, SC 29808.

Serrato M. G. 2006. Meeting Summary – Visit with Richard Hawkins on December 6, 2005, IRD-TFBUT Project File. Washington Savannah River Company, Aiken, SC. January 23, 2006.

Serrato M. G. 2007. GeoTesting Express unpublished data sheets. Washington Savannah River Company, Aiken, SC. October 3, 2006.

Shine, E. P. 2007. F-area Tank Farm Closure Cap Probability Model of Pine Tree Tap Root Penetrations of HDPE Geomembrane (U), WSRC-TR-2007-00369, Washington Savannah River Company, Aiken, SC.

Smith, G.D., Karlsson, K., and Gedde, U.W. 1992. Modelling of antioxidant loss from polyolefins in hot water applications – 1. Model and application to medium density polyethylene pipes. *Polymer Eng. and Science*, Vol. 32, No. 10, 658-667.

Strom, R. N. and Kaback, D. S. 1992. SRP Baseline Hydrogeologic Investigation: Aquifer Characterization - Groundwater Geochemistry of the Savannah River Site and Vicinity (U), WSRC-RP-92-450. Westinghouse Savannah River Company, Aiken SC. March 31, 1992.

Stutzman, P. 2001. *Contributions of NIST/NBS Researchers to the Crystallography of Construction Minerals*, Journal of Research of the National Institute of Standards and Technology, Vol. 106, No. 6, November-December 2001, pages 1051-1061.

Sun et al. (1996). Development of an Accelerated Aging Method for Evaluation of Long-Term Irradiation Effects on Ultrahigh-Molecular-Weight Polyethylene Implants. Sun, D. C., Stark, C., and Dumbleton, J. H. Irradiation of Polymers – Fundamentals and Technological Applications. Clough R. L. and Shalaby, S. W. (editors). ACS Symposium Series 620, pp 340-349. American Chemical Society, Washington, DISPOSAL CELL.

SRNL – ATG (Savannah River National Laboratory (SRNL) – Atmosphere Technology Group (ATG)) 2006. Web site: http://shweather.srs.gov/servlet/idg.Weather.Weather

Taylor, H. M. 1974. "Root Behavior as Affected by Soil Structure and Strength," The Plant Root and Its Environment, University of Virginia Press, p. 271-292.

The Nature Conservancy 2007. Heggie's Rock. (http://www.nature.org/wherewework/northamerica/states/georgia/preserves/art6696.html)

Ulrich, B., B. Benechi, W. F. Harris, P. K. Dhanna, and R. Mayer. 1981. "Chapter 5. Soil Processes," Dynamic Properties of Forest Ecosystems, IBP, Cambridge University Press.

USEPA (United States Environmental Protection Agency) 1989. Seminar Publication: Requirements for Hazardous Waste Landfill Design, Construction, and Closure, EPA/625/4-89/022, United States Environmental Protection Agency, Washington, DISPOSAL CELL. August 1989.

USEPA (United States Environmental Protection Agency) 2001. *Geosynthetic Clay Liners Used in Municipal Solid Waste Landfills*. Solid Waste and Emergency Response, EPA530-F-97-002, United States Environmental Protection Agency, Washington, DISPOSAL CELL. December 2001.

Walkinshaw, C. H. 1999. "Death of Root Tissues in Standing (Live) and Felled Loblolly Pines", 10th Biennial So. Silv. Res. Conf. pp. 573-577.

White, A. F., Blum, A. E., Schulz, M. S., Bullen, T. D., Harden, J.W., and Peterson, M. L., 1996. Chemical Weathering Rates of a Soil Chronosequence on Granitic Alluvium: I. Quantification of Mineralogical and Surface Area Changes and Calculation of Primary Silicate Reaction Rates, Geochimica et Cosmochimica Acta, Vol. 60, No. 14, pp. 2533-2550.

White, A. F., Bullen, T. D., Schulz, M. S., Blum, A. E., Huntington, T. G., and Peters, N. E., 2000. Differential Rates of Feldspar Weathering in Granitic Regoliths, Geochimica et Cosmochimica Acta, Vol. 65, No. 6, pp. 847-869.

Whyatt and Fansworth (1990). The High pH Chemical and Radiation Compatibility of Various Liner Materials. Whyatt, G. A. and Farnsworth, R. K. Geosynthetic Testing for Waste Containment Applications. Koerner, R. M. (editor). STP 1081, pp110-124. American Society of Testing and Materials, Philadelphia, PA.

Wilcox, H. 1968. "Morphological Studies of the Root of Red Pine, Pinus resinosa, Growth Characteristics and Patterns of Branching", Amer. J. Bot. 55:247-254.

Winkler, E. M. 1987. *Weathering and Weathering Rates of Natural Stone*, Environmental Geology, Vol. 9, No. 2, June, 1987, pages 85-92.

Witt, K. J. and Siegmund, M. 2001. Laboratory Testing of GCL under Changing Humidity. Proceedings of the 8th International waste Management and Landfill Symposium, Sardinia Second Conference, Euro Waste, Sardinia 2001.

WSRC 2005. Response to Action Items from Public Meetings between NRC and DOE to Discuss RAI for the Savannah River Site. CBU-PIT-2005-00203, revision 1. Westinghouse Savannah River Company, Aiken, SC. September 2005.

WSRC 2007. Life-Cycle Liquid Waste Disposition System Plan, Liquid Waste Planning Process, Rev. 14, LWO-PIT-2007-00062, Washington Savannah River Company, Aiken, SC. October 18

WSRC 2008. Saltstone Disposal Facility Hydrogeology Inputs, SDF-IP-03, Revision A, Washington Savannah River Company, Aiken, SC. March 2008.

Worrall, W. E. 1975. Clays and Ceramic Raw Materials, John Wiley and Sons, Inc. New York.

Young, M. H. and Pohlmann, K. F. 2001. Analysis of Vadose Zone Monitoring System: Computer Simulation of Water Flux: E-Area Disposal Trenches, Task Order GA0074 (KG43360-0). Division of Hydrologic Sciences, Desert Research Institute, Las Vegas, NV. August 2001.

Young, M. H. and Pohlmann, K. F. 2003. Analysis of Vadose Zone Monitoring System: Computer Simulation of Water Flux under Conditions of Variable Vegetative Cover: E-Area Disposal Trenches, Publication No. 41188. Division of Hydrologic Sciences, Desert Research Institute, Las Vegas, NV. August 2001.

Yu, A. D., Langton, C. A., and Serrato, M. G. 1993. Physical Properties Measurement Program (U), WSRC-RP-93-894. Westinghouse Savannah River Company, Aiken, SC. June 30, 1993

Zutter, B. R., R. J. Mitchell, G. R. Glover and D. H. Gjerstad. 1999. Root length and biomass in mixtures of broomsedge with loblolly pine or sweetgum. Can. J. Forest Res. 29:926-933.

Web site reference - http://abob.libs.uga.edu/bobk/rockpet.html

Web site reference - www.hermitagemuseum.org/html_En/03/hm3_2_2c.html

Web site reference - http://mc2.vicnet.net.au/home/cognit/shared_files/cupules.pdf

Web site reference - http://www.nps.gov/archeology/rockArt/arch1.htm

Web site reference - http://www.public.asu.edu/~rexweeks/Public_Access_RA_Sites.htm

Web site reference - http://www.wssc.psu.edu/index.htm

Web site reference - http://www.czen.org/wssc

Web site reference - http://stonewall.nist.gov

This page intentionally left blank.

APPENDIX A. PHYSICAL STABILITY CALCULATIONS

Scoping level calculations and/or estimations have been made in order to ensure that a physically stable closure cap configuration relative to erosion can be provided. Calculations and/or estimations for the following key items are provided below:

- Probable maximum precipitation (PMP) estimation
- Vegetative soil cover slope
- Erosion barrier riprap sizing
- Side slope riprap sizing
- Toe riprap sizing

Probable Maximum Precipitation Estimation
Estimates of the SRS-specific probable maximum precipitation (PMP) for storm (drainage) areas ranging from 1 to 1000 square miles and rainfall durations from 5 minutes to 72 hours have been made. A PMP is defined as the theoretically greatest depth of precipitation for a give duration that is physically possible over a given storm size area at a particular geographic location. These estimates are summarized in Table A-1. The SRS-specific PMP estimates for storm areas of 10 square miles, 200 square miles, and 1,000 square miles and rainfall durations of 6 to 72 hours were based on interpolation from standard maps of generalized, all-season isohyets of PMP presented in Hydrometeorological Report (HMR)-51 (Schreiner and Riedel 1978). The PMP estimates for a 1 square mile area and for rainfall durations less than 6 hours were based on procedures outlined in HMR-52 (Hansen et al. 1982). The 1-hour duration rainfall over storm areas from 1 to 1000 square mile was obtained through interpolation from the standard PMP isohyetal maps. Additional maps presented in HMR-52 were used to obtain SRS-specific scaling factors that were then applied to the 1-hour PMP value to determine 5 and 15-minute amounts. The 1 square mile PMP is considered by HMR-52 equivalent to the rainfall at any point within that area. Therefore the 1 square mile PMP is used in the riprap sizing calculations presented below. (Hunter 2005)

Table A-1. Estimated Probable Maximum Precipitation for the Savannah River Site (SRS)

Duration	Area (square miles)			
	One	Ten	Two Hundred	One Thousand
5 min	6.2	5.1	2.9	NA
15 min	9.7	8.0	4.6	NA
1 hr	19.2	15.7	9.1	5.1
6 hr	NA	31	23	16.8
12 hr	NA	37	28	22.7
24 hr	NA	43.5	35	31
48 hr	NA	48	38	33
72 hr	NA	51.5	42	36

All precipitation values are in inches
Table taken from Hunter 2005
NA = not applicable

Vegetative Soil Cover Slope

The slope of the vegetative soil cover has been evaluated using the permissible velocity method as outlined by Johnson (2002), Appendix A. The following are the initial vegetative soil cover slope assumptions which were evaluated for acceptability:

- Maximum slope length = 825 ft
- Maximum slope = 1.5% = 0.015

Calculate the drainage area in acres of the maximum slope length of the 1.5% slope vegetative soil cover on a foot-width basis:

$$A = (825 \; ft \times 1 \; ft)/43560 \; ft^2/acre = 0.0189 \; acres$$

Calculate the time of concentration for the 1.5% slope vegetative soil cover using the Kirpich Method (Nelson et al. 1986 and Johnson 2002):

$$t_c = \left(11.9L^3/H\right)^{0.385}, \quad \text{where } t_c = \text{time of concentration in hours; } L = \text{drainage length}$$
$$\text{in miles; } H = \text{elevation difference in ft}$$

L = 825 ft / 5280 ft/mile = 0.1563 miles
H (elevation difference) = 825 ft × 0.015 = 12.375 ft

$$t_c = \left(11.9 \, (0.1563)^3/12.375\right)^{0.385} = 0.1155 \; hrs = 6.9 \; \text{min}$$

Calculate the rainfall intensity for the 1.5% slope vegetative soil cover:

Rainfall intensities of 6.2 inches in five minutes and of 9.7 inches in 15 minutes are taken from Table A-1. The rainfall intensity at the time of concentration of 6.9 will be determined by linear interpolation between those from Table A-1 at 5 and 15 minutes and converted to inches per hour.

$$I_{6.9 \, min} = \left(6.2 \; in + \left[\left(\frac{6.9 \; min - 5 \; min}{15 \; min - 5 \; min}\right) \times (9.7 \; in - 6.2 \; in)\right]\right) \times \frac{60 \; min/hr}{6.9 \; min} = 59.7 \; in/hr$$

Calculate the peak flow rate using the rational formula and a flow concentration factor of 3 for the 1.5% slope vegetative soil cover:

$$Q_{cal} = FCIA, \quad \text{where } Q_{cal} = \text{calculated flow in cfs; } F = \text{flow concentration factor}$$
$$\text{(unitless); } C = \text{runoff coefficient (unitless); } I = \text{precipitation in in/hr; } A$$
$$= \text{drainage area in acres}$$

A flow concentration factor (F) of 3 is recommended by Johnson 2002.
The runoff coefficient (C) will be taken as the upper end of that for pasture and woodlands (i.e. $C = 0.45$) (Goldman et al. 1986 Table 4.1).
$I_{6.9\ min} = 59.7$ in/hr
$A = 0.0189$ acres

$$Q_{cal} = FCIA = 3(0.45)(59.7\ in/hr)(0.0189\ acres) = 1.52\ cfs$$

Calculate the flow depth using the Manning Equation for the 1.5% slope vegetative soil cover:

$$y^{5/3} = \frac{Q_{cal}n}{1.486\ S^{1/2}},$$

where y = depth in ft; Q_{cal} = flow in cfs (see value above);

n = Manning coefficient of roughness (unitless);
S = slope in fraction form

It is planned that the slope of the vegetative soil cover slope will be between 0 and 5 percent and that it will be vegetated with Bahia grass or equivalent (bamboo and pine trees are considered better than Bahia grass in terms of erosion protection). Based on the use of Bahia grass and a 0 to 5 percent slope, a maximum permissible velocity (MPV) of 5 fps has been obtained from Exhibit 7-3 of SCS 1984. Based upon Bahia grass, a retardance classification of C has been obtained from Exhibit 7-2 of SCS 1984. Determine the product of velocity (V) and hydraulic radius (R) based upon a unit width of flow of 1-ft (this is equal to the R since there are no sides in this case) and a MPV of 5 fps:

$$VR = 1\ ft \times 5\ ft/s = 5\ ft^2/s$$

Based upon a VR of 5 ft^2/s and a retardance classification of C, a Manning coefficient of roughness (n) of 0.039 has been obtained from Exhibit 7-1 of SCS 1984.

$Q_{cal} = 1.52$ cfs
$S = 0.015$

$$y^{5/3} = \frac{(Q_{cal})(n)}{1.486\ S^{1/2}} = \frac{(1.52\ cfs)(0.039)}{1.486\ (0.015)^{1/2}} = 0.3257$$
$$y = (0.3257)^{3/5} = 0.51\ ft$$

Calculate permissible velocity (V_p) for the 1.5% slope vegetative soil cover based upon the depth of flow using the velocity correction factors provided by Johnson 2002 on page A-5:

For a depth of flow of 0.51 ft, the velocity correction factor (CF) will be interpolated from the following values provided by Johnson 2002 on page A-5:

Depth of Flow (ft)	Velocity Correction Factor (CF)
0.4	0.6
0.65	0.7

$$CF = 0.6 + \left[\left(\frac{0.51\ ft - 0.4\ ft}{0.65\ ft - 0.4\ ft}\right) \times (0.7 - 0.6)\right] = 0.644$$

V_p = CF × MPV = 0.644 × 5 fps = 3.22 fps

Calculate the actual velocity (V_a) for the 1.5% vegetative soil cover and compare to the permissible velocity (V_p):

$V_a = Q_{cal}/(y \times 1\ ft) = 1.52\ cfs / (0.51\ ft \times 1\ ft) = 2.98\ fps$

V_a = 2.98 fps < V_p = 3.22 fps, therefore the 1.5 percent slope is considered a stable slope to prevent the initiation of gullying for the precipitation considered (i.e., 59.7 in/hr).

Since a maximum slope length of 825 ft with a maximum slope of 1.5% is acceptable, a 2% vegetative soil cover slope will also be evaluated for acceptability:

- Maximum slope length = 825 ft
- Maximum slope = 2.0% = 0.020

The drainage area remains the same as previously calculated for the 1.5% slope vegetative soil cover at 0.0189 acres.

Calculate the time of concentration for a 2% vegetative soil cover using the Kirpich Method (Nelson et al. 1986 and Johnson 2002):

$$t_c = \left(11.9L^3/H\right)^{0.385}, \quad \text{where } t_c = \text{time of concentration in hours; } L = \text{drainage length in miles; } H = \text{elevation difference in ft}$$

L = 825 ft / 5280 ft/mile = 0.1563 miles
H (elevation difference) = 825 ft × 0.020 = 16.5 ft

$$t_c = \left(11.9\,(0.1563)^3/16.5\right)^{0.385} = 0.1032\ hrs = 6.2\ min$$

Calculate the rainfall intensity for the 2% vegetative soil cover:

From Table A-1, rainfall intensities of 6.2 inches in five minutes and 9.7 inches in fifteen minutes are provided. The rainfall intensity at the time of concentration of 6.2 will be determined by linear interpolation between those at fifteen minutes and five minutes and then converted to inches per hour.

$$I_{6.2\,min} = \left(6.2\ in + \left[\left(\frac{6.2\ min - 5\ min}{15\ min - 5\ min} \right) \times (9.7\ in - 6.2\ in) \right] \right) \times \frac{60\ min/hr}{6.2\ min} = 64.1\ in/hr$$

Calculate the peak flow rate using the rational formula and a flow concentration factor of 3 for the 2% vegetative soil cover:

$Q_{cal} = FCIA$, where Q_{cal} = calculated flow in cfs; F = flow concentration factor (unitless); C = runoff coefficient (unitless); I = precipitation in in/hr; A = drainage area in acres

A flow concentration factor (F) of 3 is recommended by Johnson 2002.
The runoff coefficient (C) will be taken as the upper end of that for pasture and woodlands (i.e. C = 0.45) (Goldman et al. 1986 Table 4.1).
$I_{6.2\,min}$ = 64.1 in/hr
A = 0.0189 acres

$$Q_{cal} = FCIA = 3(0.45)(64.1\ in/hr)(0.0189\ acres) = 1.64\ cfs$$

Calculate the flow depth using the Manning Equation for the 2% vegetative soil cover:

$$y^{5/3} = \frac{(Q_{cal})(n)}{1.486\ S^{1/2}},$$ where y = depth in ft; Q_{cal} = flow in cfs (see value above); n = Manning coefficient of roughness (unitless); S = slope in fraction form

The following remain the same as previously determined for the 1.5% slope:

- Maximum permissible velocity (MPV) of 5 fps for Bahia grass on a 0 to 5 percent slope (Exhibit 7-3 of SCS 1984)
- A retardance classification of C for Bahia grass (Exhibit 7-2 of SCS 1984)
- The product of velocity (V) and hydraulic radius (R) of 5 ft^2/s remain
- Manning coefficient of roughness (n) of 0.039 (Exhibit 7-1 of SCS 1984)

$Q_{cal} = 1.64$ cfs
S = 0.020

$$y^{5/3} = \frac{Q_{cal}n}{1.486\ S^{1/2}} = \frac{(1.64\ cfs)(0.039)}{1.486\ (0.020)^{1/2}} = 0.3044$$
$$y = (0.3043)^{3/5} = 0.49\ ft$$

Calculate permissible velocity (V_p) for the 2% vegetative soil cover based upon the depth of flow using the velocity correction factors provided by Johnson 2002 on page A-5:

For a depth of flow of 0.49 ft, the velocity correction factor (CF) will be interpolated from the following values provided by Johnson 2002 on page A-5:

Depth of Flow (ft)	Velocity Correction Factor (CF)
0.4	0.6
0.65	0.7

$$CF = 0.6 + \left[\left(\frac{0.49\ ft - 0.4\ ft}{0.65\ ft - 0.4\ ft} \right) \times (0.7 - 0.6) \right] = 0.636$$

$V_p = CF \times MPV = 0.636 \times 5$ fps = 3.18 fps

Calculate the actual velocity (V_a) for the vegetative soil cover and compare to the permissible velocity (V_p):

$V_a = Q_{cal}/(y \times 1\ ft) = 1.64$ cfs $/ (0.49\ ft \times 1\ ft) = 3.35$ fps

$V_a = 3.35$ fps $> V_p = 3.18$ fps, therefore the 2 percent slope is *not* considered a stable slope that prevents the initiation of gullying for the precipitation considered (i.e. 64.1 in/hr).

Based upon the above, a maximum 825-ft slope length at a maximum 1.5 percent slope will be considered acceptable for the SDF closure cap vegetative soil cover. Maximum acceptable slopes for portions of the closure cap with slope lengths less than 825 ft may be greater than 1.5 percent, if it is determined that they are considered stable slopes that prevent the initiation of gullying versus a PMP event during the actual closure cap design process.

Erosion Barrier Riprap Sizing and Thickness

The riprap for the erosion barrier (i.e. riprap located 3 ft beneath the cap surface) has been sized per the Abt and Johnson Method (Abt and Johnson 1991 and Johnson 2002 Appendix D Section 2). The erosion barrier is assumed to have the same slope length and slope as the overlying vegetative soil cover (i.e. the erosion barrier and overlying vegetative soil cover are parallel). Therefore the following are the erosion barrier slope length and slope used to determine the riprap size:

- Maximum slope length = 825 ft
- Maximum slope = 1.5% = 0.015

The erosion barrier drainage area on a foot-width basis (A), time of concentration in hours (t_c), and rainfall intensity ($I_{4.8min}$) are the same as that previously calculated for the 2% vegetative soil cover:

- A = 0.0189 acres
- t_c = 6.9 min
- $I_{6.9\,min}$ = 59.7 in/hr

Calculate the peak flow rate using the rational formula and a flow concentration factor of 5:

$Q_{cal} = FCIA$, where Q_{cal} = calculated flow in cfs; F = flow concentration factor (unitless); C = runoff coefficient (unitless); I = precipitation in in/hr; A = drainage area in acres

A conservative flow concentration factor (F) of 5 (rather than 3, as used for the cap surface) has been utilized for the erosion barrier. The factor of 5 has been used for the erosion barrier since it is overlain by a 3-ft thick soil layer, which could potentially be subject to gully erosion. However the vegetative soil cover has been designed to prevent the initiation of gullying due to a PMP event. Designing both the vegetative soil cover and erosion barrier in consideration of a PMP event provides defense-in-depth and additional assurance of physical stability.

The voids within the stone of the erosion barrier will be filled with a yet-to-be-determined material. In order to be conservative, the runoff coefficient (C) will be taken as the lower end of that for concrete (i.e. C = 0.8) (Goldman et al. 1986; Table 4.1).

$Q_{cal} = FCIA = 5(0.8)(59.7\ in/hr)(0.0189\ acres) = 4.51\ cfs$

Calculate the required size of the riprap using the Abt and Johnson Method (Abt and Johnson 1991 and Johnson 2002 Appendix D Section 2):

$$D_{50} = 5.23 \, S^{0.43} \, Q_{design}^{0.56},$$

where D_{50} = median size of riprap in inches; S = slope in fraction form; Q_{design} = 1.35 $Q_{failure}$; $Q_{failure}$ = Q_{cal} (flow calculated above in cfs)

The flow at failure ($Q_{failure}$) is the flow required to move the riprap such that the underlying filter fabric or bedding stone is exposed. In order to design for no movement of the riprap the design flow (Q_{design}) is utilized, which increases the failure flow ($Q_{failure}$) by a factor that represents the experimental ratio of "the unit discharge at movement to unit discharge at failure" (Abt and Johnson 1991).

Q_{design} = 1.35 Q_{cal} = 1.35 (4.51 cfs) = 6.09 cfs
S = 0.015

$$D_{50} = 5.23 \, S^{0.43} \, Q_{design}^{0.56} = 5.23 \, (0.015)^{0.43} \, (6.09 \, cfs)^{0.56} = 2.36 \; inches$$

Using the Abt and Johnson 1991 method, the required D_{50} (median size) of the erosion barrier riprap was determined to be 2.36 in. As a conservative measure, and to provide consistency between this cap design and other onsite-cap designs, the 2.36 in. size will be rounded-up to 2.5 in. (the value determined for the 2% slope used for the F-Area Tank Farm closure cap in Phifer et al. 2007).

The D_{50} 2.5 in. erosion barrier rock size is consistent with Type B riprap from Table F-3 of Johnson 2002 or Size R-20 riprap from Table 1 of ASTM 1997. Johnson 2002 recommends a riprap layer thickness of not "less than 1.5 times the mean stone diameter (D_{50}) or the D_{100} whichever is greater." NCSU 1991 recommends that the riprap layer thickness be at least 1.5 times the maximum stone diameter (D_{100}). Since the NCSU 1991 criterion is more conservative, it will be used.

Calculate the thickness of the erosion barrier:

The D_{100} for Type B riprap ≈ 5" and for Size R-20 ≈ 7.5 in

Thickness = 1.5 (D_{100}) = 1.5 (7.5 in) = 11.25 in ≈ 12 in

Side Slope Riprap Sizing
The riprap for the side slopes have been sized per the Abt and Johnson Method (Abt and Johnson 1991 and Johnson 2002 Appendix D Section 2). The sizing is based upon the "worst case" for side slope length, the southeasternmost corner area, and is calculated by adding the times-of-concentration for the vegetative soil cover, the side slope, and the four benches built into the side slope.

Calculate the drainage area of the side slope excluding on a foot-width basis:

Assume a maximum slope = 3H:1V (33.3% or 0.333)
Assume a maximum 100 ft elevation difference between the southeast edge of the SDF closure cap surface (assume a slope-surface elevation of ~330 ft-msl) and the toe of the side slope (assume a toe elevation of ~230 ft-msl; see Figure A-1).
Slope length = 100 ft / 0.333 = 300 ft

$$A = (300 \ ft \times 1 \ ft)/43560 \ ft^2/acre = 0.0069 \ acres$$

Calculate the drainage area of the benches on a foot-wide basis:

Assume a maximum slope = 1.5% or 0.015
Assume a maximum slope length of 4 benches x 10-ft/bench = 40 ft

$$A = (40 \ ft \times 1 \ ft)/43560 \ ft^2/acre = 0.0009 \ acres$$

Calculate the time of concentration for the side slope using the Kirpich Method (Nelson et al. 1986 and Johnson 2002):

$$t_c = (11.9L^3/H)^{0.385}, \quad \text{where } t_c = \text{time of concentration in hours; } L = \text{drainage length in miles; } H = \text{elevation difference in ft}$$

The time of concentration for the side slope is the summation of the time of concentration for the vegetative soil cover plus, that of the four, 10-ft wide benches within the side slope, plus that of the side slope itself.

t_c for vegetative soil cover was previously calculated as 0.1155 hrs (6.93 min)

calculate t_c for side slope *per se*:

L = 300 ft / 5280 ft/mile = 0.0568 miles
H = 100 ft
$$t_c = (11.9 (0.0568)^3/100)^{0.385} = 0.0160 \ hrs = 0.96 \ min$$

calculate t_c for 4 benches:

L = 40 ft / 5280 ft/mile = 0.0076 miles
H = 40 ft x 0.015 = 0.6 ≈ 1

$$t_c = (11.9 (0.0076)^3/1)^{0.385} = 0.0093 \ hrs = 0.56 \ min$$

total t_c for side slope = 6.93 min + 0.96 min + 0.56 min = 8.45 min

Calculate the rainfall intensity for the side slope:

Rainfall intensities of 6.2 inches in five minutes and of 9.7 inches in 15 minutes are taken from Table A-1. The rainfall intensity at the time of concentration of 8.45 min will be determined by linear interpolation between those from Table A-1 at 5 and 15 minutes and converted to inches per hour.

$$I_{8.45\ min} = \left(6.2\ in + \left[\left(\frac{8.45\ min - 5\ min}{15\ min - 5\ min} \right) \times (9.7\ in - 6.2\ in) \right] \right) \times \frac{60\ min/hr}{8.45\ min} = 52.6\ in/hr$$

Calculate the peak flow rate using the rational formula and a flow concentration factor of 5:

$Q_{cal} = FCIA$, where Q_{cal} = calculated flow in cfs; F = flow concentration factor (unitless); C = runoff coefficient (unitless); I = precipitation in in/hr; A = drainage area in acres

A conservative flow concentration factor (F) of 5 has been utilized for the side slope. The factor of 5 has been used for the side slope, since the top slope feeds into the side slope.

The runoff coefficient for the side slope will be taken as 0.8, since it is on a barren steep slope (Goldman et al. 1986 Table 4.1).

$I_{8.45\ min}$ = 52.6 in/hr
The area (A) is equal to the side slope area itself (i.e. 0.0069 acres) plus the upgradient area of the erosion barrier or vegetative soil cover (i.e. 0.0189 acres)
A = 0.0069 acres + 0.0009 + 0.0189 acres = 0.0267 acres

$Q_{cal} = FCIA = 5(0.8)(52.6\ in/hr)(0.0267\ acres) = 5.62\ cfs$

Calculate the required size of the riprap using the Abt and Johnson Method (Abt and Johnson 1991 and Johnson 2002 Appendix D Section 2):

$D_{50} = 5.23\ S^{0.43}\ Q_{design}^{0.56}$, where D_{50} = median size of riprap in inches; S = slope in fraction form; Q_{design} = 1.35 $Q_{failure}$; $Q_{failure}$ = Q_{cal} (flow calculated above in cfs)

The flow at failure ($Q_{failure}$) is the flow required to move the riprap such that the underlying filter fabric or bedding stone is exposed. In order to design for no movement of the riprap the design flow (Q_{design}) is utilized, which increases the failure flow ($Q_{failure}$) by a factor that represents the experimental ratio of "the unit discharge at movement to unit discharge at failure" (Abt and Johnson 1991).

$Q_{design} = 1.35\ Q_{cal} = 1.35\ (5.62\ \text{cfs}) = 7.59\ \text{cfs}$

$D_{50} = 5.23\ S^{0.43}\ Q_{design}^{0.56} = 5.23\ (0.33)^{0.43}\ (7.59\ cfs)^{0.56} = 10.1\ inches$

Using the Abt and Johnson 1991 method, the required D_{50} (median size) of the side slope riprap was determined to be 10.1 in. Therefore the side slope riprap will consist of rock consistent with Type D riprap from Table F-3 of Johnson 2002 or Size R-150 riprap from Table 1 of ASTM 1997. As stated above the more conservative NCSU 1991 criterion that requires a riprap layer thickness at least 1.5 times the maximum stone diameter (D_{100}) will be used.

Calculate the thickness of the side slope riprap:

The D_{100} for Type D riprap is between 12 and 18 in and for Size R-150 ≈ 14 in

Thickness = 1.5 (D_{100}) = 1.5 (14 in) = 21 in

However a 21 in placement is not typical, therefore a 24 in layer will be used.

Toe Riprap Sizing
The riprap for the toe has been sized per the Abt Method (Johnson 2002 Appendix D Section 6).

Calculate the peak flow rate off the combined erosion barrier or vegetative soil cover and side slope using the rational formula and a flow concentration factor of 3:

$Q_{cal} = FCIA$, where Q_{cal} = calculated flow in cfs; F = flow concentration factor (unitless); C = runoff coefficient (unitless); I = precipitation in in/hr; A = drainage area in acres

A flow concentration factor of 3 is recommended by Johnson 2002. A flow concentration factor of 5 is not used for the toe riprap although it is used for the erosion barrier and side slope riprap. Since the side riprap has been designed using a flow concentration factor of 5 and designed to prevent movement of its riprap, therefore channeling and the formation of gullies in the side slope which feed into the toe should be prevented. Therefore a flow concentration factor of 3 is considered appropriate for the toe.

The runoff coefficient (i.e. 0.8), precipitation (i.e. 52.6 in/hr), and drainage area (0.0267) are the same as that of the side slope.

$Q_{cal} = FCIA = 3(0.8)(52.6\ in/hr)(0.0267\ acres) = 3.37\ cfs$

Calculate the required size of the riprap using the Abt Method (Johnson 2002 Appendix D Section 6):

$$D_{50} = 10.46 \, S^{0.43} \, Q_{cal}^{0.56}, \quad \text{where } D_{50} = \text{median size of riprap in inches; } S = \text{slope in fraction form} = 0.33 \text{ (see above for side slope); } Q_{cal} = \text{flow calculated above in cfs}$$

$$D_{50} = 10.46 \, (0.33)^{0.43} \, (3.37 \, cfs)^{0.56} = 12.82 \, inches$$

Using the Abt and Johnson 1991 method, the required D_{50} (median size) of the toe riprap was determined to be 12.82 in. Therefore the toe riprap will consist of rock consistent with Type D riprap from Table F-3 of Johnson 2002 or Size R-300 riprap from Table 1 of ASTM 1997. Johnson 2002 recommends a toe riprap thickness of 3 times the mean stone diameter (D_{50}) and a toe width of 15 times the mean stone diameter (D_{50}).

Calculate the thickness and width of the toe riprap:

The D_{50} for Type D riprap is between 10 and 12 in and for Size R-300 ≈ 14 in

Thickness = 3 (D_{50}) = 3 (14 in) = 42 in

Calculate the toe width:

Width = 15 (D_{50}) = 15 (14 in) = 210 ins = 17.5 ft

A 20 ft toe width will be used.

Erosion Barrier, Side Slope, and Toe Riprap Summary
Table A- 2 provides a summary of the erosion barrier, side slope, and toe riprap requirements. Erosion barrier, side slope, and toe riprap size may be smaller for portions of the closure cap with shorter slope lengths than those used to determine the requirements outlined in Table A- 2, if it is determined that the smaller sized riprap is stable versus a PMP event during the actual closure cap design process.

Table A- 2. Erosion Barrier, Side Slope, and Toe Riprap Requirements Summary

Location	Riprap Requirements
Erosion barrier	A 1 ft thick layer of rock consistent with Type B riprap from Table F-3 of Johnson 2002 or Size R-20 riprap from Table 1 of ASTM 1997. Voids within the stone layer shall be filled.
Side slope	A 2 ft thick layer of rock consistent with Type D riprap from Table F-3 of Johnson 2002 or Size R-150 riprap from Table 1 of ASTM 1997. The riprap shall be underlain with a stone bedding layer consisting of a 6 in thick layer of well-graded crushed stone with either the gradation shown in Table F-4 of Johnson 2002 or that of Figure 8 of ASTM 1997 (i.e. FS-2 filter/bedding stone).
Toe	A 3-ft 6-in thick layer of rock consistent with Type D riprap from Table F-3 of Johnson 2002 or Size R-300 riprap from Table 1 of ASTM 1997, which extends out 20 ft from the bottom of the side slope.

Figure A-1. Saltstone Cap Southeastern Corner Configuration
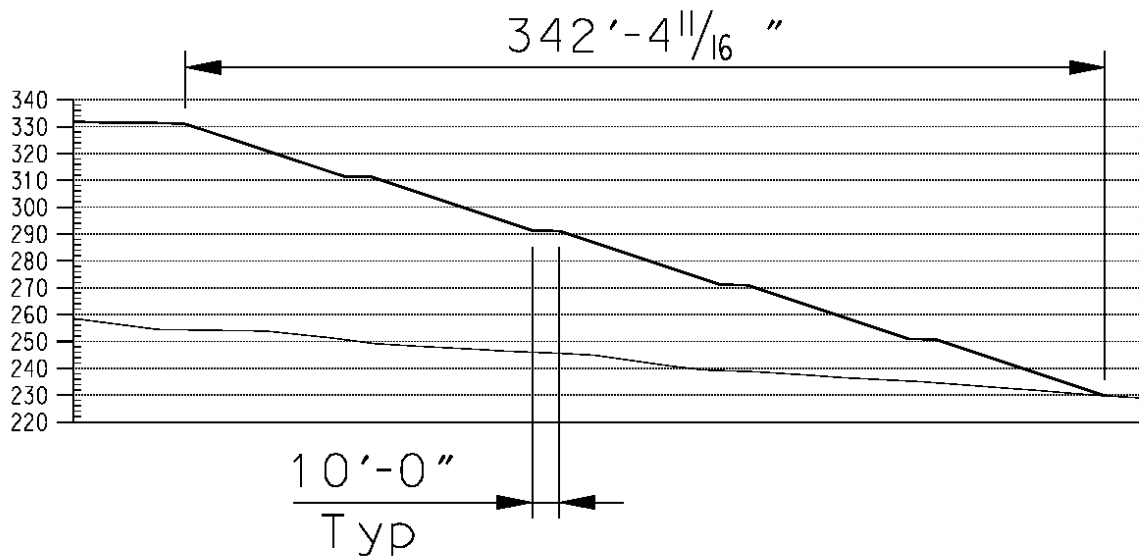
This page intentionally left blank.

APPENDIX B. AUGUSTA SYNTHETIC PRECIPITATION MODIFIED WITH SRS SPECIFIC AVERAGE MONTHLY PRECIPITATION DATA OVER 100 YEARS

This appendix is available in CD format due to its size - (file name: Fprec.d4)

This page intentionally left blank.

APPENDIX C. AUGUSTA SYNTHETIC TEMPERATURE MODIFIED WITH SRS SPECIFIC AVERAGE MONTHLY TEMPERATURE DATA OVER 100 YEARS

This appendix is available in CD format due to its size - (file name: Ftemp.d7)

This page intentionally left blank.

APPENDIX D. AUGUSTA SYNTHETIC SOLAR RADIATION DATA OVER 100 YEARS

This appendix is available in CD format due to its size - (file name: Fsolar.d13)

This page intentionally left blank.

APPENDIX E. AUGUSTA EVAPOTRANSPIRATION

(file name: Fevap.d11)

```
1
AUGUSTA               GEORGIA
33.22        68 323 3.5    22.    6.5  68.0 70.0 77.0 73.0
```

This page intentionally left blank.

APPENDIX F.
EROSION BARRIER MATERIAL PROPERTY CALCULATIONS

Erosion Barrier with CLSM as Infill

Determine the combined soil material properties for the Type B riprap from Table F-3 of Johnson 2002 or Size R-20 riprap from Table 1 of ASTM 1997 filled with a Controlled Low Strength Material (CLSM) or Flowable Fill (Phifer and Nelson 2003):

Type B riprap consists of stone ranging in size from a maximum of 5% by weight less than ½-inches to a maximum size of approximately 8-inches. Size R-20 riprap consists of stone ranging in size from a maximum of 15% by weight less than 3-inches to a maximum size of approximately 8-inches.

The following are porosity references for coarse grained materials:

Material	Porosity, η (vol/vol)	Source
Gravel	0.25 to 0.40	Freeze and Cherry 1979 Table 2.4
Well sorted sand or gravel	0.25 to 0.50	Fetter 1988 Table 4.2
Ottawa sand	0.33 to 0.44	Lamb and Whitman 1969 Table 3.2
HELP model default soil #21 (gravel or poorly graded gravel)	0.397	Schroeder et al. 1994b Table 1

It is assumed that the rock that will be utilized will be granite from regional quarries. The table on Weights and Properties of Materials in Glover 2001 provides a broken granite specific gravity of 1.65 and a weight per cubic foot of 103 (this specific gravity and weight per cubic foot represent the bulk density of the broken granite). As outlined in Section 4.4.9 the stone shall have a minimum specific gravity of 2.65 (this specific gravity represents the particle density of the granite stone). Based upon this bulk density of 1.65 g/cm^3 and particle density of
2.65 g/cm^3, a porosity of the stone can be determined as follows (Hillel 1982):

$$\eta = 1 - \frac{\rho_b}{\rho_p}, \quad \text{where } \eta = \text{porosity}; \rho_b = \text{dry bulk density of 1.65 g/cm}^3; \rho_p = \text{particle}$$

density as 2.65 g/cm^3

$$\eta = 1 - \frac{1.65 \ g/cm^3}{2.65 \ g/cm^3} = 0.38$$

The 0.38 calculated stone porosity falls within that of the above referenced porosity ranges for coarse materials and is very close to the HELP model default soil #21 (gravel or poorly graded gravel) porosity of 0.397 (Schroeder et al. 1994b Table 1). Therefore a porosity of 0.38 will be assumed for the erosion barrier stone.

From Table 6-27 of Phifer et al. 2006 the following recommended CLSM property values were obtained, which will be utilized in determining the combined rip rap/CLSM properties:

- Effective porosity (η) = 0.328
- Saturated hydraulic conductivity (K_{sat}) = 2.2E-06 cm/s

See the notes from Table for the HELP model definition of field capacity and wilting point. Volumetric moisture content can be determined as follows (Hillel 1982):

$$\theta_v = \eta s, \quad \text{where } \theta_v = \text{volumetric moisture content; } \eta = \text{porosity; } s = \text{saturation}$$

CLSM curve data was obtained from the Phifer et al. 2006, Table 6-48. From this data the field capacity (volumetric water content at 0.33 bars or 337 cm-H_2O) and wilting point (volumetric water content at 15 bars or 15,310 cm-H_2O) of the CLSM were derived by linear interpolation:

Suction Head Ψ (cm-H_2O)	Saturation s (vol/vol)
300	0.8888
400	0.8401
14,200	0.2517
16,400	0.2443

The following provides the linear interpolation used to determine the CLSM field capacity and wilting point, respectively, based upon the above CLSM characteristic curve data, which will be utilized in determining the combined rip rap/CLSM properties:

Field capacity = θ_v at 337 cm-H_2O = $\eta \times s$ at 337 cm-H_2O =

$$0.328 \times \left(0.8401 + \left[\left(\frac{400 - 337}{400 - 300} \right) (0.8888 - 0.8401) \right] \right) = 0.286$$

Wilting point = θ_v at 15,310 cm-H_2O = $\eta \times s$ at 15,310 cm-H_2O =

$$0.328 \times \left(0.2443 + \left[\left(\frac{16,400 - 15,310}{16,400 - 14,200} \right) (0.2517 - 0.2443) \right] \right) = 0.081$$

The following table provides the summary CLSM properties:

Property	Property Value
Porosity, η (vol/vol)	0.328
Field capacity (vol/vol)	0.286
Wilting point (vol/vol)	0.081
Saturated hydraulic conductivity (K_{sat})	2.2E-06 cm/s

The matrix of an individual granite stone itself is considered impermeable and non-porous. The porosity of a layer of granite stone is considered to be 0.38 as outlined above. When the granite stone porosity is filled with CLSM, the resultant hydraulic properties, which are area or volume based, become that of the CLSM times the granite stone porosity. The resultant hydraulic properties are shown below:

Property	Property Value
Porosity, η (vol/vol)	$0.328 \times 0.38 = 0.125$
Field capacity (vol/vol)	$0.286 \times 0.38 = 0.109$
Wilting point (vol/vol)	$0.081 \times 0.38 = 0.031$
Saturated hydraulic conductivity (K_{sat})	2.2E-06 cm/s $\times$ 0.38 = 8.36E-07 cm/s

Erosion Barrier with Sandy Soil as Infill

Configuration #1a differs from Configuration #1 in using sandy soil properties rather than CLSM properties for the Erosion Barrier infill. Since the material finally selected for the erosion barrier could be something other than CLSM, this configuration is presented to contrast the infiltration results of using a higher hydraulic conductivity infill material with those of a lower hydraulic conductivity, e.g., CLSM infill. The sandy soil properties will be taken as those of the lower vadose zone (LVZ) from Phifer et al. (2006). This represents an SRS sandy soil which can be obtained on-site for use in closure cap construction.

Determine the combined soil material properties for the Type B riprap from Table F-3 of Johnson 2002 or Size R-20 riprap from Table 1 of ASTM 1997 filled with LVZ soil (Phifer et al., 2006):

Type B riprap consists of stone ranging in size from a maximum of 5% by weight less than ½-inches to a maximum size of approximately 8-inches. Size R-20 riprap consists of stone ranging in size from a maximum of 15% by weight less than 3-inches to a maximum size of approximately 8-inches.

The following are porosity references for coarse grained materials:

Material	Porosity, η (vol/vol)	Source
Gravel	0.25 to 0.40	Freeze and Cherry 1979 Table 2.4
Well sorted sand or gravel	0.25 to 0.50	Fetter 1988 Table 4.2
Ottawa sand	0.33 to 0.44	Lamb and Whitman 1969 Table 3.2
HELP model default soil #21 (gravel or poorly graded gravel)	0.397	Schroeder et al. 1994b Table 1

It is assumed that the rock used will be granite from regional quarries. The table on Weights and Properties of Materials in Glover 2001 provides a broken granite specific gravity of 1.65 and a weight per cubic foot of 103 (this specific gravity and weight per cubic foot represent the bulk density of the broken granite). As outlined in Section 4.4.9 the stone shall have a minimum specific gravity of 2.65 (this specific gravity represents the particle density of the granite stone). Based upon this bulk density of 1.65 g/cm^3 and particle density of 2.65 g/cm^3, a porosity of the stone can be determined as follows (Hillel 1982):

$$\eta = 1 - \frac{\rho_b}{\rho_p}, \quad \text{where } \eta = \text{porosity}; \rho_b = \text{dry bulk density of 1.65 g/cm}^3; \rho_p = \text{particle}$$

$$\text{density as 2.65 g/cm}^3$$

$$\eta = 1 - \frac{1.65 \; g/cm^3}{2.65 \; g/cm^3} = 0.38$$

The 0.38 calculated stone porosity falls within that of the above referenced porosity ranges for coarse materials and is very close to the HELP model default soil #21 (gravel or poorly graded gravel) porosity of 0.397 (Schroeder et al. 1994b Table 1). Therefore a porosity of 0.38 will be assumed for the erosion barrier stone.

From Table 5-18 of Phifer et al. 2006 the following recommended LVZ soil property values were obtained, which will be utilized in determining the combined rip rap/sandy soil properties:

- Effective porosity (η) = 0.39
- Saturated hydraulic conductivity (K_{sat}) = 3.3E-04 cm/s

See the notes from Table for the HELP model definition of field capacity and wilting point. Volumetric moisture content can be determined as follows (Hillel 1982):

$$\theta_v = \eta s, \quad \text{where } \theta_v = \text{volumetric moisture content}; \eta = \text{porosity}; s = \text{saturation}$$

LVZ soil curve data was obtained from the Phifer et al. 2006, Table 5-19. From this data the field capacity (volumetric water content at 0.33 bars or 337 cm-H_2O) and wilting point (volumetric water content at 15 bars or 15,310 cm-H_2O) of the LVZ soil were derived by linear interpolation:

Suction Head Ψ (cm-H_2O)	Saturation s (vol/vol)
331	0.650
381	0.637
14,400	0.467
16,600	0.463

The following provides the linear interpolation used to determine the LVZ soil field capacity and wilting point, respectively, based upon the above LVZ soil characteristic curve data, which will be utilized in determining the combined rip rap/CLSM properties:

Field capacity = θ_v at 337 cm-H_2O = $\eta \times s$ at 337 cm-H_2O =

$$0.39 \times \left(0.637 + \left[\left(\frac{381-337}{381-331} \right)(0.650 - 0.637) \right] \right) = 0.253$$

Wilting point = θ_v at 15,310 cm-H_2O = $\eta \times s$ at 15,310 cm-H_2O =

$$0.39 \times \left(0.463 + \left[\left(\frac{16,600-15,310}{16,600-14,400} \right)(0.467 - 0.463) \right] \right) = 0.181$$

The following table provides the summary LVZ soil properties:

Property	Property Value
Porosity, η (vol/vol)	0.39
Field capacity (vol/vol)	0.253
Wilting point (vol/vol)	0.181
Saturated hydraulic conductivity (K_{sat})	3.3E-04 cm/s

The matrix of an individual granite stone itself is considered impermeable and non-porous. The porosity of a layer of granite stone is considered to be 0.38 as outlined above. When the granite stone porosity is filled with sandy soil, the resultant hydraulic properties, which are area or volume based, become that of the sandy soil porosity times the granite stone porosity. The resultant hydraulic properties are shown below:

Property	Property Value
Porosity, η (vol/vol)	$0.39 \times 0.38 = 0.15$
Field capacity (vol/vol)	$0.253 \times 0.38 = 0.10$
Wilting point (vol/vol)	$0.181 \times 0.38 = 0.07$
Saturated hydraulic conductivity (K_{sat})	3.3E-04 cm/s $\times$ 0.38 = 1.3E-04 cm/s

APPENDIX G.
HELP MODEL INPUT FOR INITIAL SDF CLOSURE CAP INFILTRATION

HELP Model Input Data for SDF Closure Cap (Erosion Barrier with Sandy Soil Infill; Year 0):

Input Parameter (HELP Model Query)	Generic Input Parameter Value
Landfill area =	0.0189 acres
Percent of area where runoff is possible =	100%
Do you want to specify initial moisture storage? (Y/N)	Y
Amount of water or snow on surface =	0 inches
CN Input Parameter (HELP Model Query)	CN Input Parameter Value
Slope =	2 %
Slope length =	825 ft
Soil Texture =	4 (HELP model default soil texture)
Vegetation =	4 (i.e., a good stand of grass)
HELP Model Computed Curve Number = 44.6	

Layer	Layer Number	Layer Type
Topsoil	1	1 (vertical percolation layer)
Upper Backfill	2	1 (vertical percolation layer)
Erosion Barrier	3	1 (vertical percolation layer)
Middle Backfill	4	1 (vertical percolation layer)
Lateral Drainage Layer	5	2 (lateral drainage layer)
HDPE Geomembrane	6	4 (geomembrane liner)
GCL	7	3 (barrier soil liner)
Foundation Layer (Upper 1-ft of lower backfill; 1.0E-06)	8	1 (vertical percolation layer)
Foundation Layer (lower backfill; 1.0E-03)	9	1 (vertical percolation layer)

	Layer Type	Layer Thickness (in)	Soil Texture No.	Total Porosity (Vol/Vol)	Field Capacity (Vol/Vol)	Wilting Point (Vol/Vol)	Initial Moisture (Vol/Vol)
1	1	6		0.396	0.109	0.047	0.109
2	1	30		0.35	0.252	0.181	0.252
3	1	12		0.15	0.10	0.07	0.10
4	1	12		0.35	0.252	0.181	0.252
5	2	12		0.417	0.045	0.018	0.045
6	4	0.06					
7	3	0.2		0.750	0.747	0.400	0.750
8	1	12		0.35	0.252	0.181	0.252
9	1	72		0.457	0.131	0.058	0.131

HELP Model Input Data for SDF Closure Cap (Year 0) – continued:

	Layer Type	Sat. Hyd. Conductivity (cm/sec)	Drainage Length (ft)	Drain Slope (%)	Leachate Recirc. (%)	Recirc. to Layer (#)	Subsurface Inflow (in/yr)
1	1	3.1E-03					
2	1	4.1E-05					
3	1	1.3E-04					
4	1	4.1E-05					
5	2	5.0E-02	825	4			
6	4	2.0E-13					
7	3	5.0E-09					
8	1	1.0E-06					
9	1	1.0E-03					

	Layer Type	Geomembrane Pinhole Density (#/acre)	Geomembrane Instal. Defects (#/acre)	Geomembrane Placement Quality	Geotextile Transmissivity (cm^2/sec)
1	1				
2	1				
3	1				
4	1				
5	2				
6	4	1	4	2	
7	3				
8	1				
9	1				

The lack of values in the table for particular parameters in particular layers denotes that no HELP model input was required for that parameter in that layer. No data are missing from the table.

Closure cap configuration described in 4 and Table of Section 4.3, with sandy soil as Erosion Barrier infill rather than CLSM .

APPENDIX H.
DETAILED HELP MODEL ANNUAL WATER BALANCE DATA

Detailed HELP Model Annual Water Balance Data for Configuration #1a (Year 0):

Simulation	Prec (in/yr)	Runoff (in/yr)	Evap (in/yr)	Lateral Drainage (in/yr)	Infiltration thru GCL (in/yr)	Change in Water Storage (in/yr)
1	40.07	0.000	31.653	4.674	0.00009	3.743
2	57.14	0.000	32.094	25.219	0.00114	-0.175
3	52.64	0.000	31.091	21.130	0.00134	0.417
4	47.88	0.952	38.428	9.002	0.00018	-0.503
5	50.57	0.000	34.394	14.093	0.00031	2.083
6	42.28	0.000	27.895	13.158	0.00034	1.227
7	39.35	0.515	30.611	14.807	0.00036	-6.584
8	49.46	0.509	31.514	15.519	0.00035	1.917
9	48.59	0.000	33.583	14.013	0.00030	0.994
10	53.97	0.000	33.906	19.125	0.00245	0.936
11	57.63	2.054	32.433	21.871	0.00287	1.269
12	46.71	0.000	29.208	20.020	0.00119	-2.519
13	38.58	0.000	30.409	7.619	0.00015	0.552
14	41.49	0.375	27.779	13.369	0.00042	-0.033
15	44.94	1.022	32.623	13.451	0.00029	-2.156
16	54.78	0.403	32.090	21.261	0.00173	1.024
17	29.81	0.000	21.667	9.165	0.00020	-1.022
18	49.55	0.000	34.895	11.998	0.00025	2.657
19	55.50	0.731	33.774	21.918	0.00251	-0.926
20	68.56	0.000	37.426	27.170	0.00111	3.963
21	51.14	0.000	33.876	19.158	0.00116	-1.895
22	51.22	0.000	36.715	15.447	0.00034	-0.942
23	47.94	0.000	36.529	14.831	0.00068	-3.421
24	59.17	1.199	31.240	23.092	0.00213	3.637
25	47.73	0.026	30.420	16.247	0.00038	1.037
26	50.56	0.194	31.935	17.538	0.00096	0.892
27	37.02	0.000	32.181	8.539	0.00018	-3.701
28	56.03	0.788	35.960	20.278	0.00091	-0.997
29	39.77	0.000	29.485	8.588	0.00017	1.697
30	46.55	0.299	33.864	12.716	0.00026	-0.328
31	39.45	0.060	28.844	13.692	0.00033	-3.146
32	45.35	0.375	29.807	13.016	0.00029	2.151
33	42.23	0.000	31.905	8.297	0.00016	2.027
34	37.81	0.000	27.339	11.779	0.00027	-1.307
35	48.19	0.286	34.212	14.470	0.00032	-0.778
36	62.28	3.520	34.056	20.336	0.00085	4.367

Detailed HELP Model Annual Water Balance Data for Configuration #1a (Year 0) – Continued:

Simulation	Prec (in/yr)	Runoff (in/yr)	Evap (in/yr)	Lateral Drainage (in/yr)	Infiltration thru GCL (in/yr)	Change in Water Storage (in/yr)
37	55.96	0.000	40.483	16.055	0.00037	-0.579
38	40.26	0.000	28.229	13.330	0.00030	-1.299
39	60.02	2.338	35.097	22.212	0.00318	0.369
40	59.62	0.734	37.281	21.810	0.00053	-0.207
41	47.60	0.000	31.582	15.355	0.00036	0.663
42	50.44	0.521	34.130	16.392	0.00037	-0.603
43	39.42	0.061	26.350	11.449	0.00024	1.559
44	48.61	0.000	33.998	14.369	0.00033	0.243
45	57.35	0.931	34.969	27.145	0.00358	-5.699
46	47.49	0.000	31.999	11.887	0.00027	3.604
47	38.98	0.000	31.666	9.265	0.00019	-1.951
48	42.99	0.000	32.694	9.297	0.00018	0.999
49	53.01	1.660	34.281	13.805	0.00030	3.264
50	55.17	0.038	38.102	20.038	0.00050	-3.008
51	46.16	0.000	31.248	11.786	0.00026	3.126
52	42.63	0.000	33.721	13.951	0.00033	-5.043
53	50.93	0.000	32.529	18.186	0.00042	0.215
54	54.24	0.582	28.380	20.018	0.00093	5.259
55	50.46	0.218	33.032	16.939	0.00055	0.270
56	56.39	1.117	38.507	21.660	0.00055	-4.894
57	41.99	0.000	27.957	13.188	0.00033	0.845
58	68.60	0.196	35.690	29.632	0.00234	3.079
59	48.67	0.089	33.998	14.821	0.00038	-0.239
60	58.12	0.000	34.682	23.126	0.00243	0.310
61	54.90	2.184	31.315	21.428	0.00400	-0.032
62	56.29	0.885	33.384	25.216	0.00321	-3.198
63	49.13	0.373	34.348	15.382	0.00034	-0.974
64	54.54	0.357	32.296	18.810	0.00056	3.077
65	45.05	0.000	32.908	13.493	0.00030	-1.351
66	37.07	0.000	29.770	9.605	0.00020	-2.305
67	40.17	0.000	25.014	10.780	0.00023	4.376
68	58.08	0.000	35.387	24.503	0.00241	-1.812
69	36.31	0.000	27.124	10.264	0.00021	-1.078
70	42.67	0.996	31.917	13.057	0.00031	-3.300
71	48.88	0.000	35.418	10.344	0.00023	3.118
72	47.36	0.511	32.766	17.179	0.00041	-3.096
73	35.81	0.000	26.571	8.543	0.00018	0.696
74	49.81	0.686	29.647	16.006	0.00039	3.472

Detailed HELP Model Annual Water Balance Data for Configuration #1a (Year 0) – Continued:

Simulation	Prec (in/yr)	Runoff (in/yr)	Evap (in/yr)	Lateral Drainage (in/yr)	Infiltration thru GCL (in/yr)	Change in Water Storage (in/yr)
75	56.43	3.806	34.455	17.456	0.00040	0.713
76	45.86	0.000	32.561	15.138	0.00035	-1.839
77	56.76	0.000	39.129	18.383	0.00063	-0.753
78	39.15	0.000	29.546	8.964	0.00020	0.639
79	48.87	0.000	30.932	13.743	0.00105	4.194
80	58.52	0.982	33.493	27.411	0.00496	-3.371
81	53.34	0.000	35.510	16.525	0.00037	1.305
82	55.18	0.000	35.585	18.264	0.00068	1.331
83	53.60	2.607	34.853	20.405	0.00209	-4.267
84	47.82	0.000	34.139	12.820	0.00034	0.861
85	44.69	0.000	30.905	10.088	0.00020	3.697
86	60.77	0.000	35.879	27.609	0.00280	-2.721
87	48.34	1.123	29.579	14.361	0.00052	3.277
88	36.18	0.000	26.171	15.954	0.00214	-5.947
89	58.29	2.732	35.148	17.826	0.00082	2.583
90	60.08	1.421	30.575	23.354	0.00324	4.726
91	55.49	0.000	35.936	22.105	0.00169	-2.553
92	44.51	0.202	32.165	13.119	0.00030	-0.977
93	35.83	0.000	29.650	9.732	0.00021	-3.553
94	45.02	0.000	32.964	10.173	0.00020	1.883
95	44.54	0.000	27.674	18.660	0.00282	-1.797
96	53.18	0.108	35.755	13.943	0.00033	3.375
97	48.03	0.359	31.471	16.924	0.00042	-0.724
98	62.58	1.090	41.484	16.928	0.00044	3.078
99	48.78	0.684	31.561	20.295	0.00175	-3.762
100	49.29	0.000	35.882	10.372	0.00020	3.036
Summary Statistics						
Count	100	100	100	100	100	100
Maximum	68.60	3.806	41.484	29.632	0.00496	5.259
Average	49.14	0.429	32.573	16.075	0.00088	0.065
Median	48.83	0.000	32.592	15.368	0.00037	0.257
Minimum	29.81	0.000	21.667	4.674	0.00009	-6.584
Std Dev	7.69	0.765	3.383	5.255	0.00102	2.635

Configuration #1a: Closure cap configuration described in Table and Table of Section 4.3, with sandy soil infilling the erosion barrier. (i.e., composite barrier, lateral drainage and erosion barrier with sandy soil infill)

This page intentionally left blank.

APPENDIX I.
SDF CLOSURE CAP DEGRADED PROPERTY VALUE CALCULATIONS

Closure Cap Area Affected by Pine Tree Root Penetration to Upper Drainage Layer/GCL/HDPE

Mature pine trees on the Saltstone Closure Cap are assumed to each have 4 roots to 6 feet and 1 root to 12 feet. Cap layers at greater than 12 ft depth are assumed to not be affected by pine root intrusion.

The Saltstone Closure Cap surface slopes at 1.5%. The Upper Drainage Layer, GCL, and HDPE slope at 4%. The digression between the cap surface slope and Upper Drainage Layer/GCL/HDPE slopes is:

$$4\% - 1.5\% = 2.5\%$$

So, the Upper Drainage Layer/GCL/HDPE increases in depth at a rate of 2.5%, or 2.5 feet per 100 feet of slope run.

The Upper Drainage Layer top is located a minimum 5 ft below the cap surface at the cap apex. The GCL/HDPE are located a minimum of 6 ft below the cap surface at the cap apex. With a digression rate of 2.5%, the top of the Upper Drainage Layer depth will increase by 7 ft (reach 12 ft beneath the cap surface) at the following distance from the cap apex:

Distance for Upper Drainage Layer to reach 7 ft additional depth = 7 ft/0.025 = 280 ft

The top of the GCL/HDPE will increase by 6 ft (reach 12 ft beneath the cap surface) at the following distance from the cap apex:

Distance for GCL/HDPE to reach 6 ft additional depth = 6 ft/0.025 = 240 ft

Therefore, less than one-half of the HELP-modeled closure cap area can have an Upper Drainage Layer, GCL, or HDPE subject to pine root penetration. However, the HELP model is not designed to assign different properties to any single layer (e.g., assign a root-affected permeability to the topographically upper-280 ft of the Upper Drainage Layer and a non-root affected permeability to the lower-545 ft of the Upper Drainage Layer). So, the Upper Drainage Layer, GCL, and HDPE layers will be conservatively modeled as being at the minimum depth, with each entire layer subject to root contact.

Pine Tree Succession of the Vegetative Cover

The following assumptions associated with pine tree succession discussed in Section 7.2 affect the timing of pine tree succession on the SDF Closure Cap:

- A 100-year institutional control period begins after closure cap installation during which the initial bahia grass vegetative cover is maintained and pine trees are excluded.

- 40 years after the end of institutional control it is conservatively assumed that pine trees will be established over the entire 400-ft, clear-cut buffer area surrounding the cap.
- 80 years after the end of institutional control it is assumed that the establishment of pine seedlings on top of the closure cap will begin. The 40-yr delay is assumed to result due to the 30 ft to 70 ft elevation increase from the surrounding landscape to the cap surface.
- It will take approximately 30 years for the tap roots to reach a 6-foot depth and the remainder of the tree's life (i.e. 70 years) for the root to go its full depth.
- The distance across the cap in the predominant wind direction (southwest to northeast) ranges from about 1,350 to 1,600 ft. It is conservatively assumed the average distance is 1,400 ft. Therefore, it will take approximately 7 cycles of pine seedling to mature pine trees (i.e. approximately 200 ft in each 40-year cycle) to establish mature pine over the entire cap
- 360 years after the end of institutional control it is assumed that the entire cap is dominated by mature loblolly pine.
- Complete turnover of the 400 mature trees per acre occurs every 100 years (i.e. 400 mature trees per acre die every 100 years in a staggered manner).

These pine tree succession assumptions discussed in Section 7.2 result in the following vegetative cover pine tree succession time-line:

Year	Occurrence
0	Construction of SDF Closure Cap
100	End of 100-year institutional control period
140	Pine tree seedlings established along the SDF Closure Cap perimeter
180	Pine tree roots first established on the SDF Closure Cap
210	Pine tree roots first reach 6 ft depth on SDF Closure Cap
220	Mature pine trees established over one-seventh of the SDF Closure Cap.
260	Mature pine trees established over two-sevenths of the SDF Closure Cap
300	Mature pine trees established over three-sevenths of the SDF Closure Cap.
340	Mature pine trees established over four-sevenths of the SDF Closure Cap
380	Mature pine trees established over five-sevenths of the SDF Closure Cap
420	Mature pine trees established over six-sevenths of the SDF Closure Cap
460	Mature pine trees established over the entire SDF Closure Cap
460 to 10,000	Complete turnover of mature trees occurs every 100 years

Along with the above vegetative cover pine tree succession time-line, the assumption that there are 400 mature trees per acre with 4 roots to 6 feet and 1 root to 12 feet as discussed in Section 7.2 impacts the number of pine roots at any one time and the cumulative number of roots produced over time.

Year	Live Mature Pine Trees (#/acre)	Live Mature 6-foot Roots (#/acre)	Cumulative Number of 6-foot Roots Produced (#/acre)	Live Mature 12-foot Roots (#/acre)	Cumulative Number of 12-foot Roots Produced (#/acre)
0	0	0	0	0	0
100	0	0	0	0	0
140	0	0	0	0	0
180	0	0	0	0	0
210	57	229	229	57	57
220	57	229	229	57	57
260	114	457	457	114	114
300	171	686	686	171	171
340	229	914	914	229	229
380	286	1143	1143	286	286
420	343	1371	1371	343	343
460	400	1600	1600	400	400
560	400	1600	3200	400	800
660	400	1600	4800	400	1200
760	400	1600	6400	400	1600
860	400	1600	8000	400	2000
960	400	1600	9600	400	2400
1060	400	1600	11200	400	2800
1160	400	1600	12800	400	3200
1260	400	1600	14400	400	3600
1360	400	1600	16000	400	4000
1460	400	1600	17600	400	4400
1560	400	1600	19200	400	4800
1660	400	1600	20800	400	5200
1760	400	1600	22400	400	5600
1860	400	1600	24000	400	6000
1960	400	1600	25600	400	6400
2060	400	1600	27200	400	6800
2160	400	1600	28800	400	7200
2260	400	1600	30400	400	7600
2360	400	1600	32000	400	8000
2460	400	1600	33600	400	8400
2560	400	1600	35200	400	8800
2660	400	1600	36800	400	9200
2760	400	1600	38400	400	9600
2860	400	1600	40000	400	10000
2960	400	1600	41600	400	10400
3060	400	1600	43200	400	10800
3160	400	1600	44800	400	11200
3260	400	1600	46400	400	11600
3360	400	1600	48000	400	12000
3460	400	1600	49600	400	12400

[1] It is assumed that the tap roots of a 30 year old tree reach a depth of 6 feet.

Year	Live Mature Pine Trees (#/acre)	Live Mature 6-foot Roots (#/acre)	Cumulative Number of 6-foot Roots Produced (#/acre)	Live Mature 12-foot Roots (#/acre)	Cumulative Number of 12-foot Roots Produced (#/acre)
3560	400	1600	51200	400	12800
3660	400	1600	52800	400	13200
3760	400	1600	54400	400	13600
3860	400	1600	56000	400	14000
3960	400	1600	57600	400	14400
4060	400	1600	59200	400	14800
4160	400	1600	60800	400	15200
4260	400	1600	62400	400	15600
4360	400	1600	64000	400	16000
4460	400	1600	65600	400	16400
4560	400	1600	67200	400	16800
4660	400	1600	68800	400	17200
4760	400	1600	70400	400	17600
4860	400	1600	72000	400	18000
4960	400	1600	73600	400	18400
5060	400	1600	75200	400	18800
5160	400	1600	76800	400	19200
5260	400	1600	78400	400	19600
5360	400	1600	80000	400	20000
5460	400	1600	81600	400	20400
5560	400	1600	83200	400	20800
5660	400	1600	84800	400	21200
5760	400	1600	86400	400	21600
5860	400	1600	88000	400	22000
5960	400	1600	89600	400	22400
6060	400	1600	91200	400	22800
6160	400	1600	92800	400	23200
6260	400	1600	94400	400	23600
6360	400	1600	96000	400	24000
6460	400	1600	97600	400	24400
6560	400	1600	99200	400	24800
6660	400	1600	100800	400	25200
6760	400	1600	102400	400	25600
6860	400	1600	104000	400	26000
6960	400	1600	105600	400	26400
7060	400	1600	107200	400	26800
7160	400	1600	108800	400	27200

Year	Live Mature Pine Trees (#/acre)	Live Mature 6-foot Roots (#/acre)	Cumulative Number of 6-foot Roots Produced (#/acre)	Live Mature 12-foot Roots (#/acre)	Cumulative Number of 12-foot Roots Produced (#/acre)
7260	400	1600	110400	400	27600
7360	400	1600	112000	400	28000
7460	400	1600	113600	400	28400
7560	400	1600	115200	400	28800
7660	400	1600	116800	400	29200
7760	400	1600	118400	400	29600
7860	400	1600	120000	400	30000
7960	400	1600	121600	400	30400
8060	400	1600	123200	400	30800
8160	400	1600	124800	400	31200
8260	400	1600	126400	400	31600
8360	400	1600	128000	400	32000
8460	400	1600	129600	400	32400
8560	400	1600	131200	400	32800
8660	400	1600	132800	400	33200
8760	400	1600	134400	400	33600
8860	400	1600	136000	400	34000
8960	400	1600	137600	400	34400
9060	400	1600	139200	400	34800
9160	400	1600	140800	400	35200
9260	400	1600	142400	400	35600
9360	400	1600	144000	400	36000
9460	400	1600	145600	400	36400
9560	400	1600	147200	400	36800
9660	400	1600	148800	400	37200
9760	400	1600	150400	400	37600
9860	400	1600	152000	400	38000
9960	400	1600	153600	400	38400
10060	400	1600	155200	400	38800

Erosion of the Soil above the Erosion Barrier

For the institutional control to pine forest land use scenario, it is assumed that the closure cap will be vegetated with bahia grass during the institutional control period (see Sections 4.4.12 and 7.2), with a combination of bahia and pine trees for a period immediately following the institutional control period, and with a pine forest thereafter. The projected erosion rate for both the topsoil and upper backfill layers has been determined utilizing the Universal Soil Loss Equation (Goldman et al. 1986). The Universal Soil Loss Equation is expressed as:

$A = R \times K \times LS \times C \times P$, where A = soil loss (tons/acre/year); R = rainfall erosion index (100 ft·ton/acre per in/hr); K = soil erodability factor, tons/acre per unit of R; LS = slope length and steepness factor, dimensionless; C = vegetative cover factor, dimensionless; P = erosion control practice factor, dimensionless

The following are estimated parameter values based upon Goldman et al. 1986 and Horton and Wilhite 1978:

- From Figure 5.2 of Goldman et al. (1986), R is seen to be slightly greater than 250 but significantly less than 300 100 ft·ton/acre per in/hr for the SRS location. Horton and Wilhite (1978) utilized an R value of 260 100 ft·ton/acre per in/hr for previous SRS Burial Grounds erosion estimates. Therefore an R value of 260 100 ft·ton/acre per in/hr will be utilized.
- As outlined in Section 5.4.1, typical SRS topsoil would generally be classified as silty sand (SM) materials under the Unified Soil Classification System (USCS) or as loamy sand (LS) or sandy loam (SL) in the United States Department of Agriculture (USDA) soil textural classification (i.e., textural triangle). If it is assumed that the topsoil is a sandy loam that consists of 70% sand, 25% silt, and 5% clay, the K is seen to equal approximately 0.28 tons/acre per unit of R from Figure 5.6 of Goldman et al. (1986).
- As outlined in Section 5.4.2, typical SRS control compacted backfill would generally be classified as clayey sand (SC) materials under USCS or as sandy clay loam (SCL) in the USDA soil textural classification (i.e. textural triangle). If it is assumed that the backfill is a sandy clay loam that consists of 50% sand, 30% clay, and 20% silt, the K is seen to equal approximately 0.20 tons/acre per unit of R from Figure 5.6 of Goldman et al. (1986).
- For a slope length of 825 feet and a slope of 1.5% (see Section 4.2) the LS value from Table 5.5 of Goldman et al. (1986) must be interpolated. Table 5.5 lists an LS value of 0.19 for a slope length of 800 to 900 ft, with a 1% slope. It lists values of 0.37 and 0.39 for 800 ft and 900 ft slope lengths, respectively, for a 2% slope. The interpolated LS value for an 825 ft long, 2% slope is: ((0.39 – 0.37) x (825-800)/(900-800)) + 0.37 = 0.38. The LS value for an 825 ft long, 1.5% slope is then (0.19 + 0.38)/2 = 0.29.
- For a bahia grass vegetative cover, the C factor will be taken as that of a meadow at 0.004 (Horton and Wilhite 1978).
- For a pine forest, the C factor will be taken as that of a natural successional forest at 0.001 (Horton and Wilhite 1978).
- No supporting practices are associated with the closure cap therefore P equals 1.

Based upon the Universal Soil Loss Equation and the parameter values listed above the following are the estimated soil losses:

- Topsoil with a bahia grass vegetative cover has an estimated soil loss of 0.084 tons/acre/year ($A = 260 \times 0.28 \times 0.29 \times 0.004 \times 1$).
- Topsoil with a pine forest has an estimated soil loss of 0.021 tons/acre/year ($A = 260 \times 0.28 \times 0.29 \times 0.001 \times 1$).
- Backfill with a bahia grass vegetative cover has an estimated soil loss of 0.060 tons/acre/year ($A = 260 \times 0.20 \times 0.29 \times 0.004 \times 1$).
- Backfill with a pine forest has an estimated soil loss of 0.015 tons/acre/year ($A = 260 \times 0.20 \times 0.29 \times 0.001 \times 1$).

Based upon the dry bulk density the estimated soil loss can be converted to a loss in terms of depth of loss per year. Yu et al. (1993) provides the following information, from which the average dry bulk density (i.e. approximately 1.67 g/cm^3 or 104 lbs/ft^3) of the two SRS topsoil samples tested can be determined:

Parameter	Top Soil – 1 [1]	Top Soil – 2 [2]
Sample length (cm)	7.59	7.59
Sample area (cm^2)	11.76	11.76
Sample dry weight (g)	148.81	149.75
Sample dry bulk density (g/cm^3)	1.667	1.678

[1] Yu et al. (1993) page 2-72
[2] Yu et al. (1993) page 2-84

Phifer et al. (2006) Table 5-18 provides a dry bulk density value of 1.71 g/cm^3 or 107 lbs/ft^3 for control compacted backfill. Based upon these dry bulk densities the estimated soil loss calculated above was converted to a depth of loss per year as follows:

- Topsoil with a bahia grass vegetative cover has an estimated depth of soil loss of approximately 4.5E-04 inches/year
$$(Loss = \frac{0.084 \, tons / acre / year \times 2000 \, lbs / ton \times 12 \, inches / foot}{43560 \, ft^2 / acre \times 104 \, lbs / ft^3}$$
- Topsoil with a pine forest has an estimated depth of soil loss of approximately 1.1E-04 inches/year ($Loss = \dfrac{0.021 \, tons / acre / year \times 2000 \, lbs / ton \times 12 \, inches / foot}{43560 \, ft^2 / acre \times 104 \, lbs / ft^3}$
- Backfill with a bahia grass vegetative cover has an estimated depth of soil loss of approximately 3.1E-04 inches/year
$$(Loss = \frac{0.060 \, tons / acre / year \times 2000 \, lbs / ton \times 12 \, inches / foot}{43560 \, ft^2 / acre \times 107 \, lbs / ft^3}$$
- Backfill with a pine forest has an estimated depth of soil loss of approximately 7.7E-05 inches/year ($Loss = \dfrac{0.015 \, tons / acre / year \times 2000 \, lbs / ton \times 12 \, inches / foot}{43560 \, ft^2 / acre \times 107 \, lbs / ft^3}$

The following provides a summary of the estimated topsoil and upper backfill soil losses due to erosion for both bahia grass and pine forest vegetative cover:

Soil-Vegetation Condition	Estimated Soil Loss (tons/acre/year)	Estimated Soil Loss (inches/year)
Topsoil with a bahia grass vegetative cover	0.084	4.5E-04
Topsoil with a pine forest	0.021	1.1E-04
Backfill with a bahia grass vegetative cover	0.060	3.1E-04
Backfill with a pine forest	0.015	7.7E-05

In order to maximize the erosion rate utilized the bahia erosion rate, which is higher, will be used until it is assumed that mature pine trees cover the entire closure cap at year 460.

Topsoil Thickness over Time Calculation:

Year	Thickness
0	6" – (0 years × 4.5E-04 inches/year) = 6"
100	6" – (100 years × 4.5E-04 inches/year) = 5.96"
180	6" – (180 years × 4.5E-04 inches/year) = 5.92"
220	6" – (220 years × 4.5E-04 inches/year) = 5.90"
300	6" – (300 years × 4.5E-04 inches/year) = 5.87"
380	6" – (380 years × 4.5E-04 inches/year) = 5.83"
460	6" – (460 years × 4.5E-04 inches/year) = 5.79"
560	5.79" – [(560 years – 460 years) × 1.1E-04 inches/year)] = 5.78"
1,000	5.79" – [(1,000 years – 460 years) × 1.1E-04 inches/year)] = 5.73"
1,800	5.79" – [(1,800 years – 460 years) × 1.1E-04 inches/year)] = 5.64"
3,200	5.79" – [(3,200 years – 460 years) × 1.1E-04 inches/year)] = 5.49"
5,412	5.79" – [(5,412 years – 460 years) × 1.1E-04 inches/year)] = 5.25"
5,600	5.79" – [(5,600 years – 460 years) × 1.1E-04 inches/year)] = 5.23"
10,000	5.79" – [(10,000 years – 460 years) × 1.1E-04 inches/year)] = 4.74"

Since the topsoil does not completely erode away within the 10,000 years of interest, no reduction in the upper backfill layer occurs.

Silting-in of the Upper Lateral Drainage Layer

As outlined in Section 7.5.1 silting-in of the upper lateral drainage layer will be evaluated as follows:

- Over time colloidal clay migrates with the water flux from the overlying middle backfill to the underlying 1-foot-thick upper lateral drainage layer at a concentration of 63 mg of colloidal clay per liter of water flux.
- This water-flux driven clay accumulates in the lower drainage layer from the bottom up. The hydraulic conductivity of the clay-filled drainage layer is reduced from 5.0E-02 cm/s to that of the overlying backfill, 4.1E-05 cm/s. The hydraulic conductivity of the upper, non-clay-filled drainage layer remains at 5.0E-02 cm/s. The thickness of the clay-filled portion increases with time, while the thickness of the non-filled portion decreases with time, resulting in an overall decrease in hydraulic conductivity for the lower drainage layer.
- Hydraulic conductivity and other parameters for the middle backfill are assumed to not change.

The following are the intact hydraulic properties of the middle backfill and upper lateral drainage layer:

Hydraulic Parameter	Middle Backfill	Upper Lateral Drainage Layer
K_{sat} (cm/s)	4.1E-05	5.0E-02
η	0.35	0.417
FC	0.252	0.045
WP	0.181	0.018

Determine clay mass to fill upper lateral drainage layer void volume (0.417) on cu ft basis:
- Assume clay bulk density is 1.1 g/cm^3 (Hillel 1982).
- For a 1-ft^2 area of a 1-ft thick drainage layer: Void Volume = 0.417 x 1 ft^3 = 0.417 ft^3
- Convert 0.417 ft^3 to cm^3: 0.417 ft^3 x 28316.85 cm^3/ft^3 = 11,808.1 cm^3
- Clay mass per ft^3 = 1.1 g/cm^3 x 11,808.1 cm^3 = 12,988.9 g

Determine the flux of water into the upper lateral drainage layer from the following results of the HELP model run for the initial configuration conditions (see Section 5.6):
- Precipitation = 49.14 in/yr
- Runoff = 0.334 in/yr
- Evapotranspiration = 32.569 in/yr
- Flux of water into lateral drainage layer = Precipitation – (Runoff + Evapotranspiration)
- Flux of water into lateral drainage layer = 49.14 in/yr – (0.334 in/yr + 32.569 in/yr)
- Flux of water into lateral drainage layer = 16.237 in/yr

This is the flux of water based on the initial cap conditions. Previous HELP modeling for SDF indicates this value is very close to that based on the 10,000-year degraded cap conditions (accounting for top soil erosion, erosion barrier changes, and changes to the upper GCL and lower drainage layer; Phifer and Nelson 2003). The values are sufficiently close that the initial value can be used.

Determine the yearly clay migration into the upper lateral drainage layer:
- Flux of water into lateral drainage layer = 16.237 in/yr
- Colloidal clay concentration = 63 mg/L
- Flux through a 1 ft^2 area = 16.237 in/yr × ft/12 in × 1 ft^2
- Flux through a 1 ft^2 area = 1.35 ft^3/yr
- Clay flux = 1.35 ft^3/yr × 63 mg/L × 2.831685E-02 m^3/ft^3 × 1000 L/m^3
- Clay flux = 2,408 mg/yr = 2.4 g/yr

Determine the time it takes the 12,988.9 g of clay to migrate from the middle backfill to the lateral drainage layer:
- Time = 12,988.9 g ÷ 2.4 g/yr
- Time = 5,412 yr

Determine total flux of water into the upper lateral drainage layer (on square-ft basis) required to fill the void space with clay:
- Assume water flux contains 63 mg/L colloidal clay.
- Volume of water = (12,988.9 g x 1,000 mg/g)/(63 mg/L x 28.31685 L/ft^3) = 7,280.9 ft^3

Determine upper lateral drainage layer hydraulic property variation with time assuming silting-in results in water-flux driven clay accumulation in the lower drainage layer from the bottom up:
- It will be assumed that water-flux driven clay accumulates in the upper lateral drainage layer from the bottom up, filling the void space of the drainage layer with clay at a density of 1.1 g/cm^3 (Hillel 1982). The hydraulic conductivity of the clay-filled drainage layer is reduced from 5.0E-02 cm/s to that of the overlying backfill, 4.1E-05 cm/s. The hydraulic conductivity of the upper, non-clay-filled drainage layer remains at 5.0E-02 cm/s. The thickness of the clay-filled portion increases with time, while the thickness of the non-filled portion decreases with time, resulting in an overall decrease in hydraulic conductivity for the lower drainage layer until the upper lateral drainage layer is completely infilled at year 5,412.
- The following are the initial hydraulic properties of the middle backfill and lateral drainage layer:

Hydraulic Parameter	Initial Middle Backfill	Initial Lateral Drainage Layer
K_{sat} (cm/s)	4.1E-05	5.0E-02
η	0.35	0.417
FC	0.252	0.045
WP	0.181	0.018

Determine fraction change for each year:

Year	Fraction
0	$0 \div 5{,}412 = 0$
100	$100 \div 5{,}412 = 0.018$
180	$180 \div 5{,}412 = 0.033$
220	$220 \div 5{,}412 = 0.041$
300	$300 \div 5{,}412 = 0.055$
380	$380 \div 5{,}412 = 0.070$
460	$460 \div 5{,}412 = 0.085$
560	$560 \div 5{,}412 = 0.103$
1,000	$1000 \div 5{,}412 = 0.185$
1,800	$1800 \div 5{,}412 = 0.333$
3,200	$3{,}200 \div 5{,}412 = 0.591$
5,412	1.0
5,600	1.0
10,000	1.0

Determine the porosity of the clay-filled portion of the upper drainage layer:

Porosity of the clay:

Assumed clay bulk density, $\rho_b = 1.1$ g/cm^2
Assumed clay particle density, $\rho_p = 2.6$ g/cm^2

Resulting clay porosity, $n = 1 - \rho_b/\rho_p = 1 - (1.1 \text{ g/cm}^2/2.6 \text{ g/cm}^2) = 0.58$

Porosity of the clay-filled portion of the upper drainage layer = porosity of clean portion x porosity of clay
Porosity (n) of the clay filled portion = 0.417 x 0.58 = 0.24

Determine the field capacity and wilting point of the clay-filled portion of the upper drainage layer:

Will assume that the field capacity and wilting point of the clay-filled portion have the same ratio versus its porosity of 0.24 as the equivalent ratio for kaolin clay.

From WSRC (2002) the following kaolin properties are found: n = 0.56; FC = 0.55; WP = 0.50

FC = 0.24 x (0.55/0.56) ≈ 0.24, however since in the HELP model, FC cannot be the same value as n, a value of 0.236 will be used for FC

WP = 0.24 x (0.50/0.56) ≈ 0.21

Determine the equivalent horizontal hydraulic conductivity of the upper lateral drainage layer over time:

The equivalent horizontal hydraulic conductivity for horizontal flow in a series of horizontal layers with different saturated hydraulic conductivities can be determined from the following equation from Phifer and Nelson (2003), after Freeze and Cherry (1979):

$K_h = (K_{filled} \times F) + (K_{clean} \times (1-F))$, where F is the fraction of the upper drainage layer filled

Year	Equivalent Upper Drainage Layer K_h (cm/sec)
0	0.05
100	(0.000041 x 0.018) + (0.05 x (1 - 0.018)) = 0.0491
180	(0.000041 x 0.033) + (0.05 x (1 - 0.033)) = 0.0484
220	(0.000041 x 0.041) + (0.05 x (1 - 0.041)) = 0.0480
300	(0.000041 x 0.055) + (0.05 x (1 - 0.055)) = 0.0473
380	(0.000041 x 0.070) + (0.05 x (1 - 0.070)) = 0.0465
460	(0.000041 x 0.085) + (0.05 x (1 - 0.085)) = 0.0458
560	(0.000041 x 0.103) + (0.05 x (1 - 0.103)) = 0.0449
1,000	(0.000041 x 0.185) + (0.05 x (1 - 0.185)) = 0.0408
1,800	(0.000041 x 0.333) + (0.05 x (1 - 0.333)) = 0.0334
3,200	(0.000041 x 0.591) + (0.05 x (1 - 0.591)) = 0.0205
5,412	(0.000041 x 1.0) + (0.05 x (1 - 1.0)) = 0.000041
5,600	(0.000041 x 1.0) + (0.05 x (1 - 1.0)) = 0.000041
10,000	(0.000041 x 1.0) + (0.05 x (1 - 1.0)) = 0.000041

Determine the equivalent n, FC, and WP of the upper drainage layer over time:
In an analogous manner to that for K, the equivalent n, FC, and WP can be determined based upon the fraction filled as follows:

$n = (n_{filled} \times F) + (n_{clean} \times (1 - F))$

$FC = (FC_{filled} \times F) + (FC_{clean} \times (1 - F))$

$WP = (WP_{filled} \times F) + (WP_{clean} \times (1 - F))$

Year	Equivalent Upper Drainage Layer Porosity (n)
0	(0.24 x 0) + (0.417 x (1 - 0)) = 0.417
100	(0.24 x 0.018) + (0.417 x (1 - 0.018)) = 0.414
180	(0.24 x 0.033) + (0.417 x (1 - 0.033)) = 0.411
220	(0.24 x 0.041) + (0.417 x (1 - 0.041)) = 0.410
300	(0.24 x 0.055) + (0.417 x (1 - 0.055)) = 0.407
380	(0.24 x 0.070) + (0.417 x (1 - 0.070)) = 0.405
460	(0.24 x 0.085) + (0.417 x (1 - 0.085)) = 0.402
560	(0.24 x 0.103) + (0.417 x (1 - 0.103)) = 0.399
1,000	(0.24 x 0.185) + (0.417 x (1 - 0.185)) = 0.384
1,800	(0.24 x 0.333) + (0.417 x (1 - 0.333)) = 0.358
3,200	(0.24 x 0.591) + (0.417 x (1 - 0.591)) = 0.312
5,412	(0.24 x 1.0) + (0.417 x (1 - 1.0)) = 0.24
5,600	(0.24 x 1.0) + (0.417 x (1 - 1.0)) = 0.24
10,000	(0.24 x 1.0) + (0.417 x (1 - 1.0)) = 0.24

Year	Equivalent Upper Drainage Layer FC
0	(0.236 x 0) + (0.045 x (1 - 0)) = 0.045
100	(0.236 x 0.018) + (0.045 x (1 - 0.018)) = 0.0484
180	(0.236 x 0.033) + (0.045 x (1 - 0.033)) = 0.0513
220	(0.236 x 0.041) + (0.045 x (1 - 0.041)) = 0.0528
300	(0.236 x 0.055) + (0.045 x (1 - 0.055)) = 0.0555
380	(0.236 x 0.070) + (0.045 x (1 - 0.070)) = 0.0584
460	(0.236 x 0.085) + (0.045 x (1 - 0.085)) = 0.0612
560	(0.236 x 0.103) + (0.045 x (1 - 0.103)) = 0.0647
1,000	(0.236 x 0.185) + (0.045 x (1 - 0.185)) = 0.0803
1,800	(0.236 x 0.333) + (0.045 x (1 - 0.333)) = 0.1086
3,200	(0.236 x 0.591) + (0.045 x (1 - 0.591)) = 0.1579
5,412	(0.236 x 1.0) + (0.045 x (1 - 1.0)) = 0.236
5,600	(0.236 x 1.0) + (0.045 x (1 - 1.0)) = 0.236
10,000	(0.236 x 1.0) + (0.045 x (1 - 1.0)) = 0.236

Year	Equivalent Upper Drainage Layer WP
0	(0.21 x 0) + (0.018 x (1 - 0)) = 0.018
100	(0.21 x 0.018) + (0.018 x (1 - 0.018)) = 0.0215
180	(0.21 x 0.033) + (0.018 x (1 - 0.033)) = 0.0243
220	(0.21 x 0.041) + (0.018 x (1 - 0.041)) = 0.0259
300	(0.21 x 0.055) + (0.018 x (1 - 0.055)) = 0.0286
380	(0.21 x 0.070) + (0.018 x (1 - 0.070)) = 0.0314
460	(0.21 x 0.085) + (0.018 x (1 - 0.085)) = 0.0343
560	(0.21 x 0.103) + (0.018 x (1 - 0.103)) = 0.0378
1,000	(0.21 x 0.185) + (0.018 x (1 - 0.185)) = 0.0535
1,800	(0.21 x 0.333) + (0.018 x (1 - 0.333)) = 0.0819
3,200	(0.21 x 0.591) + (0.018 x (1 - 0.591)) = 0.1315
5,412	(0.21 x 1.0) + (0.018 x (1 - 1.0)) = 0.21
5,600	(0.21 x 1.0) + (0.018 x (1 - 1.0)) = 0.21
10,000	(0.21 x 1.0) + (0.018 x (1 - 1.0)) = 0.21

Summary Upper Lateral Drainage Layer Hydraulic Properties with Time:

Year	Equivalent K_h (cm/sec)	Porosity (n)	FC	WP
0	5.00E-02	0.417	0.045	0.018
100	4.91E-02	0.414	0.0484	0.0215
180	4.84E-02	0.411	0.0513	0.0243
220	4.80E-02	0.410	0.0528	0.0259
300	4.73E-02	0.407	0.0555	0.0286
380	4.65E-02	0.405	0.0584	0.0314
460	4.58E-02	0.402	0.0612	0.0343
560	4.49E-02	0.399	0.0647	0.0378
1,000	4.08E-02	0.384	0.0803	0.0535
1,800	3.34E-02	0.358	0.1086	0.0819
3,200	2.05E-02	0.312	0.1579	0.1315
5,412	4.10E-05	0.240	0.236	0.210
5,600	4.10E-05	0.240	0.236	0.210
10,000	4.10E-05	0.240	0.236	0.210

Root Penetration of the Upper Lateral Drainage Layer

For the institutional control to pine forest land use scenario, it is assumed that the closure cap will be vegetated with bahia grass during the institutional control period (see Sections 4.4.12 and 7.2), with a combination of bahia and pine trees for a period immediately following the institutional control period, and with a pine forest thereafter. From the calculations above, it is assumed that mature pine trees will be established over one-seventh of the SDF Closure Cap by year 220; over two-sevenths of the cap by year 260; over three-sevenths of the cap by year 300, over four-sevenths of the cap by year 340, over five-sevenths of the cap by year 380, over six-sevenths of the cap by year 420, and over the entire cap by year 460. As discussed in Section 7.5.2, roots will represent an impermeable volume within the lateral drainage layer prior to their decomposition.

From Section 7.2, the following assumptions were made relative to the establishment of a pine forest on the closure cap that results in root penetration through the lateral drainage layer and a subsequent impermeable volume in the layer due to roots:

- The closure cap will eventually be covered with approximately 400 mature trees per acre.
- Each mature tree will have 4 roots to 6 feet and 1 root to 12 feet. The roots are 3 inches in diameter at a depth of 1 foot and 0.25 inches in diameter at either 6 or 12 feet, whichever is applicable.
- Deep roots will be maintained and enlarge with yearly growth over the life of the tree.
- Trees are expected to die at approximately 100 years, and it is anticipated that decomposition of deep roots will occur over a 30 year period.
- Prior to decomposition the roots represent an impermeable volume within the lateral drainage layer

The following two impermeable root volume cases will be considered:

- No erosion (in which case the lateral drainage layer will be located 5 to 6 feet below the ground surface)
- All material above the erosion barrier eroded away (in which case the lateral drainage layer will be located 2 to 3 feet below the ground surface)

General calculations applicable to both cases:

Maximum number of trees/acre with deep roots:
Considering both live and dead trees prior to decomposition of roots
Number = 400 live trees/acre + [(30 yrs/100 yrs) × 400 dead trees/acre]
Number = 520 trees/acre with deep roots

Taper of 6' root per foot:
3" diameter at 1' depth and 0.25" at 6'
$(3"-0.25")/(6'-1') = 0.55"/ft$

Taper of 12' root per foot:
3" diameter at 1' depth and 0.25" at 12'

$(3''-0.25'')/(12'-1') = 0.25''/ft$

No erosion case volume calculation:

Root Diameter for 6' roots at 5':
  Diameter = 0.25" + [(6' − 5') × 0.55"/ft] = 0.80"
Area of 6' roots at 5':
  Area = ¼πD^2 = ¼π(0.80")^2 = 0.50 in^2
Root Diameter for 6' roots at 6':
  Diameter = 0.25" + [(6' − 6') × 0.55"/ft] = 0.25"
Area of for 6' roots at 6':
  Area = ¼πD^2 = ¼π(0.25")^2 = 0.05 in^2
Average Area of 6' roots between 5' and 6':
  Average Area = (0.50 in^2 + 0.05 in^2)/2 = 0.28 in^2
Volume of 6' roots between 5' and 6' within the lateral drainage layer:
  Volume = (0.28 in^2/144 in^2/ft^2) × 1 ft = 1.94E-03 ft^3
Volume of 6' roots between 5' and 6'/acre within the lateral drainage layer:
  Volume = 520 trees/acre × 4-6' roots/tree × 1.94E-03 ft^3/6' root
  Volume = 4.04 ft^3/acre

Root Diameter for 12' roots at 5':
  Diameter = 0.25" + [(12' − 5') × 0.25"/ft] = 2.0"
Area of 12' roots at 5':
  Area = ¼πD^2 = ¼π(2.0")^2 = 3.14 in^2
Root Diameter for 12' roots at 6':
  Diameter = 0.25" + [(12' − 6') × 0.25"/ft] = 1.75"
Area of for 12' roots at 6':
  Area = ¼πD^2 = ¼π(1.75")^2 = 2.41 in^2
Average Area of 12' roots between 5' and 6':
  Average Area = (3.14 in^2 + 2.41 in^2)/2 = 2.78 in^2
Volume of 12' roots between 5' and 6' within the lateral drainage layer:
  Volume = (2.78 in^2/144 in^2/ft^2) × 1 ft = 1.93E-02 ft^3
Volume of 12' roots between 5' and 6'/acre within the lateral drainage layer:
  Volume = 520 trees/acre × 1-12' root/tree × 1.93E-02 ft^3/12' root
  Volume = 10.04 ft^3/acre

Total Volume of impermeable roots in the lateral drainage layer:
  Total Volume = 4.04 ft^3/acre + 10.04 ft^3/acre = 14.08 ft^3/acre

Volume of lateral drainage layer per acre:
  Volume = 43560 ft^2/acre × 1-foot thick lateral drainage layer
  Volume = 43560 ft^3/acre

Volume percent of lateral drainage layer occupied by impermeable roots:
  Volume percent = (14.08 ft^3/acre / 43560 ft^3/acre) × 100 = 0.032%

All material above the erosion barrier eroded away case volume calculation:

Root Diameter for 6' roots at 2':
    Diameter = 0.25" + [(6' − 2') × 0.55"/ft] = 2.45"
Area of for 6' roots at 2':
    Area = ¼πD^2 = ¼π(2.45")^2 = 4.71 in^2
Root Diameter for 6' roots at 3':
    Diameter = 0.25" + [(6' − 3') × 0.55"/ft] = 1.90"
Area of for 6' roots at 3':
    Area = ¼πD^2 = ¼π(1.90")^2 = 2.84 in^2
Average Area of 6' roots between 2' and 3':
    Average Area = (4.71 in^2 + 2.84 in^2)/2 = 3.78 in^2
Volume of 6' roots between 2' and 3' within the lateral drainage layer:
    Volume = (3.78 in^2/144 in^2/ft^2) × 1 ft = 2.63E-02 ft^3
Volume of 6' roots between 2' and 3'/acre within the lateral drainage layer:
    Volume = 520 trees/acre × 4-6' roots/tree × 2.63E-02 ft^3/6' root
    Volume = 54.70 ft^3/acre

Root Diameter for 12' roots at 2':
    Diameter = 0.25" + [(12' − 2') × 0.25"/ft] = 2.75"
Area of for 12' roots at 2':
    Area = ¼πD^2 = ¼π(2.75")^2 = 5.94 in^2
Root Diameter for 12' roots at 3':
    Diameter = 0.25" + [(12' − 3') × 0.25"/ft] = 2.50"
Area of for 12' roots at 3':
    Area = ¼πD^2 = ¼π(2.50")^2 = 4.91 in^2
Average Area of 12' roots between 2' and 3':
    Average Area = (5.94 in^2 + 4.91 in^2)/2 = 5.43 in^2
Volume of 12' roots between 2' and 3' within the lateral drainage layer:
    Volume = (5.43 in^2/144 in^2/ft^2) × 1 ft = 3.77E-02 ft^3
Volume of 12' roots between 5' and 6'/acre within the lateral drainage layer:
    Volume = 520 trees/acre × 1-6' root/tree × 3.77E-02 ft^3/12' root
    Volume = 19.60 ft^3/acre

Total Volume of impermeable roots in the lateral drainage layer:
    Total Volume = 54.70 ft^3/acre + 19.60 ft^3/acre = 74.30 ft^3/acre

Volume of lateral drainage layer per acre:
    Volume = 43560 ft^2/acre × 1-foot thick lateral drainage layer
    Volume = 43560 ft^3/acre

Volume percent of lateral drainage layer occupied by impermeable roots:
    Volume percent = (74.30 ft^3/acre / 43560 ft^3/acre) × 100 = 0.17%

Based upon the above calculations the roots within the lateral drainage layer will represent an impermeable volume at any time that ranges from 0.032 to 0.17 percent, depending upon the extent of erosion above the erosion barrier. In order to compensate for the presence of the roots within the lateral drainage layer the saturated hydraulic conductivity of the layer will be reduced by multiplying by 0.998 once the pine forest has been established on the closure cap. The conductivity will be reduced at year 300 when three-sevenths of the SDF Closure Cap is anticipated to be covered in mature pine trees. This factor is based upon the worse case percent volume of roots in the layer (i.e. approximately 0.2 percent).

Antioxidant Depletion, Thermal Oxidation, and Tensile Stress Cracking of the HDPE

HDPE Geomembrane Antioxidant Depletion

Antioxidant time of depletion for the HDPE within the SDF Closure Cap has been estimated utilizing the methodology of Mueller and Jakob (2003). They utilized the van't Hoff rule for the temperature dependence of antioxidant depletion time and their measured antioxidant depletion time of 5 years for HDPE geomembranes immersed in 80°C de-ionized water.

van't Hoff rule:

$$t_1(T) = t_1(T') \, e^{\frac{E_a}{R}\left[\frac{1}{T} - \frac{1}{T'}\right]}$$, where $t_1(T)$ = antioxidant depletion period in years at the ambient temperature of the HDPE; $t_1(T')$ = antioxidant depletion period in years at test temperature of 80°C (i.e. 5 years); E_a = depletion process activation energy; R = universal gas constant (8.319 J/mol K); T = ambient temperature of the HDPE in K (K = 273.15 + °C); T' = test temperature in K = 273.15 + 80°C = 353.15

van't Hoff rule with substitution of 5 year time of depletion in 80°C de-ionized water:

$$t_1(T) = 5 \; yrs \; e^{\frac{E_a}{8.319 \, J/mol \, K}\left[\frac{1}{T} - \frac{1}{353.15 \, K}\right]}$$, where $t_1(T)$ = antioxidant depletion period in years at the ambient temperature of the HDPE; E_a = depletion process activation energy; T = ambient temperature of the HDPE in K (K = 273.15 + °C)

As outlined in Section 7.6.2.4, Needham et al. (2004) concluded that, "Values of activation energy of 60-75 kJ/mol appear a reasonable, conservative estimate." Therefore for determination of a conservative antioxidant time of depletion for a HDPE geomembrane within the SDF Closure Cap, an activation energy of 60 kJ/mol will be utilized. This results in the following equation:

$$t_1(T) = 5 \; yrs \; e^{\frac{60,000 \, J/mol}{8.319 \, J/mol \, K}\left[\frac{1}{T} - \frac{1}{353.15 \, K}\right]}$$, where $t_1(T)$ = antioxidant depletion period in years at the ambient temperature of the HDPE; T = ambient temperature of the HDPE in K (K = 273.15 + °C)

Sappington et al. (2005) determined the subsurface temperatures within a well (DIW-1-2) screened within a shallow water table aquifer (approximately 10 feet to the water table surface) at SRS. The average monthly temperature measurements taken by Sappington et al. (2005) during 2002, 2003, and 2004 are provided below along with the yearly average (21.64°C) and median (21.03 °C). These subsurface temperatures are considered representative of that that the SDF Closure Cap HDPE geomembrane will experience since it is located at a comparable shallow depth of 6 feet below ground surface (see Table). Therefore the antioxidant depletion period for the SDF Closure Cap HDPE geomembrane has been estimated based upon an average subsurface temperature of approximately 22 °C.

Month	DIW-1-2 Average Monthly Temperature (°C)
January	19.52
February	19.40
March	17.54
April	19.46
May	21.20
June	20.79
July	24.43
August	25.26
September	24.92
October	23.56
November	22.70
December	20.87
Average	21.64
Median	21.03

As seen in the calculation below antioxidant depletion is anticipated to occur in the SDF Closure Cap HDPE geomembrane in 275 years after burial.

$$K = 273.15 + {}^{o}C$$
$$K = 273.15 + 22\,{}^{o}C$$
$$K = 295.15$$

$$t_1(T) = 5\ yrs\ e^{\frac{60,000\ J/mol}{8.319\ J/mol\ K}\left[\frac{1}{T}-\frac{1}{353.15\ K}\right]},$$ where $t_1(T)$ = antioxidant depletion period in years at the ambient temperature of the HDPE; T = ambient temperature of the HDPE in K (K = 295.15)

$$t_1(T) = 5\ yrs\ e^{\frac{60,000\ J/mol}{8.319\ J/mol\ K}\left[\frac{1}{295.15}-\frac{1}{353.15\ K}\right]}$$
$$t_1(T) = 5\ yrs\ e^{4.01}$$
$$t_1(T) = 276.66\ yrs \approx 275\ yrs$$

Needham et al. (2004) Model of HDPE Geomembrane Hole Generation due to Antioxidant Depletion, Thermal Oxidation, and Tensile Stress Cracking

It is assumed that the HDPE geomembrane will degrade over time consistent with the "fair" case degradation outlined by Needham et al. (2004). HDPE degradation results in holes in the HDPE, while the intact portion of the HDPE is assumed to maintain it initial effective hydraulic conductivity of 2.0E-13 cm/s (see Section 5.4.5).

Estimation of Duration of Different Stages of Defect Generation in the SDF Closure Cap HDPE geomembrane based upon the Methodology of Needham et al. (2004):

Stage	Duration (years)	Cumulative (years)	Comments - Assumptions
1	0	0	SDF Closure Cap construction
2	0	0	No operations anticipated on the SDF Closure Cap after construction; only monitoring and maintenance activities anticipated
3	10	10	No hole generation during this stage; minimum recommended period (Needham et al., 2004)
4	285	295	Oxidation estimated to commence after 275 year antioxidant depletion period plus 20 year induction period (i.e. 295 years) after construction
5	50	345	Period of further stress cracking during oxidation; recommended period (Needham et al., 2004)
6	9,655	10,000	Continuing deterioration through 10,000 years

Estimation of Hole Type and Size per Stage of Defect Generation in the SDF Closure Cap HDPE geomembrane based upon the Methodology of Needham et al. (2004):

Hole Type	Individual Hole Size (mm^2)	Stage					
		1 [1]		2 [2]		3	
		# of holes	holes size	# of holes	holes size	# of holes	holes size
pinholes	2.5	20	50	0	0	0	0
holes	50	10	500	0	0	0	0
tears	5000	0	0	0	0	0	0
small cracks	10	0	0	0	0	0	0
large cracks	1000	0	0	0	0	0	0
total (# of holes/stage)		30	total	0	total	0	-
total (mm^2/hectare)		550	total	0	total	0	

Hole Type	Individual Hole Size (mm^2)	Stage					
		4		5		6 [3]	
		# of holes	holes size	# of holes	holes size	# of holes	holes size
pinholes	2.5	0	0	0	0	20	50
holes	50	0	0	0	0	10	500
tears	5000	0	0	0	0	0	0
small cracks	10	75	750	100	1000	175	1750
large cracks	1000	35	35000	50	50000	85	85000
total (# of holes/stage)		110	total	150	total	290	-
total (mm^2/hectare)		35750	total	51000	total	87300	

The individual hole size for pinholes, holes, and tears is taken as the midpoint in the range provided by Needham et al. (2004)

The individual hole size for small cracks and large cracks is taken as that recommended by Needham et al. (2004)

The number of holes is the most likely number or average number from Needham et al. (2004) for the "fair" case except where noted below:

[1] The anticipated SDF Closure Cap configuration with the HDPE geomembrane on a maximum 4% slope and associated construction methodology and quality assurance (see Section 4.4.3) seem to preclude the generation of tears during construction.

[2] No operations at the F-Area Tank Farm are anticipated after installation of the SDF Closure Cap. Only monitoring and maintenance activities are anticipated. Therefore no holes, tears, or cracks generation due to operations are anticipated.

[3] # of holes and holes size is per 100 years

Estimation of Number and Size of Holes Generated per Stage for the Needham et al. (2004) Fair Case:

Stage	Cumulative (years)	Number of Holes Generated for the Needham et al. (2004) Fair Case (#)	Size of Holes Generated for the Needham et al. (2004) Fair Case (mm^2 / Hectare)
1	0	30	550
2	0	0	0
3	10	0	0
4	295	110	35,750
5	345	150	51,000
6	10,000	290 / 100 years	87,300 / 100 years

This results in the following cumulative number and area of holes over time in the HDPE

Stage	Year	Total Stage # of Holes (#/hectare)	Total Cumulative # of Holes (#/hectare)	Total Cumulative # of Holes (#/acre)	Total Stage Hole Size (mm^2/hectare)	Total Cumulative Hole Size (mm^2/hectare)	Total Cumulative Hole Size (cm^2/acres)	Average Single Hole Size (cm^2)
1	0	30	30	12	550	550	2	0.2
2	0	0	30	12	0	550	2	0.2
3	10	0	30	12	0	550	2	0.2
4	295	110	140	57	35,750	36300	147	2.6
5	345	150	290	117	51,000	87300	353	3.0
6	445	290	580	235	87,300	174600	707	3.0
6	545	290	870	352	87,300	261900	1060	3.0
6	645	290	1160	469	87,300	349200	1413	3.0
6	745	290	1450	587	87,300	436500	1766	3.0
6	845	290	1740	704	87,300	523800	2120	3.0
6	945	290	2030	822	87,300	611100	2473	3.0
6	1045	290	2320	939	87,300	698400	2826	3.0
6	1145	290	2610	1056	87,300	785700	3180	3.0
6	1245	290	2900	1174	87,300	873000	3533	3.0
6	1345	290	3190	1291	87,300	960300	3886	3.0
6	1445	290	3480	1408	87,300	1047600	4240	3.0
6	1545	290	3770	1526	87,300	1134900	4593	3.0
6	1645	290	4060	1643	87,300	1222200	4946	3.0
6	1745	290	4350	1760	87,300	1309500	5299	3.0
6	1845	290	4640	1878	87,300	1396800	5653	3.0
6	1945	290	4930	1995	87,300	1484100	6006	3.0
6	2045	290	5220	2113	87,300	1571400	6359	3.0
6	2145	290	5510	2230	87,300	1658700	6713	3.0
6	2245	290	5800	2347	87,300	1746000	7066	3.0
6	2345	290	6090	2465	87,300	1833300	7419	3.0
6	2445	290	6380	2582	87,300	1920600	7773	3.0

Stage	Year	Total Stage # of Holes (#/hectare)	Total Cumulative # of Holes (#/hectare)	Total Cumulative # of Holes (#/acre)	Total Stage Hole Size (mm^2/hectare)	Total Cumulative Hole Size (mm^2/hectare)	Total Cumulative Hole Size (cm^2/acres)	Average Single Hole Size (cm^2)
6	2545	290	6670	2699	87,300	2007900	8126	3.0
6	2645	290	6960	2817	87,300	2095200	8479	3.0
6	2745	290	7250	2934	87,300	2182500	8832	3.0
6	2845	290	7540	3051	87,300	2269800	9186	3.0
6	2945	290	7830	3169	87,300	2357100	9539	3.0
6	3045	290	8120	3286	87,300	2444400	9892	3.0
6	3145	290	8410	3403	87,300	2531700	10246	3.0
6	3245	290	8700	3521	87,300	2619000	10599	3.0
6	3345	290	8990	3638	87,300	2706300	10952	3.0
6	3445	290	9280	3756	87,300	2793600	11306	3.0
6	3545	290	9570	3873	87,300	2880900	11659	3.0
6	3645	290	9860	3990	87,300	2968200	12012	3.0
6	3745	290	10150	4108	87,300	3055500	12365	3.0
6	3845	290	10440	4225	87,300	3142800	12719	3.0
6	3945	290	10730	4342	87,300	3230100	13072	3.0
6	4045	290	11020	4460	87,300	3317400	13425	3.0
6	4145	290	11310	4577	87,300	3404700	13779	3.0
6	4245	290	11600	4694	87,300	3492000	14132	3.0
6	4345	290	11890	4812	87,300	3579300	14485	3.0
6	4445	290	12180	4929	87,300	3666600	14839	3.0
6	4545	290	12470	5047	87,300	3753900	15192	3.0
6	4645	290	12760	5164	87,300	3841200	15545	3.0
6	4745	290	13050	5281	87,300	3928500	15898	3.0
6	4845	290	13340	5399	87,300	4015800	16252	3.0
6	4945	290	13630	5516	87,300	4103100	16605	3.0
6	5045	290	13920	5633	87,300	4190400	16958	3.0
6	5145	290	14210	5751	87,300	4277700	17312	3.0
6	5245	290	14500	5868	87,300	4365000	17665	3.0

Stage	Year	Total Stage # of Holes (#/hectare)	Total Cumulative # of Holes (#/hectare)	Total Cumulative # of Holes (#/acre)	Total Stage Hole Size (mm^2/hectare)	Total Cumulative Hole Size (mm^2/hectare)	Total Cumulative Hole Size (cm^2/acres)	Average Single Hole Size (cm^2)
6	5345	290	14790	5985	87,300	4452300	18018	3.0
6	5445	290	15080	6103	87,300	4539600	18372	3.0
6	5545	290	15370	6220	87,300	4626900	18725	3.0
6	5645	290	15660	6338	87,300	4714200	19078	3.0
6	5745	290	15950	6455	87,300	4801500	19431	3.0
6	5845	290	16240	6572	87,300	4888800	19785	3.0
6	5945	290	16530	6690	87,300	4976100	20138	3.0
6	6045	290	16820	6807	87,300	5063400	20491	3.0
6	6145	290	17110	6924	87,300	5150700	20845	3.0
6	6245	290	17400	7042	87,300	5238000	21198	3.0
6	6345	290	17690	7159	87,300	5325300	21551	3.0
6	6445	290	17980	7276	87,300	5412600	21904	3.0
6	6545	290	18270	7394	87,300	5499900	22258	3.0
6	6645	290	18560	7511	87,300	5587200	22611	3.0
6	6745	290	18850	7628	87,300	5674500	22964	3.0
6	6845	290	19140	7746	87,300	5761800	23318	3.0
6	6945	290	19430	7863	87,300	5849100	23671	3.0
6	7045	290	19720	7981	87,300	5936400	24024	3.0
6	7145	290	20010	8098	87,300	6023700	24378	3.0
6	7245	290	20300	8215	87,300	6111000	24731	3.0
6	7345	290	20590	8333	87,300	6198300	25084	3.0
6	7445	290	20880	8450	87,300	6285600	25437	3.0
6	7545	290	21170	8567	87,300	6372900	25791	3.0
6	7645	290	21460	8685	87,300	6460200	26144	3.0
6	7745	290	21750	8802	87,300	6547500	26497	3.0
6	7845	290	22040	8919	87,300	6634800	26851	3.0
6	7945	290	22330	9037	87,300	6722100	27204	3.0
6	8045	290	22620	9154	87,300	6809400	27557	3.0

Stage	Year	Total Stage # of Holes (#/hectare)	Total Cumulative # of Holes (#/hectare)	Total Cumulative # of Holes (#/acre)	Total Stage Hole Size (mm^2/hectare)	Total Cumulative Hole Size (mm^2/hectare)	Total Cumulative Hole Size (cm^2/acres)	Average Single Hole Size (cm^2)
6	8145	290	22910	9272	87,300	6896700	27911	3.0
6	8245	290	23200	9389	87,300	6984000	28264	3.0
6	8345	290	23490	9506	87,300	7071300	28617	3.0
6	8445	290	23780	9624	87,300	7158600	28970	3.0
6	8545	290	24070	9741	87,300	7245900	29324	3.0
6	8645	290	24360	9858	87,300	7333200	29677	3.0
6	8745	290	24650	9976	87,300	7420500	30030	3.0
6	8845	290	24940	10093	87,300	7507800	30384	3.0
6	8945	290	25230	10210	87,300	7595100	30737	3.0
6	9045	290	25520	10328	87,300	7682400	31090	3.0
6	9145	290	25810	10445	87,300	7769700	31444	3.0
6	9245	290	26100	10563	87,300	7857000	31797	3.0
6	9345	290	26390	10680	87,300	7944300	32150	3.0
6	9445	290	26680	10797	87,300	8031600	32503	3.0
6	9545	290	26970	10915	87,300	8118900	32857	3.0
6	9645	290	27260	11032	87,300	8206200	33210	3.0
6	9745	290	27550	11149	87,300	8293500	33563	3.0
6	9845	290	27840	11267	87,300	8380800	33917	3.0
6	9945	290	28130	11384	87,300	8468100	34270	3.0
6	10045	290	28420	11501	87,300	8555400	34623	3.0

Determine total cumulative number of HDPE holes and hole size per acre for the years to be modeled by linear interpolation from adjacent values:

Year (Yr$_x$)	Total Cumulative # of Holes [1] (#/acre)	Total Cumulative Hole Size [2] (cm^2/acres)	Adjacent Values from which Linear Interpolation Made		
			Adjacent Years	Adjacent Total Cumulative # of Holes (#/acre)	Adjacent Total Cumulative Hole Size (cm^2/acres)
			Yr$_1$	#H$_1$	HS$_1$
			Yr$_2$	#H$_2$	HS$_2$
0	12	2	0	12	2
			0	12	2
100	26	48	10	12	2
			295	57	147
180	39	88	10	12	2
			295	57	147
220	45	109	10	12	2
			295	57	147
300	63	168	295	57	147
			345	117	353
380	158	477	345	117	353
			445	235	707
460	253	760	445	235	707
			545	352	1060
560	370	1113	545	352	1060
			645	469	1413
1,000	886	2667	945	822	2473
			1045	939	2826
1,800	1825	5494	1745	1760	5299
			1845	1878	5653
3,200	3468	10440	3145	3403	10246
			3245	3521	10599
5,412	6064	18255	5345	5985	18018
			5445	6103	18372
5,600	6285	18919	5545	6220	18725
			5645	6338	19078
10,000	11448	34464	9945	11384	34270
			10045	11501	34623

[1] Total Cumulative # of Holes (#/acre) = #H$_1$ + (((Yr$_x$ – Yr$_1$) / (Yr$_2$ – Yr$_1$)) × (#H$_2$ - #H$_1$))
[2] Total Cumulative Hole Size (cm^2/acres) = HS$_1$ + (((Yr$_x$ – Yr$_1$) / (Yr$_2$ – Yr$_1$)) × (HS$_2$ - HS$_1$))

Divalent Cation Degradation of the GCL

As outlined in Section 7.7.4 and Table , it will be assumed that the sodium bentonite GCL is converted to calcium-magnesium-bentonite GCL, resulting in an order of magnitude increase in saturated hydraulic conductivity. During the 100-year institutional period, it will be assumed the GCL consists of sodium bentonite with a saturated hydraulic conductivity of 5.0E-09 cm/s. After the 100-year institutional period, it will be assumed the GCL consists of calcium-magnesium-bentonite with a saturated hydraulic conductivity of 5.0E-08 cm/s.

Root Penetration of the Composite Hydraulic Barrier

The chart below provides a comparison of the number of holes in the HDPE geomembrane versus the number of pine tree roots over time. As seen there are significantly more pine tree roots than HDPE geomembrane holes.

HDPE Geomembrane Holes and Pine Tree Roots with Time
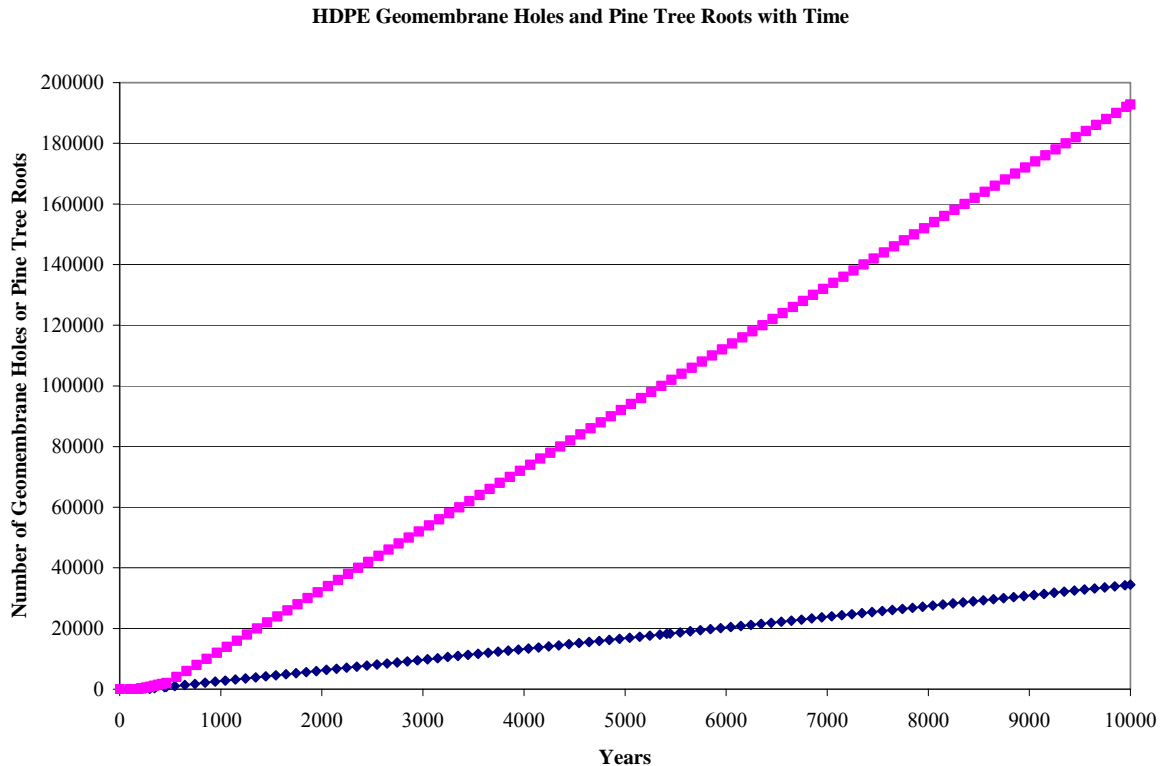
As a conservative estimation of root penetration through the GCL, it will be assumed that every HDPE geomembrane hole generated over time is penetrated by a root that subsequently penetrates the GCL, once significant roots are available to penetrate. It will be assumed that significant roots are available for penetration at year 300 and beyond (at year 300, three-sevenths of the closure cap is assumed to be covered by mature trees). As discussed in Section 7.7.2, this is a conservative estimation because much of the upper lateral drainage layer, GCL, and HDPE area will be located below the 12-ft maximum depth of root penetration, and thereby not be affected by roots at all.

Determine average projected area of roots at the depth of the HDPE geomembrane as though the HDPE geomembrane was not present:

The root area at the depth of the HDPE geomembrane will be determined based upon its depth at year 10,000, since this will result in the maximum root area. From the topsoil erosion calculations above the thickness of topsoil at 10,000 years is reduced from 6 to 4.74 inches. Therefore the thickness of materials above the HDPE geomembrane at year 10,000 is:

Thickness = 6' – ((6" – 4.74")/12"/ft) = 5.90'

Root Diameter for 6' roots at 5.90':
  Diameter = 0.25" + [(6' – 5.90') × 0.55"/ft] = 0.31"
Area of 6' roots at 5.88':
  Area = ¼πD^2 = ¼π(0.31")^2 = 0.08 in^2 × 6.4516 cm^2/in^2 = 0.52 cm^2

Root Diameter for 12' roots at 5.90':
  Diameter = 0.25" + [(12' – 5.90') × 0.25"/ft] = 1.78"
Area of 12' roots at 5.90':
  Area = ¼πD^2 = ¼π(1.78")^2 = 2.49 in^2 × 6.4516 cm^2/in^2 = 16.06 cm^2

Average root area at 5.90':
  4-6' roots per tree
  1-12' root per tree
  Average = ((4 × 0.52 cm^2) + (1 × 16.06 cm^2))/(4 + 1) = 3.63 cm^2

As seen in the tabulated HDPE hole generation calculations above, at 345 years the average hole diameter in the HDPE geomembrane is 3.0 cm^2, which is near the average root area of 3.63 cm^2 at the depth of the HDPE geomembrane. The average root area was determined as though the HDPE geomembrane was not present. As outlined in Section 7.6.6, roots are not known to enlarge existing geomembrane defects (Badu-Tweneboah et al. 1999). Therefore the size of hole produced in the composite barrier (HDPE and GCL) through root penetration will be assumed to be that of the average hole diameter in the HDPE geomembrane (i.e., 3.0 cm^2).

Based upon the conservative assumption that every HDPE hole is penetrated by a root at year 300 and beyond and assuming that such holes produced by root penetration are 3.0 cm^2, only the following two composite barrier conditions will be assumed:

- HDPE geomembrane with holes overlying an intact GCL prior to year 300, or
- HDPE geomembrane and underlying GCL with holes (GCL holes produced by root penetration through all HDPE geomembrane holes) at year 300 and beyond.

The HELP model allows the input of up to 999,999 one square centimeter installation defects per acre for a geomembrane liner; therefore the total cumulative hole size shown below for each year to be modeled will be used as the number of one square centimeter installation defects per acre for input into the HELP model. This results in more holes than determined but maintains the area of holes determined.

Year	Total Cumulative Number of Holes (number/acre)	Total Cumulative Hole Size (cm^2/acre)
0	12	2
100	26	48
180	39	88
220	45	109
300	63	168
380	158	477
460	253	760
560	370	1113
1,000	886	2667
1,800	1825	5494
3,200	3468	10440
5,412	6064	18255
5,600	6285	18919
10,000	11448	34464

Based upon recommendations from Schroeder et al. (1994a) and Schroeder et al. (1994b) discussed in Section 5.4.5, the initial hole size used for year 0 HELP modeling of the SDF Closure Cap was taken as 4 geomembrane installation defects at a total area of 4 cm^2/acre (additionally it included 1 pinhole with an area of 7.84E-03 cm^2/acre). Based upon this, the number and size of holes shown above using the Needham et al. (2004) methodology will be modified. The greater number of holes and greater area of holes for the initial condition (i.e., year 0) produced by the Needham et al. (2004) methodology or based upon the Section 5.4.5 initial assumptions will be used. For the initial conditions this results in 12 holes/acre with an area of 4 cm^2. Therefore the total cumulative hole size shown above will be increased by 2 cm^2/acre for each time period considered as shown below.

Year	Total Cumulative Number of Holes (number/acre)	Total Cumulative Hole Size (cm^2/acre)
0	12	4
100	26	50
180	39	90
220	45	111
300	63	170
380	158	479
460	253	760
560	370	1115
1,000	886	2669
1,800	1825	5496
3,200	3468	10442
5,412	6064	18257
5,600	6285	18921
10,000	11448	34466

Since the HELP model can not handle holes in a barrier soil liner (i.e., the GCL), the GCL must either be ignored in the HELP modeling or combined with the HDPE geomembrane for all cases at year 300 and beyond.

Based upon the above, the HELP model will be run with the following representations of the composite hydraulic barrier (HDPE geomembrane and GCL):

- At or before year 100, the HDPE geomembrane and GCL will be modeled as separate layers with holes in the HDPE geomembrane and an intact GCL with a Ksat = 5.0E-09 cm/s.
- After year 100 but before year 300, the HDPE geomembrane and GCL will be modeled as separate layers with holes in the HDPE geomembrane and an intact GCL with a Ksat = 5.0E-08 cm/s.
- At and beyond year 300, the HDPE geomembrane and GCL will be modeled as a combined layer with holes all the way through and with a K_{sat} = 8.7E-13 cm/s and a thickness of 0.260" for intact portions (calculations for the combined Ksat are shown below – the HELP model input field limits the number of digits to 14 and does not allow the input of scientific notation)

Determine the equivalent K_{sat} for the intact portions of the combined HDPE geomembrane and GCL for year 300 and beyond:

- Intact HDPE geomembrane assumed to always have a K_{sat} = 2E-13 cm/s and a thickness of 0.060 inches
- Beyond 100 years the intact GCL is assumed to have a K_{sat} = 5E-08 cm/s and a thickness of 0.20 inches

Equivalent K_{sat} for flow perpendicular to layering (Freeze and Cherry 1979):

$$K_v = \frac{d}{\sum_{i=1}^{n} d_i / K_i},$$ where K_v = combined saturated hydraulic conductivity of

combined layers; d = total thickness of all layers combined; di = thickness of ith layer; K_i = saturated hydraulic conductivity of ith layer

At 300 years and beyond:

$$K_v = \frac{0.20" + 0.060"}{\dfrac{0.20"}{5E-08 \, cm/s} + \dfrac{0.060"}{2E-13 \, cm/s}} = 8.7E-13 \, cm/s$$

Summary SDF Closure Cap Degraded Property Values for Entry into the HELP Model

Topsoil Thickness over Time:

Year	Thickness (inches)
0	6.00
100	5.96
180	5.92
220	5.90
300	5.87
380	5.83
460	5.79
560	5.78
1,000	5.73
1,800	5.64
3,200	5.49
5,412	5.25
5,600	5.23
10,000	4.74

Upper Lateral Drainage Layer K_{sat}, n, FC, and WP with Time:

Year	K_{sat} (cm/s)	n	FC	WP
0	5.00E-02	0.417	0.0450	0.0180
100	4.91E-02	0.414	0.0484	0.0215
180	4.84E-02	0.411	0.0513	0.0243
220	4.80E-02	0.410	0.0528	0.0259
300	4.72E-02 (4.73E-02)	0.407	0.0555	0.0286
380	4.64E-02 (4.65E-02)	0.405	0.0584	0.0314
460	4.57E-02 (4.58E-02)	0.402	0.0612	0.0343
560	4.48E-02 (4.49E-02)	0.399	0.0647	0.0378
1,000	4.07E-02 (4.08E-02)	0.384	0.0803	0.0535
1,800	3.33E-02 (3.34E-02)	0.358	0.1086	0.0819
3,200	2.05E-02 (2.05E-02)	0.312	0.1579	0.1315
5,412	4.09E-05 (4.10E-05)	0.240	0.2360	0.2100
5,600	4.09E-05 (4.10E-05)	0.240	0.2360	0.2100
10,000	4.09E-05 (4.10E-05)	0.240	0.2360	0.2100

In order to compensate for the presence of the roots within the lateral drainage layer, the saturated hydraulic conductivity of the layer will be reduced by a factor of 0.998 at year 300 and beyond due to the presence of mature pine trees on the SDF Closure Cap. The original K_{sat} prior to reduction by the 0.998 factor is shown in parenthesis.

GCL K$_{sat}$ with time:

Year	K$_{sat}$ (cm/s)
0	5.0E-09
100	5.0E-09
180	5.0E-08
220	5.0E-08

Number of 1 cm^2 holes per acre in the HDPE Geomembrane with time for input to the HELP model:

Year	Number of 1 cm^2 Holes (number/acre)
0	4
100	50
180	90
220	111

Number of 1 cm^2 holes per acre in the composite hydraulic barrier (HDPE Geomembrane and GCL) with time for input to the HELP model:

Year	Number of 1 cm^2 Holes (number/acre)
300	170
380	479
460	760
560	1115
1,000	2669
1,800	5496
3,200	10442
5,412	18257
5,600	18921
10,000	34466

Will run the HELP model with the following representations of the intact composite hydraulic barrier at year 300 and beyond:

- K$_{sat}$ = 8.7E-13 cm/s with a thickness of 0.260"

HELP Model Input Data Tables presented in Appendix J are set up for representation of the intact composite hydraulic barrier at year 300 and beyond with K$_{sat}$ = 8.7E-13 cm/s with a thickness of 0.260".

Lower Drainage Layer Silting-In Over Time

It is assumed that colloidal clay migration (63 mg/L colloidal clay) from the 84-inch (average) thick lower backfill into the 24-inch thick lower drainage layer is driven by water flux through the GCL. This water-flux-driven clay is assumed to accumulate in the lower drainage layer from the bottom up. The hydraulic conductivity of the clay-filled drainage layer is reduced from 5.0E-02 cm/s to that of the overlying backfill, 4.1E-05 cm/s. The hydraulic conductivity of the upper, non-clay-filled drainage layer remains at 5.0E-02 cm/s. The thickness of the clay-filled portion increases with time, while the thickness of the non-filled portion decreases with time, resulting in an overall decrease in hydraulic conductivity for the lower drainage layer.

To determine infiltration through the upper GCL, the HELP model was run for each time-step with degraded properties for each layer except the lower drainage layer. The results are as follows:

Infiltration Through GCL With Time	
Year After Cap Construction	**Infiltration Through GCL (in/year)**
0	0.00042
100	0.00333
180	0.04520
220	0.05676
300	0.17110
380	0.47236
460	0.72342
560	1.0211
1,000	2.2638
1,800	4.340
3,200	6.795
5,412	10.6
5,600	10.6
10000	10.6

It is assumed there is a linear increase in infiltration between time-steps. Determine the cumulative volume of water through the lower drainage layer over time:

Cumulative Volume of Water Through LDL With Time				
Year After Cap Construction	Water Infiltration Through GCL (in/year)	Time-Step Water Volume (inches)[1]	Cumulative Water Volume (inches)[2]	Cumulative Water Volume Over One Sq. Ft. Area (ft^3)[3]
0	0.00042	0.0000	0.00000	0.00000
100	0.00333	0.1875	0.18750	0.01563
180	0.04520	1.9412	2.12870	0.17739
220	0.05676	2.0392	4.16790	0.34733
300	0.17110	9.1144	13.28230	1.10686
380	0.47236	25.7384	39.02070	3.25173
460	0.72342	47.8312	86.85190	7.23766
560	1.0211	87.226	174.0779	14.5065
1,000	2.2638	722.678	896.7559	74.7297
1,800	4.340	2641.52	3538.276	294.856
3,200	6.795	7794.5	11332.776	944.398
5,412	10.6	19238.9	30571.7	2547.6
5,600	10.6	1992.8	32564.5	2713.7
10,000	10.6	46640.0	79204.5	6600.4

[1]Volume = $(I_1 \times (T_2 - T_1)) + (0.5 \times (I_2 - I_1)(T_2 - T_1))$, where I = infiltration at time-step 1 or 2; T = year at time-step 1 or 2.
[2]Cumulative Volume = previous cumulative volume + volume at current time-step.
[3]Cumulative Volume over one ft^2 area = (Cumulative Volume/12 in/ft) x 1 ft^2.

The following are the intact hydraulic properties of the middle backfill and upper lateral drainage layer:

Hydraulic Parameter	Middle Backfill	Upper Lateral Drainage Layer
K_{sat} (cm/s)	4.1E-05	5.0E-02
η	0.35	0.417
FC	0.252	0.045
WP	0.181	0.018

Determine clay mass to fill lower lateral drainage layer void volume (0.417) on cu ft basis:
- Assume clay bulk density is 1.1 g/cm^3 (Hillel 1982).
- For a 1-ft^2 area of a 2-ft thick drainage layer: Void Volume = 0.417 x 2 ft^3 = 0.834 ft^3
- Convert 0.834 ft^3 to cm^3: 0.834 ft^3 x 28316.85 cm^3/ft^3 = 23,616.3 cm^3
- Clay mass per ft^3 = 1.1 g/cm^3 x 23,616.3 cm^3 = 25,977.9 g

Determine total flux of water into the lower drainage layer required to fill the void space with clay:

Assume water flux contains 63 mg/L colloidal clay.

Volume of water = (25,977.9 g x 1,000 mg/g)/(63 mg/L x 28.31685 L/ft^3) = 14,562 ft^3

Determine the mass of clay that has migrated into the lower drainage layer at the end of each time-step:

Mass of Clay Migrated Into Lower Drainage Layer at End of Each Time Step					
Year After Cap Construction	Cumulative Volume Over One Sq. Ft. Area (ft^3)	Clay Concentration (mg/L)	L/ft^3	g/mg	Mass of Clay into LDL (g)
0	0.00000	63.000	28.317	1000.000	0.00000
100	0.01563	63.000	28.317	1000.000	0.02787
180	0.17739	63.000	28.317	1000.000	0.31646
220	0.34733	63.000	28.317	1000.000	0.61961
300	1.10686	63.000	28.317	1000.000	1.97459
380	3.25173	63.000	28.317	1000.000	5.80095
460	7.23766	63.000	28.317	1000.000	12.91170
560	14.5065	63.000	28.317	1000.000	25.8790
1,000	74.7297	63.000	28.317	1000.000	133.3148
1,800	294.856	63.000	28.317	1000.000	526.012
3,200	944.398	63.000	28.317	1000.000	1684.770
5,412	2547.6	63.000	28.317	1000.000	4544.9
5,600	2713.7	63.000	28.317	1000.000	4841.1
10,000	6600.4	63.000	28.317	1000.000	11774.8

Mass of Clay = (Cumulative Volume (ft^3) x Clay Concentration (mg/L) x 28.31685 L/ft^3)/(1,000 mg/g)

Determine the fraction of the lower drainage layer filled at the end of each time-step:

Fraction of Lower Drainage Layer Filled With Clay at End of Each Time Step			
Year After Cap Construction	Mass of Clay into LDL (g)	Clay Mass per 2 ft^3 (per ft^2 area LDL; g)	Fraction of LDL Filled
0	0.00000	25,977.9	0.000
100	0.02787	25,977.9	0.000
180	0.31646	25,977.9	0.000
220	0.61961	25,977.9	0.000
300	1.97459	25,977.9	0.000
380	5.80095	25,977.9	0.000
460	12.91170	25,977.9	0.000
560	25.8790	25,977.9	0.001
1,000	133.3148	25,977.9	0.005
1,800	526.012	25,977.9	0.020
3,200	1684.770	25,977.9	0.065
5,412	4544.9	25,977.9	0.175
5,600	4841.1	25,977.9	0.186
10,000	11774.8	25,977.9	0.453

Fraction of Lower Drainage Layer = Mass of Clay (g)/Clay Mass (g) per ft^3

Determine Equivalent Hydraulic Conductivity of the lower drainage layer over time (see Phifer and Nelson (2003) for details):

Lower Drainage Layer Saturated Hydraulic Conductivity Over Time					
Year After Cap Construction	K_{filled} (cm/s)	Fraction of LDL Filled	K_{clean} (cm/s)	1 - Fraction of LDL Filled	Hydraulic Conductivity (cm/s)
0	4.1E-05	0.000	5.0E-02	1.000	5.000E-02
100	4.1E-05	0.000	5.0E-02	1.000	5.000E-02
180	4.1E-05	0.000	5.0E-02	1.000	5.000E-02
220	4.1E-05	0.000	5.0E-02	1.000	5.000E-02
300	4.1E-05	0.000	5.0E-02	1.000	5.000E-02
380	4.1E-05	0.000	5.0E-02	1.000	4.999E-02
460	4.1E-05	0.000	5.0E-02	1.000	4.998E-02
560	4.1E-05	0.001	5.0E-02	0.999	4.995E-02
1,000	4.1E-05	0.005	5.0E-02	0.995	4.974E-02
1,800	4.1E-05	0.020	5.0E-02	0.980	4.899E-02
3,200	4.1E-05	0.065	5.0E-02	0.935	4.676E-02
5,412	4.1E-05	0.175	5.0E-02	0.825	4.126E-02
5,600	4.1E-05	0.186	5.0E-02	0.814	4.069E-02
10,000	4.1E-05	0.453	5.0E-02	0.547	2.736E-02

LDL = Lower Drainage Layer; K_{filled} = Hydraulic Conductivity of clay-filled LDL; K_{clean} = Hydraulic Conductivity of non-clay-filled LDL
Equivalent K = (K_{filled} x Fraction of LDL filled) + (K_{clean} x (1- Fraction of LDL filled))

In an analogous manner, equivalent porosity, field capacity, and wilting point for the lower drainage layer can be determined based upon the fraction filled as follows (see Phifer and Nelson (2003) for details):

Lower Drainage Layer Porosity Over Time					
Year After Cap Construction	Porosity (filled)	Fraction of LDL Filled	Porosity (clean)	1 - Fraction of LDL Filled	Porosity (vol/vol)
0	0.350	0.000	0.417	1.000	0.417
100	0.350	0.000	0.417	1.000	0.417
180	0.350	0.000	0.417	1.000	0.417
220	0.350	0.000	0.417	1.000	0.417
300	0.350	0.000	0.417	1.000	0.417
380	0.350	0.000	0.417	1.000	0.417
460	0.350	0.000	0.417	1.000	0.417
560	0.350	0.001	0.417	0.999	0.417
1,000	0.350	0.005	0.417	0.995	0.417
1,800	0.350	0.020	0.417	0.980	0.416
3,200	0.350	0.065	0.417	0.935	0.413
5,412	0.350	0.175	0.417	0.825	0.405
5,600	0.350	0.186	0.417	0.814	0.405
10,000	0.350	0.453	0.417	0.547	0.387

Equivalent Porosity = (Porosity$_{filled}$ x Fraction of LDL filled) + (Porosity$_{clean}$ x (1- Fraction of LDL filled))

Lower Drainage Layer Field Capacity Over Time					
Year After Cap Construction	Field Capacity (filled)	Fraction of LDL Filled	Field Capacity (clean)	1 - Fraction of LDL Filled	Equivalent Field Capacity (vol/vol)
0	0.252	0.000	0.045	1.000	0.045
100	0.252	0.000	0.045	1.000	0.045
180	0.252	0.000	0.045	1.000	0.045
220	0.252	0.000	0.045	1.000	0.045
300	0.252	0.000	0.045	1.000	0.045
380	0.252	0.000	0.045	1.000	0.045
460	0.252	0.000	0.045	1.000	0.045
560	0.252	0.001	0.045	0.999	0.045
1,000	0.252	0.005	0.045	0.995	0.046
1,800	0.252	0.020	0.045	0.980	0.049
3,200	0.252	0.065	0.045	0.935	0.058
5,412	0.252	0.175	0.045	0.825	0.081
5,600	0.252	0.186	0.045	0.814	0.084
10000	0.252	0.453	0.045	0.547	0.139

Equivalent Field Capacity = (Field Capacity$_{filled}$ x Fraction of LDL filled) + (Field Capacity$_{clean}$ x (1- Fraction of LDL filled))

Lower Drainage Layer Wilting Point Over Time					
Year After Cap Construction	Wilting Point (filled)	Fraction of LDL Filled	Wilting Point (clean)	1 - Fraction of LDL Filled	Equivalent Wilting Point (vol/vol)
0	0.181	0.000	0.018	1.000	0.018
100	0.181	0.000	0.018	1.000	0.018
180	0.181	0.000	0.018	1.000	0.018
220	0.181	0.000	0.018	1.000	0.018
300	0.181	0.000	0.018	1.000	0.018
380	0.181	0.000	0.018	1.000	0.018
460	0.181	0.000	0.018	1.000	0.018
560	0.181	0.001	0.018	0.999	0.018
1,000	0.181	0.005	0.018	0.995	0.019
1,800	0.181	0.020	0.018	0.980	0.021
3,200	0.181	0.065	0.018	0.935	0.029
5,412	0.181	0.175	0.018	0.825	0.047
5,600	0.181	0.186	0.018	0.814	0.048
10000	0.181	0.453	0.018	0.547	0.092

Equivalent Wilting Point = (Wilting Point$_{filled}$ x Fraction of LDL filled) + (Wilting Point$_{clean}$ x (1- Fraction of LDL filled))

Summary of Lower Drainage Layer Hydraulic Properties with Time:

Lower Drainage Layer Hydraulic Properties With Time				
Year After Cap Construction	Hydraulic Conductivity (cm/s)	Porosity (vol/vol)	Field Capacity (vol/vol)	Wilting Point (vol/vol)
0	5.000E-02	0.417	0.045	0.018
100	5.000E-02	0.417	0.045	0.018
180	5.000E-02	0.417	0.045	0.018
220	5.000E-02	0.417	0.045	0.018
300	5.000E-02	0.417	0.045	0.018
380	4.999E-02	0.417	0.045	0.018
460	4.998E-02	0.417	0.045	0.018
560	4.995E-02	0.417	0.045	0.018
1,000	4.974E-02	0.417	0.046	0.019
1,800	4.899E-02	0.416	0.049	0.021
3,200	4.676E-02	0.413	0.058	0.029
5,412	4.126E-02	0.405	0.081	0.047
5,600	4.069E-02	0.405	0.084	0.048
10,000	2.736E-02	0.387	0.139	0.092

Degradation of HDPE Surrounding Disposal cells

HDPE will be placed over and around individual disposal cells (see Figure 8). Degradation of this HDPE is evaluated following the methods outlined in Phifer (2005). Degradation is expressed in terms of the fraction or percentage area of HDPE geomembrane consisting of holes over time.

Estimation of Size of Holes Generated per Stage for the Needham et al. (2004) Fair Case:		
Stage	Cumulative Years	Size of Holes Generated (MM^2/Hectare)
1	0	550
2	2	0
3	10	0
4	90	35,750
5	140	51,000
6	10,000	87,300 per 100 years

Total Stage Hole Sizes (from above table) for Years Used for Interpolation (in following table)		
Year of Value Interpolated	Cumulative Years Used for Interpolation (earlier year/later year)	Total Stage Hole Sizes (mm^2/Hectare) Used for Interpolation (earlier year size/later year size)
0	0	550
100	90/140	36,300/87,300
180	140/240	87,300/174,600
220	140/240	87,300/174,600
300	240/340	174,600/261,900
380	340/440	261,900/349,200
460	440/540	349,200/436,500
560	540/640	436,500/523,800
1000	940/1040	785,700/873,000
1800	1740/1840	1,484,100/1,571,400
3200	3140/3240	2,706,300/2,793,600
5412	5340/5440	4,626,900/4,714,200
5600	5540/5640	4,801,500/4,888,800
10,000	9940/10,040	8,642,700/8,730,000

		Interpolated Cumulative Area of Holes[1]	
Year	Total Cumulative Hole Size[2] (mm2/Hectare)	Fraction of HDPE Membrane with Holes[3]	Percentage of HDPE Membrane with Holes[4]
0	550	5.50E-08	5.50E-06
100	46500	4.65E-06	4.65E-04
180	122220	1.22E-05	1.22E-03
220	157140	1.57E-05	1.57E-03
300	226980	2.27E-05	2.27E-03
380	296820	2.97E-05	2.97E-03
460	366660	3.67E-05	3.67E-03
560	453960	4.54E-05	4.54E-03
1000	838080	8.38E-05	8.38E-03
1800	1536480	1.54E-04	1.54E-02
3200	2758680	2.76E-04	2.76E-02
5412	4689756	4.69E-04	4.69E-02
5600	4853880	4.85E-04	4.85E-02
10000	8695080	8.70E-04	8.70E-02

[1]Using Phifer 2005, page D-6

[2]Total Cumulative Hole Size = earlier year hole size + (year interpolated - earlier year) / (later year - earlier year) * (later year hole size - earlier year hole size)

[3]Fraction of HDPE geomembrane with holes = Total cumulative hole size/10,000,000,000 mm^2/Hectare

[4]Percentage with holes = Fraction with Holes/100

Degradation of GCL Overlying Disposal cells

The Saltstone disposal cell design includes a sodium bentonite GCL in conjunction with the HDPE geomembrane as a hydraulic/diffusional barrier to contaminant migration from the Saltstone disposal cell. The GCL will be placed on the disposal cell concrete roof with an overlying HDPE geomembrane. It will also be placed on the disposal cell concrete mud mat with an overlying HDPE geomembrane. Bentonite is a swelling-type, monmorillonite clay, with very low hydraulic conductivity. Its purpose in being coupled with the HDPE is to fill any holes or tears in the HDPE, providing a redundant and "HDPE healing" low-permeability layer.

Swelling of bentonite clays results from an increase in the thickness of the electrostatic double layer, a term used to describe the diffuse layer of cations held in solution by the attractive forces of the negatively charged clay particles. The thickness of the double-layer can be impacted by both the electrolyte concentration and valence of the cations comprising the hydrating solution. As salt concentration or cation valence increases in the ambient solution, the double-layer thickness decreases (Dixon and Phifer 2006).

Dixon and Phifer (2006) reports the results of permeability testing on a sodium bentonite GCL exposed to three different solutions: simulated groundwater, simulated Saltstone leachate, and simulated Saltstone pore fluid. The average saturated hydraulic conductivity of GCL samples permeated with simulated groundwater is 6.8E-10 cm/sec. The average saturated hydraulic conductivity for GCL samples permeated with Saltstone leachate is similar to that of GCL permeated with simulated groundwater, 9.1E-10 cm/sec. The average saturated hydraulic conductivity for GCL samples permeated with Saltstone pore fluid is 8.5E-8 cm/sec.

All of these values are well below the 1.0E-7 cm/sec performance criterion, indicating that a GCL can be appropriately used in conjunction with an HDPE geomembrane as a hydraulic/diffusional barrier to contaminant migration from Saltstone disposal cells.

Since the GCL used in association with Saltstone disposal cells will be in contact with concrete and could be exposed to a Ca^{+2}–containing salt solution, it will be assigned the following conservative saturated hydraulic conductivities:
- 0 to 100 years – 5E-09 cm/s
- beyond 100 years – 1.0E-07 cm/s

APPENDIX J.
HELP MODEL INPUT FOR SDF CLOSURE CAP OVER 10,000 YEARS

HELP Model Input Data for Year 0:

Input Parameter (HELP Model Query)	Generic Input Parameter Value
Landfill area =	0.0189 acres
Percent of area where runoff is possible =	100%
Do you want to specify initial moisture storage? (Y/N)	Y
Amount of water or snow on surface =	0 inches
CN Input Parameter (HELP Model Query)	CN Input Parameter Value
Slope =	1.5 %
Slope length =	825 ft
Soil Texture =	4 (HELP model default soil texture)
Vegetation =	4 (i.e., a good stand of grass)
HELP Model Computed Curve Number = 44.0	

Layer	Layer Number	Layer Type
Topsoil	1	1 (vertical percolation layer)
Upper Backfill	2	1 (vertical percolation layer)
Erosion Barrier	3	1 (vertical percolation layer)
Middle Backfill	4	1 (vertical percolation layer)
Lateral Drainage Layer	5	2 (lateral drainage layer)
HDPE Geomembrane	6	4 (geomembrane liner)
GCL	7	3 (barrier soil liner)
Foundation Layer (1E-06)	8	1 (vertical percolation layer)
Lower Backfill	9	1 (vertical percolation layer)

	Layer Type	Layer Thickness (in)	Soil Texture No.	Total Porosity (Vol/Vol)	Field Capacity (Vol/Vol)	Wilting Point (Vol/Vol)	Initial Moisture (Vol/Vol)
1	1	6		0.396	0.109	0.047	0.109
2	1	30		0.35	0.252	0.181	0.252
3	1	12		0.15	0.10	0.07	0.10
4	1	12		0.35	0.252	0.181	0.252
5	2	12		0.417	0.045	0.018	0.045
6	4	0.06					
7	3	0.2		0.750	0.747	0.400	0.750
8	1	12		0.35	0.252	0.181	0.252
9	1	72		0.35	0.252	0.181	0.252

HELP Model Input Data for Year 0 – continued:

	Layer Type	Sat. Hyd. Conductivity (cm/sec)	Drainage Length (ft)	Drain Slope (%)	Leachate Recirc. (%)	Recirc. to Layer (#)	Subsurface Inflow (in/yr)
1	1	3.1E-03					
2	1	4.1E-05					
3	1	1.3E-04					
4	1	4.1E-05					
5	2	5.0E-02	825	4			
6	4	2.0E-13					
7	3	5.0E-09					
8	1	1.0E-06					
9	1	4.1.E-05					

	Layer Type	Geomembrane Pinhole Density (#/acre)	Geomembrane Instal. Defects (#/acre)	Geomembrane Placement Quality	Geotextile Transmissivity (cm^2/sec)
1	1				
2	1				
3	1				
4	1				
5	2				
6	4	1	4	2	
7	3				
8	1				
9	1				

The lack of values in the table for particular parameters in particular layers denotes that no HELP model input was required for that parameter in that layer. No data are missing from the table.
Input File: SSYr0.D10; Output File: SSYr0.OUT

HELP Model Input Data for Year 100:

Input Parameter (HELP Model Query)	Generic Input Parameter Value
Landfill area =	0.0189 acres
Percent of area where runoff is possible =	100%
Do you want to specify initial moisture storage? (Y/N)	Y
Amount of water or snow on surface =	0 inches
CN Input Parameter (HELP Model Query)	CN Input Parameter Value
Slope =	1.5 %
Slope length =	825 ft
Soil Texture =	4 (HELP model default soil texture)
Vegetation =	4 (i.e., a good stand of grass)

HELP Model Computed Curve Number = 44.0		
Layer	Layer Number	Layer Type
Topsoil	1	1 (vertical percolation layer)
Upper Backfill	2	1 (vertical percolation layer)
Erosion Barrier	3	1 (vertical percolation layer)
Middle Backfill	4	1 (vertical percolation layer)
Lateral Drainage Layer	5	2 (lateral drainage layer)
HDPE Geomembrane	6	4 (geomembrane liner)
GCL	7	3 (barrier soil liner)
Foundation Layer (1E-06)	8	1 (vertical percolation layer)
Lower Backfill	9	1 (vertical percolation layer)

	Layer Type	Layer Thickness (in)	Soil Texture No.	Total Porosity (Vol/Vol)	Field Capacity (Vol/Vol)	Wilting Point (Vol/Vol)	Initial Moisture (Vol/Vol)
1	1	5.96		0.396	0.109	0.047	0.109
2	1	30		0.35	0.252	0.181	0.252
3	1	12		0.15	0.10	0.07	0.10
4	1	12		0.35	0.252	0.181	0.252
5	2	12		0.414	0.0484	0.0215	0.0484
6	4	0.06					
7	3	0.2		0.750	0.747	0.400	0.750
8	1	12		0.35	0.252	0.181	0.252
9	1	72		0.35	0.252	0.181	0.252

HELP Model Input Data for Year 100 – continued:

	Layer Type	Sat. Hyd. Conductivity (cm/sec)	Drainage Length (ft)	Drain Slope (%)	Leachate Recirc. (%)	Recirc. to Layer (#)	Subsurface Inflow (in/yr)
1	1	3.1E-03					
2	1	4.1E-05					
3	1	1.3E-04					
4	1	4.1E-05					
5	2	4.91E-02	825	4			
6	4	2.0E-13					
7	3	5.0E-09					
8	1	1.0E-06					
9	1	4.1E-05					

	Layer Type	Geomembrane Pinhole Density (#/acre)	Geomembrane Instal. Defects (#/acre)	Geomembrane Placement Quality	Geotextile Transmissivity (cm^2/sec)
1	1				
2	1				
3	1				
4	1				
5	2				
6	4	1	50	2	
7	3				
8	1				
9	1				

The lack of values in the table for particular parameters in particular layers denotes that no HELP model input was required for that parameter in that layer. No data are missing from the table.

Input File: SSYr100.D10; Output File: SSYr100.OUT

HELP Model Input Data for Year 180:

Input Parameter (HELP Model Query)	Generic Input Parameter Value
Landfill area =	0.0189 acres
Percent of area where runoff is possible =	100%
Do you want to specify initial moisture storage? (Y/N)	Y
Amount of water or snow on surface =	0 inches
CN Input Parameter (HELP Model Query)	CN Input Parameter Value
Slope =	1.5 %
Slope length =	825 ft
Soil Texture =	4 (HELP model default soil texture)
Vegetation =	4 (i.e., a good stand of grass)
HELP Model Computed Curve Number = 44.0	

Layer	Layer Number	Layer Type
Topsoil	1	1 (vertical percolation layer)
Upper Backfill	2	1 (vertical percolation layer)
Erosion Barrier	3	1 (vertical percolation layer)
Middle Backfill	4	1 (vertical percolation layer)
Lateral Drainage Layer	5	2 (lateral drainage layer)
HDPE Geomembrane	6	4 (geomembrane liner)
GCL	7	3 (barrier soil liner)
Foundation Layer (1E-06)	8	1 (vertical percolation layer)
Lower Backfill	9	1 (vertical percolation layer)

	Layer Type	Layer Thickness (in)	Soil Texture No.	Total Porosity (Vol/Vol)	Field Capacity (Vol/Vol)	Wilting Point (Vol/Vol)	Initial Moisture (Vol/Vol)
1	1	5.92		0.396	0.109	0.047	0.109
2	1	30		0.35	0.252	0.181	0.252
3	1	12		0.15	0.10	0.07	0.10
4	1	12		0.35	0.252	0.181	0.252
5	2	12		0.411	0.0513	0.0243	0.0513
6	4	0.06					
7	3	0.2		0.750	0.747	0.400	0.750
8	1	12		0.35	0.252	0.181	0.252
9	1	72		0.35	0.252	0.181	0.252

HELP Model Input Data for Year 180 – continued:

	Layer Type	Sat. Hyd. Conductivity (cm/sec)	Drainage Length (ft)	Drain Slope (%)	Leachate Recirc. (%)	Recirc. to Layer (#)	Subsurface Inflow (in/yr)
1	1	3.1E-03					
2	1	4.1E-05					
3	1	1.3E-04					
4	1	4.1E-05					
5	2	4.84E-02	825	4			
6	4	2.0E-13					
7	3	5.0E-08					
8	1	1.0E-06					
9	1	4.1E-05					

	Layer Type	Geomembrane Pinhole Density (#/acre)	Geomembrane Instal. Defects (#/acre)	Geomembrane Placement Quality	Geotextile Transmissivity (cm^2/sec)
1	1				
2	1				
3	1				
4	1				
5	2				
6	4	1	90	2	
7	3				
8	1				
9	1				

The lack of values in the table for particular parameters in particular layers denotes that no HELP model input was required for that parameter in that layer. No data are missing from the table.
Input File: SSYr180.D10; Output File: SSYr180.OUT

HELP Model Input Data for Year 220:

Input Parameter (HELP Model Query)	Generic Input Parameter Value
Landfill area =	0.0189 acres
Percent of area where runoff is possible =	100%
Do you want to specify initial moisture storage? (Y/N)	Y
Amount of water or snow on surface =	0 inches
CN Input Parameter (HELP Model Query)	CN Input Parameter Value
Slope =	1.5 %
Slope length =	825 ft
Soil Texture =	4 (HELP model default soil texture)
Vegetation =	4 (i.e., a good stand of grass)

HELP Model Computed Curve Number = 44.0		
Layer	Layer Number	Layer Type
Topsoil	1	1 (vertical percolation layer)
Upper Backfill	2	1 (vertical percolation layer)
Erosion Barrier	3	1 (vertical percolation layer)
Middle Backfill	4	1 (vertical percolation layer)
Lateral Drainage Layer	5	2 (lateral drainage layer)
HDPE Geomembrane	6	4 (geomembrane liner)
GCL	7	3 (barrier soil liner)
Foundation Layer (1E-06)	8	1 (vertical percolation layer)
Lower Backfill	9	1 (vertical percolation layer)

	Layer Type	Layer Thickness (in)	Soil Texture No.	Total Porosity (Vol/Vol)	Field Capacity (Vol/Vol)	Wilting Point (Vol/Vol)	Initial Moisture (Vol/Vol)
1	1	5.90		0.396	0.109	0.047	0.109
2	1	30		0.35	0.252	0.181	0.252
3	1	12		0.15	0.10	0.07	0.10
4	1	12		0.35	0.252	0.181	0.252
5	2	12		0.410	0.0528	0.0259	0.0528
6	4	0.06					
7	3	0.2		0.750	0.747	0.400	0.750
8	1	12		0.35	0.252	0.181	0.252
9	1	72		0.35	0.252	0.181	0.250

HELP Model Input Data for Year 220 – continued:

	Layer Type	Sat. Hyd. Conductivity (cm/sec)	Drainage Length (ft)	Drain Slope (%)	Leachate Recirc. (%)	Recirc. to Layer (#)	Subsurface Inflow (in/yr)
1	1	3.1E-03					
2	1	4.1E-05					
3	1	1.3E-04					
4	1	4.1E-05					
5	2	4.80E-02	825	4			
6	4	2.0E-13					
7	3	5.0E-08					
8	1	1.0E-06					
9	1	4.1E-05					

	Layer Type	Geomembrane Pinhole Density (#/acre)	Geomembrane Instal. Defects (#/acre)	Geomembrane Placement Quality	Geotextile Transmissivity (cm^2/sec)
1	1				
2	1				
3	1				
4	1				
5	2				
6	4	1	111	2	
7	3				
8	1				
9	1				

The lack of values in the table for particular parameters in particular layers denotes that no HELP model input was required for that parameter in that layer. No data are missing from the table.
Input File: SSYr220.D10; Output File: SSYr220.OUT

HELP Model Input Data for Year 300:

Input Parameter (HELP Model Query)	Generic Input Parameter Value
Landfill area =	0.0189 acres
Percent of area where runoff is possible =	100%
Do you want to specify initial moisture storage? (Y/N)	Y
Amount of water or snow on surface =	0 inches
CN Input Parameter (HELP Model Query)	CN Input Parameter Value
Slope =	1.5 %
Slope length =	825 ft
Soil Texture =	4 (HELP model default soil texture)
Vegetation =	4 (i.e., a good stand of grass)
HELP Model Computed Curve Number = 44.0	

Layer	Layer Number	Layer Type
Topsoil	1	1 (vertical percolation layer)
Upper Backfill	2	1 (vertical percolation layer)
Erosion Barrier	3	1 (vertical percolation layer)
Middle Backfill	4	1 (vertical percolation layer)
Lateral Drainage Layer	5	2 (lateral drainage layer)
HDPE Geomembrane & GCL	6	4 (geomembrane liner)
Foundation Layer (1E-06)	7	1 (vertical percolation layer)
Lower Backfill	8	1 (vertical percolation layer)

	Layer Type	Layer Thickness (in)	Soil Texture No.	Total Porosity (Vol/Vol)	Field Capacity (Vol/Vol)	Wilting Point (Vol/Vol)	Initial Moisture (Vol/Vol)
1	1	5.87		0.396	0.109	0.047	0.109
2	1	30		0.35	0.252	0.181	0.252
3	1	12		0.15	0.10	0.07	0.10
4	1	12		0.35	0.252	0.181	0.252
5	2	12		0.407	0.0555	0.0286	0.0555
6	4	0.26					
7	1	12		0.35	0.252	0.181	0.252
8	1	72		0.35	0.252	0.181	0.252

HELP Model Input Data for Year 300 – continued:

	Layer Type	Sat. Hyd. Conductivity (cm/sec)	Drainage Length (ft)	Drain Slope (%)	Leachate Recirc. (%)	Recirc. to Layer (#)	Subsurface Inflow (in/yr)
1	1	3.1E-03					
2	1	4.1E-05					
3	1	1.3E-04					
4	1	4.1E-05					
5	2	4.72E-02	825	4			
6	4	8.7E-13					
7	1	1.0E-06					
8	1	4.1E-05					

	Layer Type	Geomembrane Pinhole Density (#/acre)	Geomembrane Instal. Defects (#/acre)	Geomembrane Placement Quality	Geotextile Transmissivity (cm^2/sec)
1	1				
2	1				
3	1				
4	1				
5	2				
6	4	1	170	2	
7	1				
8	1				

The lack of values in the table for particular parameters in particular layers denotes that no HELP model input was required for that parameter in that layer. No data are missing from the table.
Input File: SSYr300.D10; Output File: SSYr300.OUT

HELP Model Input Data for Year 380:

Input Parameter (HELP Model Query)		Generic Input Parameter Value	
Landfill area =		0.0189 acres	
Percent of area where runoff is possible =		100%	
Do you want to specify initial moisture storage? (Y/N)		Y	
Amount of water or snow on surface =		0 inches	
CN Input Parameter (HELP Model Query)		CN Input Parameter Value	
Slope =		1.5 %	
Slope length =		825 ft	
Soil Texture =		4 (HELP model default soil texture)	
Vegetation =		4 (i.e., a good stand of grass)	
HELP Model Computed Curve Number = 44.0			
Layer		Layer Number	Layer Type
Topsoil		1	1 (vertical percolation layer)
Upper Backfill		2	1 (vertical percolation layer)
Erosion Barrier		3	1 (vertical percolation layer)
Middle Backfill		4	1 (vertical percolation layer)
Lateral Drainage Layer		5	2 (lateral drainage layer)
HDPE Geomembrane & GCL		6	4 (geomembrane liner)
Foundation Layer (1E-06)		7	1 (vertical percolation layer)
Lower Backfill		8	1 (vertical percolation layer)

	Layer Type	Layer Thickness (in)	Soil Texture No.	Total Porosity (Vol/Vol)	Field Capacity (Vol/Vol)	Wilting Point (Vol/Vol)	Initial Moisture (Vol/Vol)
1	1	5.83		0.396	0.109	0.047	0.109
2	1	30		0.35	0.252	0.181	0.252
3	1	12		0.15	0.10	0.07	0.10
4	1	12		0.35	0.252	0.181	0.252
5	2	12		0.405	0.0584	0.0314	0.0584
6	4	0.26					
7	1	12		0.35	0.252	0.181	0.252
8	1	72		0.35	0.252	0.181	0.252

HELP Model Input Data for Year 380 – continued:

	Layer Type	Sat. Hyd. Conductivity (cm/sec)	Drainage Length (ft)	Drain Slope (%)	Leachate Recirc. (%)	Recirc. To Layer (#)	Subsurface Inflow (in/yr)
1	1	3.1E-03					
2	1	4.1E-05					
3	1	1.3E-04					
4	1	4.1E-05					
5	2	4.64E-02	825	4			
6	4	8.7E-13					
7	1	1.0E-06					
8	1	4.1E-05					

	Layer Type	Geomembrane Pinhole Density (#/acre)	Geomembrane Instal. Defects (#/acre)	Geomembrane Placement Quality	Geotextile Transmissivity (cm^2/sec)
1	1				
2	1				
3	1				
4	1				
5	2				
6	4	1	479	2	
7	1				
8	1				

The lack of values in the table for particular parameters in particular layers denotes that no HELP model input was required for that parameter in that layer. No data are missing from the table.
Input File: SSYr380.D10; Output File: SSYr380.OUT

HELP Model Input Data for Year 460:

Input Parameter (HELP Model Query)	Generic Input Parameter Value
Landfill area =	0.0189 acres
Percent of area where runoff is possible =	100%
Do you want to specify initial moisture storage? (Y/N)	Y
Amount of water or snow on surface =	0 inches
CN Input Parameter (HELP Model Query)	CN Input Parameter Value
Slope =	1.5 %
Slope length =	825 ft
Soil Texture =	4 (HELP model default soil texture)
Vegetation =	4 (i.e., a good stand of grass)
HELP Model Computed Curve Number = 44.0	

Layer	Layer Number	Layer Type
Topsoil	1	1 (vertical percolation layer)
Upper Backfill	2	1 (vertical percolation layer)
Erosion Barrier	3	1 (vertical percolation layer)
Middle Backfill	4	1 (vertical percolation layer)
Lateral Drainage Layer	5	2 (lateral drainage layer)
HDPE Geomembrane & GCL	6	4 (geomembrane liner)
Foundation Layer (1E-06)	7	1 (vertical percolation layer)
Lower Backfill	8	1 (vertical percolation layer)

	Layer Type	Layer Thickness (in)	Soil Texture No.	Total Porosity (Vol/Vol)	Field Capacity (Vol/Vol)	Wilting Point (Vol/Vol)	Initial Moisture (Vol/Vol)
1	1	5.79		0.396	0.109	0.047	0.109
2	1	30		0.35	0.252	0.181	0.252
3	1	12		0.15	0.10	0.07	0.10
4	1	12		0.35	0.252	0.181	0.252
5	2	12		0.402	0.0612	0.0343	0.0612
6	4	0.26					
7	1	12		0.35	0.252	0.181	0.252
8	1	72		0.35	0.252	0.181	0.252

HELP Model Input Data for Year 460 – continued:

	Layer Type	Sat. Hyd. Conductivity (cm/sec)	Drainage Length (ft)	Drain Slope (%)	Leachate Recirc. (%)	Recirc. to Layer (#)	Subsurface Inflow (in/yr)
1	1	3.1E-03					
2	1	4.1E-05					
3	1	1.3E-04					
4	1	4.1E-05					
5	2	4.57E-02	825	4			
6	4	8.7E-13					
7	1	1.0E-06					
8	1	4.1E-05					

	Layer Type	Geomembrane Pinhole Density (#/acre)	Geomembrane Instal. Defects (#/acre)	Geomembrane Placement Quality	Geotextile Transmissivity (cm^2/sec)
1	1				
2	1				
3	1				
4	1				
5	2				
6	4	1	760	2	
7	1				
8	1				

The lack of values in the table for particular parameters in particular layers denotes that no HELP model input was required for that parameter in that layer. No data are missing from the table.
Input File: SSYr460.D10; Output File: SSYr460.OUT

HELP Model Input Data for Year 560:

Input Parameter (HELP Model Query)	Generic Input Parameter Value
Landfill area =	0.0189 acres
Percent of area where runoff is possible =	100%
Do you want to specify initial moisture storage? (Y/N)	Y
Amount of water or snow on surface =	0 inches
CN Input Parameter (HELP Model Query)	CN Input Parameter Value
Slope =	1.5 %
Slope length =	825 ft
Soil Texture =	4 (HELP model default soil texture)
Vegetation =	4 (i.e., a good stand of grass)

HELP Model Computed Curve Number = 44.0		
Layer	Layer Number	Layer Type
Topsoil	1	1 (vertical percolation layer)
Upper Backfill	2	1 (vertical percolation layer)
Erosion Barrier	3	1 (vertical percolation layer)
Middle Backfill	4	1 (vertical percolation layer)
Lateral Drainage Layer	5	2 (lateral drainage layer)
HDPE Geomembrane & GCL	6	4 (geomembrane liner)
Foundation Layer (1E-06)	7	1 (vertical percolation layer)
Lower Backfill	8	1 (vertical percolation layer)

	Layer Type	Layer Thickness (in)	Soil Texture No.	Total Porosity (Vol/Vol)	Field Capacity (Vol/Vol)	Wilting Point (Vol/Vol)	Initial Moisture (Vol/Vol)
1	1	5.78		0.396	0.109	0.047	0.109
2	1	30		0.35	0.252	0.181	0.252
3	1	12		0.15	0.10	0.07	0.10
4	1	12		0.35	0.252	0.181	0.252
5	2	12		0.399	0.0647	0.0378	0.0647
6	4	0.26					
7	1	12		0.35	0.252	0.181	0.252
8	1	72		0.35	0.252	0.181	0.252

HELP Model Input Data for Year 560 – continued:

	Layer Type	Sat. Hyd. Conductivity (cm/sec)	Drainage Length (ft)	Drain Slope (%)	Leachate Recirc. (%)	Recirc. to Layer (#)	Subsurface Inflow (in/yr)
1	1	3.1E-03					
2	1	4.1E-05					
3	1	1.3E-04					
4	1	4.1E-05					
5	2	4.48E-02	825	4			
6	4	8.7E-13					
7	1	1.0E-06					
8	1	4.1E-05					
	Layer Type	Geomembrane Pinhole Density (#/acre)	Geomembrane Instal. Defects (#/acre)		Geomembrane Placement Quality	Geotextile Transmissivity (cm^2/sec)	
1	1						
2	1						
3	1						
4	1						
5	2						
6	4	1	1,115		2		
7	1						
8	1						

The lack of values in the table for particular parameters in particular layers denotes that no HELP model input was required for that parameter in that layer. No data are missing from the table.
Input File: SSYr560.D10; Output File: SSYr560.OUT

HELP Model Input Data for Year 1,000:

Input Parameter (HELP Model Query)	Generic Input Parameter Value
Landfill area =	0.0189 acres
Percent of area where runoff is possible =	100%
Do you want to specify initial moisture storage? (Y/N)	Y
Amount of water or snow on surface =	0 inches
CN Input Parameter (HELP Model Query)	CN Input Parameter Value
Slope =	1.5 %
Slope length =	825 ft
Soil Texture =	4 (HELP model default soil texture)
Vegetation =	4 (i.e., a good stand of grass)
HELP Model Computed Curve Number = 44.0	

Layer	Layer Number	Layer Type
Topsoil	1	1 (vertical percolation layer)
Upper Backfill	2	1 (vertical percolation layer)
Erosion Barrier	3	1 (vertical percolation layer)
Middle Backfill	4	1 (vertical percolation layer)
Lateral Drainage Layer	5	2 (lateral drainage layer)
HDPE Geomembrane & GCL	6	4 (geomembrane liner)
Foundation Layer (1E-06)	7	1 (vertical percolation layer)
Lower Backfill	8	1 (vertical percolation layer)

	Layer Type	Layer Thickness (in)	Soil Texture No.	Total Porosity (Vol/Vol)	Field Capacity (Vol/Vol)	Wilting Point (Vol/Vol)	Initial Moisture (Vol/Vol)
1	1	5.73		0.396	0.109	0.047	0.109
2	1	30		0.35	0.252	0.181	0.252
3	1	12		0.15	0.10	0.07	0.10
4	1	12		0.35	0.252	0.181	0.252
5	2	12		0.384	0.0803	0.0535	0.0803
6	4	0.26					
7	1	12		0.35	0.252	0.181	0.252
8	1	72		0.35	0.252	0.181	0.252

HELP Model Input Data for Year 1,000 – continued:

	Layer Type	Sat. Hyd. Conductivity (cm/sec)	Drainage Length (ft)	Drain Slope (%)	Leachate Recirc. (%)	Recirc. To Layer (#)	Subsurface Inflow (in/yr)
1	1	3.1E-03					
2	1	4.1E-05					
3	1	1.3E-04					
4	1	4.1E-05					
5	2	4.07E-02	825	4			
6	4	8.7E-13					
7	1	1.0E-06					
8	1	4.1E-05					

	Layer Type	Geomembrane Pinhole Density (#/acre)	Geomembrane Instal. Defects (#/acre)	Geomembrane Placement Quality	Geotextile Transmissivity (cm^2/sec)
1	1				
2	1				
3	1				
4	1				
5	2				
6	4	1	2,669	2	
7	1				
8	1				

The lack of values in the table for particular parameters in particular layers denotes that no HELP model input was required for that parameter in that layer. No data are missing from the table.
Input File: SSYr1000.D10; Output File: SSYr1000.OUT

HELP Model Input Data for Year 1,800:

Input Parameter (HELP Model Query)	Generic Input Parameter Value
Landfill area =	0.0189 acres
Percent of area where runoff is possible =	100%
Do you want to specify initial moisture storage? (Y/N)	Y
Amount of water or snow on surface =	0 inches
CN Input Parameter (HELP Model Query)	CN Input Parameter Value
Slope =	1.5%
Slope length =	825 ft
Soil Texture =	4 (HELP model default soil texture)
Vegetation =	4 (i.e., a good stand of grass)

HELP Model Computed Curve Number = 44.0		
Layer	Layer Number	Layer Type
Topsoil	1	1 (vertical percolation layer)
Upper Backfill	2	1 (vertical percolation layer)
Erosion Barrier	3	1 (vertical percolation layer)
Middle Backfill	4	1 (vertical percolation layer)
Lateral Drainage Layer	5	2 (lateral drainage layer)
HDPE Geomembrane & GCL	6	4 (geomembrane liner)
Foundation Layer (1E-06)	7	1 (vertical percolation layer)
Lower Backfill	8	1 (vertical percolation layer)

	Layer Type	Layer Thickness (in)	Soil Texture No.	Total Porosity (Vol/Vol)	Field Capacity (Vol/Vol)	Wilting Point (Vol/Vol)	Initial Moisture (Vol/Vol)
1	1	5.64		0.396	0.109	0.047	0.109
2	1	30		0.35	0.252	0.181	0.252
3	1	12		0.15	0.10	0.07	0.10
4	1	12		0.35	0.252	0.181	0.252
5	2	12		0.358	0.1086	0.0819	0.1086
6	4	0.26					
7	1	12		0.35	0.252	0.181	0.252
8	1	72		0.35	0.252	0.181	0.252

HELP Model Input Data for Year 1,800 – continued:

	Layer Type	Sat. Hyd. Conductivity (cm/sec)	Drainage Length (ft)	Drain Slope (%)	Leachate Recirc. (%)	Recirc. to Layer (#)	Subsurface Inflow (in/yr)
1	1	3.1E-03					
2	1	4.1E-05					
3	1	1.3E-04					
4	1	4.1E-05					
5	2	3.33E-02	825	4			
6	4	8.7E-13					
7	1	1.0E-06					
8	1	4.1E-05					
	Layer Type	Geomembrane Pinhole Density (#/acre)		Geomembrane Instal. Defects (#/acre)	Geomembrane Placement Quality		Geotextile Transmissivity (cm^2/sec)
1	1						
2	1						
3	1						
4	1						
5	2						
6	4	1		5,496	2		
7	1						
8	1						

The lack of values in the table for particular parameters in particular layers denotes that no HELP model input was required for that parameter in that layer. No data are missing from the table.
Input File: SSYr1800.D10; Output File: SSYr1800.OUT

HELP Model Input Data for Year 3,200:

Input Parameter (HELP Model Query)	Generic Input Parameter Value
Landfill area =	0.0189 acres
Percent of area where runoff is possible =	100%
Do you want to specify initial moisture storage? (Y/N)	Y
Amount of water or snow on surface =	0 inches
CN Input Parameter (HELP Model Query)	CN Input Parameter Value
Slope =	1.5%
Slope length =	825 ft
Soil Texture =	4 (HELP model default soil texture)
Vegetation =	4 (i.e., a good stand of grass)
HELP Model Computed Curve Number = 44.0	

Layer	Layer Number	Layer Type
Topsoil	1	1 (vertical percolation layer)
Upper Backfill	2	1 (vertical percolation layer)
Erosion Barrier	3	1 (vertical percolation layer)
Middle Backfill	4	1 (vertical percolation layer)
Lateral Drainage Layer	5	2 (lateral drainage layer)
HDPE Geomembrane & GCL	6	4 (geomembrane liner)
Foundation Layer (1E-06)	7	1 (vertical percolation layer)
Lower Backfill	8	1 (vertical percolation layer)

	Layer Type	Layer Thickness (in)	Soil Texture No.	Total Porosity (Vol/Vol)	Field Capacity (Vol/Vol)	Wilting Point (Vol/Vol)	Initial Moisture (Vol/Vol)
1	1	5.49		0.396	0.109	0.047	0.109
2	1	30		0.35	0.252	0.181	0.252
3	1	12		0.15	0.10	0.07	0.10
4	1	12		0.35	0.252	0.181	0.252
5	2	12		0.312	0.1579	0.1315	0.1579
6	4	0.26					
7	1	12		0.35	0.252	0.181	0.252
8	1	72		0.35	0.252	0.181	0.252

HELP Model Input Data for Year 3,200 – continued:

	Layer Type	Sat. Hyd. Conductivity (cm/sec)	Drainage Length (ft)	Drain Slope (%)	Leachate Recirc. (%)	Recirc. to Layer (#)	Subsurface Inflow (in/yr)
1	1	3.1E-03					
2	1	4.1E-05					
3	1	1.3E-04					
4	1	4.1E-05					
5	2	2.05E-02	825	4			
6	4	8.7E-13					
7	1	1.0E-06					
8	1	4.1E-05					
	Layer Type	Geomembrane Pinhole Density (#/acre)	Geomembrane Instal. Defects (#/acre)	Geomembrane Placement Quality	Geotextile Transmissivity (cm^2/sec)
1	1				
2	1				
3	1				
4	1				
5	2				
6	4	1	10,442	2	
7	1				
8	1				

The lack of values in the table for particular parameters in particular layers denotes that no HELP model input was required. No data are missing from the table.
Input File: SSYr3200.D10; Output File: SSYr3200.OUT

HELP Model Input Data for Year 5,412:

Input Parameter (HELP Model Query)			Generic Input Parameter Value			
Landfill area =			0.0189 acres			
Percent of area where runoff is possible =			100%			
Do you want to specify initial moisture storage? (Y/N)			Y			
Amount of water or snow on surface =			0 inches			
CN Input Parameter (HELP Model Query)			CN Input Parameter Value			
Slope =			1.5%			
Slope length =			825 ft			
Soil Texture =			4 (HELP model default soil texture)			
Vegetation =			4 (i.e., a good stand of grass)			
HELP Model Computed Curve Number = 44.0						
Layer		Layer Number		Layer Type		
Topsoil		1		1 (vertical percolation layer)		
Upper Backfill		2		1 (vertical percolation layer)		
Erosion Barrier		3		1 (vertical percolation layer)		
Middle Backfill		4		1 (vertical percolation layer)		
Lateral Drainage Layer		5		2 (lateral drainage layer)		
HDPE Geomembrane & GCL		6		4 (geomembrane liner)		
Foundation Layer (1E-06)		7		1 (vertical percolation layer)		
Lower Backfill		8		1 (vertical percolation layer)		

	Layer Type	Layer Thickness (in)	Soil Texture No.	Total Porosity (Vol/Vol)	Field Capacity (Vol/Vol)	Wilting Point (Vol/Vol)	Initial Moisture (Vol/Vol)
1	1	5.25		0.396	0.109	0.047	0.109
2	1	30		0.35	0.252	0.181	0.252
3	1	12		0.15	0.10	0.07	0.10
4	1	12		0.35	0.252	0.181	0.252
5	2	12		0.240	0.236	0.210	0.236
6	4	0.26					
7	1	12		0.35	0.252	0.181	0.252
8	1	72		0.35	0.252	0.181	0.252

HELP Model Input Data for Year 5,412 – continued:

	Layer Type	Sat. Hyd. Conductivity (cm/sec)	Drainage Length (ft)	Drain Slope (%)	Leachate Recirc. (%)	Recirc. to Layer (#)	Subsurface Inflow (in/yr)
1	1	3.1E-03					
2	1	4.1E-05					
3	1	1.3E-04					
4	1	4.1E-05					
5	2	4.09E-05	825	4			
6	4	8.7E-13					
7	1	1.0E-06					
8	1	4.1E-05					

	Layer Type	Geomembrane Pinhole Density (#/acre)	Geomembrane Instal. Defects (#/acre)	Geomembrane Placement Quality	Geotextile Transmissivity (cm^2/sec)
1	1				
2	1				
3	1				
4	1				
5	2				
6	4	1	18,257	2	
7	1				
8	1				

The lack of values in the table for particular parameters in particular layers denotes that no HELP model input was required. No data are missing from the table.
Input File: SSYr5412.D10; Output File: SSYr5412.OUT

HELP Model Input Data for Year 5,600:

Input Parameter (HELP Model Query)	Generic Input Parameter Value
Landfill area =	0.0189 acres
Percent of area where runoff is possible =	100%
Do you want to specify initial moisture storage? (Y/N)	Y
Amount of water or snow on surface =	0 inches
CN Input Parameter (HELP Model Query)	CN Input Parameter Value
Slope =	1.5%
Slope length =	825 ft
Soil Texture =	4 (HELP model default soil texture)
Vegetation =	4 (i.e., a good stand of grass)

HELP Model Computed Curve Number = 44.0		
Layer	Layer Number	Layer Type
Topsoil	1	1 (vertical percolation layer)
Upper Backfill	2	1 (vertical percolation layer)
Erosion Barrier	3	1 (vertical percolation layer)
Middle Backfill	4	1 (vertical percolation layer)
Lateral Drainage Layer	5	2 (lateral drainage layer)
HDPE Geomembrane & GCL	6	4 (geomembrane liner)
Foundation Layer (1E-06)	7	1 (vertical percolation layer)
Lower Backfill	8	1 (vertical percolation layer)

	Layer Type	Layer Thickness (in)	Soil Texture No.	Total Porosity (Vol/Vol)	Field Capacity (Vol/Vol)	Wilting Point (Vol/Vol)	Initial Moisture (Vol/Vol)
1	1	5.23		0.396	0.109	0.047	0.109
2	1	30		0.35	0.252	0.181	0.252
3	1	12		0.15	0.10	0.07	0.10
4	1	12		0.35	0.252	0.181	0.252
5	2	12		0.240	0.236	0.210	0.236
6	4	0.26					
7	1	12		0.35	0.252	0.181	0.252
8	1	72		0.35	0.252	0.181	0.252

HELP Model Input Data for Year 5,600 – continued:

	Layer Type	Sat. Hyd. Conductivity (cm/sec)	Drainage Length (ft)	Drain Slope (%)	Leachate Recirc. (%)	Recirc. to Layer (#)	Subsurface Inflow (in/yr)
1	1	3.1E-03					
2	1	4.1E-05					
3	1	1.3E-04					
4	1	4.1E-05					
5	2	4.09E-05	825	4			
6	4	8.7E-13					
7	1	1.0E-06					
8	1	4.1E-05					

	Layer Type	Geomembrane Pinhole Density (#/acre)	Geomembrane Instal. Defects (#/acre)	Geomembrane Placement Quality	Geotextile Transmissivity (cm^2/sec)
1	1				
2	1				
3	1				
4	1				
5	2				
6	4	1	18,921	2	
7	1				
8	1				

The lack of values in the table for particular parameters in particular layers denotes that no HELP model input was required. No data are missing from the table.
Input File: SSYr5600; Output File: SSYr5600.OUT

HELP Model Input Data for Year 10,000:

Input Parameter (HELP Model Query)	Generic Input Parameter Value
Landfill area =	0.0189 acres
Percent of area where runoff is possible =	100%
Do you want to specify initial moisture storage? (Y/N)	Y
Amount of water or snow on surface =	0 inches
CN Input Parameter (HELP Model Query)	CN Input Parameter Value
Slope =	1.5%
Slope length =	825 ft
Soil Texture =	4 (HELP model default soil texture)
Vegetation =	4 (i.e., a good stand of grass)

HELP Model Computed Curve Number = 44.0		
Layer	Layer Number	Layer Type
Topsoil	1	1 (vertical percolation layer)
Upper Backfill	2	1 (vertical percolation layer)
Erosion Barrier	3	1 (vertical percolation layer)
Middle Backfill	4	1 (vertical percolation layer)
Lateral Drainage Layer	5	2 (lateral drainage layer)
HDPE Geomembrane & GCL	6	4 (geomembrane liner)
Foundation Layer (1E-06)	7	1 (vertical percolation layer)
Lower Backfill	8	1 (vertical percolation layer)

	Layer Type	Layer Thickness (in)	Soil Texture No.	Total Porosity (Vol/Vol)	Field Capacity (Vol/Vol)	Wilting Point (Vol/Vol)	Initial Moisture (Vol/Vol)
1	1	4.74		0.396	0.109	0.047	0.109
2	1	30		0.35	0.252	0.181	0.252
3	1	12		0.15	0.10	0.07	0.10
4	1	12		0.35	0.252	0.181	0.252
5	2	12		0.240	0.236	0.210	0.236
6	4	0.26					
7	1	12		0.35	0.252	0.181	0.252
8	1	72		0.35	0.252	0.181	0.252

HELP Model Input Data for Year 10,000 – continued:

	Layer Type	Sat. Hyd. Conductivity (cm/sec)	Drainage Length (ft)	Drain Slope (%)	Leachate Recirc. (%)	Recirc. to Layer (#)	Subsurface Inflow (in/yr)
1	1	3.1E-03					
2	1	4.1E-05					
3	1	1.3E-04					
4	1	4.1E-05					
5	2	4.09E-05	825	4			
6	4	8.7E-13					
7	1	1.0E-06					
8	1	4.1E-05					

	Layer Type	Geomembrane Pinhole Density (#/acre)	Geomembrane Instal. Defects (#/acre)	Geomembrane Placement Quality	Geotextile Transmissivity (cm^2/sec)
1	1				
2	1				
3	1				
4	1				
5	2				
6	4	1	34,466	2	
7	1				
8	1				

The lack of values in the table for particular parameters in particular layers denotes that no HELP model input was required. No data are missing from the table.
Input File: SSY10000.D10; Output File: SSY10000.OUT

APPENDIX K.
SDF DETAILED HELP MODEL ANNUAL WATER BALANCE DATA OVER TIME

Detailed HELP Model Annual Water Balance Data (Year 0):

Simulation	Precip-itation (in/yr)	Runoff (in/yr)	Evapotrans-piration (in/yr)	Lateral Drainage (in/yr)	Infiltration thru GCL (in/yr)	Change in Water Storage (in/yr)
1	40.07	0.000	31.653	5.012	0.00007	3.405
2	57.14	0.000	32.094	25.559	0.00047	-0.514
3	52.64	0.000	31.091	21.023	0.00039	0.525
4	47.88	0.952	38.428	8.618	0.00011	-0.118
5	50.57	0.000	34.394	14.579	0.00021	1.597
6	42.28	0.000	27.895	13.293	0.00020	1.092
7	39.35	0.515	30.611	14.087	0.00021	-5.863
8	49.46	0.496	31.513	15.683	0.00023	1.768
9	48.59	0.000	33.584	14.162	0.00020	0.844
10	53.97	0.000	33.801	19.476	0.00128	0.691
11	57.63	0.519	32.485	23.117	0.00169	1.508
12	46.71	0.000	29.261	20.064	0.00043	-2.616
13	38.58	0.000	30.408	7.630	0.00010	0.542
14	41.49	0.375	27.772	12.974	0.00021	0.369
15	44.94	1.022	32.596	13.504	0.00019	-2.182
16	54.78	0.403	32.071	21.680	0.00080	0.625
17	29.81	0.000	21.668	8.670	0.00013	-0.527
18	49.55	0.000	34.875	12.483	0.00017	2.192
19	55.5	0.731	33.801	21.711	0.00056	-0.743
20	68.56	0.000	37.421	28.076	0.00050	3.062
21	51.14	0.000	33.889	18.378	0.00032	-1.128
22	51.22	0.000	36.717	15.709	0.00023	-1.206
23	47.94	0.000	36.519	14.232	0.00024	-2.811
24	59.17	1.197	31.104	23.866	0.00053	3.002
25	47.73	0.026	30.422	15.851	0.00024	1.430
26	50.56	0.194	31.902	18.033	0.00045	0.431
27	37.02	0.000	32.179	7.802	0.00011	-2.961
28	56.03	0.788	35.941	20.372	0.00036	-1.072
29	39.77	0.000	29.486	8.656	0.00012	1.628
30	46.55	0.299	33.879	12.899	0.00018	-0.527
31	39.45	0.060	28.852	13.314	0.00021	-2.776
32	45.35	0.375	29.810	13.095	0.00020	2.069
33	42.23	0.000	31.920	8.650	0.00011	1.660
34	37.81	0.000	27.329	11.345	0.00017	-0.864
35	48.19	0.286	34.232	14.683	0.00021	-1.011
36	62.28	3.520	34.055	20.928	0.00034	3.776

Detailed HELP Model Annual Water Balance Data (Year 0) – Continued:

Simulation	Precip-itation (in/yr)	Runoff (in/yr)	Evapotrans-piration (in/yr)	Lateral Drainage (in/yr)	Infiltration thru GCL (in/yr)	Change in Water Storage (in/yr)
37	55.96	0.000	40.470	15.504	0.00023	-0.014
38	40.26	0.000	28.231	13.337	0.00020	-1.308
39	60.02	0.757	35.069	24.051	0.00266	0.140
40	59.62	0.734	37.266	22.143	0.00035	-0.523
41	47.6	0.000	31.552	14.972	0.00023	1.076
42	50.44	0.521	34.131	16.257	0.00024	-0.469
43	39.42	0.061	26.348	11.368	0.00016	1.643
44	48.61	0.000	34.012	14.426	0.00022	0.172
45	57.35	0.000	34.920	27.972	0.00115	-5.544
46	47.49	0.000	32.002	12.424	0.00019	3.064
47	38.98	0.000	31.676	8.662	0.00012	-1.357
48	42.99	0.000	32.707	9.431	0.00013	0.852
49	53.01	1.660	34.259	14.000	0.00020	3.091
50	55.17	0.038	38.068	20.492	0.00033	-3.429
51	46.16	0.000	31.254	11.461	0.00017	3.445
52	42.63	0.000	33.706	13.594	0.00021	-4.670
53	50.93	0.000	32.529	18.477	0.00028	-0.076
54	54.24	0.582	28.380	21.065	0.00036	4.212
55	50.46	0.218	33.032	16.123	0.00025	1.086
56	56.39	1.110	38.507	21.161	0.00034	-4.388
57	41.99	0.000	27.957	13.283	0.00020	0.750
58	68.6	0.196	35.690	31.238	0.00061	1.475
59	48.67	0.089	33.998	13.095	0.00020	1.488
60	58.12	0.000	34.682	23.625	0.00139	-0.189
61	54.9	0.818	31.330	23.023	0.00234	-0.274
62	56.29	0.676	33.394	24.986	0.00161	-2.768
63	49.13	0.373	34.389	15.138	0.00022	-0.770
64	54.54	0.357	32.299	19.237	0.00031	2.648
65	45.05	0.000	32.895	13.204	0.00019	-1.049
66	37.07	0.000	29.786	9.315	0.00013	-2.031
67	40.17	0.000	25.008	11.236	0.00016	3.926
68	58.08	0.000	35.404	24.617	0.00044	-1.941
69	36.31	0.000	27.132	9.791	0.00013	-0.613
70	42.67	0.996	31.928	12.960	0.00020	-3.214
71	48.88	0.000	35.433	10.298	0.00015	3.149
72	47.36	0.511	32.743	17.261	0.00027	-3.156
73	35.81	0.000	26.582	8.445	0.00012	0.783
74	49.81	0.686	29.649	16.586	0.00025	2.889

Detailed HELP Model Annual Water Balance Data (Year 0) – Continued:

Simulation	Precip-itation (in/yr)	Runoff (in/yr)	Evapotrans-piration (in/yr)	Lateral Drainage (in/yr)	Infiltration thru GCL (in/yr)	Change in Water Storage (in/yr)
75	56.43	3.794	34.422	17.306	0.00026	0.909
76	45.86	0.000	32.558	14.927	0.00022	-1.625
77	56.76	0.000	39.094	18.548	0.00029	-0.882
78	39.15	0.000	29.545	8.739	0.00013	0.866
79	48.87	0.000	30.969	14.078	0.00045	3.823
80	58.52	0.000	33.441	28.582	0.00269	-3.505
81	53.34	0.000	35.503	16.716	0.00025	1.121
82	55.18	0.000	35.565	18.131	0.00030	1.484
83	53.6	1.004	34.982	21.310	0.00138	-3.697
84	47.82	0.000	34.131	13.107	0.00020	0.582
85	44.69	0.000	30.890	10.407	0.00014	3.393
86	60.77	0.000	35.862	27.603	0.00052	-2.696
87	48.34	1.111	29.576	14.473	0.00029	3.180
88	36.18	0.000	26.170	15.266	0.00079	-5.256
89	58.29	2.732	35.158	18.661	0.00035	1.739
90	60.08	0.200	30.458	24.690	0.00122	4.731
91	55.49	0.000	35.952	22.554	0.00049	-3.016
92	44.51	0.202	32.164	12.478	0.00018	-0.334
93	35.83	0.000	29.650	9.256	0.00013	-3.076
94	45.02	0.000	32.964	10.183	0.00013	1.874
95	44.54	0.000	27.674	18.482	0.00111	-1.617
96	53.18	0.108	35.709	14.078	0.00022	3.285
97	48.03	0.359	31.468	17.114	0.00026	-0.910
98	62.58	1.090	41.484	17.430	0.00027	2.576
99	48.78	0.684	31.534	19.955	0.00041	-3.393
100	49.29	0.000	35.871	10.134	0.00013	3.284
Summary Statistics						
Count	100	100	100	100	100	100
Maximum	68.60	3.794	41.484	31.238	0.00269	4.731
Average	49.14	0.334	32.569	16.177	0.00042	0.062
Median	48.83	0.000	32.577	15.055	0.00023	0.271
Minimum	29.81	0.000	21.668	5.012	0.00007	-5.863
Std Dev	7.69	0.652	3.380	5.539	0.00050	2.404

Detailed HELP Model Annual Water Balance Data (Year 100):

Simulation	Precip- itation (in/yr)	Runoff (in/yr)	Evapotrans- piration (in/yr)	Lateral Drainage (in/yr)	Infiltration thru GCL (in/yr)	Change in Water Storage (in/yr)
1	40.07	0.000	31.645	5.024	0.00030	3.400
2	57.14	0.000	32.085	25.563	0.00319	-0.511
3	52.64	0.000	31.055	21.052	0.00284	0.530
4	47.88	0.960	38.437	8.609	0.00053	-0.127
5	50.57	0.000	34.397	14.593	0.00116	1.579
6	42.28	0.000	27.901	13.277	0.00115	1.101
7	39.35	0.523	30.611	14.065	0.00126	-5.850
8	49.46	0.504	31.564	15.628	0.00134	1.764
9	48.59	0.000	33.572	14.175	0.00105	0.842
10	53.97	0.000	33.899	19.372	0.01257	0.693
11	57.63	0.527	32.484	23.085	0.01626	1.527
12	46.71	0.000	29.239	20.090	0.00342	-2.627
13	38.58	0.000	30.421	7.611	0.00049	0.539
14	41.49	0.381	27.792	12.951	0.00127	0.358
15	44.94	1.027	32.620	13.471	0.00107	-2.179
16	54.78	0.421	32.072	21.657	0.00716	0.624
17	29.81	0.000	21.662	8.672	0.00070	-0.527
18	49.55	0.000	34.892	12.465	0.00091	2.193
19	55.5	0.732	33.845	21.665	0.00491	-0.748
20	68.56	0.000	37.414	28.095	0.00330	3.048
21	51.14	0.000	33.842	18.413	0.00214	-1.118
22	51.22	0.000	36.697	15.732	0.00124	-1.209
23	47.94	0.000	36.530	14.216	0.00161	-2.808
24	59.17	1.203	31.115	23.837	0.00423	3.010
25	47.73	0.031	30.414	15.862	0.00142	1.421
26	50.56	0.200	31.924	17.997	0.00355	0.435
27	37.02	0.000	32.197	7.790	0.00055	-2.968
28	56.03	0.794	35.908	20.390	0.00241	-1.064
29	39.77	0.000	29.479	8.669	0.00061	1.621
30	46.55	0.306	33.965	12.766	0.00092	-0.488
31	39.45	0.066	28.859	13.327	0.00128	-2.803
32	45.35	0.382	29.773	13.126	0.00113	2.068
33	42.23	0.000	31.922	8.647	0.00055	1.661
34	37.81	0.000	27.338	11.338	0.00094	-0.867
35	48.19	0.293	34.204	14.705	0.00117	-1.013
36	62.28	3.528	34.023	20.951	0.00224	3.776

Detailed HELP Model Annual Water Balance Data (Year 100) – Continued:

Simulation	Precip-itation (in/yr)	Runoff (in/yr)	Evapotrans-piration (in/yr)	Lateral Drainage (in/yr)	Infiltration thru GCL (in/yr)	Change in Water Storage (in/yr)
37	55.96	0.000	40.450	15.524	0.00131	-0.016
38	40.26	0.000	28.237	13.320	0.00111	-1.299
39	60.02	0.906	35.035	23.918	0.02579	0.154
40	59.62	0.746	37.258	22.141	0.00208	-0.534
41	47.6	0.000	31.554	14.964	0.00133	1.073
42	50.44	0.514	34.105	16.292	0.00137	-0.478
43	39.42	0.068	26.329	11.395	0.00086	1.623
44	48.61	0.000	33.980	14.441	0.00128	0.188
45	57.35	0.000	34.910	27.979	0.01045	-5.545
46	47.49	0.000	32.009	12.411	0.00107	3.062
47	38.98	0.000	31.701	8.631	0.00059	-1.352
48	42.99	0.000	32.698	9.470	0.00062	0.821
49	53.01	1.667	34.192	14.040	0.00112	3.110
50	55.17	0.049	38.099	20.432	0.00209	-3.412
51	46.16	0.000	31.211	11.497	0.00094	3.451
52	42.63	0.000	33.770	13.537	0.00125	-4.678
53	50.93	0.000	32.519	18.492	0.00162	-0.083
54	54.24	0.595	28.391	21.028	0.00243	4.225
55	50.46	0.224	33.001	16.186	0.00147	1.047
56	56.39	1.122	38.532	21.087	0.00208	-4.354
57	41.99	0.000	27.980	13.321	0.00118	0.687
58	68.6	0.204	35.664	31.193	0.00440	1.536
59	48.67	0.082	33.981	13.123	0.00119	1.480
60	58.12	0.000	34.707	23.592	0.01321	-0.186
61	54.9	0.924	31.328	22.888	0.02273	-0.248
62	56.29	0.683	33.382	24.983	0.01550	-2.767
63	49.13	0.391	34.410	15.096	0.00121	-0.777
64	54.54	0.364	32.294	19.237	0.00190	2.637
65	45.05	0.000	32.927	13.170	0.00107	-1.055
66	37.07	0.000	29.771	9.328	0.00067	-2.038
67	40.17	0.000	25.010	11.235	0.00089	3.917
68	58.08	0.000	35.387	24.637	0.00301	-1.947
69	36.31	0.000	27.104	9.808	0.00070	-0.602
70	42.67	1.003	31.955	12.928	0.00116	-3.217
71	48.88	0.000	35.422	10.312	0.00085	3.145
72	47.36	0.517	32.743	17.253	0.00163	-3.154
73	35.81	0.000	26.599	8.431	0.00065	0.780
74	49.81	0.694	29.601	16.615	0.00147	2.899

Detailed HELP Model Annual Water Balance Data for (Year 100) – Continued:

Simulation	Precip- itation (in/yr)	Runoff (in/yr)	Evapotrans- piration (in/yr)	Lateral Drainage (in/yr)	Infiltration thru GCL (in/yr)	Change in Water Storage (in/yr)
75	56.43	3.807	34.458	17.262	0.00145	0.901
76	45.86	0.000	32.522	14.965	0.00129	-1.629
77	56.76	0.000	39.110	18.525	0.00175	-0.877
78	39.15	0.000	29.528	8.750	0.00072	0.871
79	48.87	0.000	30.960	14.087	0.00393	3.819
80	58.52	0.000	33.416	28.587	0.02767	-3.490
81	53.34	0.000	35.530	16.687	0.00140	1.114
82	55.18	0.000	35.567	18.130	0.00190	1.475
83	53.6	1.152	34.966	21.161	0.01289	-3.687
84	47.82	0.000	34.216	13.015	0.00119	0.580
85	44.69	0.000	30.918	10.398	0.00072	3.365
86	60.77	0.000	35.831	27.615	0.00370	-2.682
87	48.34	1.123	29.594	14.442	0.00207	3.174
88	36.18	0.000	26.148	15.280	0.00773	-5.256
89	58.29	2.738	35.133	18.674	0.00252	1.741
90	60.08	0.207	30.431	24.701	0.01182	4.735
91	55.49	0.000	35.940	22.557	0.00390	-3.013
92	44.51	0.207	32.162	12.494	0.00105	-0.360
93	35.83	0.000	29.648	9.245	0.00070	-3.063
94	45.02	0.000	32.934	10.217	0.00065	1.869
95	44.54	0.000	27.620	18.521	0.01113	-1.608
96	53.18	0.115	35.707	14.064	0.00129	3.287
97	48.03	0.364	31.462	17.124	0.00156	-0.922
98	62.58	1.104	41.480	17.413	0.00165	2.581
99	48.78	0.689	31.556	19.934	0.00312	-3.403
100	49.29	0.000	35.864	10.135	0.00063	3.291
Summary Statistics						
Count	100	100	100	100	100	100
Maximum	68.60	3.807	41.480	31.193	0.02767	4.735
Average	49.14	0.341	32.567	16.168	0.00333	0.062
Median	48.83	0.000	32.571	15.030	0.00133	0.273
Minimum	29.81	0.000	21.662	5.024	0.00030	-5.850
Std Dev	7.69	0.658	3.382	5.532	0.00516	2.403

Detailed HELP Model Annual Water Balance Data (Year 180):

Simulation	Precip-itation (in/yr)	Runoff (in/yr)	Evapotrans-piration (in/yr)	Lateral Drainage (in/yr)	Infiltration thru GCL (in/yr)	Change in Water Storage (in/yr)
1	40.07	0.000	31.629	5.046	0.00376	3.394
2	57.14	0.000	32.001	25.602	0.04349	-0.464
3	52.64	0.000	31.089	20.979	0.04021	0.568
4	47.88	0.967	38.416	8.620	0.00662	-0.135
5	50.57	0.000	34.397	14.578	0.01487	1.588
6	42.28	0.000	27.894	13.281	0.01489	1.094
7	39.35	0.530	30.602	14.039	0.01627	-5.833
8	49.46	0.512	31.576	15.594	0.01727	1.767
9	48.59	0.000	33.575	14.162	0.01335	0.841
10	53.97	0.000	33.851	19.271	0.17381	0.808
11	57.63	0.535	32.434	22.906	0.22295	1.647
12	46.71	0.000	29.226	20.061	0.05039	-2.686
13	38.58	0.000	30.406	7.615	0.00614	0.488
14	41.49	0.385	27.784	12.934	0.01657	0.341
15	44.94	1.032	32.606	13.470	0.01375	-2.208
16	54.78	0.446	32.060	21.556	0.09982	0.672
17	29.81	0.000	21.660	8.658	0.00902	-0.559
18	49.55	0.000	34.887	12.461	0.01161	2.159
19	55.5	0.795	33.752	21.633	0.07173	-0.719
20	68.56	0.000	37.422	28.069	0.04444	3.042
21	51.14	0.000	33.812	18.382	0.02975	-1.101
22	51.22	0.000	36.713	15.713	0.01586	-1.249
23	47.94	0.000	36.544	14.178	0.02156	-2.822
24	59.17	1.210	31.131	23.759	0.06219	3.038
25	47.73	0.037	30.391	15.863	0.01852	1.397
26	50.56	0.208	31.914	17.948	0.04902	0.448
27	37.02	0.000	32.219	7.758	0.00688	-3.001
28	56.03	0.799	35.909	20.357	0.03261	-1.065
29	39.77	0.000	29.464	8.681	0.00767	1.590
30	46.55	0.313	33.879	12.860	0.01173	-0.537
31	39.45	0.072	28.851	13.289	0.01667	-2.790
32	45.35	0.390	29.789	13.081	0.01452	2.059
33	42.23	0.000	31.925	8.653	0.00688	1.615
34	37.81	0.000	27.338	11.311	0.01212	-0.868
35	48.19	0.301	34.166	14.730	0.01500	-1.030
36	62.28	3.535	34.023	20.920	0.03060	3.785

Detailed HELP Model Annual Water Balance Data (Year 180) – Continued:

Simulation	Precip-itation (in/yr)	Runoff (in/yr)	Evapotrans-piration (in/yr)	Lateral Drainage (in/yr)	Infiltration thru GCL (in/yr)	Change in Water Storage (in/yr)
37	55.96	0.000	40.413	15.534	0.01691	-0.009
38	40.26	0.000	28.235	13.313	0.01424	-1.318
39	60.02	0.867	34.991	23.684	0.34987	0.386
40	59.62	0.758	37.227	22.136	0.02706	-0.570
41	47.6	0.000	31.591	14.918	0.01719	1.020
42	50.44	0.507	34.112	16.264	0.01776	-0.492
43	39.42	0.076	26.343	11.361	0.01089	1.597
44	48.61	0.000	33.993	14.415	0.01662	0.168
45	57.35	0.000	34.915	27.843	0.14565	-5.464
46	47.49	0.000	32.005	12.396	0.01380	3.029
47	38.98	0.000	31.624	8.688	0.00748	-1.376
48	42.99	0.000	32.699	9.495	0.00784	0.757
49	53.01	1.674	34.167	14.042	0.01440	3.094
50	55.17	0.058	38.067	20.407	0.02739	-3.382
51	46.16	0.000	31.223	11.487	0.01219	3.422
52	42.63	0.000	33.808	13.472	0.01620	-4.681
53	50.93	0.000	32.538	18.456	0.02096	-0.090
54	54.24	0.607	28.376	21.012	0.03370	4.226
55	50.46	0.232	33.001	16.145	0.01904	1.052
56	56.39	1.136	38.494	21.078	0.02732	-4.342
57	41.99	0.000	27.949	13.339	0.01528	0.671
58	68.6	0.211	35.661	31.141	0.05875	1.573
59	48.67	0.075	33.994	13.105	0.01557	1.458
60	58.12	0.003	34.687	23.460	0.18154	-0.122
61	54.9	0.945	31.325	22.574	0.30191	0.002
62	56.29	0.690	33.367	24.798	0.21072	-2.666
63	49.13	0.405	34.447	15.025	0.01549	-0.920
64	54.54	0.371	32.276	19.237	0.02493	2.595
65	45.05	0.000	32.936	13.139	0.01368	-1.076
66	37.07	0.000	29.787	9.302	0.00851	-2.066
67	40.17	0.000	24.984	11.196	0.01134	3.951
68	58.08	0.000	35.383	24.680	0.04118	-2.009
69	36.31	0.000	27.087	9.792	0.00888	-0.609
70	42.67	1.010	31.929	12.931	0.01505	-3.235
71	48.88	0.000	35.442	10.280	0.01087	3.121
72	47.36	0.523	32.737	17.229	0.02126	-3.158
73	35.81	0.000	26.558	8.462	0.00826	0.753
74	49.81	0.723	29.595	16.600	0.01907	2.872

Detailed HELP Model Annual Water Balance Data (Year 180) – Continued:

Simulation	Precip-itation (in/yr)	Runoff (in/yr)	Evapotrans-piration (in/yr)	Lateral Drainage (in/yr)	Infiltration thru GCL (in/yr)	Change in Water Storage (in/yr)
75	56.43	3.820	34.426	17.254	0.01868	0.907
76	45.86	0.000	32.541	14.921	0.01662	-1.629
77	56.76	0.000	39.105	18.514	0.02412	-0.887
78	39.15	0.000	29.545	8.729	0.00930	0.841
79	48.87	0.000	30.977	14.007	0.05507	3.856
80	58.52	0.000	33.385	28.286	0.36710	-3.242
81	53.34	0.000	35.537	16.666	0.01807	1.071
82	55.18	0.000	35.577	18.099	0.02560	1.442
83	53.6	1.209	34.959	20.943	0.17670	-3.618
84	47.82	0.000	34.226	12.990	0.01544	0.517
85	44.69	0.000	30.850	10.457	0.00904	3.326
86	60.77	0.000	35.831	27.575	0.05145	-2.666
87	48.34	1.135	29.587	14.403	0.02884	3.170
88	36.18	0.000	26.152	15.174	0.10832	-5.232
89	58.29	2.744	35.121	18.654	0.03501	1.725
90	60.08	0.214	30.451	24.514	0.16863	4.793
91	55.49	0.000	35.938	22.535	0.05514	-3.062
92	44.51	0.211	32.168	12.448	0.01342	-0.397
93	35.83	0.000	29.610	9.267	0.00889	-3.098
94	45.02	0.000	32.955	10.186	0.00809	1.837
95	44.54	0.000	27.592	18.412	0.15683	-1.541
96	53.18	0.122	35.708	14.032	0.01681	3.256
97	48.03	0.370	31.462	17.102	0.02024	-0.943
98	62.58	1.117	41.455	17.407	0.02160	2.567
99	48.78	0.695	31.564	19.892	0.04235	-3.408
100	49.29	0.000	35.857	10.134	0.00783	3.259
Summary Statistics						
Count	100	100	100	100	100	100
Maximum	68.60	3.820	41.455	31.141	0.36710	4.793
Average	49.14	0.346	32.559	16.130	0.04520	0.063
Median	48.83	0.000	32.574	14.973	0.01723	0.364
Minimum	29.81	0.000	21.660	5.046	0.00376	-5.833
Std Dev	7.69	0.662	3.381	5.497	0.07009	2.395

Detailed HELP Model Annual Water Balance Data (Year 220):

Simulation	Precip- itation (in/yr)	Runoff (in/yr)	Evapotrans- piration (in/yr)	Lateral Drainage (in/yr)	Infiltration thru GCL (in/yr)	Change in Water Storage (in/yr)
1	40.07	0.000	31.620	5.056	0.00470	3.392
2	57.14	0.000	32.016	25.576	0.05670	-0.454
3	52.64	0.000	31.090	20.950	0.05112	0.595
4	47.88	0.970	38.395	8.650	0.00830	-0.151
5	50.57	0.000	34.420	14.578	0.01857	1.563
6	42.28	0.000	27.901	13.255	0.01850	1.109
7	39.35	0.533	30.585	14.037	0.02026	-5.825
8	49.46	0.516	31.402	15.768	0.02190	1.757
9	48.59	0.000	33.583	14.143	0.01661	0.847
10	53.97	0.000	33.812	19.268	0.21829	0.819
11	57.63	0.539	32.458	22.828	0.27711	1.704
12	46.71	0.000	29.248	20.018	0.06465	-2.695
13	38.58	0.000	30.391	7.628	0.00765	0.444
14	41.49	0.373	27.700	13.023	0.02193	0.346
15	44.94	1.035	32.630	13.441	0.01708	-2.210
16	54.78	0.458	32.069	21.509	0.12614	0.684
17	29.81	0.000	21.667	8.649	0.01123	-0.569
18	49.55	0.000	34.878	12.459	0.01448	2.171
19	55.50	0.772	33.763	21.630	0.09504	-0.720
20	68.56	0.000	37.429	28.063	0.05570	3.036
21	51.14	0.000	33.821	18.401	0.03723	-1.147
22	51.22	0.000	36.727	15.646	0.01973	-1.200
23	47.94	0.000	36.546	14.170	0.02835	-2.820
24	59.17	1.213	31.121	23.749	0.08060	3.052
25	47.73	0.040	30.412	15.836	0.02305	1.390
26	50.56	0.211	31.882	17.948	0.06283	0.459
27	37.02	0.000	32.210	7.775	0.00859	-3.016
28	56.03	0.802	35.891	20.370	0.04113	-1.066
29	39.77	0.000	29.482	8.657	0.00952	1.586
30	46.55	0.317	33.916	12.868	0.01469	-0.584
31	39.45	0.076	28.830	13.241	0.02065	-2.726
32	45.35	0.393	29.813	13.065	0.01812	2.045
33	42.23	0.000	31.966	8.606	0.00851	1.620
34	37.81	0.000	27.326	11.322	0.01514	-0.868
35	48.19	0.304	34.134	14.753	0.01877	-1.025
36	62.28	3.537	34.024	20.909	0.03856	3.791

Detailed HELP Model Annual Water Balance Data (Year 220) – Continued:

Simulation	Precip-itation (in/yr)	Runoff (in/yr)	Evapotrans-piration (in/yr)	Lateral Drainage (in/yr)	Infiltration thru GCL (in/yr)	Change in Water Storage (in/yr)
37	55.96	0.000	40.409	15.528	0.02107	-0.001
38	40.26	0.000	28.237	13.327	0.01778	-1.332
39	60.02	0.887	35.016	23.543	0.43035	0.503
40	59.62	0.765	37.224	22.128	0.03379	-0.607
41	47.60	0.000	31.570	14.928	0.02144	1.023
42	50.44	0.503	34.100	16.282	0.02220	-0.497
43	39.42	0.079	26.336	11.363	0.01358	1.592
44	48.61	0.000	34.008	14.393	0.02069	0.169
45	57.35	0.000	34.922	27.789	0.18216	-5.441
46	47.49	0.000	32.005	12.411	0.01727	3.004
47	38.98	0.000	31.692	8.608	0.00923	-1.379
48	42.99	0.000	32.673	9.518	0.00981	0.757
49	53.01	1.678	34.167	14.034	0.01794	3.094
50	55.17	0.062	38.079	20.382	0.03412	-3.376
51	46.16	0.000	31.202	11.540	0.01537	3.386
52	42.63	0.000	33.822	13.426	0.02003	-4.652
53	50.93	0.000	32.532	18.457	0.02617	-0.089
54	54.24	0.614	28.390	20.980	0.04237	4.235
55	50.46	0.235	33.003	16.136	0.02373	1.054
56	56.39	1.143	38.490	21.074	0.03409	-4.345
57	41.99	0.000	27.944	13.358	0.01908	0.651
58	68.60	0.215	35.639	31.124	0.07108	1.604
59	48.67	0.072	33.993	13.105	0.01942	1.450
60	58.12	0.006	34.711	23.387	0.22822	-0.097
61	54.90	0.978	31.340	22.437	0.37304	0.088
62	56.29	0.694	33.367	24.755	0.26411	-2.666
63	49.13	0.413	34.473	14.991	0.01924	-1.042
64	54.54	0.375	32.295	19.206	0.03105	2.496
65	45.05	0.000	32.952	13.121	0.01703	-1.078
66	37.07	0.000	29.764	9.318	0.01062	-2.059
67	40.17	0.000	25.002	11.175	0.01408	3.958
68	58.08	0.000	35.371	24.686	0.05239	-2.005
69	36.31	0.000	27.106	9.771	0.01101	-0.607
70	42.67	1.014	31.914	12.940	0.01878	-3.233
71	48.88	0.000	35.432	10.289	0.01355	3.121
72	47.36	0.526	32.733	17.223	0.02659	-3.150
73	35.81	0.000	26.533	8.475	0.01030	0.765
74	49.81	0.739	29.609	16.578	0.02375	2.862

Detailed HELP Model Annual Water Balance Data (Year 220) – Continued:

Simulation	Precip-itation (in/yr)	Runoff (in/yr)	Evapotrans-piration (in/yr)	Lateral Drainage (in/yr)	Infiltration thru GCL (in/yr)	Change in Water Storage (in/yr)
75	56.43	3.827	34.393	17.269	0.02336	0.919
76	45.86	0.000	32.533	14.925	0.02073	-1.625
77	56.76	0.000	39.099	18.519	0.03079	-0.884
78	39.15	0.000	29.536	8.736	0.01159	0.844
79	48.87	0.000	30.964	14.000	0.07121	3.868
80	58.52	0.000	33.395	28.184	0.45894	-3.111
81	53.34	0.000	35.528	16.673	0.02254	0.991
82	55.18	0.000	35.521	18.123	0.03232	1.382
83	53.60	1.238	34.955	20.905	0.21897	-3.608
84	47.82	0.000	34.250	12.957	0.01921	0.493
85	44.69	0.000	30.834	10.464	0.01126	3.335
86	60.77	0.000	35.841	27.556	0.06502	-2.664
87	48.34	1.142	29.593	14.386	0.03640	3.169
88	36.18	0.000	26.143	15.155	0.13670	-5.236
89	58.29	2.747	35.126	18.635	0.04406	1.727
90	60.08	0.218	30.483	24.439	0.21745	4.836
91	55.49	0.000	35.948	22.502	0.07007	-3.065
92	44.51	0.214	32.146	12.466	0.01676	-0.410
93	35.83	0.000	29.634	9.237	0.01104	-3.102
94	45.02	0.000	32.816	10.333	0.01032	1.824
95	44.54	0.000	27.595	18.358	0.20168	-1.523
96	53.18	0.126	35.703	14.039	0.02100	3.233
97	48.03	0.373	31.462	17.084	0.02520	-0.940
98	62.58	1.123	41.438	17.408	0.02691	2.573
99	48.78	0.697	31.544	19.910	0.05455	-3.419
100	49.29	0.000	35.869	10.108	0.00971	3.269
Summary Statistics						
Count	100	100	100	100	100	100
Maximum	68.60	3.827	41.438	31.124	0.45894	4.836
Average	49.14	0.348	32.556	16.120	0.05676	0.064
Median	48.83	0.000	32.582	14.960	0.02191	0.395
Minimum	29.81	0.000	21.667	5.056	0.00470	-5.825
Std Dev	7.69	0.663	3.381	5.482	0.08741	2.392

Detailed HELP Model Annual Water Balance Data (Year 300):

Simulation	Precip-itation (in/yr)	Runoff (in/yr)	Evapotrans-piration (in/yr)	Lateral Drainage (in/yr)	Infiltration thru GCL (in/yr)	Change in Water Storage (in/yr)
1	40.07	0.000	31.633	5.018	0.04135	3.419
2	57.14	0.000	31.997	25.417	0.23556	-0.278
3	52.64	0.000	31.072	20.807	0.20619	0.705
4	47.88	0.976	38.43	8.546	0.07052	-0.215
5	50.57	0.000	34.41	14.497	0.12140	1.588
6	42.28	0.000	27.904	13.166	0.11084	1.091
7	39.35	0.539	30.564	13.926	0.11748	-5.808
8	49.46	0.526	31.412	15.656	0.13176	1.761
9	48.59	0.000	33.552	14.072	0.11729	0.846
10	53.97	0.000	33.722	19.217	0.36622	0.977
11	57.63	0.546	32.484	22.639	0.43917	1.801
12	46.71	0.000	29.206	19.898	0.21624	-2.752
13	38.58	0.000	30.398	7.568	0.06257	0.277
14	41.49	0.375	27.694	12.918	0.11367	0.209
15	44.94	1.038	32.63	13.350	0.11176	-2.195
16	54.78	0.477	32.039	21.367	0.28785	0.810
17	29.81	0.000	21.667	8.577	0.07189	-0.597
18	49.55	0.000	34.86	12.392	0.10324	2.098
19	55.5	0.748	33.773	21.478	0.26539	-0.601
20	68.56	0.000	37.431	27.883	0.24786	3.082
21	51.14	0.000	33.803	18.269	0.16998	-1.126
22	51.22	0.000	36.723	15.551	0.13013	-1.236
23	47.94	0.000	36.528	14.071	0.13047	-2.900
24	59.17	1.218	31.086	23.607	0.26161	3.113
25	47.73	0.044	30.416	15.715	0.13265	1.382
26	50.56	0.216	31.896	17.838	0.19275	0.432
27	37.02	0.000	32.214	7.671	0.06371	-3.061
28	56.03	0.806	35.895	20.223	0.18114	-1.054
29	39.77	0.000	29.45	8.628	0.07166	1.545
30	46.55	0.322	33.96	12.647	0.10523	-0.473
31	39.45	0.080	28.83	13.234	0.11231	-2.809
32	45.35	0.399	29.8	12.962	0.10908	2.085
33	42.23	0.000	31.932	8.593	0.07102	1.607
34	37.81	0.000	27.325	11.214	0.09416	-0.839
35	48.19	0.310	34.092	14.710	0.12318	-1.010
36	62.28	3.540	34.025	20.779	0.18393	3.846

Detailed HELP Model Annual Water Balance Data (Year 300) – Continued:

Simulation	Precip-itation (in/yr)	Runoff (in/yr)	Evapotrans-piration (in/yr)	Lateral Drainage (in/yr)	Infiltration thru GCL (in/yr)	Change in Water Storage (in/yr)
37	55.96	0.000	40.406	15.429	0.12968	-0.023
38	40.26	0.000	28.243	13.193	0.11075	-1.324
39	60.02	0.997	35.104	23.213	0.57396	0.643
40	59.62	0.774	37.197	21.999	0.18630	-0.668
41	47.6	0.000	31.583	14.810	0.12492	0.899
42	50.44	0.498	34.091	16.174	0.13596	-0.567
43	39.42	0.085	26.334	11.272	0.09404	1.531
44	48.61	0.000	34.006	14.305	0.12067	0.169
45	57.35	0.000	34.897	27.602	0.38182	-5.232
46	47.49	0.000	31.999	12.360	0.10406	2.979
47	38.98	0.000	31.666	8.530	0.07076	-1.505
48	42.99	0.000	32.711	9.452	0.07827	0.684
49	53.01	1.683	34.148	13.927	0.11662	3.159
50	55.17	0.068	38.058	20.269	0.17279	-3.321
51	46.16	0.000	31.174	11.481	0.09638	3.357
52	42.63	0.000	33.813	13.337	0.11277	-4.659
53	50.93	0.000	32.527	18.340	0.15457	-0.032
54	54.24	0.623	28.375	20.864	0.18665	4.271
55	50.46	0.239	33.014	15.993	0.13508	1.078
56	56.39	1.153	38.534	20.870	0.17745	-4.353
57	41.99	0.000	27.918	13.284	0.11200	0.623
58	68.6	0.221	35.638	30.939	0.28344	1.664
59	48.67	0.066	33.956	13.026	0.11008	1.463
60	58.12	0.012	34.638	23.287	0.40225	0.054
61	54.9	1.274	31.323	22.035	0.50004	0.069
62	56.29	0.699	33.311	24.633	0.44264	-2.784
63	49.13	0.423	34.462	14.872	0.12456	-1.121
64	54.54	0.381	32.307	19.062	0.16366	2.458
65	45.05	0.000	32.969	13.010	0.10905	-1.163
66	37.07	0.000	29.771	9.238	0.07688	-2.129
67	40.17	0.000	24.97	11.140	0.09321	3.967
68	58.08	0.000	35.347	24.521	0.22069	-1.875
69	36.31	0.000	27.109	9.713	0.08080	-0.683
70	42.67	1.019	31.92	12.831	0.10830	-3.230
71	48.88	0.000	35.421	10.229	0.08581	3.111
72	47.36	0.530	32.735	17.101	0.14494	-3.100
73	35.81	0.000	26.578	8.378	0.06997	0.719
74	49.81	0.745	29.577	16.486	0.13903	2.939

Detailed HELP Model Annual Water Balance Data (Year 300) – Continued:

Simulation	Precip-itation (in/yr)	Runoff (in/yr)	Evapotrans-piration (in/yr)	Lateral Drainage (in/yr)	Infiltration thru GCL (in/yr)	Change in Water Storage (in/yr)
75	56.43	3.837	34.391	17.137	0.14400	0.937
76	45.86	0.000	32.525	14.850	0.12498	-1.633
77	56.76	0.000	39.091	18.367	0.16698	-0.827
78	39.15	0.000	29.533	8.674	0.07280	0.778
79	48.87	0.000	30.925	13.932	0.18006	3.863
80	58.52	0.000	33.42	27.949	0.67743	-2.906
81	53.34	0.000	35.523	16.565	0.13918	0.882
82	55.18	0.000	35.5	18.020	0.16035	1.305
83	53.6	1.308	34.951	20.677	0.36824	-3.541
84	47.82	0.000	34.253	12.864	0.10872	0.478
85	44.69	0.000	30.832	10.393	0.08624	3.140
86	60.77	0.000	35.813	27.397	0.25496	-2.544
87	48.34	1.152	29.586	14.280	0.14368	3.184
88	36.18	0.000	26.139	15.028	0.25009	-5.150
89	58.29	2.752	35.114	18.525	0.17720	1.646
90	60.08	0.223	30.481	24.255	0.40865	4.975
91	55.49	0.000	35.932	22.337	0.23540	-3.028
92	44.51	0.217	32.158	12.358	0.10380	-0.511
93	35.83	0.000	29.613	9.193	0.07668	-3.231
94	45.02	0.000	32.828	10.247	0.08472	1.772
95	44.54	0.000	27.583	18.216	0.34912	-1.341
96	53.18	0.131	35.735	13.915	0.11767	3.214
97	48.03	0.379	31.459	16.962	0.14332	-1.037
98	62.58	1.132	41.463	17.255	0.14628	2.570
99	48.78	0.702	31.528	19.773	0.20419	-3.335
100	49.29	0.000	35.869	10.027	0.08276	3.221
Summary Statistics						
Count	100	100	100	100	100	100
Maximum	68.60	3.837	41.463	30.939	0.67743	4.975
Average	49.14	0.355	32.549	16.005	0.17110	0.067
Median	48.83	0.000	32.579	14.861	0.13030	0.243
Minimum	29.81	0.000	21.667	5.018	0.04135	-5.808
Std Dev	7.70	0.670	3.383	5.443	0.11529	2.385

Detailed HELP Model Annual Water Balance Data (Year 380):

Simulation	Precip-itation (in/yr)	Runoff (in/yr)	Evapotrans-piration (in/yr)	Lateral Drainage (in/yr)	Infiltration thru GCL (in/yr)	Change in Water Storage (in/yr)
1	40.07	0.000	31.634	4.957	0.11677	3.478
2	57.14	0.000	31.985	24.997	0.66859	0.123
3	52.64	0.000	31.03	20.500	0.58542	0.995
4	47.88	0.983	38.439	8.367	0.19727	-0.256
5	50.57	0.000	34.391	14.302	0.34231	1.429
6	42.28	0.000	27.881	13.029	0.31346	1.112
7	39.35	0.546	30.578	13.644	0.32891	-5.716
8	49.46	0.534	31.409	15.412	0.37073	1.722
9	48.59	0.000	33.533	13.884	0.33079	0.829
10	53.97	0.000	33.874	18.479	0.97570	1.203
11	57.63	0.554	32.427	21.930	1.17513	1.565
12	46.71	0.000	29.225	19.491	0.60418	-2.787
13	38.58	0.000	30.388	7.467	0.17643	0.176
14	41.49	0.372	27.765	12.640	0.31704	0.276
15	44.94	1.043	32.617	13.146	0.31457	-2.214
16	54.78	0.501	32.067	20.827	0.78622	1.161
17	29.81	0.000	21.661	8.439	0.20221	-0.825
18	49.55	0.000	34.846	12.237	0.29140	1.922
19	55.5	0.730	33.741	21.065	0.73100	-0.302
20	68.56	0.000	37.407	27.466	0.70366	3.166
21	51.14	0.000	33.794	17.949	0.47866	-1.141
22	51.22	0.000	36.697	15.351	0.36720	-1.439
23	47.94	0.000	36.532	13.810	0.36175	-2.771
24	59.17	1.223	30.951	23.286	0.74228	3.240
25	47.73	0.050	30.391	15.478	0.37342	1.302
26	50.56	0.221	31.913	17.453	0.53434	0.461
27	37.02	0.000	32.237	7.539	0.17901	-3.311
28	56.03	0.812	35.876	19.911	0.50996	-0.992
29	39.77	0.000	29.462	8.494	0.20165	1.510
30	46.55	0.329	33.963	12.444	0.29585	-0.616
31	39.45	0.086	28.811	13.027	0.31591	-2.695
32	45.35	0.406	29.799	12.770	0.30721	2.020
33	42.23	0.000	31.931	8.506	0.20101	1.521
34	37.81	0.000	27.31	11.014	0.26429	-0.825
35	48.19	0.317	34.08	14.505	0.34717	-0.968
36	62.28	3.545	34.004	20.474	0.52206	4.078

Detailed HELP Model Annual Water Balance Data (Year 380) – Continued:

Simulation	Precip-itation (in/yr)	Runoff (in/yr)	Evapotrans-piration (in/yr)	Lateral Drainage (in/yr)	Infiltration thru GCL (in/yr)	Change in Water Storage (in/yr)
37	55.96	0.000	40.413	15.171	0.36445	0.048
38	40.26	0.000	28.225	13.010	0.31217	-1.440
39	60.02	0.842	35.105	22.398	1.54799	0.663
40	59.62	0.787	37.207	21.648	0.52409	-0.747
41	47.6	0.000	31.58	14.576	0.35142	0.957
42	50.44	0.491	34.082	15.933	0.38286	-0.560
43	39.42	0.092	26.32	11.113	0.26498	1.494
44	48.61	0.000	34.008	14.085	0.33961	0.134
45	57.35	0.000	34.908	26.928	1.03619	-4.884
46	47.49	0.000	31.983	12.203	0.29370	2.509
47	38.98	0.000	31.672	8.365	0.19832	-1.447
48	42.99	0.000	32.698	9.301	0.22011	0.606
49	53.01	1.690	34.173	13.739	0.32887	3.118
50	55.17	0.067	38.036	19.982	0.48694	-3.103
51	46.16	0.000	31.178	11.286	0.27079	3.413
52	42.63	0.000	33.795	13.142	0.31763	-4.722
53	50.93	0.000	32.496	18.099	0.43602	-0.051
54	54.24	0.637	28.39	20.533	0.52620	4.421
55	50.46	0.246	33.012	15.731	0.37978	1.106
56	56.39	1.167	38.427	20.606	0.50075	-4.316
57	41.99	0.000	27.936	13.044	0.32041	0.519
58	68.6	0.226	35.66	30.448	0.80706	1.856
59	48.67	0.059	33.952	12.795	0.30903	1.354
60	58.12	0.019	34.654	22.609	1.07497	-0.026
61	54.9	1.168	31.341	21.314	1.31529	-0.224
62	56.29	0.707	33.309	23.873	1.16563	-2.713
63	49.13	0.438	34.473	14.630	0.35026	-1.154
64	54.54	0.388	32.252	18.826	0.46533	2.677
65	45.05	0.000	32.97	12.800	0.30661	-1.193
66	37.07	0.000	29.776	9.087	0.21613	-2.221
67	40.17	0.000	24.986	10.971	0.26244	3.836
68	58.08	0.000	35.252	24.206	0.62638	-1.615
69	36.31	0.000	27.11	9.545	0.22693	-0.705
70	42.67	1.026	31.896	12.657	0.30539	-3.316
71	48.88	0.000	35.452	10.043	0.24078	3.025
72	47.36	0.538	32.717	16.851	0.40826	-3.056
73	35.81	0.000	26.587	8.240	0.19669	0.735
74	49.81	0.745	29.613	16.213	0.39083	2.837

Detailed HELP Model Annual Water Balance Data (Year 380) – Continued:

Simulation	Precip- itation (in/yr)	Runoff (in/yr)	Evapotrans- piration (in/yr)	Lateral Drainage (in/yr)	Infiltration thru GCL (in/yr)	Change in Water Storage (in/yr)
75	56.43	3.850	34.42	16.834	0.40425	1.141
76	45.86	0.000	32.513	14.608	0.35139	-1.545
77	56.76	0.000	39.097	18.085	0.46457	-0.839
78	39.15	0.000	29.556	8.519	0.20438	0.674
79	48.87	0.000	30.955	13.607	0.49797	3.938
80	58.52	0.000	33.418	26.968	1.65155	-2.954
81	53.34	0.000	35.512	16.328	0.39216	0.716
82	55.18	0.000	35.603	17.604	0.44927	1.550
83	53.6	1.258	34.958	20.100	1.00000	-3.488
84	47.82	0.000	34.267	12.650	0.30559	0.148
85	44.69	0.000	30.833	10.272	0.24366	3.116
86	60.77	0.000	35.825	26.889	0.72121	-2.213
87	48.34	1.163	29.59	14.009	0.40627	3.093
88	36.18	0.000	26.139	14.576	0.67649	-5.130
89	58.29	2.758	35.112	18.228	0.49765	1.486
90	60.08	0.231	30.462	23.576	1.10187	5.133
91	55.49	0.000	35.891	21.969	0.66109	-3.007
92	44.51	0.221	32.158	12.139	0.29142	-0.600
93	35.83	0.000	29.64	9.014	0.21487	-3.330
94	45.02	0.000	32.91	10.010	0.23645	1.654
95	44.54	0.000	27.588	17.654	0.90874	-0.990
96	53.18	0.138	35.726	13.690	0.33085	2.991
97	48.03	0.385	31.457	16.722	0.40392	-0.968
98	62.58	1.146	41.433	17.018	0.41234	2.664
99	48.78	0.707	31.559	19.351	0.57051	-3.221
100	49.29	0.000	35.866	9.882	0.23312	2.987
Summary Statistics						
Count	100	100	100	100	100	100
Maximum	68.60	3.850	41.433	30.448	1.65155	5.133
Average	49.14	0.354	32.548	15.706	0.47236	0.073
Median	48.83	0.000	32.565	14.592	0.36583	0.162
Minimum	29.81	0.000	21.661	4.957	0.11677	-5.716
Std Dev	7.69	0.669	3.379	5.305	0.29946	2.366

Detailed HELP Model Annual Water Balance Data (Year 460):

Simulation	Precip-itation (in/yr)	Runoff (in/yr)	Evapotrans-piration (in/yr)	Lateral Drainage (in/yr)	Infiltration thru GCL (in/yr)	Change in Water Storage (in/yr)
1	40.07	0.000	31.631	4.921	0.18667	3.517
2	57.14	0.000	32.013	24.584	1.05586	0.500
3	52.64	0.000	31.059	20.123	0.93277	1.087
4	47.88	0.990	38.424	8.236	0.31263	-0.505
5	50.57	0.000	34.35	14.129	0.54448	1.510
6	42.28	0.000	27.894	12.846	0.49786	1.202
7	39.35	0.553	30.587	13.425	0.52119	-5.770
8	49.46	0.539	31.406	15.197	0.58867	1.733
9	48.59	0.000	33.483	13.750	0.52756	0.839
10	53.97	0.000	33.756	18.180	1.40098	0.960
11	57.63	0.564	32.454	21.460	1.61899	1.505
12	46.71	0.000	29.196	19.162	0.94472	-2.636
13	38.58	0.000	30.393	7.362	0.28007	0.133
14	41.49	0.377	27.656	12.518	0.51333	0.467
15	44.94	1.048	32.609	12.972	0.49987	-2.280
16	54.78	0.526	32.018	20.456	1.20222	1.126
17	29.81	0.000	21.625	8.311	0.32065	-0.866
18	49.55	0.000	34.914	12.048	0.46188	1.893
19	55.5	0.708	33.805	20.603	1.13267	-0.192
20	68.56	0.000	37.44	27.051	1.12446	3.322
21	51.14	0.000	33.747	17.683	0.76476	-1.400
22	51.22	0.000	36.714	15.131	0.58280	-1.373
23	47.94	0.000	36.511	13.581	0.58578	-2.774
24	59.17	1.229	31.003	22.814	1.17429	3.317
25	47.73	0.055	30.399	15.242	0.59219	1.164
26	50.56	0.229	31.897	17.167	0.84186	0.448
27	37.02	0.000	32.222	7.415	0.28347	-3.286
28	56.03	0.818	35.87	19.611	0.81234	-0.758
29	39.77	0.000	29.407	8.432	0.32230	1.300
30	46.55	0.337	33.969	12.268	0.46964	-0.544
31	39.45	0.093	28.841	12.789	0.49934	-2.602
32	45.35	0.413	29.791	12.592	0.48786	1.910
33	42.23	0.000	31.909	8.433	0.32090	1.455
34	37.81	0.000	27.319	10.820	0.41804	-0.649
35	48.19	0.324	34.209	14.183	0.54642	-1.015
36	62.28	3.552	34.019	20.151	0.83376	4.141

Detailed HELP Model Annual Water Balance Data (Year 460) – Continued:

Simulation	Precip-itation (in/yr)	Runoff (in/yr)	Evapotrans-piration (in/yr)	Lateral Drainage (in/yr)	Infiltration thru GCL (in/yr)	Change in Water Storage (in/yr)
37	55.96	0.000	40.402	14.945	0.57808	-0.018
38	40.26	0.000	28.231	12.834	0.49581	-1.514
39	60.02	0.850	35.091	21.976	1.99735	0.479
40	59.62	0.801	37.197	21.339	0.83183	-0.547
41	47.6	0.000	31.6	14.341	0.55679	0.852
42	50.44	0.484	34.1	15.688	0.60707	-0.463
43	39.42	0.099	26.33	10.937	0.41994	1.492
44	48.61	0.000	33.988	13.908	0.54001	0.170
45	57.35	0.000	34.928	26.380	1.55524	-4.973
46	47.49	0.000	31.974	12.058	0.46735	2.469
47	38.98	0.000	31.68	8.223	0.31388	-1.338
48	42.99	0.000	32.683	9.191	0.35029	0.518
49	53.01	1.697	34.161	13.553	0.52239	3.291
50	55.17	0.065	38.076	19.676	0.77222	-2.995
51	46.16	0.000	31.18	11.135	0.43031	3.191
52	42.63	0.000	33.775	12.944	0.50367	-4.702
53	50.93	0.000	32.518	17.826	0.69142	0.035
54	54.24	0.650	28.376	20.281	0.83658	4.449
55	50.46	0.253	33.019	15.474	0.60150	0.876
56	56.39	1.179	38.386	20.304	0.79443	-4.080
57	41.99	0.000	27.929	12.864	0.51416	0.397
58	68.6	0.231	35.668	29.993	1.28592	1.983
59	48.67	0.052	33.983	12.541	0.48774	1.092
60	58.12	0.026	34.646	22.184	1.53805	0.001
61	54.9	1.176	31.322	20.878	1.78121	-0.359
62	56.29	0.714	33.313	23.367	1.61580	-2.603
63	49.13	0.452	34.484	14.393	0.55494	-1.022
64	54.54	0.396	32.285	18.534	0.74055	2.663
65	45.05	0.000	33.003	12.574	0.48498	-1.227
66	37.07	0.000	29.769	8.949	0.34274	-2.173
67	40.17	0.000	24.962	10.863	0.41856	3.804
68	58.08	0.000	35.258	23.829	1.00465	-1.446
69	36.31	0.000	27.109	9.390	0.35945	-0.898
70	42.67	1.033	31.929	12.435	0.48319	-3.192
71	48.88	0.000	35.463	9.889	0.38184	2.954
72	47.36	0.545	32.726	16.592	0.64734	-2.918
73	35.81	0.000	26.513	8.187	0.31464	0.618
74	49.81	0.746	29.604	16.018	0.62184	2.844

Detailed HELP Model Annual Water Balance Data (Year 460) – Continued:

Simulation	Precip- itation (in/yr)	Runoff (in/yr)	Evapotrans- piration (in/yr)	Lateral Drainage (in/yr)	Infiltration thru GCL (in/yr)	Change in Water Storage (in/yr)
75	56.43	3.824	34.426	16.619	0.64263	1.270
76	45.86	0.000	32.492	14.424	0.55863	-1.720
77	56.76	0.000	39.061	17.840	0.73838	-0.764
78	39.15	0.000	29.534	8.413	0.32500	0.558
79	48.87	0.000	30.949	13.341	0.77731	3.959
80	58.52	0.000	33.379	26.483	2.20654	-3.113
81	53.34	0.000	35.523	16.075	0.62172	0.900
82	55.18	0.004	35.562	17.345	0.71456	1.559
83	53.6	1.251	34.929	19.700	1.42727	-3.666
84	47.82	0.000	34.283	12.478	0.48549	0.254
85	44.69	0.000	30.821	10.141	0.38728	3.141
86	60.77	0.000	35.842	26.481	1.13452	-2.032
87	48.34	1.167	29.595	13.751	0.65229	2.968
88	36.18	0.000	26.144	14.217	0.99719	-5.328
89	58.29	2.764	35.091	17.981	0.79127	1.672
90	60.08	0.238	30.434	23.076	1.61427	5.018
91	55.49	0.000	35.922	21.587	1.04425	-2.908
92	44.51	0.226	32.149	11.941	0.46159	-0.680
93	35.83	0.000	29.624	8.887	0.34114	-3.287
94	45.02	0.000	32.814	9.965	0.37912	1.663
95	44.54	0.000	27.549	17.290	1.30503	-1.024
96	53.18	0.145	35.728	13.501	0.52546	3.035
97	48.03	0.389	31.46	16.477	0.64095	-0.848
98	62.58	1.160	41.438	16.786	0.65492	2.615
99	48.78	0.713	31.568	18.978	0.89930	-3.330
100	49.29	0.000	35.881	9.721	0.36923	3.030
Summary Statistics						
Count	100	100	100	100	100	100
Maximum	68.60	3.824	41.438	29.993	2.20654	5.018
Average	49.14	0.357	32.544	15.456	0.72342	0.075
Median	48.83	0.000	32.564	14.367	0.58429	0.326
Minimum	29.81	0.000	21.625	4.921	0.18667	-5.770
Std Dev	7.69	0.669	3.384	5.199	0.40729	2.358

Detailed HELP Model Annual Water Balance Data (Year 560):

Simulation	Precip-itation (in/yr)	Runoff (in/yr)	Evapotrans-piration (in/yr)	Lateral Drainage (in/yr)	Infiltration thru GCL (in/yr)	Change in Water Storage (in/yr)
1	40.07	0.000	31.62	4.862	0.27597	3.588
2	57.14	0.000	31.996	24.116	1.55105	1.008
3	52.64	0.000	31.065	19.679	1.37295	0.806
4	47.88	0.992	38.428	8.063	0.45796	-0.630
5	50.57	0.000	34.356	13.888	0.80088	1.653
6	42.28	0.000	27.892	12.622	0.73209	1.103
7	39.35	0.555	30.555	13.172	0.76510	-5.755
8	49.46	0.542	31.422	14.901	0.86375	1.839
9	48.59	0.000	33.441	13.561	0.77874	0.892
10	53.97	0.000	33.765	17.825	1.75765	0.676
11	57.63	0.568	32.449	21.013	2.04413	1.533
12	46.71	0.000	29.208	18.733	1.37718	-2.532
13	38.58	0.000	30.393	7.231	0.41161	0.072
14	41.49	0.373	27.752	12.183	0.74649	0.522
15	44.94	1.049	32.607	12.729	0.73399	-2.141
16	54.78	0.533	32.032	20.041	1.61369	0.949
17	29.81	0.000	21.646	8.124	0.46909	-0.930
18	49.55	0.000	34.945	11.821	0.67806	2.024
19	55.5	0.741	33.803	20.079	1.60787	-0.225
20	68.56	0.000	37.43	26.566	1.65410	3.608
21	51.14	0.000	33.785	17.268	1.12354	-1.723
22	51.22	0.000	36.731	14.849	0.85576	-1.309
23	47.94	0.000	36.474	13.307	0.86324	-2.899
24	59.17	1.230	30.983	22.319	1.71907	3.482
25	47.73	0.057	30.389	14.958	0.86975	1.043
26	50.56	0.231	31.906	16.830	1.19451	0.430
27	37.02	0.000	32.205	7.255	0.41491	-3.256
28	56.03	0.819	35.848	19.255	1.19630	-0.554
29	39.77	0.000	29.425	8.269	0.47297	1.096
30	46.55	0.338	33.954	12.070	0.69143	-0.377
31	39.45	0.095	28.842	12.533	0.73229	-2.744
32	45.35	0.415	29.776	12.379	0.71777	2.032
33	42.23	0.000	31.906	8.305	0.47291	1.361
34	37.81	0.000	27.316	10.603	0.61300	-0.559
35	48.19	0.326	34.24	13.905	0.80155	-0.937
36	62.28	3.554	34.016	19.797	1.21932	3.987

Detailed HELP Model Annual Water Balance Data (Year 560) – Continued:

Simulation	Precip-itation (in/yr)	Runoff (in/yr)	Evapotrans-piration (in/yr)	Lateral Drainage (in/yr)	Infiltration thru GCL (in/yr)	Change in Water Storage (in/yr)
37	55.96	0.000	40.391	14.646	0.84762	-0.040
38	40.26	0.000	28.244	12.602	0.72879	-1.527
39	60.02	0.924	35.105	21.557	2.34615	0.400
40	59.62	0.804	37.193	20.955	1.22234	-0.388
41	47.6	0.000	31.598	14.066	0.81721	0.722
42	50.44	0.482	34.088	15.407	0.89211	-0.369
43	39.42	0.101	26.322	10.745	0.61736	1.455
44	48.61	0.000	33.993	13.655	0.79347	0.179
45	57.35	0.000	34.917	25.836	2.09770	-5.031
46	47.49	0.000	31.982	11.855	0.68768	2.522
47	38.98	0.000	31.676	8.055	0.46008	-1.345
48	42.99	0.000	32.673	9.043	0.51577	0.551
49	53.01	1.699	34.146	13.335	0.76923	3.401
50	55.17	0.065	38.089	19.312	1.13590	-3.077
51	46.16	0.000	31.187	10.920	0.63152	3.073
52	42.63	0.000	33.783	12.673	0.73795	-4.647
53	50.93	0.000	32.502	17.527	1.01745	0.222
54	54.24	0.653	28.37	19.928	1.24256	4.398
55	50.46	0.254	33.018	15.157	0.88151	0.672
56	56.39	1.182	38.371	19.916	1.16600	-3.968
57	41.99	0.000	27.9	12.624	0.76535	0.388
58	68.6	0.232	35.633	29.487	1.90532	2.149
59	48.67	0.050	33.968	12.273	0.71419	0.785
60	58.12	0.028	34.67	21.737	1.98548	0.122
61	54.9	1.236	31.324	20.430	2.17172	-0.487
62	56.29	0.716	33.319	22.905	2.05054	-2.522
63	49.13	0.456	34.427	14.174	0.81790	-0.893
64	54.54	0.398	32.248	18.236	1.09469	2.556
65	45.05	0.000	32.991	12.344	0.71246	-1.237
66	37.07	0.000	29.749	8.792	0.50384	-2.159
67	40.17	0.000	24.98	10.674	0.61554	3.869
68	58.08	0.000	35.288	23.339	1.47670	-1.511
69	36.31	0.000	27.116	9.186	0.52619	-0.925
70	42.67	1.035	31.949	12.184	0.70858	-3.141
71	48.88	0.000	35.439	9.730	0.56220	3.009
72	47.36	0.549	32.744	16.272	0.94999	-2.843
73	35.81	0.000	26.522	8.024	0.46153	0.462
74	49.81	0.747	29.591	15.766	0.91598	2.992

Detailed HELP Model Annual Water Balance Data (Year 560) – Continued:

Simulation	Precip-itation (in/yr)	Runoff (in/yr)	Evapotrans-piration (in/yr)	Lateral Drainage (in/yr)	Infiltration thru GCL (in/yr)	Change in Water Storage (in/yr)
75	56.43	3.827	34.403	16.327	0.94470	1.232
76	45.86	0.000	32.454	14.189	0.82232	-1.856
77	56.76	0.000	39.09	17.469	1.08291	-0.694
78	39.15	0.000	29.543	8.240	0.47642	0.461
79	48.87	0.000	30.952	13.073	1.06815	3.932
80	58.52	0.000	33.369	25.949	2.75913	-3.114
81	53.34	0.000	35.502	15.802	0.91454	1.022
82	55.18	0.006	35.583	16.982	1.05612	1.470
83	53.6	1.264	34.92	19.257	1.81675	-3.720
84	47.82	0.000	34.266	12.294	0.71597	0.339
85	44.69	0.000	30.807	9.989	0.57082	3.221
86	60.77	0.000	35.839	25.939	1.67165	-2.119
87	48.34	1.162	29.591	13.468	0.95123	3.099
88	36.18	0.000	26.166	13.880	1.28034	-5.564
89	58.29	2.766	35.089	17.643	1.16565	2.012
90	60.08	0.240	30.437	22.562	2.13956	4.785
91	55.49	0.000	35.911	21.136	1.50893	-2.792
92	44.51	0.227	32.148	11.706	0.67721	-0.801
93	35.83	0.000	29.64	8.685	0.49892	-3.284
94	45.02	0.000	32.84	9.764	0.55579	1.781
95	44.54	0.000	27.55	16.881	1.70527	-1.187
96	53.18	0.147	35.736	13.254	0.77200	3.094
97	48.03	0.391	31.462	16.178	0.94188	-0.746
98	62.58	1.164	41.439	16.502	0.96355	2.535
99	48.78	0.714	31.532	18.569	1.31333	-3.386
100	49.29	0.000	35.879	9.545	0.54250	3.120
Summary Statistics						
Count	100	100	100	100	100	100
Maximum	68.60	3.827	41.439	29.487	2.75913	4.785
Average	49.14	0.359	32.543	15.158	1.02113	0.078
Median	48.83	0.000	32.555	14.120	0.85950	0.364
Minimum	29.81	0.000	21.646	4.862	0.27597	-5.755
Std Dev	7.69	0.672	3.381	5.092	0.50833	2.371

Detailed HELP Model Annual Water Balance Data (Year 1,000):

Simulation	Precip-itation (in/yr)	Runoff (in/yr)	Evapotrans-piration (in/yr)	Lateral Drainage (in/yr)	Infiltration thru GCL (in/yr)	Change in Water Storage (in/yr)
1	40.07	0.000	31.616	4.534	0.67862	3.919
2	57.14	0.000	32.011	22.074	3.64684	1.525
3	52.64	0.000	31.03	18.009	3.09946	0.638
4	47.88	1.001	38.413	7.317	1.09485	-0.933
5	50.57	0.000	34.38	12.822	1.95022	2.278
6	42.28	0.000	27.884	11.616	1.81704	0.523
7	39.35	0.564	30.558	11.894	1.82034	-5.739
8	49.46	0.555	31.414	13.690	2.09337	2.063
9	48.59	0.000	33.437	12.498	1.89220	0.906
10	53.97	0.000	33.7	16.678	3.03461	0.317
11	57.63	0.708	32.399	19.332	3.56100	1.650
12	46.71	0.000	29.176	17.229	2.94169	-2.269
13	38.58	0.000	30.405	6.641	0.99634	-0.186
14	41.49	0.379	27.674	11.112	1.80570	0.342
15	44.94	1.055	32.596	11.686	1.77774	-1.718
16	54.78	0.563	32.044	18.523	3.16550	1.071
17	29.81	0.000	21.641	7.385	1.12466	-1.537
18	49.55	0.000	34.827	11.058	1.67345	2.809
19	55.5	0.722	33.724	18.401	3.32055	-0.679
20	68.56	0.000	37.424	24.433	3.92166	3.960
21	51.14	0.000	33.76	15.752	2.57737	-2.149
22	51.22	0.000	36.722	13.683	2.07869	-0.944
23	47.94	0.000	36.467	12.086	1.98188	-3.544
24	59.17	1.239	30.991	20.434	3.66955	4.119
25	47.73	0.064	30.396	13.682	2.09879	0.804
26	50.56	0.239	31.909	15.533	2.57546	0.314
27	37.02	0.000	32.201	6.523	0.98275	-3.355
28	56.03	0.826	35.841	17.584	2.87683	-0.492
29	39.77	0.000	29.379	7.679	1.15805	1.017
30	46.55	0.347	33.863	11.182	1.68863	-0.056
31	39.45	0.102	28.812	11.438	1.76268	-3.187
32	45.35	0.424	29.769	11.368	1.73882	2.475
33	42.23	0.000	31.952	7.673	1.15227	1.394
34	37.81	0.000	27.303	9.648	1.47052	-0.933
35	48.19	0.323	34.261	12.803	1.94598	-0.653
36	62.28	3.562	34.016	18.171	2.96499	4.155

Detailed HELP Model Annual Water Balance Data (Year 1,000) – Continued:

Simulation	Precip-itation (in/yr)	Runoff (in/yr)	Evapotrans-piration (in/yr)	Lateral Drainage (in/yr)	Infiltration thru GCL (in/yr)	Change in Water Storage (in/yr)
37	55.96	0.000	40.371	13.401	2.04500	-0.514
38	40.26	0.000	28.261	11.504	1.75349	-1.387
39	60.02	1.280	35.091	19.949	3.69910	0.390
40	59.62	0.821	37.198	19.212	2.95448	0.206
41	47.6	0.000	31.558	12.879	1.97346	0.318
42	50.44	0.476	34.103	14.094	2.15204	-0.229
43	39.42	0.110	26.319	9.870	1.49541	1.097
44	48.61	0.000	34.01	12.518	1.92533	0.245
45	57.35	0.000	34.901	23.657	4.23510	-5.199
46	47.49	0.000	31.967	10.988	1.68171	3.155
47	38.98	0.000	31.67	7.311	1.10050	-1.948
48	42.99	0.000	32.687	8.332	1.25293	1.060
49	53.01	1.708	34.174	12.248	1.86343	3.256
50	55.17	0.062	38.06	17.785	2.78700	-3.240
51	46.16	0.000	31.194	9.933	1.51436	2.850
52	42.63	0.000	33.81	11.543	1.77296	-4.525
53	50.93	0.000	32.479	16.140	2.47211	0.661
54	54.24	0.670	28.391	18.318	3.01136	4.652
55	50.46	0.262	33	13.843	2.12126	0.038
56	56.39	1.185	38.458	18.031	2.78291	-4.117
57	41.99	0.000	27.847	11.616	1.86786	0.404
58	68.6	0.239	35.607	27.127	4.55146	2.816
59	48.67	0.041	33.969	11.024	1.69112	0.005
60	58.12	0.037	34.653	20.210	3.64504	0.440
61	54.9	1.527	31.341	18.767	3.59849	-0.715
62	56.29	0.725	33.271	21.094	3.75515	-2.242
63	49.13	0.474	34.458	12.928	1.96677	-0.932
64	54.54	0.405	32.246	16.772	2.65638	2.606
65	45.05	0.000	33.025	11.251	1.71197	-1.317
66	37.07	0.000	29.762	8.010	1.20983	-2.414
67	40.17	0.000	24.959	9.911	1.50806	4.208
68	58.08	0.000	35.292	21.323	3.49101	-1.484
69	36.31	0.000	27.093	8.372	1.26487	-0.941
70	42.67	1.044	31.943	11.121	1.75834	-3.456
71	48.88	0.000	35.448	8.920	1.35977	3.180
72	47.36	0.567	32.734	14.915	2.29708	-2.758
73	35.81	0.000	26.538	7.356	1.11606	0.151
74	49.81	0.749	29.616	14.533	2.26982	3.759

Detailed HELP Model Annual Water Balance Data (Year 1,000) – Continued:

Simulation	Precip- itation (in/yr)	Runoff (in/yr)	Evapotrans- piration (in/yr)	Lateral Drainage (in/yr)	Infiltration thru GCL (in/yr)	Change in Water Storage (in/yr)
75	56.43	3.884	34.362	14.918	2.27556	0.782
76	45.86	0.000	32.488	12.936	1.97675	-1.886
77	56.76	0.000	39.026	16.073	2.57706	-0.640
78	39.15	0.000	29.55	7.531	1.14843	0.087
79	48.87	0.000	30.989	12.089	2.11688	3.948
80	58.52	0.030	33.403	24.002	4.64697	-2.968
81	53.34	0.000	35.522	14.521	2.21594	1.279
82	55.18	0.013	35.476	15.638	2.50148	1.248
83	53.6	1.871	34.768	17.344	3.09135	-3.830
84	47.82	0.000	34.242	11.323	1.79171	0.364
85	44.69	0.000	30.811	9.220	1.38891	3.565
86	60.77	0.000	35.781	23.727	3.93060	-2.412
87	48.34	1.057	29.602	12.447	2.08647	3.600
88	36.18	0.000	26.151	12.750	2.28616	-6.223
89	58.29	2.773	35.082	16.301	2.66005	3.020
90	60.08	0.249	30.48	20.709	4.02179	4.295
91	55.49	0.000	35.901	19.302	3.32251	-2.459
92	44.51	0.232	32.141	10.709	1.63450	-1.357
93	35.83	0.000	29.642	7.860	1.18992	-3.436
94	45.02	0.000	32.827	8.984	1.34785	2.384
95	44.54	0.000	27.526	15.590	2.99088	-1.864
96	53.18	0.156	35.755	12.153	1.86757	3.165
97	48.03	0.397	31.454	14.886	2.28505	-0.667
98	62.58	1.179	41.393	15.202	2.40917	2.714
99	48.78	0.721	31.56	16.885	2.84901	-3.360
100	49.29	0.000	35.834	8.777	1.31499	3.053
Summary Statistics						
Count	100	100	100	100	100	100
Maximum	68.60	3.884	41.393	27.127	4.64697	4.652
Average	49.14	0.376	32.533	13.909	2.26380	0.084
Median	48.83	0.000	32.542	12.904	2.06184	0.226
Minimum	29.81	0.000	21.641	4.534	0.67862	-6.223
Std Dev	7.69	0.694	3.377	4.685	0.89125	2.514

Detailed HELP Model Annual Water Balance Data (Year 1,800):

Simulation	Precip-itation (in/yr)	Runoff (in/yr)	Evapotrans-piration (in/yr)	Lateral Drainage (in/yr)	Infiltration thru GCL (in/yr)	Change in Water Storage (in/yr)
1	40.07	0	31.628	3.882	1.46494	4.537
2	57.14	0	31.886	18.994	6.94064	1.559
3	52.64	0	31.024	15.516	5.59796	0.367
4	47.88	1.017	38.386	6.018	2.26770	-0.923
5	50.57	0	34.379	10.803	4.14682	2.535
6	42.28	0	27.862	9.709	3.62576	0.546
7	39.35	0.58	30.538	9.871	3.71440	-6.127
8	49.46	0.571	31.431	11.403	4.34979	2.27
9	48.59	0	33.416	10.523	4.01870	0.773
10	53.97	0	33.912	14.496	5.14298	0.514
11	57.63	1.429	32.388	16.470	5.70088	1.461
12	46.71	0	29.159	14.741	5.35773	-2.167
13	38.58	0	30.384	5.566	2.10616	-0.056
14	41.49	0.383	27.652	9.341	3.44268	-0.085
15	44.94	1.064	32.571	9.750	3.70831	-1.698
16	54.78	0.617	32.047	15.969	5.80226	1.383
17	29.81	0	21.638	6.038	2.30847	-1.906
18	49.55	0	34.843	9.333	3.56328	3.228
19	55.5	0.913	33.721	15.932	5.52043	-0.788
20	68.56	0	37.442	20.736	7.81415	3.78
21	51.14	0	33.8	13.291	4.89941	-2.094
22	51.22	0	36.712	11.431	4.37809	-0.318
23	47.94	0	36.428	10.125	3.75487	-4.253
24	59.17	1.251	30.867	17.999	6.33925	4.381
25	47.73	0.077	30.406	11.427	4.33091	0.751
26	50.56	0.254	31.883	13.462	4.87035	0.723
27	37.02	0	32.189	5.198	1.97115	-3.927
28	56.03	0.839	35.767	15.132	5.38901	-0.615
29	39.77	0	29.468	6.392	2.43151	1.211
30	46.55	0.364	33.883	9.368	3.56653	0.033
31	39.45	0.118	28.831	9.399	3.58405	-3.497
32	45.35	0.44	29.746	9.505	3.61870	2.616
33	42.23	0	31.933	6.557	2.48491	1.828
34	37.81	0	27.303	7.895	3.02246	-1.484
35	48.19	0.306	34.115	10.839	4.15974	-0.488
36	62.28	3.575	34.002	15.604	5.78914	4.69

Detailed HELP Model Annual Water Balance Data (Year 1,800) – Continued:

Simulation	Precip-itation (in/yr)	Runoff (in/yr)	Evapotrans-piration (in/yr)	Lateral Drainage (in/yr)	Infiltration thru GCL (in/yr)	Change in Water Storage (in/yr)
37	55.96	0	40.238	11.117	4.23774	-1.082
38	40.26	0	28.237	9.608	3.67751	-1.328
39	60.02	2.276	35.091	16.895	5.90450	0.373
40	59.62	0.85	37.219	15.977	6.15136	0.349
41	47.6	0	31.595	10.645	4.08539	0.366
42	50.44	0.492	34.096	11.626	4.47718	-0.368
43	39.42	0.118	26.301	8.313	3.17677	0.924
44	48.61	0	34.009	10.484	3.90986	0.504
45	57.35	0	34.887	20.639	7.13245	-5.503
46	47.49	0	31.967	9.331	3.57788	3.869
47	38.98	0	31.67	5.949	2.25657	-2.572
48	42.99	0	32.741	6.975	2.64549	1.143
49	53.01	1.724	34.193	10.271	3.86958	3.332
50	55.17	0.058	38.054	15.014	5.63319	-3.039
51	46.16	0	31.15	8.326	3.13186	2.527
52	42.63	0	33.774	9.633	3.54491	-4.439
53	50.93	0	32.392	13.593	5.16885	0.586
54	54.24	0.7	28.381	15.606	5.64407	4.956
55	50.46	0.276	32.982	11.713	4.38844	0.469
56	56.39	1.218	38.377	14.994	5.70778	-4.988
57	41.99	0	27.817	9.924	3.64117	0.694
58	68.6	0.268	35.612	23.692	8.27997	2.638
59	48.67	0.025	33.939	9.028	3.37841	-0.029
60	58.12	0.652	34.64	17.287	6.11044	0.561
61	54.9	2.092	31.323	16.173	5.37163	-0.525
62	56.29	1.13	33.249	18.185	6.47776	-2.255
63	49.13	0.506	34.444	10.708	4.10986	-1.197
64	54.54	0.418	32.213	14.289	5.35000	3.084
65	45.05	0	32.747	9.525	3.62021	-1.571
66	37.07	0	29.757	6.578	2.50456	-2.654
67	40.17	0	24.979	8.455	3.25176	4.44
68	58.08	0	35.231	18.294	6.51891	-1.223
69	36.31	0	27.066	6.832	2.60432	-1.114
70	42.67	1.06	31.864	9.440	3.49029	-3.707
71	48.88	0	35.438	7.428	2.85590	3.159
72	47.36	0.586	32.726	12.435	4.77047	-2.841
73	35.81	0	26.531	6.125	2.34479	0.077
74	49.81	0.749	29.573	12.446	4.65966	4.119

Detailed HELP Model Annual Water Balance Data (Year 1,800) – Continued:

Simulation	Precip-itation (in/yr)	Runoff (in/yr)	Evapotrans-piration (in/yr)	Lateral Drainage (in/yr)	Infiltration thru GCL (in/yr)	Change in Water Storage (in/yr)
75	56.43	3.939	34.341	12.331	4.74275	0.542
76	45.86	0	32.502	10.711	4.12822	-1.685
77	56.76	0	38.988	13.601	5.07791	-0.634
78	39.15	0	29.537	6.268	2.36953	-0.195
79	48.87	0	30.982	10.686	3.70822	4.031
80	58.52	0.843	33.423	20.745	7.06688	-2.61
81	53.34	0	35.499	12.174	4.68622	1.664
82	55.18	0.026	35.439	13.215	4.91543	0.998
83	53.6	2.423	34.765	14.476	5.11966	-4.298
84	47.82	0	34.249	9.670	3.58666	0.392
85	44.69	0	30.801	7.813	2.96809	4.091
86	60.77	0	35.764	20.259	7.34433	-2.514
87	48.34	1.118	29.613	10.625	3.82215	3.284
88	36.18	0	26.15	11.040	3.77468	-6.363
89	58.29	2.786	35.051	14.054	5.18417	3.157
90	60.08	0.74	30.417	17.854	6.07988	4.409
91	55.49	0	35.865	16.967	6.03740	-2.495
92	44.51	0.24	32.127	9.053	3.35552	-1.419
93	35.83	0	29.666	6.354	2.42419	-3.287
94	45.02	0	32.813	7.514	2.84039	2.279
95	44.54	0.041	27.507	13.756	4.74762	-2.186
96	53.18	0.172	35.737	10.284	3.78317	3.383
97	48.03	0.411	31.447	12.523	4.73137	-0.769
98	62.58	1.207	41.367	12.807	4.76228	3.203
99	48.78	0.734	31.55	14.586	5.19735	-3.454
100	49.29	0.001	35.803	7.279	2.74889	2.872
Summary Statistics						
Count	100	100	100	100	100	100
Maximum	68.60	3.939	41.367	23.692	8.27997	4.956
Average	49.14	0.437	32.515	11.789	4.34049	0.089
Median	48.83	0.001	32.537	10.821	4.13752	0.358
Minimum	29.81	0.000	21.638	3.882	1.46494	-6.363
Std Dev	7.69	0.755	3.371	4.119	1.41389	2.667

Detailed HELP Model Annual Water Balance Data (Year 3,200):

Simulation	Precip-itation (in/yr)	Runoff (in/yr)	Evapotrans-piration (in/yr)	Lateral Drainage (in/yr)	Infiltration thru GCL (in/yr)	Change in Water Storage (in/yr)
1	40.07	0.000	31.635	2.588	2.99804	5.817
2	57.14	0.000	31.789	16.309	9.58485	0.851
3	52.64	0.101	31.102	12.336	8.83725	0.238
4	47.88	1.044	38.298	3.833	4.41289	-1.006
5	50.57	0.000	34.335	8.070	6.97170	2.5
6	42.28	0.000	27.819	6.652	6.15669	1.537
7	39.35	0.607	30.464	7.808	6.13237	-7.26
8	49.46	0.613	31.406	8.602	7.18295	2.247
9	48.59	0.000	33.538	7.377	7.26874	0.961
10	53.97	1.148	33.954	10.750	7.78469	1.11
11	57.63	4.005	32.392	11.645	7.77003	0.813
12	46.71	0.000	29.221	11.601	8.58223	-2.078
13	38.58	0.000	30.346	3.734	3.95262	0.592
14	41.49	0.389	27.682	7.306	5.27292	-0.879
15	44.94	1.081	32.460	7.112	6.33542	-1.861
16	54.78	1.071	32.231	11.967	9.26978	1.499
17	29.81	0.000	21.667	4.409	3.75908	-1.966
18	49.55	0.000	34.789	6.696	6.59669	3.722
19	55.5	2.35	33.676	11.581	8.32263	-1.033
20	68.56	0.000	37.432	17.392	10.62935	4.055
21	51.14	0.000	33.680	10.984	7.89404	-2.495
22	51.22	0.000	36.603	8.238	7.84363	-0.404
23	47.94	0.000	36.433	7.862	5.67657	-3.946
24	59.17	2.084	31.401	14.013	9.02238	4.446
25	47.73	0.099	30.375	8.865	6.91508	0.361
26	50.56	0.302	31.843	11.096	7.23096	1.298
27	37.02	0.000	31.939	3.735	3.56594	-4.324
28	56.03	0.886	35.681	12.482	8.08085	-0.811
29	39.77	0.000	29.457	4.539	4.38554	1.837
30	46.55	0.391	33.839	6.501	6.67423	-0.238
31	39.45	0.142	28.778	7.328	5.37407	-3.867
32	45.35	0.427	29.761	7.384	5.75782	2.604
33	42.23	0.000	31.883	4.639	4.73186	2.317
34	37.81	0.000	27.355	5.613	5.01894	-2.018
35	48.19	0.279	34.240	7.889	7.11671	-0.081
36	62.28	3.595	33.957	12.410	8.92212	4.525

Detailed HELP Model Annual Water Balance Data (Year 3,200) – Continued:

Simulation	Precip-itation (in/yr)	Runoff (in/yr)	Evapotrans-piration (in/yr)	Lateral Drainage (in/yr)	Infiltration thru GCL (in/yr)	Change in Water Storage (in/yr)
37	55.96	0.000	40.271	7.893	7.21311	-0.911
38	40.26	0.000	28.253	7.552	6.10903	-1.478
39	60.02	4.561	35.034	12.080	7.97245	0.529
40	59.62	0.901	37.120	12.785	9.98912	0.01
41	47.6	0.000	31.563	8.274	6.39218	0.509
42	50.44	0.519	34.095	8.756	7.20117	-0.519
43	39.42	0.13	26.297	5.869	5.61785	1.057
44	48.61	0.000	33.995	8.141	6.36787	0.544
45	57.35	3.52	34.849	15.302	8.76708	-5.706
46	47.49	0.000	31.970	7.454	5.70795	3.967
47	38.98	0.000	31.646	4.046	3.98249	-2.552
48	42.99	0.000	32.633	4.905	4.94157	1.206
49	53.01	1.751	34.193	7.347	6.85867	3.54
50	55.17	0.081	37.981	11.842	7.95047	-2.6
51	46.16	0.000	31.144	6.387	5.71351	2.201
52	42.63	0.000	33.742	7.615	5.67910	-4.813
53	50.93	0.000	32.356	10.386	8.49045	0.636
54	54.24	0.751	28.423	12.672	7.58409	5.661
55	50.46	0.299	32.975	9.663	7.37942	-0.08
56	56.39	1.269	38.397	11.873	8.56601	-5.312
57	41.99	0.000	27.818	7.517	6.10272	1.231
58	68.6	0.745	35.750	18.441	10.35122	4.455
59	48.67	0.000	33.903	8.906	6.06663	-2.234
60	58.12	2.434	34.651	12.442	8.75280	0.845
61	54.9	4.353	31.582	11.830	7.03069	0.17
62	56.29	3.401	33.140	13.586	9.65566	-3.206
63	49.13	0.533	34.450	7.895	6.81056	-1.337
64	54.54	0.444	32.271	11.754	7.99506	3.365
65	45.05	0.000	32.852	6.902	6.07673	-1.37
66	37.07	0.000	29.744	4.395	4.47669	-2.881
67	40.17	0.000	24.963	6.642	5.16571	4.471
68	58.08	0.695	35.580	14.700	9.25775	-1.202
69	36.31	0.000	27.025	4.764	4.44646	-1.406
70	42.67	1.087	31.870	7.223	5.66920	-3.464
71	48.88	0.000	35.468	5.745	4.51044	2.953
72	47.36	0.621	32.691	10.158	7.03381	-2.938
73	35.81	0.000	26.524	4.497	3.97806	0.132
74	49.81	0.738	29.551	9.418	7.98077	4.556

Detailed HELP Model Annual Water Balance Data (Year 3,200) – Continued:

Simulation	Precip-itation (in/yr)	Runoff (in/yr)	Evapotrans-piration (in/yr)	Lateral Drainage (in/yr)	Infiltration thru GCL (in/yr)	Change in Water Storage (in/yr)
75	56.43	3.988	34.321	8.863	8.25878	0.247
76	45.86	0.000	32.516	8.094	6.57066	-1.854
77	56.76	0.000	39.017	10.411	8.25441	-0.374
78	39.15	0.000	29.530	4.794	3.80454	-0.337
79	48.87	0.264	30.939	8.358	5.39681	4.38
80	58.52	4.739	33.315	15.302	9.23574	-2.612
81	53.34	0.000	35.432	9.200	7.71769	1.228
82	55.18	0.05	35.528	9.812	8.10077	1.47
83	53.6	3.721	34.952	11.060	6.92025	-4.767
84	47.82	0.000	34.234	7.669	5.89494	0.796
85	44.69	0.000	30.801	5.296	5.43971	4.296
86	60.77	0.707	36.838	16.351	9.56622	-2.737
87	48.34	1.147	29.608	7.947	5.96095	3.44
88	36.18	1.51	26.137	8.166	5.31956	-6.772
89	58.29	2.808	35.363	11.577	7.49120	3.169
90	60.08	3.188	30.455	12.750	7.91046	4.949
91	55.49	0.021	35.601	13.849	8.77156	-1.924
92	44.51	0.249	32.099	7.422	5.70970	-2.064
93	35.83	0.000	29.692	5.141	4.22932	-3.417
94	45.02	0.000	32.790	4.838	5.55045	1.923
95	44.54	1.636	27.551	9.941	6.83865	-2.375
96	53.18	0.195	35.684	8.086	6.13133	3.55
97	48.03	0.432	31.447	9.687	7.71069	-0.473
98	62.58	1.255	41.328	9.387	7.40407	3.868
99	48.78	1.462	31.539	11.574	8.29288	-4.321
100	49.29	0.025	35.763	4.733	5.12755	2.866
Summary Statistics						
Count	100	100	100	100	100	100
Maximum	68.60	4.739	41.328	18.441	10.62935	5.817
Average	49.14	0.768	32.527	8.993	6.79485	0.092
Median	48.83	0.136	32.488	8.202	6.88687	0.204
Minimum	29.81	0.000	21.667	2.588	2.99804	-7.260
Std Dev	7.69	1.221	3.377	3.368	1.70035	2.897

Detailed HELP Model Annual Water Balance Data (Year 5,412):

Simulation	Precip-itation (in/yr)	Runoff (in/yr)	Evapotrans-piration (in/yr)	Lateral Drainage (in/yr)	Infiltration thru GCL (in/yr)	Change in Water Storage (in/yr)
1	40.07	0.000	31.566	0.065	5.30347	7.717
2	57.14	6.687	35.896	0.651	12.01312	1.894
3	52.64	7.501	32.013	0.770	11.96040	0.402
4	47.88	1.085	39.26	0.349	9.56774	-3.538
5	50.57	0.918	34.217	0.359	11.84732	4.386
6	42.28	3.339	28.564	0.545	10.47649	-0.665
7	39.35	2.850	31.454	0.416	10.20734	-7.108
8	49.46	2.337	33.477	0.345	11.61482	3.206
9	48.59	0.000	34.881	0.251	12.19848	1.291
10	53.97	6.596	35.008	0.395	10.32398	1.646
11	57.63	12.611	33.028	0.502	10.97853	-0.227
12	46.71	4.077	31.156	0.552	12.44982	-0.785
13	38.58	0.000	30.329	0.142	8.32428	-0.217
14	41.49	4.660	28.761	0.305	8.08932	-2.077
15	44.94	1.433	34.641	0.304	10.77869	-1.727
16	54.78	6.354	33.009	0.419	12.28924	3.973
17	29.81	2.034	22.587	0.304	7.26211	-4.599
18	49.55	0.000	35.322	0.180	11.64727	4.623
19	55.5	8.366	35.648	0.502	12.41581	-1.432
20	68.56	12.843	38.634	0.894	12.44982	3.740
21	51.14	4.022	35.796	0.479	11.74539	-1.088
22	51.22	0.326	37.558	0.511	12.41581	0.595
23	47.94	6.698	36.987	0.492	8.87898	-6.606
24	59.17	10.270	32.045	0.563	11.18029	6.603
25	47.73	4.541	31.677	0.465	11.36674	-0.626
26	50.56	6.488	32.284	0.560	10.39571	1.137
27	37.02	0.000	32.15	0.228	8.26097	-5.524
28	56.03	6.970	38.579	0.532	10.90000	-0.306
29	39.77	0.000	29.493	0.161	9.03531	1.652
30	46.55	0.378	34.717	0.203	11.38827	0.343
31	39.45	3.678	30.108	0.392	7.84630	-4.484
32	45.35	1.673	31.208	0.314	10.30107	2.694
33	42.23	0.000	31.908	0.082	7.96179	3.355
34	37.81	2.132	28.575	0.326	8.17667	-3.288
35	48.19	0.526	36.944	0.296	12.01205	0.421
36	62.28	9.716	34.759	0.590	12.01325	5.286

Detailed HELP Model Annual Water Balance Data (Year 5,412) – Continued:

Simulation	Precip-itation (in/yr)	Runoff (in/yr)	Evapotrans-piration (in/yr)	Lateral Drainage (in/yr)	Infiltration thru GCL (in/yr)	Change in Water Storage (in/yr)
37	55.96	3.179	42.137	0.590	10.62996	-1.657
38	40.26	2.196	28.661	0.401	10.47257	-1.115
39	60.02	10.467	36.481	0.548	11.80802	1.345
40	59.62	7.202	38.369	0.801	12.44982	0.893
41	47.6	3.781	31.924	0.502	11.48790	-0.095
42	50.44	3.254	34.775	0.498	12.41581	-0.502
43	39.42	0.859	27.535	0.437	9.81868	-0.429
44	48.61	2.429	35.124	0.447	10.69059	0.710
45	57.35	13.177	37.797	0.678	10.83655	-6.041
46	47.49	1.317	32.087	0.335	8.52411	6.539
47	38.98	1.057	32.503	0.321	8.98063	-5.466
48	42.99	0.000	33.02	0.118	9.28617	1.810
49	53.01	2.150	34.425	0.307	12.41581	4.053
50	55.17	6.047	38.849	0.592	11.49613	-1.945
51	46.16	2.862	32.222	0.414	8.69478	1.278
52	42.63	2.663	35.038	0.425	9.68648	-5.630
53	50.93	1.907	34.054	0.493	12.13839	3.604
54	54.24	9.861	30.265	0.615	11.52497	1.974
55	50.46	3.752	33.565	0.378	11.97420	0.791
56	56.39	6.496	41.446	0.636	11.89135	-4.648
57	41.99	1.418	29.418	0.250	10.44200	0.942
58	68.6	16.561	36.116	0.906	12.41581	2.690
59	48.67	3.761	34.657	0.347	9.17273	-0.847
60	58.12	7.171	37.864	0.649	12.40704	1.574
61	54.9	12.818	32.114	0.598	9.45565	-0.147
62	56.29	9.492	35.327	0.654	12.41581	-1.503
63	49.13	2.117	37.012	0.482	12.16246	-2.888
64	54.54	4.892	33.166	0.542	11.42188	4.763
65	45.05	2.778	32.998	0.346	11.95502	-3.038
66	37.07	0.000	30.403	0.182	8.09578	-3.308
67	40.17	0.465	25.262	0.264	9.48097	5.570
68	58.08	9.974	36.373	0.701	11.94406	-0.075
69	36.31	0.000	27.435	0.323	10.91015	-2.843
70	42.67	3.390	33.344	0.303	8.96877	-4.406
71	48.88	0.681	36.517	0.231	8.47238	2.939
72	47.36	3.969	34.612	0.412	11.11957	-2.342
73	35.81	0.387	27.126	0.191	7.49676	0.075
74	49.81	2.028	32.048	0.345	10.77909	6.329

Detailed HELP Model Annual Water Balance Data (Year 5,412) – Continued:

Simulation	Precip- itation (in/yr)	Runoff (in/yr)	Evapotrans- piration (in/yr)	Lateral Drainage (in/yr)	Infiltration thru GCL (in/yr)	Change in Water Storage (in/yr)
75	56.43	7.542	36.688	0.536	12.34211	-0.691
76	45.86	2.795	32.876	0.438	12.09978	-2.352
77	56.76	3.439	40.478	0.381	12.26720	0.209
78	39.15	0.684	29.92	0.282	8.41509	-1.285
79	48.87	3.966	31.659	0.404	8.64606	4.501
80	58.52	12.163	35.646	0.670	11.94453	-1.113
81	53.34	2.687	36.757	0.514	12.28173	1.137
82	55.18	5.590	36.392	0.559	11.95364	0.686
83	53.6	12.319	35.402	0.516	9.69424	-6.048
84	47.82	2.294	35.137	0.290	9.44669	2.315
85	44.69	0.706	30.793	0.136	9.29627	3.812
86	60.77	12.766	37.43	0.773	10.79039	-0.995
87	48.34	4.981	30.041	0.455	11.11258	1.756
88	36.18	6.170	27.338	0.370	8.19050	-7.809
89	58.29	8.403	36.795	0.444	8.81954	5.750
90	60.08	14.267	31.658	0.597	12.18943	1.369
91	55.49	6.537	36.212	0.769	12.41581	-0.445
92	44.51	1.062	32.797	0.498	10.18246	-0.802
93	35.83	1.368	29.654	0.266	9.45129	-4.244
94	45.02	0.000	32.684	0.141	10.54666	1.581
95	44.54	6.538	29.073	0.386	9.66974	-2.680
96	53.18	3.274	36.95	0.371	9.36370	3.449
97	48.03	3.957	33.158	0.384	11.55729	0.442
98	62.58	4.876	42.385	0.577	12.07541	2.699
99	48.78	6.098	31.953	0.565	12.39194	-2.228
100	49.29	0.064	36.094	0.193	11.06189	0.963
Summary Statistics						
Count	100	100	100	100	100	100
Maximum	68.60	16.561	42.385	0.906	12.44982	7.717
Average	49.14	4.422	33.623	0.432	10.60621	0.096
Median	48.83	3.365	33.411	0.418	10.90508	0.142
Minimum	29.81	0.000	22.587	0.065	5.30347	-7.809
Std Dev	7.69	3.973	3.606	0.178	1.58201	3.295

Detailed HELP Model Annual Water Balance Data (Year 5,600):

Simulation	Precip-itation (in/yr)	Runoff (in/yr)	Evapotrans-piration (in/yr)	Lateral Drainage (in/yr)	Infiltration thru GCL (in/yr)	Change in Water Storage (in/yr)
1	40.07	0.000	31.600	0.063	5.30224	7.687
2	57.14	6.678	35.886	0.647	12.01303	1.917
3	52.64	7.505	31.995	0.768	11.97520	0.404
4	47.88	1.089	39.244	0.347	9.56693	-3.509
5	50.57	0.904	34.237	0.357	11.85767	4.356
6	42.28	3.345	28.566	0.543	10.46999	-0.666
7	39.35	2.854	31.430	0.415	10.22368	-7.096
8	49.46	2.341	33.503	0.343	11.59117	3.180
9	48.59	0.000	34.876	0.248	12.20214	1.311
10	53.97	6.602	34.950	0.394	10.37708	1.646
11	57.63	12.619	33.068	0.499	10.93671	-0.256
12	46.71	4.078	31.146	0.550	12.44982	-0.751
13	38.58	0.000	30.313	0.143	8.33574	-0.213
14	41.49	4.675	28.777	0.303	8.07432	-2.091
15	44.94	1.405	34.666	0.302	10.77772	-1.721
16	54.78	6.375	33.023	0.415	12.28261	3.948
17	29.81	2.018	22.565	0.302	7.27580	-4.571
18	49.55	0.000	35.337	0.180	11.63540	4.618
19	55.5	8.374	35.645	0.501	12.41581	-1.435
20	68.56	12.850	38.630	0.890	12.44982	3.739
21	51.14	4.023	35.793	0.478	11.74515	-1.086
22	51.22	0.307	37.582	0.507	12.41581	0.594
23	47.94	6.702	37.001	0.490	8.86169	-6.614
24	59.17	10.294	32.028	0.561	11.17681	6.608
25	47.73	4.543	31.674	0.464	11.36429	-0.613
26	50.56	6.495	32.296	0.558	10.38174	1.125
27	37.02	0.000	32.147	0.228	8.26586	-5.528
28	56.03	6.973	38.574	0.530	10.89712	-0.298
29	39.77	0.000	29.504	0.161	9.02521	1.651
30	46.55	0.375	34.729	0.203	11.38459	0.336
31	39.45	3.679	30.088	0.391	7.85975	-4.472
32	45.35	1.676	31.216	0.314	10.30967	2.675
33	42.23	0.000	31.898	0.083	7.95840	3.368
34	37.81	2.132	28.588	0.324	8.16070	-3.288
35	48.19	0.527	36.924	0.297	12.02804	0.434
36	62.28	9.741	34.754	0.589	12.00127	5.270

Detailed HELP Model Annual Water Balance Data for (Year 5,600) – Continued:

Simulation	Precip-itation (in/yr)	Runoff (in/yr)	Evapotrans-piration (in/yr)	Lateral Drainage (in/yr)	Infiltration thru GCL (in/yr)	Change in Water Storage (in/yr)
37	55.96	3.180	42.122	0.587	10.64265	-1.650
38	40.26	2.200	28.654	0.400	10.47575	-1.116
39	60.02	10.469	36.455	0.548	11.82187	1.349
40	59.62	7.208	38.382	0.797	12.44982	0.883
41	47.6	3.782	31.927	0.500	11.48657	-0.095
42	50.44	3.258	34.764	0.497	12.41581	-0.495
43	39.42	0.864	27.532	0.436	9.81894	-0.431
44	48.61	2.435	35.125	0.446	10.68869	0.705
45	57.35	13.175	37.778	0.676	10.85619	-6.028
46	47.49	1.313	32.097	0.334	8.52431	6.524
47	38.98	1.057	32.504	0.319	8.97501	-5.452
48	42.99	0.000	33.038	0.117	9.27085	1.798
49	53.01	2.159	34.418	0.307	12.41581	4.054
50	55.17	6.061	38.829	0.591	11.50912	-1.946
51	46.16	2.883	32.198	0.413	8.69851	1.287
52	42.63	2.664	35.038	0.424	9.68236	-5.639
53	50.93	1.934	34.033	0.492	12.13784	3.601
54	54.24	9.890	30.275	0.612	11.48757	1.975
55	50.46	3.753	33.582	0.377	11.95745	0.791
56	56.39	6.501	41.443	0.634	11.88732	-4.647
57	41.99	1.422	29.420	0.249	10.43916	0.941
58	68.6	16.540	36.143	0.901	12.41581	2.691
59	48.67	3.769	34.634	0.346	9.19049	-0.837
60	58.12	7.182	37.861	0.647	12.40122	1.554
61	54.9	12.823	32.128	0.595	9.43950	-0.141
62	56.29	9.498	35.329	0.652	12.41581	-1.505
63	49.13	2.107	37.002	0.481	12.17480	-2.863
64	54.54	4.901	33.161	0.540	11.42200	4.744
65	45.05	2.778	32.989	0.346	11.96084	-3.034
66	37.07	0.000	30.414	0.182	8.09011	-3.318
67	40.17	0.442	25.289	0.261	9.47799	5.603
68	58.08	9.981	36.374	0.699	11.93873	-0.103
69	36.31	0.000	27.440	0.322	10.90104	-2.836
70	42.67	3.399	33.347	0.301	8.95243	-4.391
71	48.88	0.695	36.492	0.231	8.48528	2.922
72	47.36	3.982	34.613	0.413	11.11170	-2.348
73	35.81	0.401	27.106	0.190	7.50176	0.092
74	49.81	2.039	32.041	0.344	10.77885	6.314

Detailed HELP Model Annual Water Balance Data (Year 5,600) – Continued:

Simulation	Precip-itation (in/yr)	Runoff (in/yr)	Evapotrans-piration (in/yr)	Lateral Drainage (in/yr)	Infiltration thru GCL (in/yr)	Change in Water Storage (in/yr)
75	56.43	7.552	36.694	0.532	12.32885	-0.691
76	45.86	2.799	32.893	0.436	12.07906	-2.346
77	56.76	3.443	40.540	0.378	12.25764	0.155
78	39.15	0.638	29.936	0.280	8.39611	-1.250
79	48.87	3.975	31.637	0.402	8.66357	4.536
80	58.52	12.165	35.667	0.667	11.93171	-1.140
81	53.34	2.673	36.760	0.508	12.29176	1.143
82	55.18	5.588	36.410	0.555	11.94156	0.685
83	53.6	12.315	35.297	0.520	9.79846	-6.025
84	47.82	2.293	35.165	0.288	9.41929	2.292
85	44.69	0.706	30.775	0.136	9.31912	3.811
86	60.77	12.768	37.431	0.770	10.79111	-0.995
87	48.34	5.004	30.009	0.454	11.12244	1.756
88	36.18	6.170	27.340	0.369	8.18612	-7.812
89	58.29	8.408	36.792	0.444	8.81971	5.754
90	60.08	14.309	31.643	0.598	12.16316	1.368
91	55.49	6.552	36.200	0.767	12.41581	-0.444
92	44.51	1.068	32.794	0.496	10.18112	-0.802
93	35.83	1.368	29.650	0.265	9.44800	-4.227
94	45.02	0.000	32.711	0.140	10.52511	1.549
95	44.54	6.542	29.063	0.385	9.66860	-2.661
96	53.18	3.277	36.974	0.369	9.34311	3.450
97	48.03	3.965	33.156	0.383	11.55486	0.443
98	62.58	4.915	42.350	0.576	12.07783	2.694
99	48.78	6.102	31.948	0.563	12.39147	-2.225
100	49.29	0.067	36.103	0.192	11.05051	0.952
Summary Statistics						
Count	100	100	100	100	100	100
Maximum	68.60	16.540	42.350	0.901	12.44982	7.687
Average	49.14	4.426	33.622	0.431	10.60515	0.096
Median	48.83	3.372	33.425	0.415	10.89908	0.124
Minimum	29.81	0.000	22.565	0.063	5.30224	-7.812
Std Dev	7.69	3.976	3.606	0.177	1.58076	3.290

Detailed HELP Model Annual Water Balance Data (Year 10,000):

Simulation	Precip- itation (in/yr)	Runoff (in/yr)	Evapotrans- piration (in/yr)	Lateral Drainage (in/yr)	Infiltration thru GCL (in/yr)	Change in Water Storage (in/yr)
1	40.07	0.000	31.575	0.060	5.41035	7.610
2	57.14	7.040	35.705	0.590	11.93675	1.862
3	52.64	7.623	31.976	0.685	11.96880	0.399
4	47.88	1.157	39.144	0.314	9.51845	-3.392
5	50.57	1.019	34.234	0.344	11.87505	4.236
6	42.28	3.445	28.401	0.496	10.57945	-0.657
7	39.35	2.968	31.528	0.370	9.93657	-7.062
8	49.46	2.542	33.420	0.325	11.39476	3.236
9	48.59	0.000	34.940	0.257	12.25115	1.310
10	53.97	6.710	34.893	0.370	10.32053	1.675
11	57.63	12.865	32.916	0.456	11.03073	-0.175
12	46.71	4.073	31.029	0.514	12.44982	-0.818
13	38.58	0.000	30.303	0.147	8.38081	-0.253
14	41.49	4.795	28.711	0.278	8.04102	-2.094
15	44.94	1.511	34.602	0.291	10.73919	-1.720
16	54.78	6.639	33.040	0.392	12.02812	3.960
17	29.81	2.143	22.499	0.281	7.22954	-4.575
18	49.55	0.000	35.506	0.175	11.50044	4.601
19	55.5	8.605	35.520	0.462	12.41581	-1.503
20	68.56	13.022	38.565	0.803	12.44982	3.720
21	51.14	4.040	35.735	0.442	11.72615	-0.992
22	51.22	0.359	37.644	0.482	12.41581	0.508
23	47.94	6.745	36.954	0.447	8.90271	-6.604
24	59.17	10.425	32.157	0.509	10.95394	6.620
25	47.73	4.681	31.590	0.431	11.33503	-0.606
26	50.56	6.629	32.249	0.511	10.37905	1.089
27	37.02	0.000	32.069	0.209	8.24669	-5.410
28	56.03	7.151	38.491	0.485	10.84896	-0.326
29	39.77	0.000	29.484	0.157	9.02560	1.688
30	46.55	0.286	34.812	0.205	11.48492	0.335
31	39.45	3.746	30.038	0.350	7.80224	-4.494
32	45.35	1.681	31.216	0.295	10.32567	2.683
33	42.23	0.000	31.886	0.081	7.97941	3.370
34	37.81	2.252	28.414	0.309	8.12686	-3.198
35	48.19	0.600	36.924	0.304	12.06104	0.331
36	62.28	9.797	34.902	0.540	11.94384	5.173

Detailed HELP Model Annual Water Balance Data (Year 10,000) – Continued:

Simulation	Precip-itation (in/yr)	Runoff (in/yr)	Evapotrans-piration (in/yr)	Lateral Drainage (in/yr)	Infiltration thru GCL (in/yr)	Change in Water Storage (in/yr)
37	55.96	3.238	42.068	0.528	10.60639	-1.557
38	40.26	2.313	28.582	0.373	10.44351	-1.110
39	60.02	10.510	36.527	0.506	11.70666	1.213
40	59.62	7.516	38.302	0.722	12.44982	0.921
41	47.6	3.803	31.888	0.467	11.43317	0.009
42	50.44	3.480	34.666	0.455	12.41581	-0.577
43	39.42	0.856	27.455	0.399	9.78889	-0.286
44	48.61	2.633	35.063	0.407	10.66856	0.650
45	57.35	13.402	37.624	0.624	10.81856	-6.046
46	47.49	1.442	32.081	0.306	8.54380	6.440
47	38.98	1.087	32.447	0.289	8.96609	-5.335
48	42.99	0.000	33.042	0.117	9.25628	1.772
49	53.01	2.339	34.390	0.286	12.41581	3.908
50	55.17	6.173	38.795	0.536	11.43707	-1.924
51	46.16	3.037	32.137	0.378	8.64894	1.300
52	42.63	2.684	34.974	0.386	9.65536	-5.514
53	50.93	2.179	33.929	0.457	12.13342	3.488
54	54.24	10.101	30.160	0.556	11.45129	1.972
55	50.46	3.910	33.503	0.350	11.90852	0.788
56	56.39	6.659	41.287	0.577	11.83536	-4.582
57	41.99	1.535	29.370	0.226	10.35888	0.999
58	68.6	16.835	36.065	0.828	12.41581	2.571
59	48.67	3.905	34.695	0.308	8.92484	-0.728
60	58.12	7.486	37.713	0.595	12.40382	1.449
61	54.9	12.969	32.055	0.545	9.41386	-0.141
62	56.29	9.633	35.223	0.598	12.41581	-1.485
63	49.13	2.041	37.039	0.448	12.18326	-2.797
64	54.54	5.209	33.000	0.496	11.40235	4.648
65	45.05	2.840	32.807	0.316	12.05154	-2.974
66	37.07	0.000	30.486	0.176	8.03116	-3.341
67	40.17	0.591	25.289	0.246	9.39459	5.506
68	58.08	10.235	36.109	0.657	11.98793	-0.039
69	36.31	0.000	27.386	0.301	10.87248	-2.763
70	42.67	3.573	33.322	0.272	8.81567	-4.335
71	48.88	0.835	36.455	0.215	8.44584	2.894
72	47.36	4.178	34.518	0.379	11.01566	-2.401
73	35.81	0.493	27.183	0.180	7.33004	-0.026
74	49.81	2.154	32.020	0.326	10.77726	6.424

Detailed HELP Model Annual Water Balance Data (Year 10,000) – Continued:

Simulation	Precip-itation (in/yr)	Runoff (in/yr)	Evapotrans-piration (in/yr)	Lateral Drainage (in/yr)	Infiltration thru GCL (in/yr)	Change in Water Storage (in/yr)
75	56.43	7.769	36.495	0.486	12.30589	-0.643
76	45.86	2.912	32.899	0.400	11.97782	-2.389
77	56.76	3.580	40.514	0.357	12.21619	0.171
78	39.15	0.705	29.897	0.256	8.43251	-1.198
79	48.87	4.122	31.603	0.368	8.60958	4.417
80	58.52	12.243	35.546	0.612	11.93565	-1.040
81	53.34	2.937	36.662	0.497	12.22575	1.051
82	55.18	5.732	36.367	0.514	11.88624	0.680
83	53.6	12.167	35.252	0.480	9.92911	-5.897
84	47.82	2.372	35.109	0.269	9.41924	2.269
85	44.69	0.801	30.718	0.137	9.38110	3.705
86	60.77	12.912	37.347	0.707	10.74654	-0.948
87	48.34	5.147	29.977	0.412	11.09773	1.713
88	36.18	6.192	27.283	0.333	8.15144	-7.712
89	58.29	8.504	36.719	0.410	8.92491	5.664
90	60.08	14.510	31.581	0.557	12.07850	1.354
91	55.49	6.808	36.010	0.699	12.41581	-0.443
92	44.51	1.335	32.679	0.448	10.07379	-0.823
93	35.83	1.377	29.667	0.247	9.31054	-4.086
94	45.02	0.000	32.653	0.148	10.59745	1.597
95	44.54	6.656	29.019	0.355	9.69579	-2.740
96	53.18	3.194	36.936	0.333	9.56430	3.422
97	48.03	3.963	33.084	0.353	11.50107	0.512
98	62.58	5.188	42.377	0.527	11.96432	2.562
99	48.78	6.204	31.859	0.522	12.34982	-2.155
100	49.29	0.154	36.073	0.184	10.98109	0.981
Summary Statistics						
Count	100	100	100	100	100	100
Maximum	68.60	16.835	42.377	0.828	12.44982	7.610
Average	49.14	4.539	33.571	0.398	10.57611	0.095
Median	48.83	3.527	33.371	0.382	10.86072	0.090
Minimum	29.81	0.000	22.499	0.060	5.41035	-7.712
Std Dev	7.69	4.016	3.600	0.159	1.57660	3.253

This page intentionally left blank

Distribution:

T. C. Robinson, Jr., 766-H
K. H. Rosenberger, 766-H
J. L. Newman, 766-H
T. W. Coffield, 766-H
H. H. Burns, 999-W
B. T. Butcher, 773-43A
E. L. Wilhite, 773-43A
R. S. Aylward, 773-42A
M. A. Phifer, 773-42A
G. P. Flach, 773-42A
W. E. Jones, 773-42A
WPT file (2 copies), 773-43A, Rm. 213